UNIVERSITY OF NAPLES FEDERICO II

DEPARTMENT OF PHARMACY

PhD programme in Pharmaceutical Sciences

Novel (bio)sensors and LC-HRMS approaches for the accurate and sustainable monitoring of anthropogenic contaminants and emerging natural toxins

PhD student

Antonella Miglione

Coordinator
Prof.
ROSARIA MELI

Tutor
Prof. STEFANO CINTI
Cotutor
Prof. LUCIANA TARTAGLIONE

XXXVI CYCLE (2021-2023)

A mio Nonno,
e al piacere di conoscere.

.

Table of contents

Figure list

Table list

ABSTRACT

Climate change and anthropogenic activities, such as pollution, land and water exploitation, have significant impacts on both aquatic and terrestrial ecosystems, leading to environmental degradation and potential human health consequences. The natural occurrence or the introduction of contaminants into the environment may cause adverse changes that affect the health of humans, animals, and plants, as well as damage buildings and other structures. Terrestrial and freshwater ecosystems are particularly vulnerable to climate change, which can lead to changes in wildlife diseases, insect pests, extinction events, biome shifts, wildfires, and drought-related ecosystem changes. This dissertation is focused on emerging contaminants, a class of contaminants characterized by their novelty, ubiquity, and persistence and consequently, reason of challenges for traditional regulatory frameworks and analytical methods. Chapter 1 is focused on two sub-groups belonging to this macro-area: i) anthropogenic contaminants, including heavy metals, drug residues, pesticides, and so on, known to adversely affect physiological systems even when they are present in trace, and ii) emerging natural toxins (e.g. cyclic imines, cyanotoxins and palytoxins), whose risk to the environment and to humans is not fully understood and so tolerance limits for regulation are not established yet by Safety Authorities. As for the clinical practice, as well as for the environmental pollution, the first part of the therapy is represented by an early diagnosis. Consequently, the real purpose of this dissertation is to enhance both the environmental and health monitoring system by improving analytical analysis. In this context, two analytical techniques are exploited, liquid chromatography coupled to high resolution mass spectrometry (LC-HRMS), that provides high reliability towards detection, identification and quantitation of most of the emerging natural toxins in different matrices, and electrochemical (bio)sensors, applied as novel architectures in environmental and

health monitoring. In Chapter 2, the main theoretical aspects of the two techniques are briefly presented, focusing on the workflows for targeted and untargeted LC-HRMS analysis and on fabrication, modification, and architectures of electrochemical (bio)sensors. Accordingly, results obtained on these two topics are discussed: in Chapter 3, LC-HRMS approaches for the accurate and sustainable monitoring of emerging natural toxins are presented. Three class of toxins are exploited, the cyclic imines related to the mucilage samples that we analyzed in 2021, when in the north-eastern Aegean sea a mucilage episode occurred, the cyanotoxins and cyanometabolites, that have been the subject of two different studies, one related to the untargeted LC-HRMS applied to microcystin-producing cyanobacterial cultures for the evaluation of the efficiency of chlorine-based treatments commonly used for water potabilization, and the other related to the activities that I carried out as visiting PhD student at Eawag - Department of Environmental Chemistry of the Swiss Federal Institute of Aquatic Science and Technology, about the update and implementation of the CyanoMetDB, applied on the monitoring of key metabolites from cyanobacterial blooms of *Planktothrix* spp. The last toxins discussed are palytoxin and its congeners and in particular the development of a solid-phase toxin adsorption (SPATT) method based on cross-linked cyclodextrins for monitoring these compounds. In Chapter 4, novel architecture in the field of electrochemical sensors and biosensors are presented. Starting from an integrated electrochemical platform, empowered by paper, for fast nickel detection, in which the classical three electrodes configuration is printed on a polyester substrate and then combined with filter paper in order to (1) store the reagents, (2) collect real samples, and (3) preconcentrate the analyte of interest, we moved on a total paper-based electrochemical strip to detect paracetamol in wastewater, in which our paper-based electrochemical sensor is printed together with a filter paper strip, which gives the possibility of treating complex matrices

as wastewater, in situ, and represented a green alternative to common detection methods. Moving on, we proceeded with the characterization and application of porous PHBV-based bacterial polymers to realize novel bio-based electroanalytical (bio)sensors. These alternative substrates have been screen-printed with conductive inks to realize electrochemical strips and applied towards pesticide detection, highlighting the potentiality of PHBV-based materials for future sustainable application in the electroanalytical field. Finally, we focused on electrochemical biosensors for on-glove applications, in which the classical electrochemical strip is integrated in a glove and applied to the detection of pesticides directly on fruit peels. All these new architectures can be successfully implemented in the clinical field and some of these exploited applications are quickly presented in Chapter 5. In conclusion, the exploitation of I) easy-to-use and portable de-centralized approaches and II) validated and reference laboratory-bound methodologies, might represent a step forward beyond the current paradigm: each approach should be seen as an added point for the other one. The obtained information could allow a faster, more selective, cheaper, and easier detection of potentially harmful factors in different matrices, with the purpose to preserve human health and ecosystems.

The above studies resulted in 11 papers published and 2 submitted, that are listed below.

LIST OF PAPERS

1) A. Miglione, A. Raucci, F. Cristiano, M. Mancini, V. Gioia, A. Frugis, S. Cinti, Paper-based 2D configuration for the electrochemical and facile detection of paracetamol in wastewaters, *Electrochimica Acta*, 2024 (Submitted).

2) M. Simonazzi, A. Miglione, L. Tartaglione, M. Varra, C. Dell'Aversano, F. Guerrini, R. Pistocchi, L. Pezzolesi, Untargeted LC-HRMS applied to microcystin-producing cyanobacterial cultures for the evaluation of the efficiency of chlorine-based treatments commonly used for water potabilization, *Chemosphere*, 2024 (Submitted).

3) A. Miglione, F. Di Nardo, S. Cavalera, T. Serra, C. Baggiani, S. Cinti, L. Anfossi, Merging lateral flow immunoassay with electroanalysis as a novel sensing platform: prostate specific antigen detection as case of study, *Analytical Chemistry*, 2024, 96 (6), 2297-2302.

4) A. Raucci, A. Miglione, W. Cimmino, A. Cioffi, S. Singh, M. Spinelli, A. Amoresano, G. Musile, S. Cinti, Technical Evaluation of a Paper-Based Electrochemical Strip to Measure Nitrite Ions in the Forensic Field, *ACS Measurement Science Au*, 2023, 4 (1), 136-143.

5) S. Singh, A. Miglione, A. Raucci, A. Numan, S. Cinti, Towards sense and sensitivity-based electrochemical biosensors for liquid biopsy-based breast cancer detection, *TrAC Trends in Analytical Chemistry*, 2023, 163, 117050.

6) E. M.-L Janssen, M.R Jones, E. Pinto, F.Dörr, M.A Torres, F. Rios Jacinavicius, H. Mazur-Marzec, K. Szubert, R. Konkel, L. Tartaglione, C. Dell'Aversano, A. Miglione, P. McCarron, D. G Beach, C. O Miles, D. P Fewer, K. Sivonen, J. Jokela, M. Wahlsten, T. H. J Niedermeyer, F. Schanbacher, P. Leão, M. Preto, P. M D'Agostino, M. Baunach, E. Dittmann, R. Reher, S75 | CyanoMetDB | Comprehensive Database of Secondary Metabolites from Cyanobacteria, 2023, https://doi.org/10.5281/zenodo.7922070.

7) W. Cimmino, D. Migliorelli, S. Singh, A. Miglione, S. Generelli, S. Cinti, Design of a printed electrochemical strip towards miRNA-21 detection in urine samples: optimization of the experimental procedures for real sample application, *Analytical and Bioanalytical Chemistry*, 2023, 415 (18):4511-4520.

8) A. Raucci, A. Miglione, L. Lenzi, P. Fabbri, J. Di Tocco, C. Massaroni, D. Lo Presti, E. Schena, V. Pifferi, L. Falciola, W. Aidli, C. Di Natale, P. A. Netti, S. L. Woo, D. Morselli, S. Cinti, Characterization and application of porous PHBV-based bacterial polymers to realize novel bio-based electroanalytical (bio)sensors, *Sensors and Actuators B: Chemical*, 2023, 379, 133178.
9) A. Miglione, R. Di Lorenzo, L. Grumetto, M. Spinelli, A. Amoresano, S. Laneri, S. Cinti, An integrated electrochemical platform empowered by paper for fast nickel detection in cosmetics, *Electrochimica Acta*, 2022, 434, 141332.
10) A. Miglione, A. Raucci, J. Amato, S. Marzano, B. Pagano, T. Raia, M. Lucarelli, A. Fuso, S. Cinti, Printed Electrochemical Strip for the Detection of miRNA-29a: A Possible Biomarker Related to Alzheimer's Disease, *Analytical Chemistry*, 2022 94 (45), 15558-15563.
11) A. Raucci, A. Miglione, M. Spinelli, A. Amoresano, S. Cinti, A Hybrid Screen-Printed Strip for Enhanced Electroanalysis towards Lead and Cadmium in Multi-Matrices, *Journal of The Electrochemical Society,* 2022, 169, 3, 037516.
12) A. Miglione, M. Spinelli, A. Amoresano, S. Cinti, Sustainable copper electrochemical stripping onto paper-based substrate for clinical application, *ACS Measurement Science Au,* 2022, 2, 2, 177–184.
13) A. Miglione, M. Napoletano, S. Cinti, Electrochemical Biosensors for Tracing Cyanotoxins in Food and Environmental Matrices, *Biosensors,* 2021, 11 (9), 315.

CHAPTER 1. GENERAL INTRODUCTION

Climate change, anthropogenic pollution, land, and water exploitation affect the condition of aquatic and terrestrial ecosystems leading to environmental issues and human health consequences. In recent decades, environmental pollution has emerged as a pressing global issue, that arises from the introduction of contaminants into the natural environment, causing adverse changes.[1–3] As a further consequence, eutrophication of marine and fresh waters, have favored the spreading and proliferation of some noxious microorganisms able to produce natural toxins that, despite their natural occurrence in the environmental, may pose threat to human health. This multifaceted issue encompasses a wide range of contaminants and their sources, impacting air, water, and soil quality, posing concern for a multitude of specialists including eco-toxicologists, environmental biologists, eco-chemists, pathologists, and researchers from several fields.[4,5] The consequences of environmental pollution and climate changes are far-reaching, affecting ecosystems, wildlife, and human health, and demanding urgent attention from individuals, communities, and policymakers worldwide, placing a significant threat to biodiversity and ecosystems health. Contaminants disrupt ecological balance, harm wildlife, and often contribute to habitat degradation. Altered air and water quality, soil contamination, and habitat destruction can lead to the decline or extinction of plant and animal species: the survival of many societies, and of the biological support systems of the planet, is at risk. The detrimental effects on human health are related to the exposure to polluted air, water, and soil that can result in respiratory diseases, cardiovascular problems, neurological disorders, and various other health issues, in particular for the vulnerable populations, such as children and the elderly, who are the most affected and particularly at risk.[3,6–8] Addressing environmental pollution requires a concerted effort from individuals, communities, governments, and industries.

Strategies include implementing and enforcing stringent environmental regulations, promoting sustainable practices, investing in cleaner technologies, and fostering public awareness and education.[9–11] In particular, ONU established 17 goals for sustainable development to be achieved in the environmental, economic, social and institutional spheres by 2030. Briefly, I) combat climate change, II) improve health condition, reducing the number of deaths and diseases from pollution and contamination of air, water and soil, III) ensure availability and sustainable management for all water, and IV) protect oceans, seas and land, are just some of the goals for reaching a sustainable growth.[12]

In this dissertation, I will focus on a key category of substances named as "emerging contaminants" and among these on the occurrence of toxic and potentially harmful algal species for humans in environmental, food and biological matrices. Emerging contaminants include some anthropogenic contaminants (pesticides, drug residues, heavy metals, etc.),[13,14] and also some natural toxins that are not regulated by European Safety Authorities yet (e.g. cyanotoxins such as microcystins and nodularins, cylindrospermopsins, anatoxins and saxitoxins and palytoxins),[15–17] whose analytical analysis and monitoring represent a bullet point to understand the better way to minimize their impact on ecosystem and human health. What we have to considerer is that also the analytical methods used to reveal these kinds of contaminants are many and constantly evolving. The first step to be undertaken to protect/cure the ecosystem and human health is represented by an accurate monitoring. As for the clinical practice, as well as for the environmental pollution, the first part of the therapy is represented by an early diagnosis. Consequently, it is essential to improve both the environmental and health monitoring system, which represents the first attempt in managing and solving this great issue and develop effective solutions and fostering a sustainable and healthier planet for present and future generations.[13,18] During my PhD, I particularly focused on two main different

techniques, high-performance liquid chromatography (HPLC) coupled to high resolution mass spectroscopy (HRMS) for suspect and untargeted screening of natural emerging toxins in different matrices and their in-depth structural investigation, and different types and architectures of screen - printed electrochemical sensors (SPEs) and biosensors for the analysis of several anthropogenic contaminants.[19–22] Moreover, (bio)sensors has been extensively investigated for the development of novel architectures in the diagnostic field. The exploitation of I) easy-to-use and portable de-centralized approaches and II) validated and reference laboratory-bound methodologies (liquid chromatography coupled to high resolution mass spectrometry), might represent a step forward beyond the current paradigm: each approach should be seen as an added point for the other one. The obtained information could allow a faster, more selective, cheaper, and easier detection of potentially harmful factors in different matrices, with the purpose to preserve human health and ecosystems (Figure I.1).

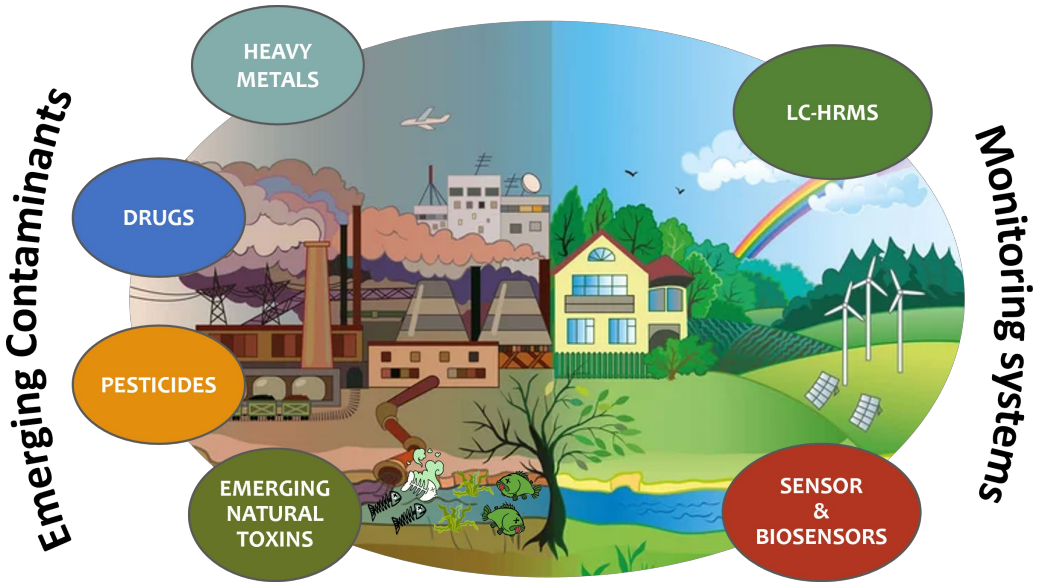

Figure I.1 LC-HRMS approaches and novel (bio)sensors for the accurate and sustainable monitoring of anthropogenic contaminants and emerging natural toxins.

1.1 EMERGING CONTAMINANTS

Emerging contaminants represent a complex and dynamic category of substances that have gained attention in recent years due to their potential impacts on environmental and human health.[23] These contaminants, often characterized by their novelty, ubiquity, and persistence, pose challenges for traditional regulatory frameworks and analytical methods. The term "emerging contaminants", rigorously refers to synthetic or naturally occurring compound and even to microorganisms that are not commonly monitored in the environment but have the potential to enter the environment and cause known or suspected adverse ecological and/or human health effects, and they include a wide range of substances, such as pharmaceuticals, personal care products, industrial chemicals, pesticides, and other compounds that have been detected in environmental media, such as water, soil, and air as well as in food sources.[11,24–26] One of the key characteristics of emerging contaminants is their relatively recent identification and recognition as potential threats to ecosystems and human well-being. As scientific knowledge and analytical techniques advance, researchers and consequently environmental regulators have become increasingly capable of detecting trace levels of substances that were previously overlooked or undetected. This heightened sensitivity has led to the identification of emerging contaminants in various environmental compartments, raising concerns about their long-term impacts on ecosystems and public health. The sources of emerging contaminants are diverse, spanning from industrial discharges and agricultural runoff to pharmaceuticals and personal care residues to microorganisms and cyanobacteria. Their introduction into the environment can occur through a variety of pathways, including direct discharges, atmospheric deposition, and the use of contaminated biosolids in agriculture or they can be naturally occurring. Once released, these contaminants can persist in the environment and may undergo complex transformation processes, further

complicating the assessment of their fate and transport. The potential risks associated with emerging contaminants extend beyond ecological concerns to encompass human health implications.[27] Studies have indicated that certain pharmaceuticals, endocrine-disrupting compounds, and even toxin-producing bacteria may enter drinking water supplies or proliferating in drinking water reservoirs, posing challenges to water treatment facilities and potentially exposing the public to low-level, chronic exposures.[28,29] The study of emerging contaminants represents a vital area of environmental research and management, as our understanding of these substances evolves alongside advances in scientific knowledge and technology. The interdisciplinary nature of this field underscores the importance of collaboration among scientists, regulators, and industry stakeholders to develop effective strategies for monitoring, mitigating, and preventing the adverse effects of emerging contaminants on both the environment and human health.

During my PhD, I focused my studies mainly on two different kinds of emerging contaminants, the anthropogenic ones, originated from human activities, and the emerging natural toxins of European concern, both described in the next paragraphs.

1.1.1 Anthropogenic contaminants

Anthropogenic contaminants represent a category of pollutants that originate from human activities, significantly impacting the environment and ecosystems. These contaminants are a testament to the extensive footprint of human civilization on the planet and underscore the need for a comprehensive understanding of the consequences of our industrial, agricultural, and societal practices. The term "anthropogenic" refers to human-induced activities, and anthropogenic contaminants encompass a broad spectrum of pollutants that find their way into air, water, soil, and various other environmental compartments and even food. Sources of anthropogenic contaminants are diverse and widespread and include industrial processes, agricultural practices, urbanization, and everyday human activities. Industrial discharges release a plethora of chemicals and toxins into the air and water, while agricultural runoff introduces pesticides, fertilizers and herbicides into soil and water systems. Urban areas contribute to anthropogenic contamination through the release of pollutants from transport, waste disposal and construction activities.[7,30,31] Anthropogenic contaminants represent a significant environmental challenge that necessitates a proactive and coordinated response. Recognizing the sources, understanding the types, and acknowledging the far-reaching consequences of these contaminants are essential for fostering a sustainable coexistence between human activities and the health of the planet. Among these, heavy metals are prominent examples of anthropogenic contaminants, representing a class of toxic elements that find their way into the environment primarily as a result of human activities. These metals, which include copper, nickel, lead, mercury, cadmium, chromium, and arsenic, have various industrial, agricultural, and urban sources, posing significant threats to ecosystems and human health.[32–35] Another significant examples of anthropogenic contaminants are represented by pesticides, originating from human activities designed to control pests in agriculture, forestry, public health,

and other settings.[29,36,37] In addition, also pharmaceuticals have emerged as a significant and complex class of anthropogenic pollutants, infiltrating aquatic ecosystems and challenging traditional notions of water quality. Pharmaceuticals, intended to enhance human health, are paradoxically posing a new environmental challenge. The presence of pharmaceutical compounds in wastewater is a result of the disposal of unused medications, incomplete metabolization within the human body, and inadequate removal during water treatment processes.[29,38,39] Consequently, it is necessary to implement early monitoring of anthropogenic contaminants through new technologies able to discriminate accurately among these different class of compounds with very different chemical features and impact on the environment and human health (Figure I.2). During my PhD, I focused on three different classes of anthropogenic compounds, heavy metals, pharmaceuticals and pesticides; specific applications are reported in Chapter 4.

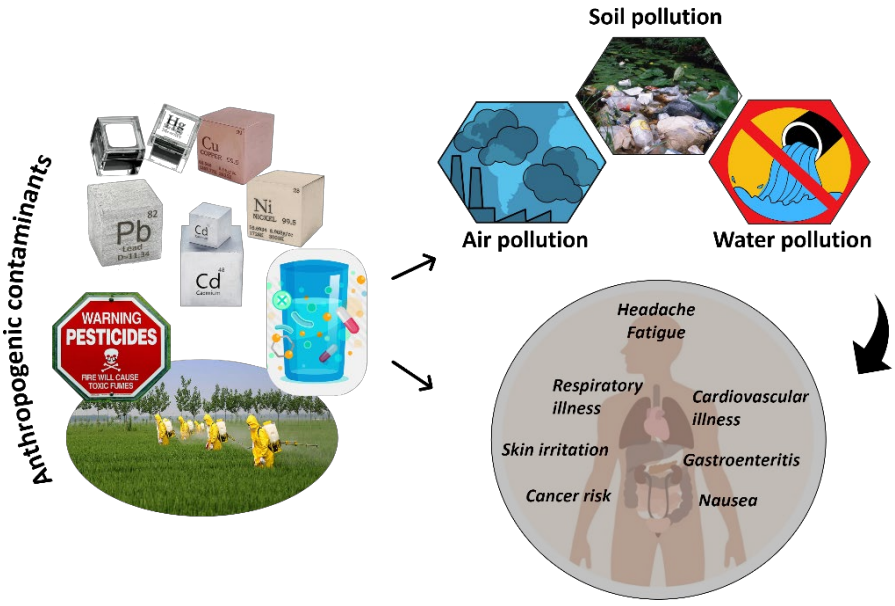

Figure I.2 Anthropogenic contaminants and their impact on the environment and human health.

1.1.1.1 Heavy metals

Heavy metals pose significant challenges as pollutants due to their toxic and nonbiodegradable characteristics, leading to bioaccumulation in ecological systems. The accurate determination of heavy metals is crucial for monitoring environmental quality, especially with the increasing pollution from industrial, agricultural, and domestic activities. These pollutants enter the environment, get absorbed by plants and animals, and subsequently accumulate, resulting in bioaccumulation. Through the food chain, these heavy metals can biomagnify within the human body through the consumption of contaminated plants, animals, or water. Some metals such as sodium (Na^+), potassium (K^+), calcium (Ca^{2+}), magnesium (Mg^{2+}), zinc (Zn^{2+}), iron (Fe^{2+}), copper (Cu^{2+}) and manganese (Mn^{2+}) are essential for life, while a large number of them are toxic as well.[34,35,40] For instance, copper (Cu) is as an essential metal playing a crucial role in various biochemical reactions as a cofactor of many metalloenzymes and in physiological regulations; nevertheless, significant changes in serum could reflect pathological disorders like neurodegenerative and oxidative stress-related diseases and diseases related to abnormal ceruloplasmin levels, e.g., Wilson's disease (WD) and Menkes' syndrome.[41,42] In addition to this, free copper ions are involved in the development of some chronic degenerative diseases whose pathophysiology is largely attributed to oxidative stress, e.g., Alzheimer's disease.[43] Nickel (Ni^{2+}) is one of the most common allergen responsible for contact dermatitis, because it is found everywhere in the environment. High exposure to nickel can cause serious health effects, such as contact dermatitis or eczema.[44,45] Mercury (Hg^+) accumulation in the body increases cardiovascular and neural diseases.[46–48] Lead (Pb^{2+}) and cadmium (Cd^{2+}) are highly toxic, and even small doses of these can lead to a number of human health problems. The principal sources of exposure are represented by ingestion of contaminated food or water, soil, dust, cigarette smoke (for cadmium) and occupational exposure. Studies suggest that cadmium

is associated with several clinical complications, mainly kidney dysfunction and bone disease, but also tumors, while people who have been exposed to lead for a long time may suffer from memory deterioration, prolonged reaction times, and reduced comprehension.[47,49–51] Acute exposure to lead causes proximal tubular renal damage. FAO/WHO (Food and Agriculture Organization of the United Nations/World Health Organization) established a provisional tolerable weekly intake (PTWI) for lead of 25 ppb body weight and of 7 ppb body weight per cadmium (420 g/week for a 60 kg person).[52,53] Considering that, these metal ions need to be readily and continuously monitored for evaluating toxic exposure for both individuals and the environment. Various standard analytical methods, including cold vapor atomic fluorescence, atomic absorption spectrometry (AAS), and inductively coupled plasma-mass spectrometry (ICP-MS), have been developed to quantify heavy metals in different matrices at ppb level.[54] While these techniques offer sensitivity and selectivity, they are limited by the need for skilled personnel, sophisticated instruments, and time-consuming procedures. In light of these experimental constraints, there is a growing need to develop user-friendly and portable methods for decentralized analyses. The emergence of portable analytical devices represents a significant trend in analytical chemistry, enabling the creation of miniaturized, sustainable, and cost-effective tools for on-site measurements.[55–57] A novel approach is represented by electrochemical sensing and biosensing, in compliance with the ASSURED (Affordable, Sensitive, Specific, User-friendly, Rapid and robust, Equipment-free and Deliverable to end-users) and REASSURED (Real-time connectivity, Ease of specimen collection, Affordable, Sensitive, Specific, User-friendly, Rapid and robust, Equipment-free or simple, and Deliverable to end-users) criteria, established by the World Health Organization (WHO).[58,59] Decentralized systems, have gained prominence for developing point-of-care tests (POCT) and have been successfully applied also for the electrochemical determination of

heavy metals.[56,60–63] In particular, paper-based screen-printed electrodes have been reported by many research groups, utilizing various substrates (e.g., chromatographic, office, and nanocellulose) for different fields of application, including heavy metals detection.[64,65] However, the choice of paper-based substrates is crucial for environmental considerations, as they pose lower risks compared to plastic substrates, the toxicity implications of which are not fully understood. Despite their advantages, paper-based substrates may exhibit non-specific adsorption and impurities, limiting their application in real-world settings. Pretreatments can be applied to mitigate these issues and reduce metal ion interactions. Given the diverse range of samples and concentration levels, there is no one-size-fits-all technique for heavy metals quantification. In this context, anodic stripping voltammetry is frequently featured in recent reviews due to its ability to achieve trace-level detection, a necessity for heavy metals with stringent limits, often in parts per billion (ppb).[66] For instance, WHO sets limits for Pb, Cd, Hg, As, and Cr in drinking water at 10, 5, 1, 10, and 50 ppb, respectively, corresponding to approximately 10^{-8} M concentration.[33] As a result, anodic stripping voltammetry plays a prominent role in addressing these challenging detection limits in heavy metal analysis. Even if paper-based substrates represent an established alternative to plastic-based ones for realizing portable electroanalytical tools, our idea is to highlight how the use of papers of different porosities is capable to enhance analysis of samples. In Chapter 4, is reported the development of an integrated device for nickel electrochemical detection in cosmetic products as example of efficient combination between chromatographic paper and electrochemical strip printed on polyester substrate.[61] A similar architecture, that exploits the advantages of the paper used as tool to enhance the sensitivity and facilitate the treatment of complex matrices towards heavy metals detection, is investigated for copper ions electrochemical detection in clinical samples and is summarized in Chapter 5.[60,63]

1.1.1.2 Pharmaceuticals

Pharmaceuticals, designed to improve human well-being, are paradoxically contributing to a new environmental challenge.[38] The disposal of unused medications, incomplete metabolization within the human body, and inefficient removal during water treatment processes, have led to the infiltration of pharmaceutical compounds into wastewater. The complexity of pharmaceutical compounds as emerging contaminants lies not only in their diverse chemical structures but also in their ability to persist in the environment. Conventional water treatment methods, designed with other contaminants in mind, may fall short in effectively removing pharmaceuticals, raising concerns about the long-term impact on the water quality of wastewater and its surrounding habitats.[67,68] For these reasons, since 2020, human pharmaceuticals were included in the list of emerging contaminants from the UNESCO and their detection and elimination were incorporated in the goal 6 (clean water and sanitation) of the 2030 Agenda for Sustainable Development Goal Targets.[69,70] It's important to note that the presence in the environment of pharmaceuticals is a complex issue, and efforts are being made to improve wastewater treatment processes to better remove pharmaceuticals, and public awareness campaigns emphasize proper disposal methods for unused medications to reduce their introduction into the environment (Figure I.3). Additionally, advancements in analytical techniques contribute to a more accurate detection and monitoring of pharmaceutical contaminants in water sources. The monitoring of pharmaceuticals as emerging contaminants typically involves analysing water samples for the presence and concentration of specific pharmaceutical compounds. Various analytical methods can be employed for this purpose, and the choice of method depends on factors such as the targeted pharmaceuticals, required sensitivity, and the type of sample being analysed. These include mainly high performance-liquid chromatography, liquid chromatography-mass spectroscopy, UV–Vis spectroscopy, flow and batch

injection analysis, as traditional analysis techniques.[71–74] Additionally, electrochemical methods provide a simple, rapid, selective detection with low-cost of systems and eco-friendly applications.[75,76] In Chapter 4, the development of a novel screen - printed electrochemical sensor for monitoring paracetamol in wastewater is discussed, highlighting the advantages of a total paper-based device, such as real-time monitoring, high sensitivity, and the potential for miniaturization, making them suitable for on-site applications.

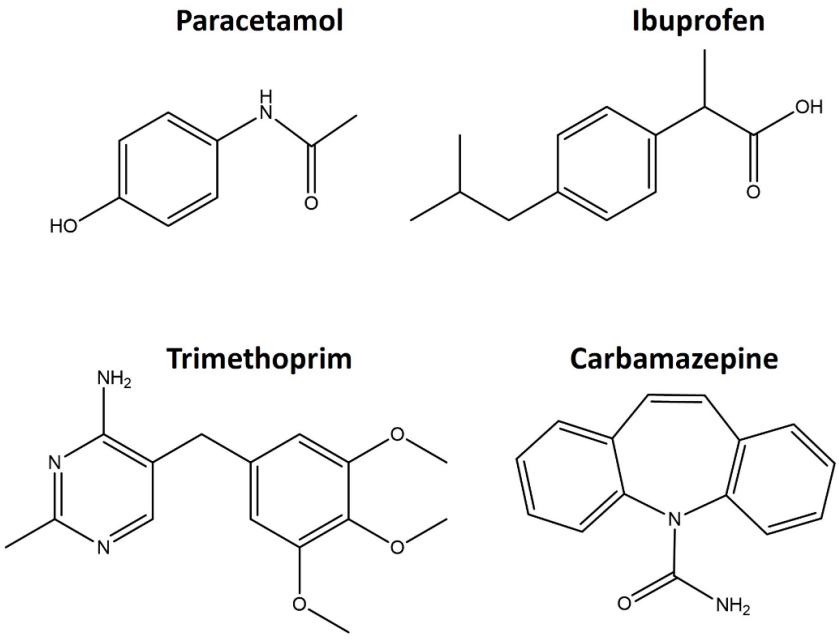

Figure I.3. Planar structures of the main exponents of the principal pharmaceutical classes found in wastewater.

1.1.1.3 Pesticides

As a key factor in increasing agricultural production, pesticides have been used worldwide on crops because of their ability to eliminate plant pests and consequently, reduce labor intensity. On the other hand, their misuse also results in excessive pesticide residues in agricultural products, affecting consumers' food safety and harming human health.[36,37] There are many types of pesticides,

classified considering their functional groups, in: carbamates, organochlorides, pyrethroids, organophosphates, and other substances (Figure I.4).[77] The total amount of pesticides applied to the environment amounts to millions of tons every year in the world causing serious pollution of the environment (in the soil, surface/water, atmosphere, etc.) and negative effects on the ecosystem. Regulation (EC) No 396/2005 sets the maximum quantities of pesticide residues permitted in products of animal or vegetable origin intended for human or animal consumption at 0.01 ppm.[78,79] Considering that, it is necessary to implement early monitoring of the health conditions of crops through new technologies in order to increase agricultural productivity and reduce food losses, so as to guarantee food security and a sustainable development. In addition, as demonstrated by the Covid-19 pandemic, the necessity of portable and wearable solutions for analyzing samples, from the medical to the environmental field, is growing day by day: an example is the development of "smart agriculture" or "precision agriculture", that has been attracting increasing attention due to its capability for using less to grow more, compared to traditional agricultural practices, improving the quality of the work environment. Smart agriculture comprises a set of technologies that combines sensors, information systems, enhanced machinery, and informed management to optimize production by accounting for variabilities and uncertainties within sustainable agricultural systems.[80–83] Among the several technologies, advanced sensing systems that monitor soil and plants health conditions and crop developments are of great importance because they collect and evaluate data, especially when crop growing conditions change in space and time, such as in case of plants diseases, weeds or pests; in this way, it is possible to make long-term spatial models that can be used to create an intelligent and sustainable agricultural system. In addition, a system where sensing devices are required to be in close contact with fruit, leaf or soil, lowers the risk of contamination, waste disposal, especially in remote areas.[81] In this scenario, the

use of sensors and biosensors capable of detecting the state of health of crops has proved to be a useful strategy for optimizing agricultural production. Nowadays, traditional techniques, such as gas chromatography (GC), gas chromatography-mass spectrometer (GC-MS) and liquid chromatography-tandem mass spectrometry (LC-MS/MS), are still the main methods used for environmental monitoring, including pesticides, but, as already said, they have some disadvantages, such as the complicated pre-treatment of the sample, high cost, time-consuming, and difficulty in realizing in-situ detection, that can't allow their application in precision agriculture.[84] Hence, economically viable and rapid analytical methods are required to assess the levels of the pesticides and other contaminants in real samples, and electroanalytical (bio)sensors represent an excellent alternative. Another step forward, is the development of wearable sensors, generally reported as electronic devices that can be incorporated into clothing or worn on the body for monitoring several health parameters; they can be applied to plants due to their capability to continually track important physiological and pathological parameters in situ, also adding the opportunity to integrate remote communication and control. Plant wearables possess a great potential as precision agriculture tools, thanks to their ability to allow a simple, precise, and continuous monitor of plant health at large scale.[81,85] In Chapter 4, the development of a scree-printed electrochemical biosensor for on-glove applications is discussed considering its use for pesticides detection directly on fruit peels. The pesticides detection is also evaluated in another application that exploits the use of porous PHBV-based bacterial polymers to realize novel bio-based electroanalytical (bio)sensors.[86]

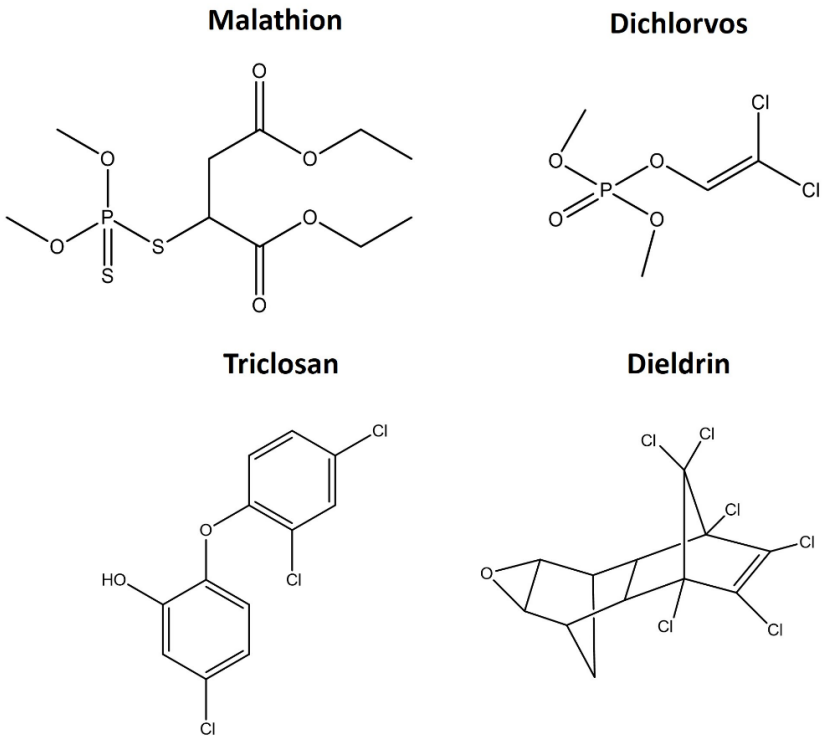

Figure I.4. Planar structures of the main pesticides used in agriculture.

1.1.2 Harmful algal species: emerging toxins

Harmful algal blooms (HABs)[87] or excessive algae growth are naturally occurring phenomena characterized by the massive and atypical proliferation of microalgae in either marine or freshwater environments which have significant impacts and adverse effects on aquatic ecosystems, human health, and economic activities. Specific atmospheric conditions in combination of different factors (water temperature, freshwater run-off, seasonal/temporal stratification, turbulence, salinity, excess or limitation of nutrients and other anthropic factors) are considered the main drivers in triggering algal proliferation. About 300 hundred species of microalgae are reported to form mass occurrence, and about one third of these species are known to produce toxic natural secondary metabolites called "*phycotoxins*" with a large variety of toxicities and modes of action that can be harmful or even lethal to humans and so posing significant challenges for water quality management and conservation efforts.[88,89] Being the main food of several herbivorous and predatory fish and filter-feeding bivalves, microalgae and the produced phycotoxins may be accumulated in edible tissues of finfish and shellfish ending up on the table of unaware consumers that get poisoned following ingestion of contaminated seafood. Besides the oral route, humans may be affected by phycotoxins even through inhalation of aerosolized toxins and direct skin contact with microalgae and/or contaminated seawaters. The main consequence is then represented by the displacement of the microalgal community with the spreading and establishment of invasive toxin-producing algal species and toxin-bearing fish species in the environment. This phenomenon leads to the appearance and distribution of the emerging toxins, once confined in tropical area, in the food-chain of temperate zones such as the Mediterranean area. [90,91] Phycotoxins can be divided in several groups, each of them including a parent compound and a certain number of structural analogues which are produced by algae or bio-transformed in seafood. Traditionally, marine

toxins have been classified in five main groups according to the poisoning syndromes recorded in humans following ingestion of contaminated seafood: paralytic shellfish poisoning (PSP), amnesic shellfish poisoning (ASP), neurotoxic shellfish poisoning (NSP), azaspiracid shellfish poisoning (AZP), and diarrhetic shellfish poisoning (DSP).[92,93] However, the classification based on the food-borne illness turned out to be inadequate for some groups of toxins and it does not consider other types of poisonings that are still not fully characterized. An alternative classification system, based on the chemical features of phycotoxins, was suggested by Quilliam et al. in 2001, and then adopted by the Joint FAO/IOC/WHO ad hoc Expert Consultation Group on Biotoxins in Bivalve Mollusks in 2005. For the first time in 2004, EC has established the maximum permitted level (MPL) for the main groups of marine toxins in bivalve molluscs, whilst one year later it settled the official methods for their detection.[90,94,95] As a consequence, national and local food safety authorities have instituted monitoring programs to survey the presence of phycotoxins in seafood. The establishment of regulatory limits associated with a strict surveillance of products turned out to be fundamental to decrease the impact of toxins on consumer safety, to manage the shellfish production by farm fisheries and for the trading of shellfish within and outside the EU borders. Currently, six groups of phycotoxins are regulated and regularly monitored in EU: azaspiracids, domoic acid, okadaic acids, pectenotoxins, saxitoxins and yessotoxins (EC/853/2004).[96] However, new HAB-related threats once confined to tropical areas are emerging together with a plethora of new structural analogues discovered in each toxin group, following analytical advancements. All these toxins are designated as "*Emerging Toxins*" by official organizations such as the European Commission (EC) and the European Food Safety Authority (EFSA), overall including non-regulated toxins in EU, known by scientists and a matter of concern for legislators but for which additional toxicological evidence are needed before further regulations can be

established. The establishment of regulatory criteria is pointed as one of the most critical issues in the field of the emerging toxins by EC and EFSA. This requires i) determination of the MPL of each toxin group in seafood, ii) development of reliable analytical methods for their determination, iii) assessment of toxin distribution throughout the food web, and iv) collection of appropriate toxicity data. Availability of adequate amounts of certified reference material (CRM) for each toxin is the cornerstone for both the validation of analytical methods and the achievement of toxicity data.[97] Currently, cyclic imines, tetrodotoxins, ciguatoxins, maitotoxins, palytoxins and cyanotoxins are listed among the emerging toxins of European concern.[98] During my PhD I focused on the development of LC-HRMS methods to analyse different classes of these emerging toxins, in particular the cyclic imines (CIs), the cyanotoxins and cyanometabolites and the palytoxin and ovatoxins (PLTX and OVTXs), in order to evaluate new monitoring and water treatments methods. A detailed description for each toxin class is reported below.

1.1.2.1 Cyclic imines

Cyclic imines (CIs) encompass a range of structurally related lipophilic compounds produced by various harmful bloom-forming marine dinoflagellates belonging to genera *Karenia*, *Alexandrium* and *Vulcanodinium*. All CIs share a characteristic structural feature being a cyclic imine unit in their structure and are classified into sub-groups: pinnatoxins (PnTXs), spirolides (SPXs), gymnodimines (GYMs), pteriatoxins (PtTXs), prorocentrolides, spiroprorocentrimines, portimines, and symbioimines (Figure I.5).[99,100] These compounds contain spiro-linked cyclic imines, macrocycles, and ether rings. They are also known as fast-acting toxins, due to the rapid onset of neurological symptoms induced in mice after intraperitoneal injection. Mode of action and molecular targets of CIs is binding and blocking muscular and neuronal nicotinic acetylcholine receptors (Ach and nAChRs), leading to asphyxia through diaphragm paralysis. The cyclic imine moiety serves as the pharmacophore responsible for their bioactivity, and the opening of this ring results in the molecule's inactivation.[101–103] Despite their global presence in tropical and temperate regions, found in extracts from natural plankton, cultured dinoflagellate microalgae, and contaminated seafood, human intoxications from CIs-contaminated seafood are rare, with the exception of PnTXs.[102] CIs are considered emerging toxicants due to their neurotoxicity, posing potential risks to consumer well-being and seafood industries. The increasing number of newly identified shellfish biotransformation products, coupled with the impact on neuromuscular transmission and their ability to cross the intestinal and blood-brain barrier, raises concerns for patients with neuromuscular disorders. Currently, the presence of CIs in seafood products is not regulated either in Europe or in other regions worldwide. In the 2010s, the EFSA Panel on Contaminants in the Food Chain expressed concerns about CIs in shellfish, stating that no provisional guideline values could be suggested due to limited

toxicological data, primarily focused on the acute toxicity of SPXs, GYMs, and PnTXs, with no information on chronic toxicity. CIs, being polar liposoluble compounds, are extracted alongside various categories of regulated lipophilic marine biotoxins (LMBs). These include toxins associated with diarrheic shellfish poisoning (DSPs, such as okadaic acid, dinophysistoxins, and pectenotoxins), neurotoxic shellfish poisoning (NSPs, like brevetoxins), and Azaspiracid Shellfish Poisoning (AZP, involving azaspiracids). Until a few years ago, the EU reference method for monitoring the presence of LMBs in seafood was the mouse bioassay (MBA). However, due to concerns about its questionable specificity, low sensitivity, and inability to explore the toxic profile of contaminated shellfish, coupled with ethical concerns related to animal distress, the MBA has been replaced by MS-based approaches.[104] In this context, the physical-chemical properties of cyclic imines, coupled with the necessity to monitor a broad array of structural congeners in a single test run, led to the adoption of reverse-phase (RP) liquid chromatography as a suitable approach for resolving complex toxin mixtures. However, the absence of chromophores in the molecules hindered the development of highly specific and sensitive RP-LC methods based on optical detection, with HPLC-UV being the sole method employed. This limitation was overcome by coupling liquid chromatography (LC) to mass spectrometry (MS), leveraging the imine function's compatibility with electrospray ionization (ESI). The use of acidic or alkaline conditions, along with optional solid phase extraction (SPE), significantly reduces matrix interference.[104] Despite the expensive instrumentation and the prerequisite of expert personnel and analytical standards, LC-MS has been designated as the method of choice for determining CIs in complex matrices. In this perspective, the continuous discovery of new CIs and their metabolites in shellfish, along with the detection of known congeners lacking appropriate standards, underscores the untargeted LC-HRMS approach as the most valid methodology for revealing new

and intriguing findings.[105] In Chapter 3, we described the application of high effective and sensitive LC-HRMS method for the identification of marine toxins in mucilage from the 2021 north-eastern Aegean Sea episode, resulting in the identification of CIs as main components of the samples.

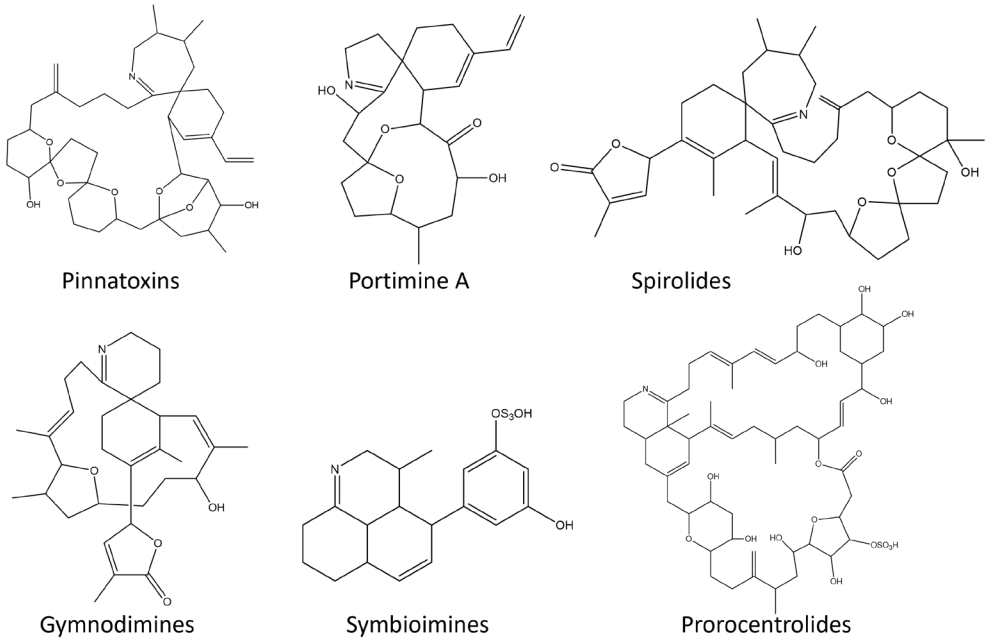

Figure I.5. Planar structures of the principal subgroups of CIs: pinnatoxins (PnTXs), portimines, spirolides (SPXs), gymnodimines (GYMs), symbioimines and prorocentrolides.

1.1.2.2 Cyanotoxins and cyanometabolites

Cyanobacteria represent major constituents of phytoplankton in aquatic ecosystems, contributing to 20-30% of the global primary production. Under certain environmental conditions (e.g., high nutrient levels, water temperature, and light intensity), cyanobacteria can massively proliferate giving rise to harmful cyanobacterial blooms.[106,107] Several studies highlight a close correlation between climate changes and the increasing magnitude, frequency, and duration of cyanobacterial blooms. They have adapted to live in a variety of environment occupying different ecological niches; as a consequence, a high biodiversity has been observed through the description of aquatic (oceans, seas, hot spring water, fresh and brackish water), terrestrial (soils, deserts, glaciers) and symbiotic (plant, lichens and primitive animals) species.[108] It follows that cyanobacteria are characterized by extremely heterogeneous metabolic profiles, with a plethora of more than 2000 bioactive secondary cyanometabolites that have been described so far. Additionally, many cyanobacteria genera such as *Microcystis* and *Planktothrix* produce toxic metabolites (i.e., cyanotoxins) characterized by different chemical structures and mechanisms of action. The main criteria adopted to properly classify cyanotoxins takes into account their mechanism of toxicity on mammals: i) microcystin and nodularin are hepatotoxins, ii) anatoxins, paralytic shellfish toxins, and BMAA belong to the neurotoxins, iii) cylindrospermopsins are cytotoxins, iv) lyngbyatoxins are dermatotoxins and v) lipopolysaccharides are irritant toxins (Figure I.6).[109,110]

Microcystins (MCs) are one of the most studied cyanotoxins, which exert acute hepatotoxic effects by targeting liver cells and inducing the inhibition of protein phosphatases as well as non-lethal chronic doses of MCs elicit tumor-promoting effects. MCs are cyclic heptapeptides characterized by the presence of L-, D- and unconventional amino acids, with a high structural heterogeneity due to multiple substitutions and modifications that can involve all the amino acid residues.

Although a substantial chemodiversity has been observed, an accurate evaluation conducted on the most substituted and conserved amino acids allowed to outline the following general structure: cyclo-(D-Ala[1]-X[2]-D-Masp[3]-Z[4]-Adda[5]-D-ϒ-Glu[6]-Mdha[7]), were Mdha is N-methyl-dehydroalanine. L-amino acids X and Z at position 2 and 4, respectively, are the most variable. Among the more than 300 known MCs variants, MC-LR containing leucine and arginine in positions 2 and 4, respectively, is considered the most common and toxic one (LD_{50} i.p. injection = 50 and 160-300 μg kg^{-1} for MC-LR and other MCs variants, respectively.[111]

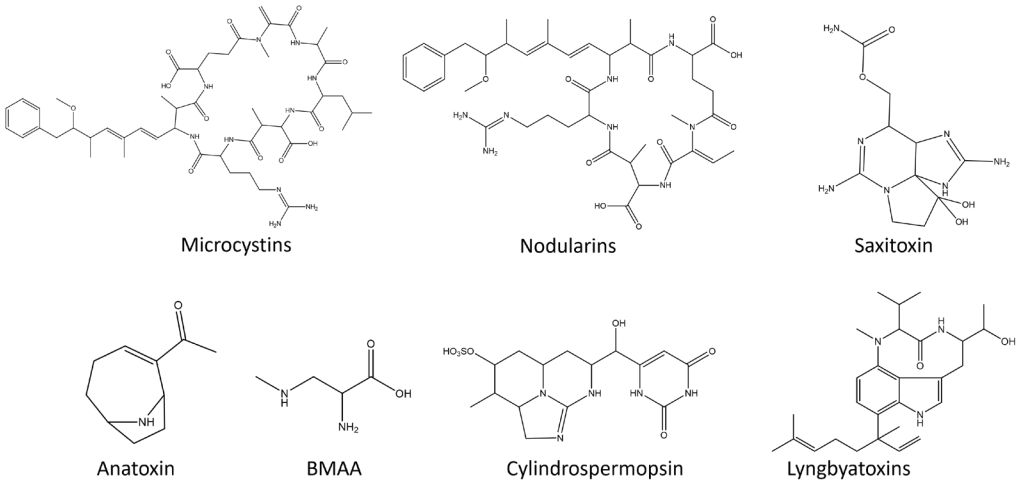

Figure I.6. Planar structures of the principal exponents of Cyanotoxins: MC-LR, NOD-R, STX, ATX-a, BMAA, CYN and LA.

Nonetheless, different and less-studied bioactive metabolites are produced by cyanobacteria, such as microginins (MGs), anabaenopeptins (APs) and cyanopeptolin-type peptides (CPtps) (Figure I.7).[109,112]

Microginins (MGs) represent an interesting category of cyanobacterial secondary metabolites, with approximately 100 congeners documented to date. They are also known as oscillaginins, cyanostatins, and nostoginins, depending on the producing organism. MGs consist of linear peptides comprising three to six amino acids, some of which may be N-methylated residues or homo variants. A

consistent structural motif is observed, featuring one or more Tyr or its homo or methylated derivative at the C-terminus, while the N-terminus is characterized by the unconventional 3-amino-2-hydroxy-decanoic acid (Ahda).

Anabaenopetins (APs) constitute a group of around 100 compounds produced by freshwater, marine, and terrestrial cyanobacteria, or even originating from symbiosis with marine sponges. Depending on the specific producing organism or the geographical location of discovery, APs have been identified by various names such as oscillamides, nodulapeptins, ferintoic acids, lyngbyaureidamides, pompanopeptin, kermamides, konbamide, mozamide, brunsvicamides, and schizopeptin. From chemical point of view, APs are cyclic hexapeptides featuring a cyclic moiety composed of five amino acids. A common structural motif, with a few exceptions, is recognized across all congeners, including a D-Lys residue at position 2, an ureido linkage between residues at positions 1 and 2, homo amino acids at position 4, and N-methyl amino acids at position 5. Variability in all other positions results in a vast structural diversity, leading to numerous analogues with masses ranging between 750 and 950 Da. The general APs structure can be reported as follows: X^1-CO-[Lys^2-X^3-X^4-MeX^5-X^6].

Cyanopeptoline-type peptides (CPtps) comprise more than 230 cyclic depsipeptides containing a β-lactone ring and featuring a characteristic 3-amino-6-hydroxy-2-piperidone (Ahp) moiety. The naming system is related to the producing cyanobacteria, so they are classified into different sub-groups: CPs, micropeptins, aeruginopeptins, microcystilide, nostopeptins, nostocyclins, oscillapeptins and somamides. Despite cyanopeptides may occur in freshwater at concentrations similar to those reported for the well-studied MCs, they have been poorly investigated from both chemical and toxicological standpoints. [18,112–114]

Currently, cyanotoxins are not regularly monitored in many countries, despite the increasing global demand for statutory regulation. Cyanotoxins have been found globally in diverse environmental and food samples, including fresh and brackish

waters, fish, shellfish, and algal dietary supplements. The primary source of exposure is likely the consumption of contaminated drinking water, often derived from surface water sources. Nevertheless, inadvertent ingestion of water during recreational activities, particularly in lakes and rivers, can contribute to oral exposure, along with the consumption of contaminated foods.[115,116] In this scenario, toxicological data are often limited to a few analogues for each sub-group, and combined toxicity resulting from the co-occurrence of different cyanotoxins should be considered for accurate risk assessment. Furthermore, the development of validated analytical methods for precise toxin determination in various matrices, along with effective extraction and clean-up methods yielding high recovery, is essential. On the basis of the available data, the World Health Organizations (WHO) has recently released provisional guidelines for MC-LR, CYN, ATX-a and STXs for chronic and short-term exposure to drinking water, and for exposure to recreational water.[117] High diversity is observed among the US, where specific guideline levels have been suggested also for domestic animals (cats and dogs); moreover, recently US National Centre for Environmental Assessment suggested a stricter maximum permitted level for MC-LR in drinking water of 0.1 μg/L.[117,118] Although regulations exist for cyanotoxins in water, none have been set for food. Health agencies require more data on cyanotoxin distribution in food, along with comprehensive toxicity studies and improved extraction procedures before recommending regulations. Effective analytical detection methods are also needed. In routine analyses, liquid chromatography coupled to mass spectrometry (LC-MS) is employed in targeted screening of selected cyanotoxins, whose reference standards are available, while no information can be easily obtained for other unknown cyanometabolites. More recently, approaches based on the untargeted analysis using LC-HRMS, together with an ever-growing comprehensive database of cyanobacterial metabolites, have been successfully used for toxic profile determination of bloom material

and cultured strains. Considering this, in chapter 3 an untargeted LC-HRMS approach applied to microcystin-producing cyanobacterial cultures for the evaluation of the efficiency of chlorine-based treatments commonly used for water potabilization, is discussed.[112,114,119]

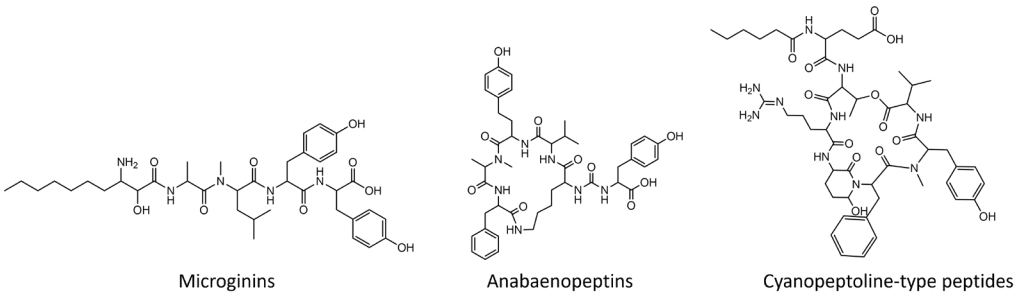

Figure I.7. Planar structures of some cyanobacterial bioactive metabolites: Microginins (microginin FR1), Anabaenopeptins (anabaenopeptin A), Cyanopeptolin-type peptides (cyanopeptoline 1020).

1.1.2.3 Palytoxin and its congeners

Palytoxin (PLTX) (Figure I.8) stands as one of the most potent non-protein and non-polymeric natural marine toxins identified thus far. It was initially discovered in 1971 in the Hawaiian *Palythoa toxica*, a tropical soft coral species belonging to the *Zoanthidae* family. Following this breakthrough, PLTX has been found in various *Palythoa* species, including *P. tuberculosa, P. vestitus, P. caribaeorum, P. mammilosa, and Palythoa aff. margaritae*, as well as in *Zoanthus* species such as *Z. solanderi* and *Z. sociatus*.[120]

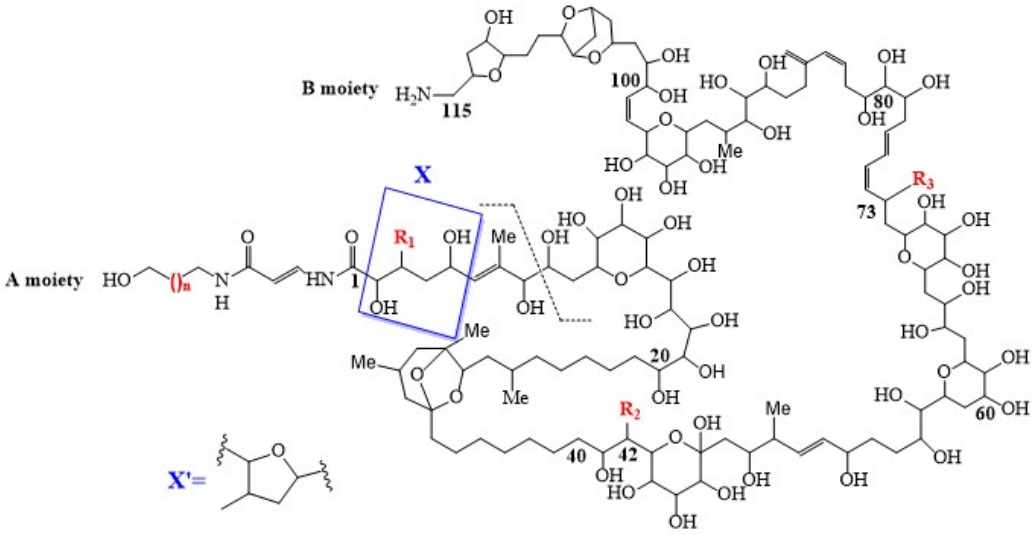

Toxin	n	R_1	R_2	R_3		Molecular formula
Palytoxin	1	Me	H	OH	X	$C_{129}H_{223}O_{54}N_3$
Homopalytoxin	2	Me	H	OH	X	$C_{130}H_{225}O_{54}N_3$
Bishomopalytoxin	3	Me	H	OH	X	$C_{131}H_{227}O_{54}N_3$
Neopalytoxin	1		H	OH	X'	$C_{129}H_{221}O_{54}N_3$
Deoxypalytoxin	1	Me	H	H	X	$C_{129}H_{223}O_{53}N_3$
42-hydroxypalytoxins (50*R*), (50*S*)	1	Me	OH	OH	X	$C_{129}H_{223}O_{55}N_3$

Figure I.8. Planar structure of PLTX and its analogues produced by *Zoanthis* species.

PLTX, a complex amphiphilic compound with high molecular weight, consists of a long, partially unsaturated aliphatic backbone containing 64 chiral centers, 8 stereogenic double bonds, 7 interspersed ether rings, 42 hydroxyl groups, two amide functions, and one primary amino group ($C_{129}H_{223}O_{54}N_3$) (Figure I.8).[121,122] Conventionally, the toxin's long alkyl chain is divided into two moieties, labelled as A side (C1-C8) and B side (C9-C129), as MS^2 experiments revealed a characteristic and intense fragment ion resulting from cleavage between C8 and C9 (*m*/*z* 327) (Figure I.8). Six PLTX analogues have been identified in extracts from *Palythoa* spp.: homoPLTX, bishomoPLTX, neoPLTX, 73-deoxyPLTX, and two diastereoisomers of 42-hydroxyPLTX (50R and 50S) (Figure I.8).[123] Conversely, the diversity of PLTX analogues significantly expand when considering toxic secondary metabolites produced by dinoflagellates of the *Ostreopsis* genus. Originally confined to tropical and sub-tropical areas, the benthic and epiphytic microalgae from the genus *Ostreopsis*, have spread and started proliferating in temperate regions, especially in the Mediterranean basin, posing health concerns due to the capability to produce e PLTX-like molecules.[124,125] Various *Ostreopsis* species, including *O. siamensis, O. ovata, O. lenticularis, O. heptagona, O. mascarenensis, O. labens, O. marina, O. belizeana, O. caribbeana,* and *O. fattorussoi*, have been identified.[125] Not all of these species have been found to be toxic, and for the toxic ones, even toxin profiles can vary among different strains in response to environmental factors or geographical distribution. The toxic secondary metabolites produced by *Ostreopsis* dinoflagellates fall into three sub-groups based on their producing organisms: ostreocins (OSTs), mascarenotoxins (McTXs), and ovatoxins (OVTXs) (Figure I.9).[127,128]

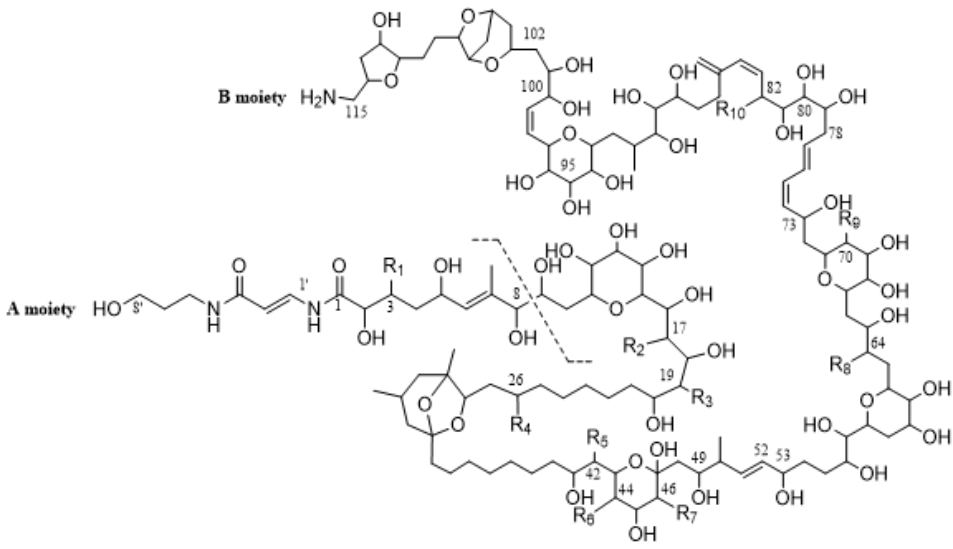

Figure I.9. Planar structure of PLTX and its analogues produced by *Ostreopsis* species.

Ovatoxins (OVTXs) is the most extensive group of PLTX congeners, consisting of 17 reported analogues (OVTX-a, b, c, d, e, f, g, h, i, j1, j2, k, isobaric PLTX, OVTa-IK2, OVTd-IK2, and OVTe-IK2). The identification of isobaric PLTX, (firstly referred to as "putative PLTX) is dated back 2005, when "*Ostreopsis* phenomenon" hit the headlines for the first time due to a severe human outbreak with a hundred people intoxicated after exposure to marine aerosols during recreational and work-related activities along the Ligurian coastline of Italy,[123] In coincidence to the toxic episode a significant proliferation of *Ostreopsis* cf. *ovata* was registered in the seawater and since 2005 recurring blooms of *O*. cf. *ovata* have been reported every year all around Italian coasts. Notably, among these PLTX analogues, OVTX-a stands out as the only one fully structurally characterized using High-Resolution Mass Spectrometry ($HRMS^2$) and Nuclear Magnetic Resonance (NMR) techniques. Structural insights or preliminary structural hints for the other congeners have been obtained through Liquid Chromatography-High-Resolution Mass Spectrometry ($LC\text{-}HRMS^2$), proving to

be a powerful tool for this purpose.[123,129,130] Currently, the lack of reference materials and well-purified fractions for most PLTX analogues hinders: i) conducting toxicological studies, ii) developing and validating effective analytical methods for detection, iii) standardizing procedures for preparative works, and iv) studying their mechanisms of action.

PLTX primarily targets the Na^+/K^+ ATPase transmembrane pump, vital for maintaining cellular membrane potential and homeostasis. By binding to the pump's extracellular moiety, PLTX inhibits the active transport of Na^+ and K^+ across the membrane, transforming the pump into a non-specific cation channel that stays open continuously. This leads to a persistent ionic imbalance within cells, causing: i) an increase in cytosolic Ca^{2+}, leading to cell death, and ii) the release of K^+ from various cell types. The latter triggers tissue depolarization, resulting in secondary pharmacological effects such as intense contractions in skeletal, smooth, and cardiac muscles, cardiovascular effects, hemolysis, prostaglandin and norepinephrine release, platelet aggregation, and inhibition of sperm motility.[131,132] PLTX exhibits toxicity in humans through multiple exposure routes. The oral route, primarily linked to consuming contaminated seafood, manifests as bitter/metallic taste, vomiting, diarrhea, muscle cramps, abdominal pain, numbness in extremities, bradycardia, difficulty breathing, and, in tropical regions, clupeotoxism. This specific syndrome results from ingesting contaminated clupeoid fish like sardines, herrings, and anchovies. Other exposure routes include dermal contact and inhalation of toxic marine aerosols, causing symptoms such as erythema, dermatitis, fever, watery rhinorrhea, pharyngeal pain, cough, headache, bronchoconstriction with dyspnea, and conjunctivitis. Additionally, studies using a mouse skin carcinogenesis model have identified PLTX as a potent tumor promoter.[133] The examination of acute toxicity through various administration routes and animal models has revealed notable differences. A recent study by Poli et al. 2018, investigated the toxic

potential of PLTX and OVTX-a through intraperitoneal (IP) and aerosol administration in rats. Higher toxicity was observed through the aerosol administration, with OVTX-a showing the highest toxicity (LD_{50} 0.031 μg/Kg) and the measured acute inhalation toxicity was 15- to 195-fold higher than that obtained by IP injection.[134] These data strongly suggested that the presence of PLTX and its analogues should be closely monitored not only in seafood, but also in the aquatic systems as the human exposure to toxic marine aerosols during recreational and/or working activities may also be more dangerous than the oral one.

Regulatory limits for PLTX and its analogues in seafood are yet to be established globally, including in the European Union (EU). Achieving regulatory standards poses challenges due to i) a focus on acute toxicity in available toxicological data, with limited chronic studies, ii) the need for effective detection methods for PLTXs in seafood, and iii) the production of certified reference material (CRM) for precise quantitation and method validation across laboratories. However, in 2009, the European Food Safety Authority (EFSA) Panel on contaminants in the food chain (CONTAM) provided provisional guidance for PLTXs in seafood. With an Acute Reference Dose (ARfD) of 0.2 μg/Kg body weight for the sum of PLTX and OSTD, an adult weighing 60 Kg should not consume more than 12 μg in a 400 g portion of edible shellfish. This corresponds to a Maximum Permitted Level (MPL) of 30 μg equivalent PLTXs/Kg.[135] The Italian Ministry of Health solicited the introduction of surveys actions to manage risks associated to *O.* cf. *ovata* blooms, defining a three-phase monitoring plan: routine, alert and emergency phases, identified by thresholds of *Ostreopsis* cf. *ovata* cells in the water. When more than 10.000 cell/L or per g of macroalgae are found we enter in the Alert stage in which an assessment of the extension of the affected area and health surveillance are required, while in the emergency phase more than 100.000 cell/L are detected or the presence of ovatoxins is detected in seafood

represents the favouring conditions for aerosol and spray formation and chemical analysis of toxins in water is requested.[136] In Chapter 3, the development of a Solid-Phase Toxin Adsorption (SPATT) method based on cross-linked cyclodextrins for monitoring palytoxin and its congeners, is discussed.

References

(1) Malhi, Y.; Franklin, J.; Seddon, N.; Solan, M.; Turner, M. G.; Field, C. B.; Knowlton, N. Climate Change and Ecosystems: Threats, Opportunities and Solutions. *Philosophical Transactions of the Royal Society B: Biological Sciences* **2020**, *375* (1794), 20190104. https://doi.org/10.1098/rstb.2019.0104.

(2) US EPA, O. *Climate Change Impacts on Ecosystems*. https://www.epa.gov/climateimpacts/climate-change-impacts-ecosystems (accessed 2024-01-13).

(3) Hao, Y.; Liu, S.; Lu, Z.-N.; Huang, J.; Zhao, M. The Impact of Environmental Pollution on Public Health Expenditure: Dynamic Panel Analysis Based on Chinese Provincial Data. *Environ Sci Pollut Res* **2018**, *25* (19), 18853–18865. https://doi.org/10.1007/s11356-018-2095-y.

(4) Manisalidis, I.; Stavropoulou, E.; Stavropoulos, A.; Bezirtzoglou, E. Environmental and Health Impacts of Air Pollution: A Review. *Frontiers in Public Health* **2020**, *8*.

(5) *Health impacts*. https://www.who.int/teams/environment-climate-change-and-health/air-quality-energy-and-health/health-impacts (accessed 2024-01-13).

(6) Shetty, S. S.; D, D.; S, H.; Sonkusare, S.; Naik, P. B.; Kumari N, S.; Madhyastha, H. Environmental Pollutants and Their Effects on Human Health. *Heliyon* **2023**, *9* (9), e19496. https://doi.org/10.1016/j.heliyon.2023.e19496.

(7) Münzel, T.; Hahad, O.; Daiber, A.; Landrigan, P. J. Soil and Water Pollution and Human Health: What Should Cardiologists Worry About? *Cardiovascular Research* **2023**, *119* (2), 440–449. https://doi.org/10.1093/cvr/cvac082.

(8) *Link between climate change and pollution: health implications — European Climate and Health Observatory*. https://climate-

adapt.eea.europa.eu/en/observatory/evidence/health-effects/pollution (accessed 2024-01-13).

(9) Hernando, M. D.; Rodríguez, A.; Vaquero, J. J.; Fernández-Alba, A. R.; García, E. Environmental Risk Assessment of Emerging Pollutants in Water: Approaches Under Horizontal and Vertical EU Legislation. *Critical Reviews in Environmental Science and Technology* **2011**, *41* (7), 699–731. https://doi.org/10.1080/10643380903140224.

(10) Food and Agriculture: Key to Achieving the 2030 Agenda for Sustainable Development. *FOOD AND AGRICULTURE*.

(11) Puri, M.; Gandhi, K.; Kumar, M. S. Emerging Environmental Contaminants: A Global Perspective on Policies and Regulations. *Journal of Environmental Management* **2023**, *332*, 117344. https://doi.org/10.1016/j.jenvman.2023.117344.

(12) Cf, O. Transforming Our World: The 2030 Agenda for Sustainable Development. *United Nations: New York, NY, USA* **2015**.

(13) Dirtu, A. C.; Van den Eede, N.; Malarvannan, G.; Ionas, A. C.; Covaci, A. Analytical Methods for Selected Emerging Contaminants in Human Matrices—a Review. *Anal Bioanal Chem* **2012**, *404* (9), 2555–2581. https://doi.org/10.1007/s00216-012-6053-0.

(14) Petrie, B.; Barden, R.; Kasprzyk-Hordern, B. A Review on Emerging Contaminants in Wastewaters and the Environment: Current Knowledge, Understudied Areas and Recommendations for Future Monitoring. *Water Research* **2015**, *72*, 3–27. https://doi.org/10.1016/j.watres.2014.08.053.

(15) Nutrition Division. *Marine Biotoxins*; FAO Food and Nutrition Paper; FAO: Rome, Italy, 2004.

(16) Bouaïcha, N.; Corbel, S. Cyanobacterial Toxins Emerging Contaminants in Soils: A Review of Sources, Fate and Impacts on Ecosystems, Plants and Animal and Human Health; 2016.

(17) Mutoti, M. I.; Edokpayi, J. N.; Mutileni, N.; Durowoju, O. S.; Munyai, F. L. Cyanotoxins in Groundwater; Occurrence, Potential Sources, Health Impacts and

Knowledge Gap for Public Health. *Toxicon* **2023**, *226*, 107077. https://doi.org/10.1016/j.toxicon.2023.107077.

(18) Institute of Medicine (US) Roundtable on Environmental Health Sciences, R.; Goldman, L.; Coussens, C. M. Overview of Environmental Health Monitoring and the Use of Indicators. In *Environmental Health Indicators: Bridging the Chasm of Public Health and the Environment: Workshop Summary*; National Academies Press (US), 2004.

(19) De Girolamo, A.; Lippolis, V.; Pascale, M. Overview of Recent Liquid Chromatography Mass Spectrometry-Based Methods for Natural Toxins Detection in Food Products. *Toxins* **2022**, *14* (5), 328. https://doi.org/10.3390/toxins14050328.

(20) Picardo, M.; Sanchís, J.; Núñez, O.; Farré, M. Suspect Screening of Natural Toxins in Surface and Drinking Water by High Performance Liquid Chromatography and High-Resolution Mass Spectrometry. *Chemosphere* **2020**, *261*, 127888. https://doi.org/10.1016/j.chemosphere.2020.127888.

(21) Khanmohammadi, A.; Jalili Ghazizadeh, A.; Hashemi, P.; Afkhami, A.; Arduini, F.; Bagheri, H. An Overview to Electrochemical Biosensors and Sensors for the Detection of Environmental Contaminants. *J IRAN CHEM SOC* **2020**, *17* (10), 2429–2447. https://doi.org/10.1007/s13738-020-01940-z.

(22) Cinti, S. Novel Paper-Based Electroanalytical Tools for Food Surveillance. *Anal Bioanal Chem* **2019**, *411* (19), 4303–4311. https://doi.org/10.1007/s00216-019-01640-5.

(23) Rosenfeld, P. E.; Feng, L. G. H. 16 - Emerging Contaminants. In *Risks of Hazardous Wastes*; Rosenfeld, P. E., Feng, L. G. H., Eds.; William Andrew Publishing: Boston, 2011; pp 215–222. https://doi.org/10.1016/B978-1-4377-7842-7.00016-7.

(24) Sarma, H. Chapter 1 - Understanding Emerging Contaminants in Soil and Water: Current Perspectives on Integrated Remediation Approaches. In *Emerging Contaminants in the Environment*; Sarma, H., Dominguez, D. C., Lee, W.-Y., Eds.; Elsevier, 2022; pp 1–38. https://doi.org/10.1016/B978-0-323-85160-2.00002-0.

(25) Ali, J.; Ali, M.; Khan, I.; Khan, A.; Rafique, Z.; Waseem, H. Chapter 7 - Advances in Biodegradation and Bioremediation of Emerging Contaminants in the Environment. In *Biological Approaches to Controlling Pollutants*; Kumar, S., Hashmi, M. Z., Eds.; Advances in Pollution Research; Woodhead Publishing, 2022; pp 121–138. https://doi.org/10.1016/B978-0-12-824316-9.00013-6.

(26) Gwenzi, W.; Kanda, A.; Muhoyi, E.; Mukura, T. J. Chapter 2 - Emerging Contaminants in the Terrestrial-Aquatic-Atmosphere Continuum: A Global Perspective. In *Emerging Contaminants in the Terrestrial-Aquatic-Atmosphere Continuum:* Gwenzi, W., Ed.; Elsevier, 2022; pp 17–25. https://doi.org/10.1016/B978-0-323-90051-5.00004-3.

(27) Stefanakis, A. I.; Becker, J. A.; Stefanakis, A. I.; Becker, J. A. *A Review of Emerging Contaminants in Water: Classification, Sources, and Potential Risks*. https://services.igi-global.com/resolvedoi/resolve.aspx?doi=10.4018/978-1-4666-9559-7.ch003. https://www.igi-global.com/gateway/chapter/www.igi-global.com/gateway/chapter/140170 (accessed 2024-01-13).

(28) Wee, S. Y.; Aris, A. Z. Occurrence and Public-Perceived Risk of Endocrine Disrupting Compounds in Drinking Water. *npj Clean Water* **2019**, *2* (1), 1–14. https://doi.org/10.1038/s41545-018-0029-3.

(29) Wee, S. Y.; Ismail, N. A. H.; Haron, D. E. M.; Yusoff, F. Md.; Praveena, S. M.; Aris, A. Z. Pharmaceuticals, Hormones, Plasticizers, and Pesticides in Drinking Water. *Journal of Hazardous Materials* **2022**, *424*, 127327. https://doi.org/10.1016/j.jhazmat.2021.127327.

(30) López-Pacheco, I. Y.; Silva-Núñez, A.; Salinas-Salazar, C.; Arévalo-Gallegos, A.; Lizarazo-Holguin, L. A.; Barceló, D.; Iqbal, H. M. N.; Parra-Saldívar, R. Anthropogenic Contaminants of High Concern: Existence in Water Resources and Their Adverse Effects. *Science of The Total Environment* **2019**, *690*, 1068–1088. https://doi.org/10.1016/j.scitotenv.2019.07.052.

(31) Rhind, S. M. Anthropogenic Pollutants: A Threat to Ecosystem Sustainability? *Philosophical Transactions of the Royal Society B: Biological Sciences* **2009**, *364* (1534), 3391–3401. https://doi.org/10.1098/rstb.2009.0122.

(32) Järup, L. Hazards of Heavy Metal Contamination. *British Medical Bulletin* **2003**, *68* (1), 167–182. https://doi.org/10.1093/bmb/ldg032.

(33) Abarca, R. R. M.; Gaudio, M. T.; Chakraborty, S.; Bhattacherjee, P. Chapter 6 - Metals Toxic Pollutants in the Environment: Anthropogenic and Geological Causes and Remediation. In *Current Trends and Future Developments on (Bio-) Membranes*; Figoli, A., Li, Y., Basile, A., Eds.; Elsevier, 2020; pp 109–124. https://doi.org/10.1016/B978-0-12-816778-6.00006-0.

(34) Vareda, J. P.; Valente, A. J. M.; Durães, L. Assessment of Heavy Metal Pollution from Anthropogenic Activities and Remediation Strategies: A Review. *Journal of Environmental Management* **2019**, *246*, 101–118. https://doi.org/10.1016/j.jenvman.2019.05.126.

(35) Tchounwou, P. B.; Yedjou, C. G.; Patlolla, A. K.; Sutton, D. J. Heavy Metal Toxicity and the Environment. In *Molecular, Clinical and Environmental Toxicology: Volume 3: Environmental Toxicology*; Luch, A., Ed.; Experientia Supplementum; Springer: Basel, 2012; pp 133–164. https://doi.org/10.1007/978-3-7643-8340-4_6.

(36) Intisar, A.; Ramzan, A.; Sawaira, T.; Kareem, A. T.; Hussain, N.; Din, M. I.; Bilal, M.; Iqbal, H. M. N. Occurrence, Toxic Effects, and Mitigation of Pesticides as Emerging Environmental Pollutants Using Robust Nanomaterials – A Review. *Chemosphere* **2022**, *293*, 133538. https://doi.org/10.1016/j.chemosphere.2022.133538.

(37) Karwal, P.; Mittal, P.; Nagar, G.; Singh, A.; Singh, I. K. Chapter 13 - Effects of Pesticides on Human Physiology, Genetics, and Evolution. In *Emerging Contaminants in the Environment*; Sarma, H., Dominguez, D. C., Lee, W.-Y., Eds.; Elsevier, 2022; pp 287–310. https://doi.org/10.1016/B978-0-323-85160-2.00005-6.

(38) Chaturvedi, P.; Shukla, P.; Giri, B. S.; Chowdhary, P.; Chandra, R.; Gupta, P.; Pandey, A. Prevalence and Hazardous Impact of Pharmaceutical and Personal Care Products and Antibiotics in Environment: A Review on Emerging Contaminants. *Environmental Research* **2021**, *194*, 110664. https://doi.org/10.1016/j.envres.2020.110664.

(39) Dhir, B. Chapter 7 - Excessive Pharmaceutical and Personal Care Products in the Environment Cause Life-Threatening Diseases. In *Emerging Contaminants in the Environment*; Sarma, H., Dominguez, D. C., Lee, W.-Y., Eds.; Elsevier, 2022; pp 159–182. https://doi.org/10.1016/B978-0-323-85160-2.00014-7.

(40) Malik, L. A.; Bashir, A.; Qureashi, A.; Pandith, A. H. Detection and Removal of Heavy Metal Ions: A Review. *Environ Chem Lett* **2019**, *17* (4), 1495–1521. https://doi.org/10.1007/s10311-019-00891-z.

(41) Schaefer, M.; Schellenberg, M.; Merle, U.; Weiss, K. H.; Stremmel, W. Wilson Protein Expression, Copper Excretion and Sweat Production in Sweat Glands of Wilson Disease Patients and Controls. *BMC Gastroenterol* **2008**, *8*, 29. https://doi.org/10.1186/1471-230X-8-29.

(42) Twomey, P. J.; Viljoen, A.; House, I. M.; Reynolds, T. M.; Wierzbicki, A. S. Relationship between Serum Copper, Ceruloplasmin, and Non-Ceruloplasmin-Bound Copper in Routine Clinical Practice. *Clin Chem* **2005**, *51* (8), 1558–1559. https://doi.org/10.1373/clinchem.2005.052688.

(43) Ventriglia, M.; Bucossi, S.; Panetta, V.; Squitti, R. Copper in Alzheimer's Disease: A Meta-Analysis of Serum, Plasma, and Cerebrospinal Fluid Studies. *Journal of Alzheimer's Disease* **2012**, *30* (4), 981–984. https://doi.org/10.3233/JAD-2012-120244.

(44) Borowska, S.; Brzóska, M. M. Metals in Cosmetics: Implications for Human Health. *Journal of Applied Toxicology* **2015**, *35* (6), 551–572. https://doi.org/10.1002/jat.3129.

(45) Costa, M.; Salnikow, K.; Cosentino, S.; Klein, C. B.; Huang, X.; Zhuang, Z. Molecular Mechanisms of Nickel Carcinogenesis. *Environ Health Perspect* **1994**, *102* (Suppl 3), 127–130.

(46) Fernandes Azevedo, B.; Barros Furieri, L.; Peçanha, F. M.; Wiggers, G. A.; Frizera Vassallo, P.; Ronacher Simões, M.; Fiorim, J.; Rossi de Batista, P.; Fioresi, M.; Rossoni, L.; Stefanon, I.; Alonso, M. J.; Salaices, M.; Valentim Vassallo, D. Toxic Effects of Mercury on the Cardiovascular and Central Nervous Systems. *BioMed Research International* **2012**, *2012*, e949048. https://doi.org/10.1155/2012/949048.

(47) Balali-Mood, M.; Naseri, K.; Tahergorabi, Z.; Khazdair, M. R.; Sadeghi, M. Toxic Mechanisms of Five Heavy Metals: Mercury, Lead, Chromium, Cadmium, and Arsenic. *Frontiers in Pharmacology* **2021**, *12*.

(48) Dickenson, C. A.; Woodruff, T. J.; Stotland, N. E.; Dobraca, D.; Das, R. Elevated Mercury Levels in Pregnant Woman Linked to Skin Cream from Mexico. *American Journal of Obstetrics and Gynecology* **2013**, *209* (2), e4–e5. https://doi.org/10.1016/j.ajog.2013.05.030.

(49) Cha, N.-R.; Lee, J.-K.; Lee, Y.-R.; Jeong, H.-J.; Kim, H.-K.; Lee, S.-Y. Determination of Iron, Copper, Zinc, Lead, Nickel and Cadmium in Cosmetic Matrices by Flame Atomic Absorption Spectroscopy. *Analytical Letters* **2010**, *43* (2), 259–268. https://doi.org/10.1080/00032710903325781.

(50) Amry, M. A.; Al-Saikhan, F.; Ayoubi, A. Toxic Effect of Cadmium Found in Eyeliner to the Eye of a 21-Year-Old Saudi Woman: A Case Report. *Saudi Pharmaceutical Journal* **2011**, *19* (4), 269–272. https://doi.org/10.1016/j.jsps.2011.05.002.

(51) Ebrahimi, M.; Khalili, N.; Razi, S.; Keshavarz-Fathi, M.; Khalili, N.; Rezaei, N. Effects of Lead and Cadmium on the Immune System and Cancer Progression. *J Environ Health Sci Engineer* **2020**, *18* (1), 335–343. https://doi.org/10.1007/s40201-020-00455-2.

(52) Loghman-Adham, M. Renal Effects of Environmental and Occupational Lead Exposure. *Environmental Health Perspectives* **1997**, *105* (9), 928–939. https://doi.org/10.1289/ehp.97105928.

(53) Goyer, R. A. Mechanisms of Lead and Cadmium Nephrotoxicity. *Toxicology Letters* **1989**, *46* (1), 153–162. https://doi.org/10.1016/0378-4274(89)90124-0.

(54) Inobeme, A.; Mathew, J. T.; Jatto, E.; Inobeme, J.; Adetunji, C. O.; Muniratu, M.; Onyeachu, B. I.; Adekoya, M. A.; Ajai, A. I.; Mann, A.; Olori, E.; Akhor, S. O.; Eziukwu, C. A.; Kelani, T.; Omali, P. I. Recent Advances in Instrumental Techniques for Heavy Metal Quantification. *Environ Monit Assess* **2023**, *195* (4), 452. https://doi.org/10.1007/s10661-023-11058-3.

(55) Singh, S.; Wang, J.; Cinti, S. Review—An Overview on Recent Progress in Screen-Printed Electroanalytical (Bio)Sensors. *ECS Sens. Plus* **2022**, *1* (2), 023401. https://doi.org/10.1149/2754-2726/ac70e2.

(56) Cinti, S.; De Lellis, B.; Moscone, D.; Arduini, F. Sustainable Monitoring of Zn (II) in Biological Fluids Using Office Paper. *Sensors and Actuators B: Chemical* **2017**, *253*, 1199–1206. https://doi.org/10.1016/j.snb.2017.07.161.

(57) Arduini, F.; Cinti, S.; Scognamiglio, V.; Moscone, D.; Palleschi, G. How Cutting-Edge Technologies Impact the Design of Electrochemical (Bio)Sensors for Environmental Analysis. A Review. *Analytica Chimica Acta* **2017**, *959*, 15–42. https://doi.org/10.1016/j.aca.2016.12.035.

(58) Urdea, M.; Penny, L. A.; Olmsted, S. S.; Giovanni, M. Y.; Kaspar, P.; Shepherd, A.; Wilson, P.; Dahl, C. A.; Buchsbaum, S.; Moeller, G.; Hay Burgess, D. C. Requirements for High Impact Diagnostics in the Developing World. *Nature* **2006**, *444 Suppl 1*, 73–79. https://doi.org/10.1038/nature05448.

(59) Land, K. J.; Boeras, D. I.; Chen, X.-S.; Ramsay, A. R.; Peeling, R. W. REASSURED Diagnostics to Inform Disease Control Strategies, Strengthen Health Systems and Improve Patient Outcomes. *Nat Microbiol* **2019**, *4* (1), 46–54. https://doi.org/10.1038/s41564-018-0295-3.

(60) Miglione, A.; Spinelli, M.; Amoresano, A.; Cinti, S. Sustainable Copper Electrochemical Stripping onto a Paper-Based Substrate for Clinical Application. *ACS Meas. Au* **2022**. https://doi.org/10.1021/acsmeasuresciau.1c00059.

(61) Miglione, A.; Lorenzo, R. D.; Grumetto, L.; Spinelli, M.; Amoresano, A.; Laneri, S.; Cinti, S. An Integrated Electrochemical Platform Empowered by Paper for Fast Nickel Detection in Cosmetics. *Electrochimica Acta* **2022**, *434*, 141332. https://doi.org/10.1016/j.electacta.2022.141332.

(62) Ortone, V.; Matino, L.; Santoro, F.; Cinti, S. Merging Office/Filter Paper-Based Tools for Pre-Concentring and Detecting Heavy Metals in Drinking Water. *Chem. Commun.* **2021**, *57* (58), 7100–7103. https://doi.org/10.1039/D1CC02481G.

(63) Raucci, A.; Miglione, A.; Spinelli, M.; Amoresano, A.; Cinti, S. A Hybrid Screen-Printed Strip for Enhanced Electroanalysis towards Lead and Cadmium in Multi-

Matrices. *J. Electrochem. Soc.* **2022**, *169* (3), 037516. https://doi.org/10.1149/1945-7111/ac5c98.

(64) Faheem, A.; Cinti, S. Non-Invasive Electrochemistry-Driven Metals Tracing in Human Biofluids. *Biosensors and Bioelectronics* **2022**, *200*, 113904. https://doi.org/10.1016/j.bios.2021.113904.

(65) Mettakoonpitak, J.; Volckens, J.; Henry, C. S. Janus Electrochemical Paper-Based Analytical Devices for Metals Detection in Aerosol Samples. *Anal. Chem.* **2020**, *92* (1), 1439–1446. https://doi.org/10.1021/acs.analchem.9b04632.

(66) Banks, C. *Electrochemistry: Volume 17*; Royal Society of Chemistry, 2023.

(67) Samal, K.; Mahapatra, S.; Hibzur Ali, M. Pharmaceutical Wastewater as Emerging Contaminants (EC): Treatment Technologies, Impact on Environment and Human Health. *Energy Nexus* **2022**, *6*, 100076. https://doi.org/10.1016/j.nexus.2022.100076.

(68) Valdez-Carrillo, M.; Abrell, L.; Ramírez-Hernández, J.; Reyes-López, J. A.; Carreón-Diazconti, C. Pharmaceuticals as Emerging Contaminants in the Aquatic Environment of Latin America: A Review. *Environ Sci Pollut Res* **2020**, *27* (36), 44863–44891. https://doi.org/10.1007/s11356-020-10842-9.

(69) Colglazier, W. Sustainable Development Agenda: 2030. *Science* **2015**, *349* (6252), 1048–1050. https://doi.org/10.1126/science.aad2333.

(70) Guppy, L.; Mehta, P.; Qadir, M. Sustainable Development Goal 6: Two Gaps in the Race for Indicators. *Sustain Sci* **2019**, *14* (2), 501–513. https://doi.org/10.1007/s11625-018-0649-z.

(71) Baranowska, I.; Kowalski, B. The Development of SPE Procedures and an UHPLC Method for the Simultaneous Determination of Ten Drugs in Water Samples. *Water Air Soil Pollut* **2010**, *211* (1), 417–425. https://doi.org/10.1007/s11270-009-0310-7.

(72) Gioia, M. G.; Andreatta, P.; Boschetti, S.; Gatti, R. Development and Validation of a Liquid Chromatographic Method for the Determination of Ascorbic Acid, Dehydroascorbic Acid and Acetaminophen in Pharmaceuticals. *Journal of Pharmaceutical and Biomedical Analysis* **2008**, *48* (2), 331–339. https://doi.org/10.1016/j.jpba.2008.01.026.

(73) Lou, H.; Yuan, H.; Ruan, Z.; Jiang, B. Simultaneous Determination of Paracetamol, Pseudoephedrine, Dextrophan and Chlorpheniramine in Human Plasma by Liquid Chromatography–Tandem Mass Spectrometry. *Journal of Chromatography B* **2010**, *878* (7), 682–688. https://doi.org/10.1016/j.jchromb.2010.01.005.

(74) Ruengsitagoon, W.; Liawruangrath, S.; Townshend, A. Flow Injection Chemiluminescence Determination of Paracetamol. *Talanta* **2006**, *69* (4), 976–983. https://doi.org/10.1016/j.talanta.2005.11.050.

(75) Baranowska, I.; Markowski, P.; Gerle, A.; Baranowski, J. Determination of Selected Drugs in Human Urine by Differential Pulse Voltammetry Technique. *Bioelectrochemistry* **2008**, *73* (1), 5–10. https://doi.org/10.1016/j.bioelechem.2008.04.022.

(76) Raymundo-Pereira, P. A.; Gomes, N. O.; Machado, S. A. S.; Oliveira, O. N. Simultaneous, Ultrasensitive Detection of Hydroquinone, Paracetamol and Estradiol for Quality Control of Tap Water with a Simple Electrochemical Method. *Journal of Electroanalytical Chemistry* **2019**, *848*, 113319. https://doi.org/10.1016/j.jelechem.2019.113319.

(77) Nicolopoulou-Stamati, P.; Maipas, S.; Kotampasi, C.; Stamatis, P.; Hens, L. Chemical Pesticides and Human Health: The Urgent Need for a New Concept in Agriculture. *Frontiers in Public Health* **2016**, *4*.

(78) *Regulation (EC) No 396/2005 of the European Parliament and of the Council of 23 February 2005 on Maximum Residue Levels of Pesticides in or on Food and Feed of Plant and Animal Origin and Amending Council Directive 91/414/EEC Text with EEA Relevance.*; 2005; Vol. 070. http://data.europa.eu/eli/reg/2005/396/oj/eng (accessed 2024-01-13).

(79) Authority (EFSA), E. F. S.; Carrasco Cabrera, L.; Medina Pastor, P. The 2019 European Union Report on Pesticide Residues in Food. *EFSA Journal* **2021**, *19* (4), e06491. https://doi.org/10.2903/j.efsa.2021.6491.

(80) Stafford, J. V. Implementing Precision Agriculture in the 21st Century. *Journal of Agricultural Engineering Research* **2000**, *76* (3), 267–275. https://doi.org/10.1006/jaer.2000.0577.

(81) Yin, H.; Cao, Y.; Marelli, B.; Zeng, X.; Mason, A. J.; Cao, C. Soil Sensors and Plant Wearables for Smart and Precision Agriculture. *Advanced Materials* **2021**, *33* (20), 2007764. https://doi.org/10.1002/adma.202007764.

(82) Lo Presti, D.; Di Tocco, J.; Massaroni, C.; Cimini, S.; De Gara, L.; Singh, S.; Raucci, A.; Manganiello, G.; Woo, S. L.; Schena, E.; Cinti, S. Current Understanding, Challenges and Perspective on Portable Systems Applied to Plant Monitoring and Precision Agriculture. *Biosensors and Bioelectronics* **2023**, *222*, 115005. https://doi.org/10.1016/j.bios.2022.115005.

(83) Zhang, N.; Wang, M.; Wang, N. Precision Agriculture—a Worldwide Overview. *Computers and Electronics in Agriculture* **2002**, *36* (2), 113–132. https://doi.org/10.1016/S0168-1699(02)00096-0.

(84) Campanale, C.; Massarelli, C.; Losacco, D.; Bisaccia, D.; Triozzi, M.; Uricchio, V. F. The Monitoring of Pesticides in Water Matrices and the Analytical Criticalities: A Review. *TrAC Trends in Analytical Chemistry* **2021**, *144*, 116423. https://doi.org/10.1016/j.trac.2021.116423.

(85) Di Tocco, J.; Lo Presti, D.; Massaroni, C.; Cinti, S.; Cimini, S.; De Gara, L.; Schena, E. Plant-Wear: A Multi-Sensor Plant Wearable Platform for Growth and Microclimate Monitoring. *Sensors* **2023**, *23* (1), 549. https://doi.org/10.3390/s23010549.

(86) Raucci, A.; Miglione, A.; Lenzi, L.; Fabbri, P.; Di Tocco, J.; Massaroni, C.; Presti, D. L.; Schena, E.; Pifferi, V.; Falciola, L.; Aidli, W.; Di Natale, C.; Netti, P. A.; Woo, S. L.; Morselli, D.; Cinti, S. Characterization and Application of Porous PHBV-Based Bacterial Polymers to Realize Novel Bio-Based Electroanalytical (Bio)Sensors. *Sensors and Actuators B: Chemical* **2023**, *379*, 133178. https://doi.org/10.1016/j.snb.2022.133178.

(87) Turner, A. D., Lewis, A. M., Bradley, K., & Maskrey, B. H. Marine invertebrate interactions with harmful algal blooms–implications for one health. *Journal of invertebrate pathology*, **2023**, 186, 107555. https://doi.org/10.1016/j.jip.2021.107555.

(88) Amorim, C. A.; Moura, A. do N. Ecological Impacts of Freshwater Algal Blooms on Water Quality, Plankton Biodiversity, Structure, and Ecosystem Functioning. *Science of The Total Environment* **2021**, *758*, 143605. https://doi.org/10.1016/j.scitotenv.2020.143605.

(89) Brooks, B. W.; Lazorchak, J. M.; Howard, M. D. A.; Johnson, M.-V. V.; Morton, S. L.; Perkins, D. A. K.; Reavie, E. D.; Scott, G. I.; Smith, S. A.; Steevens, J. A. Are Harmful Algal Blooms Becoming the Greatest Inland Water Quality Threat to Public Health and Aquatic Ecosystems? *Environmental Toxicology and Chemistry* **2016**, *35* (1), 6–13. https://doi.org/10.1002/etc.3220.

(90) Costa, P. R.; Costa, S. T.; Braga, A. C.; Rodrigues, S. M.; Vale, P. Relevance and Challenges in Monitoring Marine Biotoxins in Non-Bivalve Vectors. *Food Control* **2017**, *76*, 24–33. https://doi.org/10.1016/j.foodcont.2016.12.038.

(91) Ebrahimzadeh, G.; Alimohammadi, M.; Kahkah, M. R. R.; Mahvi, A. H. Relationship between Algae Diversity and Water Quality- a Case Study: Chah Niemeh Reservoir Southeast of Iran. *J Environ Health Sci Engineer* **2021**, *19* (1), 437–443. https://doi.org/10.1007/s40201-021-00616-x.

(92) Vilariño, N.; Louzao, M. C.; Abal, P.; Cagide, E.; Carrera, C.; Vieytes, M. R.; Botana, L. M. Human Poisoning from Marine Toxins: Unknowns for Optimal Consumer Protection. *Toxins* **2018**, *10* (8), 324. https://doi.org/10.3390/toxins10080324.

(93) Gerssen, A.; Pol-Hofstad, I. E.; Poelman, M.; Mulder, P. P. J.; van den Top, H. J.; de Boer, J. Marine Toxins: Chemistry, Toxicity, Occurrence and Detection, with Special Reference to the Dutch Situation. *Toxins (Basel)* **2010**, *2* (4), 878–904. https://doi.org/10.3390/toxins2040878.

(94) Kuramoto, M.; Arimoto, H.; Uemura, D. Bioactive Alkaloids from the Sea: A Review. *Mar Drugs* **2004**, *2* (1), 39–54.

(95) Klijnstra, M. D.; Faassen, E. J.; Gerssen, A. A Generic LC-HRMS Screening Method for Marine and Freshwater Phycotoxins in Fish, Shellfish, Water, and Supplements. *Toxins* **2021**, *13* (11), 823. https://doi.org/10.3390/toxins13110823.

(96) *Regolamento (CE) n. 853/2004 del Parlamento europeo e del Consiglio, del 29 aprile 2004, che stabilisce norme specifiche in materia di igiene per gli alimenti di origine animale*; 2004; Vol. 139. http://data.europa.eu/eli/reg/2004/853/oj/ita (accessed 2024-01-13).

(97) Bosch-Orea, C.; Kleemann, C. R.; Deolindo, C. T. P.; Molognoni, L.; Dallegrave, A.; Daguer, H.; de Oliveira Costa, A. C.; Hoff, R. B. Integrated Analysis of Marine Biotoxins and Contaminants of Emerging Concern in Bivalve Mollusks from Santa Catarina, Brazil. *Science of The Total Environment* **2023**, *905*, 167254. https://doi.org/10.1016/j.scitotenv.2023.167254.

(98) Mafra, L. L.; de Souza, D. A.; Menezes, M.; Schramm, M. A.; Hoff, R. Marine Biotoxins: Latest Advances and Challenges toward Seafood Safety, Using Brazil as a Case Study. *Current Opinion in Food Science* **2023**, *53*, 101078. https://doi.org/10.1016/j.cofs.2023.101078.

(99) Otero, A.; Chapela, M.-J.; Atanassova, M.; Vieites, J. M.; Cabado, A. G. Cyclic Imines: Chemistry and Mechanism of Action: A Review. *Chem. Res. Toxicol.* **2011**, *24* (11), 1817–1829. https://doi.org/10.1021/tx200182m.

(100) Selwood, A. I.; Wilkins, A. L.; Munday, R.; Shi, F.; Rhodes, L. L.; Holland, P. T. Portimine: A Bioactive Metabolite from the Benthic Dinoflagellate Vulcanodinium Rugosum. *Tetrahedron Letters* **2013**, *54* (35), 4705–4707. https://doi.org/10.1016/j.tetlet.2013.06.098.

(101) Molgó, J.; Marchot, P.; Aráoz, R.; Benoit, E.; Iorga, B. I.; Zakarian, A.; Taylor, P.; Bourne, Y.; Servent, D. Cyclic Imine Toxins from Dinoflagellates: A Growing Family of Potent Antagonists of the Nicotinic Acetylcholine Receptors. *Journal of Neurochemistry* **2017**, *142* (S2), 41–51. https://doi.org/10.1111/jnc.13995.

(102) Aráoz, R.; Barnes, P.; Séchet, V.; Delepierre, M.; Zinn-Justin, S.; Molgó, J.; Zakarian, A.; Hess, P.; Servent, D. Cyclic Imine Toxins Survey in Coastal European Shellfish Samples: Bioaccumulation and Mode of Action of 28-O-Palmitoyl Ester of Pinnatoxin-G. First Report of Portimine-A Bioaccumulation. *Harmful Algae* **2020**, *98*, 101887. https://doi.org/10.1016/j.hal.2020.101887.

(103)Hellyer, S. D.; Selwood, A. I.; Rhodes, L.; Kerr, D. S. Marine Algal Pinnatoxins E and F Cause Neuromuscular Block in an in Vitro Hemidiaphragm Preparation. *Toxicon* **2011**, *58* (8), 693–699. https://doi.org/10.1016/j.toxicon.2011.09.006.

(104)Bodero, M.; Gerssen, A.; Portier, L.; Klijnstra, M. D.; Hoogenboom, R. L. A. P.; Guzmán, L.; Hendriksen, P. J. M.; Bovee, T. F. H. A Strategy to Replace the Mouse Bioassay for Detecting and Identifying Lipophilic Marine Biotoxins by Combining the Neuro-2a Bioassay and LC-MS/MS Analysis. *Marine Drugs* **2018**, *16* (12), 501. https://doi.org/10.3390/md16120501.

(105)Varriale, F.; Tartaglione, L.; Cinti, S.; Milandri, A.; Dall'Ara, S.; Calfapietra, A.; Dell'Aversano, C. Development of a Data Dependent Acquisition-Based Approach for the Identification of Unknown Fast-Acting Toxins and Their Ester Metabolites. *Talanta* **2021**, *224*, 121842. https://doi.org/10.1016/j.talanta.2020.121842.

(106)Nabout, J. C.; da Silva Rocha, B.; Carneiro, F. M.; Sant'Anna, C. L. How Many Species of Cyanobacteria Are There? Using a Discovery Curve to Predict the Species Number. *Biodivers Conserv* **2013**, *22* (12), 2907–2918. https://doi.org/10.1007/s10531-013-0561-x.

(107)Chaurasia, A. Cyanobacterial Biodiversity and Associated Ecosystem Services: Introduction to the Special Issue. *Biodivers Conserv* **2015**, *24* (4), 707–710. https://doi.org/10.1007/s10531-015-0908-6.

(108)Gobler, C. J. Climate Change and Harmful Algal Blooms: Insights and Perspective. *Harmful Algae* **2020**, *91*, 101731. https://doi.org/10.1016/j.hal.2019.101731.

(109) Gkelis, S.; Lanaras, T.; Sivonen, K. Cyanobacterial Toxic and Bioactive Peptides in Freshwater Bodies of Greece: Concentrations, Occurrence Patterns, and Implications for Human Health. *Marine Drugs* **2015**, *13* (10), 6319–6335. https://doi.org/10.3390/md13106319.

(110)Du, X.; Liu, H.; Yuan, L.; Wang, Y.; Ma, Y.; Wang, R.; Chen, X.; Losiewicz, M. D.; Guo, H.; Zhang, H. The Diversity of Cyanobacterial Toxins on Structural Characterization, Distribution and Identification: A Systematic Review. *Toxins* **2019**, *11* (9), 530. https://doi.org/10.3390/toxins11090530.

(111)Catherine, A.; Bernard, C.; Spoof, L.; Bruno, M. Microcystins and Nodularins. In *Handbook of Cyanobacterial Monitoring and Cyanotoxin Analysis*; John Wiley & Sons, Ltd, 2016; pp 107–126. https://doi.org/10.1002/9781119068761.ch11.

(112)Jones, M. R.; Pinto, E.; Torres, M. A.; Dörr, F.; Mazur-Marzec, H.; Szubert, K.; Tartaglione, L.; Dell'Aversano, C.; Miles, C. O.; Beach, D. G.; McCarron, P.; Sivonen, K.; Fewer, D. P.; Jokela, J.; Janssen, E. M.-L. CyanoMetDB, a Comprehensive Public Database of Secondary Metabolites from Cyanobacteria. *Water Research* **2021**, *196*, 117017. https://doi.org/10.1016/j.watres.2021.117017.

(113)Veerapagu, M.; Jeya, K. R.; Sankara narayanan, A. Isolation of Toxin Producing Cyanobacteria from Aquatic Samples—Anabaenopsis Sp. In *Protocols for Cyanobacteria Sampling and Detection of Cyanotoxin*; Thajuddin, N., Sankara narayanan, A., Dhanasekaran, D., Eds.; Springer Nature: Singapore, 2023; pp 77–83. https://doi.org/10.1007/978-981-99-4514-6_10.

(114)Varriale, F.; Tartaglione, L.; Zervou, S.-K.; Miles, C. O.; Mazur-Marzec, H.; Triantis, T. M.; Kaloudis, T.; Hiskia, A.; Dell'Aversano, C. Untargeted and Targeted LC-MS and Data Processing Workflow for the Comprehensive Analysis of Oligopeptides from Cyanobacteria. *Chemosphere* **2023**, *311*, 137012. https://doi.org/10.1016/j.chemosphere.2022.137012.

(115)Filatova, D.; Picardo, M.; Núñez, O.; Farré, M. Analysis, Levels and Seasonal Variation of Cyanotoxins in Freshwater Ecosystems. *Trends in Environmental Analytical Chemistry* **2020**, *26*, e00091. https://doi.org/10.1016/j.teac.2020.e00091.

(116) Westrick, J. A.; Szlag, D. C.; Southwell, B. J.; Sinclair, J. A Review of Cyanobacteria and Cyanotoxins Removal/Inactivation in Drinking Water Treatment. *Anal Bioanal Chem* **2010**, *397* (5), 1705–1714. https://doi.org/10.1007/s00216-010-3709-5.

(117)Toxins, C. Microcystin-LR in Drinking-Water. Background Document for Development of WHO Guidelines for Drinking-Water Quality. *WHO: Geneva, Switzerland* **2003**.

(118)*Directive (EU) 2020/2184 of the European Parliament and of the Council of 16 December 2020 on the Quality of Water Intended for Human Consumption (Recast)*

(Text with EEA Relevance); 2020; Vol. 435. http://data.europa.eu/eli/dir/2020/2184/oj/eng (accessed 2024-01-13).

(119)Meriluoto, J.; Spoof, L.; Codd, G. A. *Handbook of Cyanobacterial Monitoring and Cyanotoxin Analysis*; Wiley, 2017.

(120)*Palytoxin: A New Marine Toxin from a Coelenterate | Science*. https://www.science.org/doi/10.1126/science.172.3982.495 (accessed 2024-01-13).

(121)Moore, R. E.; Bartolini, G. Structure of Palytoxin. *J. Am. Chem. Soc.* **1981**, *103* (9), 2491–2494. https://doi.org/10.1021/ja00399a093.

(122)Kerbrat, A. S.; Amzil, Z.; Pawlowiez, R.; Golubic, S.; Sibat, M.; Darius, H. T.; Chinain, M.; Laurent, D. First Evidence of Palytoxin and 42-Hydroxy-Palytoxin in the Marine Cyanobacterium Trichodesmium. *Marine Drugs* **2011**, *9* (4), 543–560. https://doi.org/10.3390/md9040543.

(123)Ciminiello, P.; Dell'Aversano, C.; Dello Iacovo, E.; Fattorusso, E.; Forino, M.; Grauso, L.; Tartaglione, L. High Resolution LC-MSn Fragmentation Pattern of Palytoxin as Template to Gain New Insights into Ovatoxin-a Structure. The Key Role of Calcium in MS Behavior of Palytoxins. *J. Am. Soc. Mass Spectrom.* **2012**, *23* (5), 952–963. https://doi.org/10.1007/s13361-012-0345-7.

(124)Santos, M.; Oliveira, P. B.; Moita, M. T.; David, H.; Caeiro, M. F.; Zingone, A.; Amorim, A.; Silva, A. Ocurrence of Ostreopsis in Two Temperate Coastal Bays (SW Iberia): Insights from the Plankton. *Harmful Algae* **2019**, *86*, 20–36. https://doi.org/10.1016/j.hal.2019.03.003.

(125)Scalco, E.; Brunet, C.; Marino, F.; Rossi, R.; Soprano, V.; Zingone, A.; Montresor, M. Growth and Toxicity Responses of Mediterranean Ostreopsis Cf. Ovata to Seasonal Irradiance and Temperature Conditions. *Harmful Algae* **2012**, *17*, 25–34. https://doi.org/10.1016/j.hal.2012.02.008.

(126)Accoroni, S.; Romagnoli, T.; Penna, A.; Capellacci, S.; Ciminiello, P.; Dell'Aversano, C.; Tartaglione, L.; Abboud–Abi Saab, M.; Giussani, V.; Asnaghi, V.; Chiantore, M.; Totti, C. Ostreopsis Fattorussoi Sp. Nov. (Dinophyceae), a New Benthic Toxic Ostreopsis Species from the Eastern Mediterranean Sea. *Journal of Phycology* **2016**, *52* (6), 1064–1084. https://doi.org/10.1111/jpy.12464.

(127)Tartaglione, L.; Dello Iacovo, E.; Mazzeo, A.; Casabianca, S.; Ciminiello, P.; Penna, A.; Dell'Aversano, C. Variability in Toxin Profiles of the Mediterranean Ostreopsis Cf. Ovata and in Structural Features of the Produced Ovatoxins. *Environ. Sci. Technol.* **2017**, *51* (23), 13920–13928. https://doi.org/10.1021/acs.est.7b03827.

(128)Ukena, T.; Satake, M.; Usami, M.; Oshima, Y.; Fujita, T.; Naoki, H.; Yasumoto, T. Structural Confirmation of Ostreocin-D by Application of Negative-Ion Fast-Atom Bombardment Collision-Induced Dissociation Tandem Mass Spectrometric Methods. *Rapid Communications in Mass Spectrometry* **2002**, *16* (24), 2387–2393. https://doi.org/10.1002/rcm.867.

(129)Ciminiello, P.; Dell'Aversano, C.; Iacovo, E. D.; Fattorusso, E.; Forino, M.; Tartaglione, L. LC-MS of Palytoxin and Its Analogues: State of the Art and Future Perspectives. *Toxicon* **2011**, *57* (3), 376–389. https://doi.org/10.1016/j.toxicon.2010.11.002.

(130)Tartaglione, L.; Mazzeo, A.; Dell'Aversano, C.; Forino, M.; Giussani, V.; Capellacci, S.; Penna, A.; Asnaghi, V.; Faimali, M.; Chiantore, M.; Yasumoto, T.; Ciminiello, P. Chemical, Molecular, and Eco-Toxicological Investigation of Ostreopsis Sp. from Cyprus Island: Structural Insights into Four New Ovatoxins by LC-HRMS/MS. *Anal Bioanal Chem* **2016**, *408* (3), 915–932. https://doi.org/10.1007/s00216-015-9183-3.

(131)Rossini, G. P.; Bigiani, A. Palytoxin Action on the Na+, K+-ATPase and the Disruption of Ion Equilibria in Biological Systems. *Toxicon* **2011**, *57* (3), 429–439. https://doi.org/10.1016/j.toxicon.2010.09.011.

(132)Wu, C. H. Palytoxin: Membrane Mechanisms of Action. *Toxicon* **2009**, *54* (8), 1183–1189. https://doi.org/10.1016/j.toxicon.2009.02.030.

(133)Pelin, M.; Sosa, S.; Tubaro, A. Palytoxins: Toxicological Profile. In *Marine and Freshwater Toxins*; Gopalakrishnakone, P., Haddad Jr., V., Tubaro, A., Kim, E., Kem, W. R., Eds.; Toxinology; Springer Netherlands: Dordrecht, 2016; pp 129–145. https://doi.org/10.1007/978-94-007-6419-4_19.

(134)Poli, M.; Ruiz-Olvera, P.; Nalca, A.; Ruiz, S.; Livingston, V.; Frick, O.; Dyer, D.; Schellhase, C.; Raymond, J.; Kulis, D.; Anderson, D.; McGrath, S.; Deeds, J.

Toxicity and Pathophysiology of Palytoxin Congeners after Intraperitoneal and Aerosol Administration in Rats. *Toxicon* **2018**, *150*, 235–250. https://doi.org/10.1016/j.toxicon.2018.06.067.

(135)Authority (EFSA), E. F. S. Marine Biotoxins in Shellfish – Summary on Regulated Marine Biotoxins. *EFSA Journal* **2009**, *7* (8), 1306. https://doi.org/10.2903/j.efsa.2009.1306.

(136)Funari, E.; Manganelli, M.; Testai, E. Ostreospis Cf. Ovata Blooms in Coastal Water: Italian Guidelines to Assess and Manage the Risk Associated to Bathing Waters and Recreational Activities. *Harmful Algae* **2015**, *50*, 45–56. https://doi.org/10.1016/j.hal.2015.10.008.

CHAPTER 2. ANALYTICAL TECHNIQUES

The escalation in the release of emerging contaminants (ECs) into the environment is a consequence of heightened domestic, industrial, and agricultural activities driven by rapid urbanization. This increased utilization of chemicals poses the risk of these substances permeating various environmental compartments, such as soil and the atmosphere. Entry mechanisms include volatilization, wet and dry deposition in the soil matrix, diffusive exchange, and aerosol formation processes with consequences on environmental, animals and humans' health. A substantial number of chemicals are currently in widespread use globally, resulting in the uncontrolled release of transformed residuals and metabolites of organic micro-pollutants into the environment. Despite this, the fate, behaviour, and potential consequences of these by-products remain largely unknown. It is crucial to scrutinize the altered products and metabolites, as they may exhibit harmful effects comparable to or even greater than those of the parent chemicals.[1]

The initial step in addressing the possible biological impact of ECs in the environment is the identification and quantification of the compounds present. This emphasizes the significance of employing analytical techniques to assess and monitor the levels of these contaminants.[2]

To ascertain the presence of known and unknown compounds in intricate environmental samples at minimal concentrations, it is imperative to combine cutting-edge sampling techniques with advanced analytical methodologies. The research in this domain is intense, driven by heightened public concern for environmental issues, leading to a substantial annual publication output. Additionally, a multitude of literature reviews comprehensively address various aspects of environmental investigations.[3–5] These encompass the advancement of

extraction techniques, the rapid evolution of chromatographic methods, the utilization of mass spectrometry (MS) for targeted and non-targeted analyses, and new and strategic architectures in the (bio)sensor world to improve the early monitoring of emerging contaminants (ECs) (Figure II.1).[6] This wealth of information significantly contributes to our comprehension of environmental intricacies and facilitates the development of more sophisticated analysis methods.

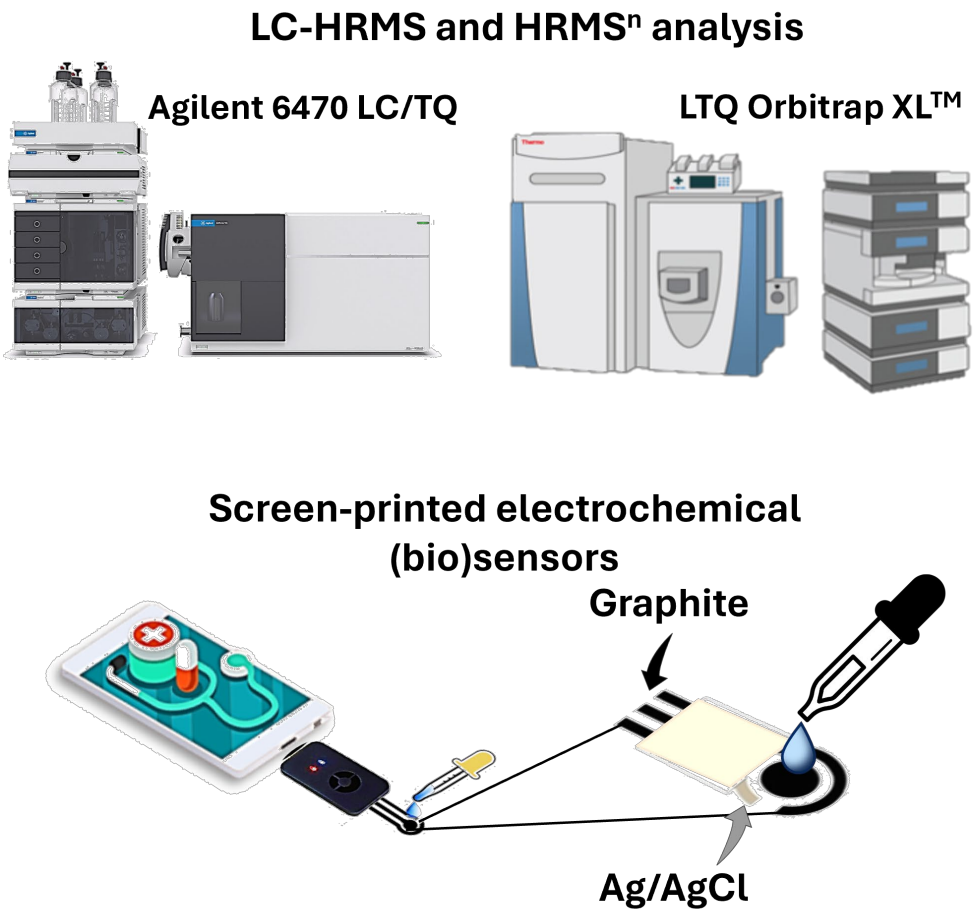

Figure II.1. LC-HRMS and HRMS^n analysis and screen-printed electrochemical (bio)sensors architectures.

2.1 LIQUID CHROMATOGRAPHY – MASS SPECTROMETRY

Qualitative-quantitative determination of emerging toxins is commonly performed through the application of analytical methods based on the combination of liquid chromatography and mass spectrometry. This ifenate technique provides several advantages, such as the high sensitivity and specificity, the possibility of examining labile and very structurally diverse toxins also when they are present in trace, accurate and precise quantification, a wide range of linear response and the possibility to obtain structural information for identification of new toxins, analogues of known toxins and metabolites.[7]

For many years, the coupling of high-performance liquid chromatography (HPLC) with a mass spectrometer (MS) has been a problem due to the nature of the eluent used. In HPLC, in fact, a liquid is used as an eluent that can reach flows of up to 5 ml min^{-1}, while the mass spectrometer, and in particular the analyzer, works at very low pressures in the order of 10^{-5} - 10^{-6} torr. Therefore, the direct injection of the eluent into the ionization source represents a critical point in the interfacing between the two instruments as it is required to ionize the analytes by removing the solvent without disturbing the vacuum inside the instrument. This problem has been solved thanks to the spread of so-called API (Atmospheric Pressure Ionization) sources, which make it possible to couple HPLC systems, operating under high pressure conditions, to mass spectrometry operating under high vacuum. Electrospray Ionization (ESI) is one of several variants of API applied between the output of an HPLC unit and the input of a mass spectrometer. Using mass spectrometry, it is possible to study any type of compound that is capable of being ionised, and whose ions can exist in the gas phase, so that depending on the nature of the molecules to be analysed, a different ionisation source is required a different ionisation source. ESI is an electron ionisation technique that is successfully applied to all those analytes that are already in ionic

form in solution or easily ionised in solution by protonation, deprotonation or by binding cations or anions. Medium polar to ionic analytes with a molecular weight between 10 and 10^6 Daltons are therefore suitable for ESI. The solvent can be volatile or moderately volatile, moderately or strongly polar and protic (e.g. isopropanol, methanol, acetonitrile, water) and volatile acids or bases are often added to it to promote ions formation. The solution containing the analytes is injected into the source through a steel capillary to which a current in the order of 3-5 kV is applied, triggering acid/base reactions in the liquid phase between the analyte and the solvent in which it is dissolved. The solution escapes from the capillary to which a high potential is applied in the form of a spray consisting of charged droplets a few microns (1-60 μm) in diameter. In this phase, the electrical potential induces charge separation in the solution, resulting in a cone-shaped deformation of the spray (Taylor cone) from the apex of which, the area of maximum charge density, begins the emission of a thin liquid jet. Eventually, the droplets emitted from the cone will move away from each other due to coulombic repulsion, generating a finely divided cloud. The progressive decrease in drop volume leads to an increase in surface charge density until the electrical repulsion exceeds the surface tension of the drop, causing it to 'burst' (Rayleigh limit) and creating a stream of bare ions that are then directed by a field gradient towards the analyzer. This mechanism is repeated in a cascade until all the solvent has evaporated, leading to the formation of desolvated analyte ions in the gas phase, which may have unit or multiple charges. Finally, the ions thus formed are drawn beyond the sampling plate by the potential of the opposite sign to that applied to the capillary.[8,9.]

The main low-resolution mass detector is the triple quadrupole (TQ). The quadrupole analyzer schematically consists of four parallel, cylindrical metallic

rods by means of which ions from the sample under investigation can be conveyed to the detector, based on their mass-to-charge ratio (m/z).

The opposite bars are held at the same potential consisting of a direct current (DC) component and an alternating current (AC) component. The resulting electric field forces the ions to travel a different oscillating trajectory (z) for each value of *m/z*. By adjusting this field, the *m/z* value of the ions passing through the quadrupole can be selected; ions with *m/z* higher or lower than the chosen value will be forced to travel along different trajectories that lead out of the electric field and thus will not reach the detector. This allows the selection of a particular ion, or the scanning of the various *m/z* by continuously varying the electric field. The triple quadrupole, in particular, is made up of three quadrupoles in series in which the first and third act as mass filters, while the central quadrupole, filled with an inert gas (nitrogen or argon), acts as a collision cell to which the radio frequency is applied, whose function is to keep the ions generated by the breakage of the parent molecule focused (Figure II.2). However, its characteristics as a destructive analyser and its low (unitary) resolution limit its use for analyses where there is no need for high performance. An analysis with this type of analyser is useful when the study is to be carried out with a targeted approach that guarantees a more sensitive and accurate detection of predetermined metabolites. However, the number of substances that can be quantified depends on the availability of reference standards.[10,11.]

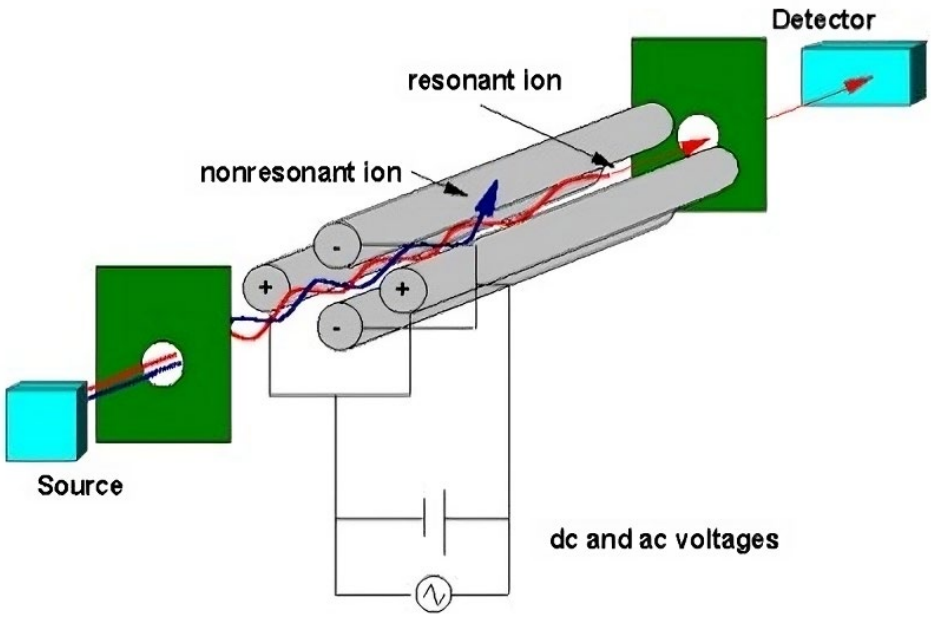

Figure II.2. Quadrupole mass analyzer.

High-resolution and high-performance mass detectors include the orbital trap analyser (Orbitrap), which is based on trapping ions in electrostatic fields. Unlike the TQ, the Orbitrap makes it possible to detect and identify not only known metabolites, but also unknown ones (untargeted approach). It consists of a spindle-shaped inner electrode and a bell-shaped outer electrode. Ions with a stable trajectory revolve around the central electrode with harmonic oscillations along its axis (Figure II.3). The frequency ω of these is proportional to the mass-to-charge ratio via the instrumental constant k.

$$\omega = \sqrt{\frac{K}{m/z}}$$

The two halves of the Orbitrap's outer electrode detect the image current produced by the oscillation of the ions. Then by means of a Fast Fourier Transformation (FFT) of the current, the axial oscillation frequencies are obtained from which, using equation 1, the mass-to-charge ratio of the ions is derived. Before reaching the Orbitrap, the electrons pass through an RF octapole (Oct1) in vacuum and reach a curved linear trap, called the C-Trap, containing nitrogen used as a collision gas (bath gas), which has the function of dissipating the kinetic energy possessed by the ions, 'cooling' them and focusing them along the curved axis of the trap. The voltages applied to the ends of the C-Trap apertures are then increased in order to create a potential barrier along its axis. These voltages are then progressively increased in order to 'squeeze' the ions into a narrow beam along its axis. This system causes the ions to enter the Orbitrap as packets of ions only a few millimetres long. When all ions of all m/z ratios have entered the Orbitrap, the voltage applied to the internal electrode is kept constant and the detection of the image currents begins.[12,13.]

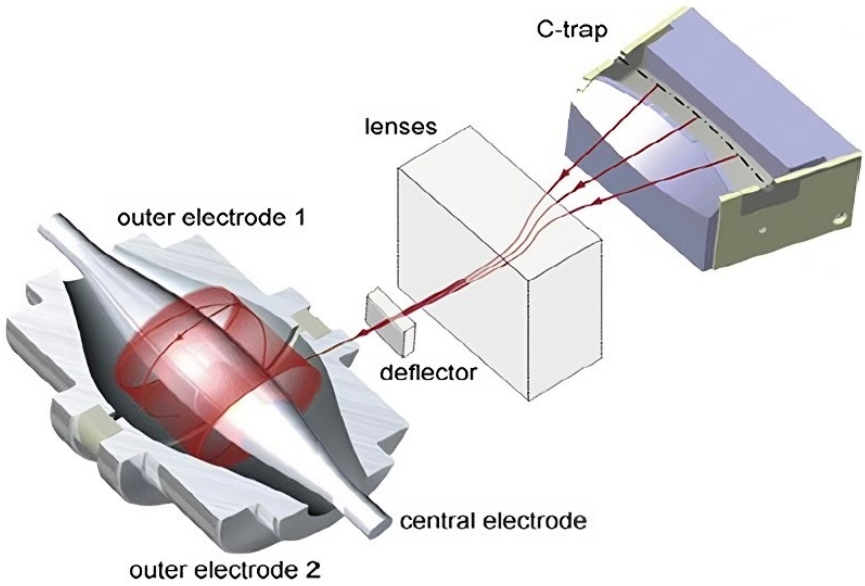

Figure II.3. Representation of stable ion trajectory in the Orbitrap analyzer.

The LC-MS analyses of emerging natural toxins that I carried out during my PhD, have been conducted mainly on an Ultimate 3000 quaternary system coupled to an LTQ Orbitrap XL^{TM} Fourier Transform MS (FTMS) hybrid linear ion trap equipped with an ESI ION MAX^{TM} source (Thermo-Fisher, San Jose, CA, USA) and also on an UHPLC (Agilent 1290 Infinity II) coupled to a Triple Quadrupole (Agilent 6470 LC/TQ) analyser equipped with an Electrospray source (Agilent JetStream Technology) for quantitative analysis.

1st step: LC-HRMS method set up

The separations will be performed on Microbore Analytical columns suitable for LC-HRMS analysis. Only reverse-phase (C8, C18 etc.) and ion-exchange stationary phases (cationic / anionic or ion-pair) can be used considering the molecular weight of the analyte, its polarity and its solubility in organic or aqueous solvents. In particular, for the analysis of Palytoxin and its congeners, the LC-HRMS methos is optimized on a Kinetex C18 column (2.6 µm 100Å 100 2.1mm; Phenomenex, Torrance, USA), while for the analysis of Microcystins and Cyclic imines a HyperClone column (3 µm BDS C8, 130 Å, 50 × 2.0 mm; Phenomenex, Torrance, USA) was used. Considering the characteristics of an ESI source, the usable mobile phases can be volatile or moderately volatile, medium or highly polar and protic (e.g. isopropanol, methanol, acetonitrile, water) and volatile acids or bases are often added to it to promote the formation of ions. The concentration of any buffers present must be kept below 20mM and volatile salts such as ammonium formate or ammonium acetate are used. In particular, for the analysis of palytoxin and ovatoxins mobile phases consist in water (eluent A) and acetonitrile–water (95:5 v/v) (eluent B), both containing 30 mM of acetic acid, while for cyanotoxins and cyclic imines analysis, mobile phases are constituted by water (eluent A) and acetonitrile–water (95:5 v/v)

(eluent B), both containing 2 mM ammonium formate and 50 mM formic acid. The elution flow typically was of 0.2 mL/min with an elution gradient developed during the optimization phase of the chromatographic method. The optimization of source parameters is also fundamental (spray voltage, capillary temperature, capillary voltage, sheath gas and auxiliary gas and tube lens voltage). In order to characterize the profile of a biomass under examination, LC-HRMS analyses were acquired on the LTQ Orbitrap XL^{TM} mass spectrometer in HR Full scan and MS/MS Data Dependent (DD) mode. The DD experiment involves the fragmentation of the most intense mass peaks present in the Full scan spectrum using two different fragmentation modes: Collision Induced Dissociation (CID) and Higher Energy Collisional Dissociation (HCD). HCD is particularly useful for its ability to operate at higher collision energies, which tends to promote the fragmentation of the peptide backbone, thus providing valuable information for the identification of peptides and proteins. HCD is preferred for its high fragmentation efficiency and the generation of extensive fragment ion spectra, especially useful in high-resolution settings like Orbitrap mass spectrometers. CID, on the other hand, is versatile and can be applied in various mass spectrometer configurations, including ion traps and quadrupoles, making it suitable for detailed structural analysis through sequential MS^n experiments. The two modes of fragmentation are complementary as they allow to obtain MS/MS spectra which generally contain different fragment ions, so the combined interpretation of both spectra provides the maximum of structural information. The purpose of DD experiments is to obtain, in a single analysis, MS/MS spectra of numerous ions thus allowing the identification of known compounds (dereplication) and, if present, also of new analogues, which share the fragmentation pattern with known ones (untargeted analysis). The optimized methods must be validated on real samples so to allow a qualitative and

quantitative determination of analytes in complex matrices that can cause an enhancement or a decrease of the signal related to the substance. The quantification of metabolites is performed using internal or external standards through the construction of calibration curves.[12] For example, the quantification of ovatoxins is carried out using a calibration curve obtained by analysing different dilution points of a non-certified standard solution of palytoxins (Wako Chemicals GmbH, Neuss, Germany). This is necessary because to date there is no standard of ovatoxins, but considering the small structural differences, we can admit the same molar response. For microcystins and cyclic imines some reference standard materials are available, and a calibration curve has been constructed for the quantification.

2nd step: sample pre-treatment

The determination of these emerging natural toxins in complex matrices through LC-MS, required specific pre-treatment of the samples, such as extraction, carried out using suitable solvents based on the analytes to be extracted; samples can be further sonicated and centrifuged several times according to the standard operating procedure. For examples, the extraction of a cyanobacterial biomass is carried out in 75% aqueous methanol (v/v) and after sonication and centrifugation, the procedure is repeated a second time using the same solvent mixture, and a third time using n-butanol. The resulting three supernatants were combined and dried under a gentle nitrogen stream and then reconstituted with the desired volume of aqueous methanol and analysed by LC-HRMS.[14] On the other hand, the extraction of ovatoxins from algal pellet required a different treatment: a methanol/water 1:1 solution (3mL x 10^6 cells) is added, vortexed, sonicated and centrifugated for three times and then the sample is ready for the LC-HRMS analysis.[15]

Sample pre-treatments including purification steps such as solid phase extraction (SPE) which remains the most popular means of extraction, concentration, and cleaning of analytes from complex sample matrices. This method employs a solid sorbent material to selectively retain the target analytes while unwanted matrix components are removed. SPE is based on the principles of selective adsorption and desorption. A solid sorbent, typically packed into a cartridge or disk, selectively interacts with the target analytes based on their chemical properties. The sample is loaded onto the SPE column, and the analytes of interest selectively adhere to the solid phase while interfering substances pass through. Various types of sorbents can be employed in SPE, such as silica, reversed-phase materials, ion-exchange resins, and molecularly imprinted polymers, for example, normal phase SPE, utilizes a polar sorbent and a nonpolar elution solvent, while the reversed-phase SPE employs a nonpolar sorbent and a polar elution solvent and the ion-exchange SPE is based on the charge of the analytes and the sorbent. The choice of sorbent depends on the physicochemical properties of the analytes and the desired selectivity (Figure II.4).[16] For examples, the SPE procedure described by Tartaglione et al. in 2016, about the extraction of palytoxin from seawater was successfully applied to evaluate the recovery yields of Palytoxin in the supernatant obtained after the incubation with cyclodextrins and eluted through SPE cartridges (Oasis HLB Cartridge, 1cc, 10mg). This procedure consists in four steps, a conditioning of the cartridge with a gradient of methanol from 100% to 0%, the loading of the sample, the washes in water and then in methanol and finally the elution of the clean fraction in methanol 80% + 0.1% TFA.[17]

Solid-phase extraction is a versatile and widely utilized technique that plays a crucial role in improving the sensitivity, accuracy, and precision of analytical methods by effectively preparing samples for subsequent analysis.

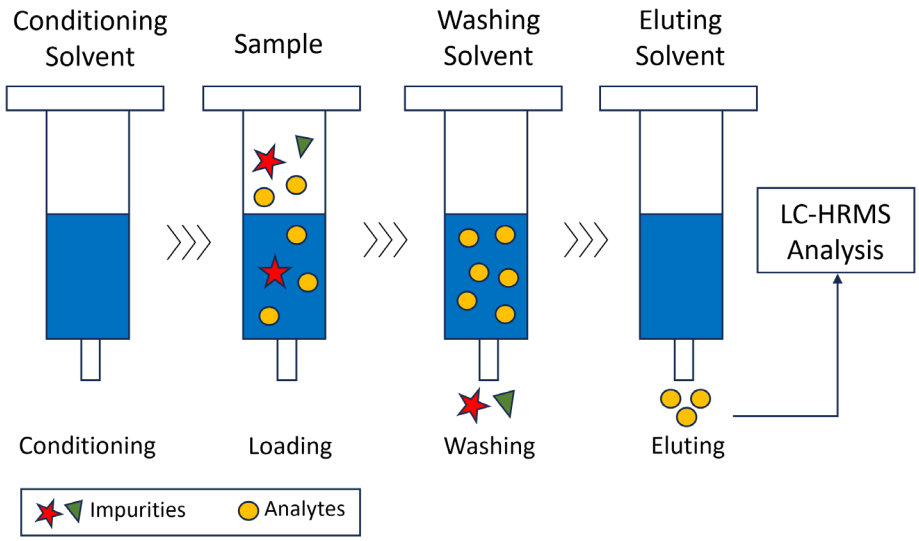

Figure II.4. Solid phase extraction (SPE) steps.

3rd step: LC-HRMSn approaches for characterization of unknown compounds

LC-HRMS^n has become a powerful tool for the complete analysis of all measurable analytes present in a sample (untargeted analysis), including those not characterized and can only be achieved using high-resolution mass spectrometers. No prior knowledge of the sample is required in an untargeted study. While different identification strategies and approaches have been used, all nontarget discovery studies share the common workflow steps of i) producing highly resolved full-scan chromatograms and/or spectra to reveal all detectable ions in the sample, ii) selecting prospective analytes features from the full-scan data, iii) assigning plausible molecular formulas, iv) MS^n ($n \geq 2$) fragmentation experiments to confirm molecular formula and reveal structural information, and v) structural proposal or analyte confirmation through matching to a database suspects.[18] In this context fits the development and the ongoing curation of the CyanoMetDB, a comprehensive, publicly-accessible database detailing these secondary metabolites would facilitate research into their occurrence, functions

and toxicological risks. The CyanoMetDB is a highly curated, flat-file, openly accessible database of cyanobacterial secondary metabolites collated from 850 peer-reviewed articles published between 1967 and 2020. CyanoMetDB contains >2010 cyanobacterial metabolites and 99 structurally related compounds. This has nearly doubled the number of entries with complete literature metadata and structural composition information compared to previously available open access databases. The dataset includes microcytsins, cyanopeptolins, other depsipeptides, anabaenopeptins, microginins, aeruginosins, cyclamides, cryptophycins, saxitoxins, spumigins, microviridins, and anatoxins among other metabolite classes.7 In particular, at the current stage of the project, we have started implementing the database by including annotated fragmentation spectra of compounds that are as detailed as possible, in order to facilitate: (1) the detection and dereplication of known cyanobacterial toxins and secondary metabolites; (2) the identification of novel natural products from cyanobacteria; (3) research on biosynthesis of cyanobacterial secondary metabolites, including substructure searches; and (4) the investigation of their abundance, persistence, and toxicity in natural environments (Figure II.5).[19]

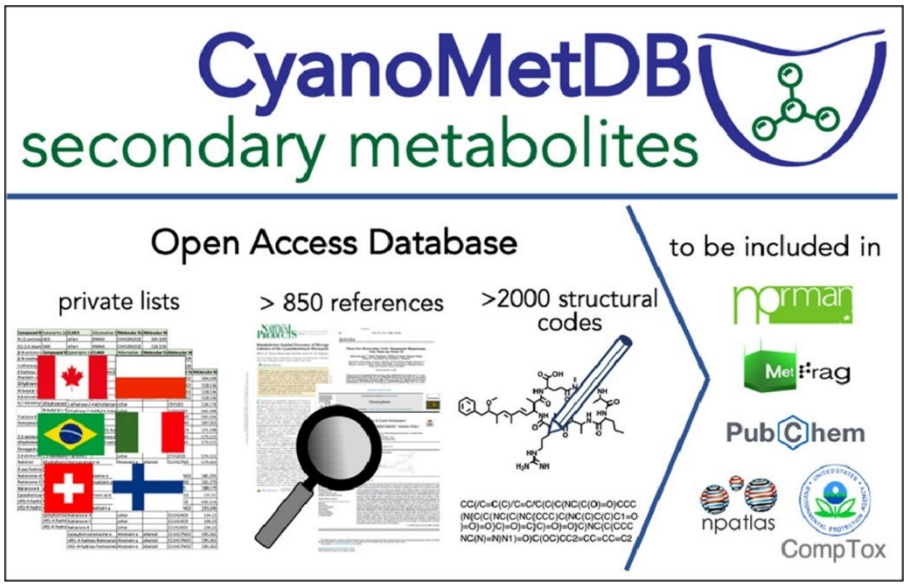

Figure II.5. CyanoMetDB, a highly curated, flat-file, openly accessible database of cyanobacterial secondary metabolites.

2.2 SENSORS AND BIOSENSORS

Sensors and biosensors are fundamental devices that play a critical role in collecting and interpreting data from the world around us. They are essential tools in various fields, spanning from industrial applications to healthcare, environmental monitoring, and scientific research. They are the sensory organs of the technological world, translating the real world into data for human interpretation or automated control systems. Sensors can detect subtle changes in their environment, making them invaluable in fields like environmental monitoring and healthcare. According to the IUPAC definition, a chemical sensor is a device that produces analytical responses based on chemical information from the analyte, encompassing the concentration of a specific sample component or overall composition analysis.[20,21] A biosensor, as per the same definition, is a type of chemical sensor wherein the recognition system employs a biochemical mechanism. Consequently, a chemical (bio)sensor serves as an analytical tool capable of detecting specific compounds or analytes in either a liquid or gas phase, offering insights into the chemical composition and concentration of the analytes in the solution. Typically, a (bio)sensor system comprises three integral components: (a) a (bio)recognition component for the specific detection of the analyte; (b) a signal transducer generating a measurable response from the analyte-(bio)recognition component; and (c) an electronic system for efficient data management. The objective in designing (bio)sensors is to create professional devices for the selective, sensitive, reproducible, rapid, cost-effective, and user-friendly detection of specific analytes.[22–24] Consequently, the miniaturization and automation of these (bio)sensors are crucial.

(Bio)sensors can be classified based on various criteria, including the transduction method, the type of recognition element used, and the application.[24] Considering the transduction method, the principal classes are represented by:

- Optical biosensors, that measure changes in light properties (e.g., absorbance, fluorescence).
- Electrochemical biosensors, that measure changes in electrical properties (e.g., current, voltage).
- Piezoelectric biosensors that measure changes in mass on a quartz crystal.
- Thermal biosensors that measure changes in heat production or absorption.

Currently, there is extensive research on electrochemical (bio)sensors, driven by their high sensitivity and stability and I worked on this kind of (bio)sensors during my PhD.

Over the last decade, significant technological advancements have been done in electrochemical (bio)sensors field; since the inception of the Clark Oxygen Electrode sensor, there have been notable enhancements in the sensitivity, selectivity, and multiplexing capabilities of modern biosensors.

According to an IUPAC recommendation in 1999, an electrochemical (bio)sensor is a self-contained integrated device, which is capable of providing specific quantitative or semi-quantitative analytical information using a recognition element (chemical receptor) which is kept in direct spatial contact with an electrochemical transduction element.[23] Electrochemical biosensors measure the current produced from oxidation and reduction reactions. The current produced can be correlated to either the concentration of the electroactive species present or its rate of production/consumption. The resulting electrical

signal is related to the recognition process by target and analyte and is proportional to the analyte concentration.

The most common configuration for running dynamic electrochemical experiments involves the use of three electrodes, the working electrode, a counter (auxiliary) electrode and a reference electrode, all connected to a commercially available potentiostat which allows the potential difference between the reference and working electrode. The reference electrode can be an Ag/AgCl, commercially available or fabricated within the laboratory. The counter electrode should be a non-reactive high surface area electrode such as platinum or carbon and the working electrode can be a plethora of configurations and compositions, indeed, researchers are trying to utilise graphene as an electrode material or as modification of the working electrode surface.

One of the major areas of interest for both centralized and non-centralized analysis is the development of portable systems and the reduction of sample volume.[25] And this interest is fulfilled by combination of electrochemical techniques with screen printed electrodes (SPEs). SPEs have revolutionized the area of decentralised electroanalysis due to their capacity to bridge the gap between lab to hand implementation. Screen printing emerges as a highly competitive technique for efficiently producing scalable and rapid printed microelectronics, benefiting from its cost-effectiveness, operational simplicity, and scalability.[22,26] This method involves the application of various inks onto ceramic, plastic, or paper substrates, providing versatility in electrode configuration, material compatibility, and modifications. It is noteworthy that ongoing research activities aim to develop screen-printed biosensors for diverse applications, such as environmental monitoring, clinical pathogen detection, biomarker development, pharmaceuticals, and the agri-food sectors.[26–28] SPEs serve as versatile platforms for detecting various biological species, including

DNA, antigen-antibody interactions, hormones, and forensic markers.[29–31] The field of screen-printed electrodes (SPEs) and screen-printed sensors is dynamically evolving, exerting a substantial impact in practical applications. The global SPEs market demonstrates remarkable growth potential, with projections indicating rapid expansion in the coming years, positioning it among the fastest-growing industries worldwide. Industry studies forecast significant development in the printed electronics sector, with the market set to surge from USD 41.2 billion in 2020 to USD 74 billion in 2030.[22] Screen-printed electrodes (SPEs) represent straightforward, cost-effective, highly sensitive, selective, and rapidly responsive techniques ideal for on-site analysis. Surprisingly, numerous companies offer SPEs, indicating a competitive market landscape. Notable players include Gamry Instrument, PalmSens, Zimmer and Peacock, Metrohm AG, Nano Research Elements, Rusens LTD., BVT Technologies, among others, but an advantage of these kind of technologies is the possibility to make them by yourself, in a customised and cost-effective way, described in the next paragraph.

1st step: screen-printed electrode fabrication

Typically, screen-printed electrodes (SPEs) comprise an inert substrate, housing a three-electrode system – namely the working electrode (WE), reference electrode (RE), and counter electrode (CE) – all printed onto a solid substrate (Figure II.6a). The use of screen printing in electrode fabrication has a rich history, with a fabrication procedure encompassing three to four key steps: the choice of the substrate, the creation of the screen-printed electrode, surface modification of the screen-printed electrode, and its subsequent applications in sensing. This process involves the application of ink or paste to the substrate, pushed through a woven mesh, and transferred onto a solid surface. Designing an effective SPE sensor involves various considerations, such as ink composition,

curing temperature, pre-treatment methods, and surface roughness. These factors collectively contribute to determining the sensor's sensitivity and selectivity, a recent focus in thick-film technology.[32–34]

- *Choice of the substrates*. The homemade production of disposable electrochemical (bio)sensors starts from the choice of the substrate, mainly paper and plastic. When a plastic sheet is used, no pre-treatment is required, while when a paper-based substrate (office or filter paper) is used, the porosity can represent a source of electrical noise due to diffusion of aqueous samples to connector: to avoid this, testing area is surrounded with a hydrophobic layer, i.e., melted wax, that prevents liquid flow toward the undesired portion of the strip. This is obtained through wax-printing (ColorQube 8580 from Xerox (USA, CT, Norwalk). Firstly, the wax pattern is drawn using common software like Paint, PowerPoint, or Adobe Illustrator. Then, a wax ink layer is printed onto the selected paper-based substrate. High temperature curing (>100°C) allows wax to melt forming a 3D hydrophobic barrier. It's possible also obtain a double layer of wax ink through wax-printing: the first wax ink layer was printed, cured and then the second layer was printed in order to obtain a more robust support. The office paper (Copy 2, 80 g/m2, Fabriano, Italy, Fabriano) is characterized by a thickness of ca. 90 mm and prepared using an ECF (elemental chlorine-free) technique, acid-free warranties, and described as ash-free. In the case of plastic-based substrates, no wax is required, because of their hydrophobic nature: an adhesive tape is enough to define the testing area.[6]

- *Screen-printing.* The next step in the screen-printed electrodes (SPEs) production consists in the effective printing of the three-electrode using a squeegee and two masks, one for the Ag/AgCl ink (Electrodag 477 SS, Acheson,

Italy, Milan), which was used to print the connections and the reference electrode, and one for the carbon ink (Electrodag 421, Acheson, Italy, Milan), which was used to print the working and counter electrodes. The diameter of the working electrode was 0.4 cm, the whole three-electrode system is ca. 2.5 cm (length) and 1 cm (width). Thermal curing, at 100°C and 60 °C for 30 and 15 min, respectively when plastic or paper are used as substrates, was necessary to make the printed ink stable for electrochemical measurements (Figure II.6a, 6b).

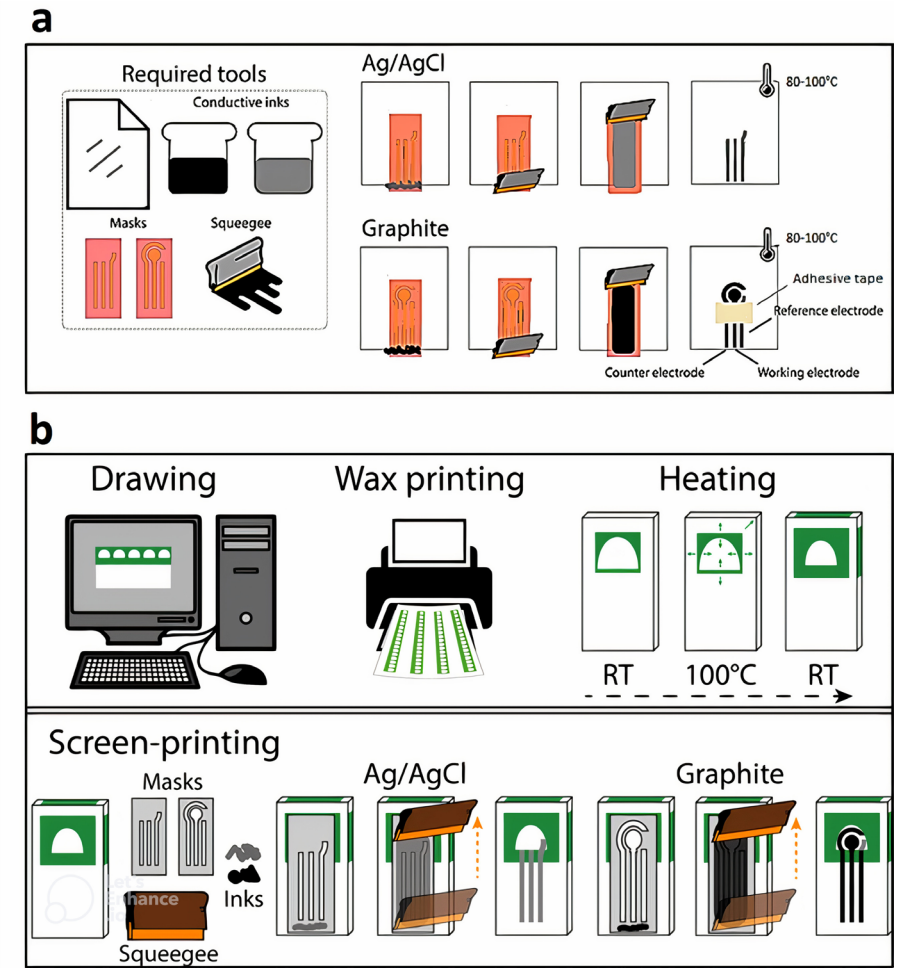

Figure II.6. Screen-printing procedure on a) polyester b) paper substrates.

2nd step: using a modifier to enhance and/or tailor electrodes performance

A strategy for increasing the performance and selectivity of electrochemical (bio)sensors is the use of nanostructured materials such as metallic nanoparticles, carbon-based nanomaterials (carbon black and graphene), carbon coatings, membranes, and even some conductive polymers can be used for enhancing performances; it depends on the analytical needs.[35–37] Gold nanoparticles (AuNPs) have unique properties, such as their high surface area, excellent conductivity, and biocompatibility, that make them ideal candidates for enhancing the sensitivity and selectivity and improve the electrochemical performance of the (bio)sensor; infact, the large surface area of the nanoparticles provides ample sites for the immobilization of recognition elements, such as specific ligands or biomolecules while the catalytic activity of gold nanoparticles contributes to the efficient electrochemical reduction of heavy metal ions, facilitating their detection at lower concentrations. The combination of screen-printed electrodes and gold nanoparticles offers a cost-effective and scalable platform for heavy metal sensing, making it suitable for various applications, including environmental monitoring, industrial safety, and water quality assessment.[38–40] The procedure applied for the synthesis of the AuNPs consists in a modified Turkevich method, in which after the cleaning of all glassware and the magnetic stir bar used with aqua regia (HCl/HNO_3 of 3:1, v/v) and piranha solution (H_2SO_4/H_2O_2 of 7:3, v/v), 9 mL of ultrapure water and 1 mL of the 10 mg/mL $HAuCl_4$ solution (30 mM) are added into the flask placed on a magnetic plate. Then, 2 mL of the 10 mg/mL trisodium citrate dihydrate solution (34 mM) are added and finally 500 μL of the 0.8 mg/mL $NaBH_4$ solution (21 mM) drop by drop. The reaction was left under stirring overnight at room temperature.[41,42] AuNPs modification is also fundamental for biological/biomimetic molecules

immobilization at the screen-printed electrode surface when the element is suitable customized with C6-SH, allowing covalent binding onto AuNPs.[43]

Carbon-based materials were mainly used into enzyme-based biosensors in order to significantly enhance the surface area-to-volume ratio, facilitating the immobilization of a greater number of enzyme molecules and thereby improving the overall enzyme–substrate interaction. Moreover, they exhibit high electrical conductivity, optical characteristics, and biocompatibility, contributing to effective signal transmission and detection. A simple and useful example is represented by carbon black, characterized by its fine particle size, typically in the nanometer range, and a high surface area. Considering the enzyme-based biosensors, the combination of carbon black and Prussian blue presents a compelling approach for enzyme immobilization on the surface of screen-printed electrodes. Prussian blue is a dark blue pigment with a complex chemical composition, historically known as Ferric Hexacyanoferrate (II). It is a coordination compound with the formula $Fe\,[Fe(CN)_6]^3 \cdot xH_2O$, and its deep blue color results from the interaction between iron (III) ions and cyanide ligands. When it is used in combination with carbon black in the enzyme-based biosensors, it contributes to the immobilization process by providing a stable and biocompatible environment for the enzymes.[44,45] Its unique chemical structure and electrochemical properties make it suitable for facilitating electron transfer during enzymatic reactions, improving the overall efficiency of the biosensor; at the same time, the carbon black has the dual function of hosting the composite and improving conductivity. This synergistic integration leverages the unique properties of both materials to enhance the overall performance of the electrode and the efficiency of enzyme immobilization. [46-48]

The use of biological/biomimetic molecules can be also considered as modification of the electrode surface towards a specific target analyte.

Considering this, (bio)sensors can be classified by the type of biological signaling mechanism they utilize DNA/nucleic acid sensors is based on recognition of the complementary single strand of DNA to form a stable hydrogen bond between two nucleic acids to become a double stranded DNA. Exposure of the target to the probe which results in hybridization of complementary ssDNA to form dsDNA will result in the production of a biochemical reaction that allows the transducer to amplify the signal into an electrical one;[29,48,50] aptasensors use aptamers (synthetic strands of nucleic acid) as the biocomponent to recognize small molecules (amino acids, oligosaccharides proteins, toxins),[43,51,52] immunosensors are composed of an antigen/antibody as bioreceptor as a tool for clinical diagnostics and enzyme-based sensors associate intimately a biocatalyst-containing a sensing layer with a transducer (Figure II.7).[46,47]

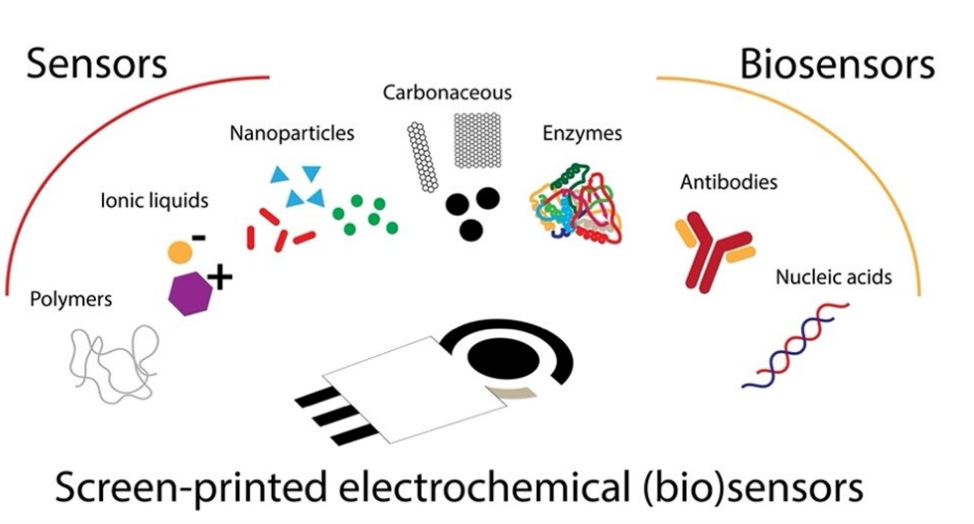

Figure II.7. Modifiers to enhance and/or tailor electrodes performance.

3rd step: electroanalysis

Depending on the architecture of the (bio), different electroanalysis techniques can be adopted to investigate and quantify various analytes.[25] The commonly used techniques are summarized below:

- Cyclic Voltammetry (CV) involves applying a potential sweep to the working electrode and measuring the resulting current. The potential is swept back and forth in a cyclic manner. It facilitates the swift determination of redox potentials specific to the electroactive species being studied, offering valuable insights into the thermodynamics of redox processes, kinetics of heterogeneous electron-transfer reactions, and the analysis of interconnected electrochemical reactions or adsorption processes.
- In the pulsed voltammetry, when a step-in pulse is applied, the current is sampled when the capacitative current (IC) decays away. To achieve this pulse widths are chosen to meet this condition. In pulse techniques such as differential pulse and square wave voltammetry, the capacitative contribution is eliminated via subtraction. The Differential Pulse Voltammetry (DPV) measures the difference between two currents just before the end of the pulse and just before its application. The difference between the two sampled currents is plotted against the staircase potential leading to a peak shaped waveform. DPV is employed for enhancing the sensitivity of electrochemical measurements, particularly for detecting low-concentration analytes.

  The Square Wave Voltammetry (SWV) applies a superimposed square wave to the potential applied during voltammetry; the currents at the end of the forward and reverse pulses are both registered as a function of staircase potential, leading to enhanced sensitivity and reduced

background noise. SWV is particularly useful for the detection of low-concentration analytes and for achieving better signal-to-noise ratios.

- In Chronoamperometry a constant potential is applied, and the resulting current is monitored as a function of time. The mass transport process throughout this process is solely governed by diffusion, and as such the current-time curve reflects the change in concentration at the electrodes surface. This involves the continuing growth of the diffusion layer associated with the depletion of reactant, thus a decrease in the concentration gradient is observed as time progresses. This technique is employed for studying electrode processes, determining kinetics, and monitoring concentration changes over time.
- Impedance Spectroscopy measures the impedance of an electrochemical system as a function of frequency. This technique provides information about the electrical properties of the electrode interface, including resistance and capacitance, and is often used for studying electrode modifications.
- Anodic Stripping Voltammetry (ASV) involves the deposition of the analyte at the working electrode by controlled potential electrolysis in a stirred solution at a suitable reduction potential, followed by a second phase in which the potential of the working electrode is scanned so that the deposited species is oxidized back to its ionic form. ASV is commonly used for the trace analysis of heavy metals and other electroactive species.

The performance of these sensors, particularly in terms of sensitivity and stability, can be significantly influenced by the current density at the working electrode. Current density is a critical parameter that describes the current per

unit area of the electrode surface and is influenced by the electrode's material, design, and the operational conditions of the sensor.[53]

In the works discussed in this dissertation, all the electrochemical measurements were carried out using portable and battery-powered instrumentation, EmStat Blue or the MultiPalmSens 4, 8 channels (PalmSens, the Netherlands), and data were recorded with PalmSens potentiostat software PsTrace interfaced with a laptop. Currents can be recorded and displayed on a laptop and/or smartphone by using a dedicated app, e.g., PStouch, which can be used with all PalmSens and EmStat potentiostats.

2.3 GENERAL OBJECTIVES

During my PhD, I focused my studies mainly on the analysis of two different classes of emerging contaminants: emerging natural toxins of European interest and anthropogenic contaminants, originating from human activities, analyzed by liquid chromatography coupled with high-resolution mass spectrometry and electrochemical screen-printed (bio)sensors, respectively. During these three years, I have had the opportunity to delve into these two analytical techniques, addressing two different and complementary aspects of analytical chemistry applied to environmental monitoring and health surveillance, with the general objectives of:

- Develop and apply LC-HRMS analysis to identify different marine and freshwater toxins and evaluate different types of decontamination treatments in the field of emerging toxins.
- Design and conceptualize new architectures in the field of sensors and (bio)sensors.

The results achieved for each of these two categories are discussed in the following chapters. Although the two analytical techniques have not been applied to the analysis of the same analytes, but in two different fields, the combination of I) easy-to-use and portable decentralized approaches and II) validated, laboratory-referenced methodologies (liquid chromatography coupled with high-resolution mass spectrometry), could represent a step forward from the current paradigm: each approach should be seen as a plus point for the other, with the common goal of preserving human health and ecosystems.

All the performed studies fall within the objectives of my PhD project and resulted in 11 papers published during these years, 2 in press and 5 under preparation.

References

(1) Rosenfeld, P. E.; Feng, L. G. H. 16 - Emerging Contaminants. In *Risks of Hazardous Wastes*; Rosenfeld, P. E., Feng, L. G. H., Eds.; William Andrew Publishing: Boston, 2011; pp 215–222. https://doi.org/10.1016/B978-1-4377-7842-7.00016-7.

(2) Khan, S.; Naushad, Mu.; Govarthanan, M.; Iqbal, J.; Alfadul, S. M. Emerging Contaminants of High Concern for the Environment: Current Trends and Future Research. *Environmental Research* **2022**, *207*, 112609. https://doi.org/10.1016/j.envres.2021.112609.

(3) Ding, X.; Lan, W.; Gu, J.-D. A Review on Sampling Techniques and Analytical Methods for Microbiota of Cultural Properties and Historical Architecture. *Applied Sciences* **2020**, *10* (22), 8099. https://doi.org/10.3390/app10228099.

(4) ENETWILD-consortium; Alves, P. C.; Gavier-Widen, D.; Ferroglio, E.; Queirós, J.; Rafael, M.; Santos, N.; Silva, T.; Gonçalves, C.; Vada, R.; Zanet, S.; Smith, G.; Gethöffer, F.; Keuling, O.; Staubach, C.; Sauter-Louis, C.; Blanco, J.; Podgorski, T.; Larska, M.; Richomme, C.; Knauf, S.; Rijks, J. M.; Pasetto, C.; Benatti, F.; Poncina, M.; Gómez, A.; Dups-Bergmann, J.; Neimanis, A.; Vicente, J. Literature Review on the Main Existing Structures and Systematic/Academic Initiatives for Surveillance in the EU for Zoonoses in the Environment and the Methods for Surveillance of Pathogens in the Environment. *EFSA Supporting Publications* **2022**, *19* (12), 7792E. https://doi.org/10.2903/sp.efsa.2022.EN-7792.

(5) Development, O. of R. &. *A Literature Review of Wipe Sampling Methods for Chemical Warfare Agents and Toxic Industrial Chemicals*. https://cfpub.epa.gov/si/si_public_record_report.cfm?Lab=NHSRC&subject=Homeland%20Security%20Research&dirEntryId=238670 (accessed 2024-01-14).

(6) Miglione, A.; Napoletano, M.; Cinti, S. Electrochemical Biosensors for Tracing Cyanotoxins in Food and Environmental Matrices. *Biosensors* **2021**, *11* (9), 315. https://doi.org/10.3390/bios11090315.

(7) De Girolamo, A.; Lippolis, V.; Pascale, M. Overview of Recent Liquid Chromatography Mass Spectrometry-Based Methods for Natural Toxins Detection

in Food Products. *Toxins* **2022**, *14* (5), 328. https://doi.org/10.3390/toxins14050328.

(8) *Mass Spectrometry: Principles and Applications, 3rd Edition | Wiley*. Wiley.com. https://www.wiley.com/en-be/Mass+Spectrometry%3A+Principles+and+Applications%2C+3rd+Edition-p-9780470033104 (accessed 2024-01-14).

(9) Hyphenated Separation Techniques. In *Fundamentals of Contemporary Mass Spectrometry*; John Wiley & Sons, Ltd, 2007; pp 151–194. https://doi.org/10.1002/9780470118498.ch5.

(10) Johnson, J. V.; Yost, R. A.; Kelley, P. E.; Bradford, D. C. Tandem-in-Space and Tandem-in-Time Mass Spectrometry: Triple Quadrupoles and Quadrupole Ion Traps. *Anal. Chem.* **1990**, *62* (20), 2162–2172. https://doi.org/10.1021/ac00219a003.

(11) Yost, R. A.; Enke, C. G. Selected Ion Fragmentation with a Tandem Quadrupole Mass Spectrometer. *J. Am. Chem. Soc.* **1978**, *100* (7), 2274–2275. https://doi.org/10.1021/ja00475a072.

(12) Zubarev, R. A.; Makarov, A. Orbitrap Mass Spectrometry. *Anal. Chem.* **2013**, *85* (11), 5288–5296. https://doi.org/10.1021/ac4001223.

(13) Vanhaecke, L.; Van Meulebroek, L.; De Clercq, N.; Bussche, J. V. High Resolution Orbitrap Mass Spectrometry in Comparison with Tandem Mass Spectrometry for Confirmation of Anabolic Steroids in Meat. *Analytica Chimica Acta* **2013**, *767*, 118–127. https://doi.org/10.1016/j.aca.2013.01.009.

(14) Christophoridis, C.; Zervou, S.-K.; Manolidi, K.; Katsiapi, M.; Moustaka-Gouni, M.; Kaloudis, T.; Triantis, T. M.; Hiskia, A. Occurrence and Diversity of Cyanotoxins in Greek Lakes. *Sci Rep* **2018**, *8* (1), 17877. https://doi.org/10.1038/s41598-018-35428-x.

(15) Tartaglione, L.; Dello Iacovo, E.; Mazzeo, A.; Casabianca, S.; Ciminiello, P.; Penna, A.; Dell'Aversano, C. Variability in Toxin Profiles of the Mediterranean Ostreopsis

Cf. Ovata and in Structural Features of the Produced Ovatoxins. *Environ. Sci. Technol.* **2017**, *51* (23), 13920–13928. https://doi.org/10.1021/acs.est.7b03827.

(16) Buszewski, B.; Szultka, M. Past, Present, and Future of Solid Phase Extraction: A Review. *Critical Reviews in Analytical Chemistry* **2012**, *42* (3), 198–213. https://doi.org/10.1080/07373937.2011.645413.

(17) Tartaglione, L.; Dell'Aversano, C.; Mazzeo, A.; Forino, M.; Wieringa, A.; Ciminiello, P. Determination of Palytoxins in Soft Coral and Seawater from a Home Aquarium. Comparison between Palythoa- and Ostreopsis-Related Inhalatory Poisonings. *Environ. Sci. Technol.* **2016**, *50* (2), 1023–1030. https://doi.org/10.1021/acs.est.5b05469.

(18) Varriale, F.; Tartaglione, L.; Zervou, S.-K.; Miles, C. O.; Mazur-Marzec, H.; Triantis, T. M.; Kaloudis, T.; Hiskia, A.; Dell'Aversano, C. Untargeted and Targeted LC-MS and Data Processing Workflow for the Comprehensive Analysis of Oligopeptides from Cyanobacteria. *Chemosphere* **2023**, *311*, 137012. https://doi.org/10.1016/j.chemosphere.2022.137012.

(19) Jones, M. R.; Pinto, E.; Torres, M. A.; Dörr, F.; Mazur-Marzec, H.; Szubert, K.; Tartaglione, L.; Dell'Aversano, C.; Miles, C. O.; Beach, D. G.; McCarron, P.; Sivonen, K.; Fewer, D. P.; Jokela, J.; Janssen, E. M.-L. CyanoMetDB, a Comprehensive Public Database of Secondary Metabolites from Cyanobacteria. *Water Research* **2021**, *196*, 117017. https://doi.org/10.1016/j.watres.2021.117017.

(20) Nagel, B.; Dellweg, H.; Gierasch, L. M. Glossary for Chemists of Terms Used in Biotechnology (IUPAC Recommendations 1992). *Pure and Applied Chemistry* **1992**, *64* (1), 143–168. https://doi.org/10.1351/pac199264010143.

(21) *Chemical Sensors: Definitions and Classification*. De Gruyter. https://www.degruyter.com/database/IUPAC/entry/iupac.63.0073/html (accessed 2024-01-14).

(22) Singh, S.; Wang, J.; Cinti, S. Review—An Overview on Recent Progress in Screen-Printed Electroanalytical (Bio)Sensors. *ECS Sens. Plus* **2022**, *1* (2), 023401. https://doi.org/10.1149/2754-2726/ac70e2.

(23) Thévenot, D. R.; Toth, K.; Durst, R. A.; Wilson, G. S. Electrochemical Biosensors: Recommended Definitions and classification1International Union of Pure and Applied Chemistry: Physical Chemistry Division, Commission I.7 (Biophysical Chemistry); Analytical Chemistry Division, Commission V.5 (Electroanalytical Chemistry).1. *Biosensors and Bioelectronics* **2001**, *16* (1), 121–131. https://doi.org/10.1016/S0956-5663(01)00115-4.

(24) Perumal, V.; Hashim, U. Advances in Biosensors: Principle, Architecture and Applications. *Journal of Applied Biomedicine* **2014**, *12* (1), 1–15. https://doi.org/10.1016/j.jab.2013.02.001.

(25) Electrochemical Sensors. In *Analytical Electrochemistry*; John Wiley & Sons, Ltd, 2006; pp 201–243. https://doi.org/10.1002/0471790303.ch6.

(26) Hayat, A.; Marty, J. L. Disposable Screen Printed Electrochemical Sensors: Tools for Environmental Monitoring. *Sensors* **2014**, *14* (6), 10432–10453. https://doi.org/10.3390/s140610432.

(27) Khanmohammadi, A.; Jalili Ghazizadeh, A.; Hashemi, P.; Afkhami, A.; Arduini, F.; Bagheri, H. An Overview to Electrochemical Biosensors and Sensors for the Detection of Environmental Contaminants. *J IRAN CHEM SOC* **2020**, *17* (10), 2429–2447. https://doi.org/10.1007/s13738-020-01940-z.

(28) Cinti, S. Novel Paper-Based Electroanalytical Tools for Food Surveillance. *Anal Bioanal Chem* **2019**, *411* (19), 4303–4311. https://doi.org/10.1007/s00216-019-01640-5.

(29) Singh, S.; Miglione, A.; Raucci, A.; Numan, A.; Cinti, S. Towards Sense and Sensitivity-Based Electrochemical Biosensors for Liquid Biopsy-Based Breast Cancer Detection. *TrAC Trends in Analytical Chemistry* **2023**, *163*, 117050. https://doi.org/10.1016/j.trac.2023.117050.

(30) Wang, L.; Lu, D.; Wang, J.; Du, D.; Zou, Z.; Wang, H.; Smith, J. N.; Timchalk, C.; Liu, F.; Lin, Y. A Novel Immunochromatographic Electrochemical Biosensor for Highly Sensitive and Selective Detection of Trichloropyridinol, a Biomarker of

Exposure to Chlorpyrifos. *Biosensors and Bioelectronics* **2011**, *26* (6), 2835–2840. https://doi.org/10.1016/j.bios.2010.11.008.

(31) Ferreira, P. C.; Ataíde, V. N.; Silva Chagas, C. L.; Angnes, L.; Tomazelli Coltro, W. K.; Longo Cesar Paixão, T. R.; Reis de Araujo, W. Wearable Electrochemical Sensors for Forensic and Clinical Applications. *TrAC Trends in Analytical Chemistry* **2019**, *119*, 115622. https://doi.org/10.1016/j.trac.2019.115622.

(32) Cinti, S.; Moscone, D.; Arduini, F. Preparation of Paper-Based Devices for Reagentless Electrochemical (Bio)Sensor Strips. *Nature Protocols* **2019**, *14* (8), 2437–2451. https://doi.org/10.1038/s41596-019-0186-y.

(33) Cinti, S.; Talarico, D.; Palleschi, G.; Moscone, D.; Arduini, F. Novel Reagentless Paper-Based Screen-Printed Electrochemical Sensor to Detect Phosphate. *Analytica Chimica Acta* **2016**, *919*, 78–84. https://doi.org/10.1016/j.aca.2016.03.011.

(34) Raucci, A.; Miglione, A.; Spinelli, M.; Amoresano, A.; Cinti, S. A Hybrid Screen-Printed Strip for Enhanced Electroanalysis towards Lead and Cadmium in Multi-Matrices. *Journal of The Electrochemical Society* **2022**, *169* (3), 037516. https://doi.org/10.1149/1945-7111/ac5c98.

(35) Alhardan, R.; Kilic, N. M.; Cevher, S. C.; Soylemez, S.; Odaci, D.; Kurbanoglu, S. Chapter 18 - Detection of Toxic Metals Using Nanostructured Biosensing Platforms. In *Novel Nanostructured Materials for Electrochemical Bio-Sensing Applications*; Manjunatha, J. G., Ed.; Elsevier, 2024; pp 463–503. https://doi.org/10.1016/B978-0-443-15334-1.00016-X.

(36) Aftab, S.; Kurbanoglu, S. Chapter 17 - Advanced Nanostructured Material-Based Biosensors in Clinical and Forensic Diagnosis. In *Novel Nanostructured Materials for Electrochemical Bio-Sensing Applications*; Manjunatha, J. G., Ed.; Elsevier, 2024; pp 429–461. https://doi.org/10.1016/B978-0-443-15334-1.00015-8.

(37) Yashaswini; Pratibha, S.; Vinay Kumar, Y. B.; Sudheer Kumar, K. H. Chapter 10 - Nanostructured Electrochemical Biosensors for Pesticides and Insecticides. In *Novel Nanostructured Materials for Electrochemical Bio-Sensing Applications*;

Manjunatha, J. G., Ed.; Elsevier, 2024; pp 195–214. https://doi.org/10.1016/B978-0-443-15334-1.00010-9.

(38) Bagheri, N.; Mazzaracchio, V.; Cinti, S.; Colozza, N.; Di Natale, C.; Netti, P. A.; Saraji, M.; Roggero, S.; Moscone, D.; Arduini, F. Electroanalytical Sensor Based on Gold-Nanoparticle-Decorated Paper for Sensitive Detection of Copper Ions in Sweat and Serum. *Anal. Chem.* **2021**, *93* (12), 5225–5233. https://doi.org/10.1021/acs.analchem.0c05469.

(39) Castañeda, M. T.; Alegret, S.; Merkoçi, A. Electrochemical Sensing of DNA Using Gold Nanoparticles. *Electroanalysis* **2007**, *19* (7–8), 743–753. https://doi.org/10.1002/elan.200603784.

(40) Miglione, A.; Spinelli, M.; Amoresano, A.; Cinti, S. Sustainable Copper Electrochemical Stripping onto a Paper-Based Substrate for Clinical Application. *ACS Meas. Au* **2022**. https://doi.org/10.1021/acsmeasuresciau.1c00059.

(41) Daruich De Souza, C.; Ribeiro Nogueira, B.; Rostelato, M. E. C. M. Review of the Methodologies Used in the Synthesis Gold Nanoparticles by Chemical Reduction. *Journal of Alloys and Compounds* **2019**, *798*, 714–740. https://doi.org/10.1016/j.jallcom.2019.05.153.

(42) Turkevich, J.; Stevenson, P. C.; Hillier, J. A Study of the Nucleation and Growth Processes in the Synthesis of Colloidal Gold. *Discuss. Faraday Soc.* **1951**, *11* (0), 55–75. https://doi.org/10.1039/DF9511100055.

(43) Miglione, A.; Raucci, A.; Amato, J.; Marzano, S.; Pagano, B.; Raia, T.; Lucarelli, M.; Fuso, A.; Cinti, S. Printed Electrochemical Strip for the Detection of miRNA-29a: A Possible Biomarker Related to Alzheimer's Disease. *Anal. Chem.* **2022**, *94* (45), 15558–15563. https://doi.org/10.1021/acs.analchem.2c03542.

(44) Aller-Pellitero, M.; Fremeau, J.; Villa, R.; Guirado, G.; Lakard, B.; Hihn, J.-Y.; del Campo, F. J. Electrochromic Biosensors Based on Screen-Printed Prussian Blue Electrodes. *Sensors and Actuators B: Chemical* **2019**, *290*, 591–597. https://doi.org/10.1016/j.snb.2019.03.100.

(45) Ricci, F.; Palleschi, G. Sensor and Biosensor Preparation, Optimisation and Applications of Prussian Blue Modified Electrodes. *Biosensors and Bioelectronics* **2005**, *21* (3), 389–407. https://doi.org/10.1016/j.bios.2004.12.001.

(46) Wooten, M. D. Electrochemical Sensors Based on Enzymes, Biopolymers and Nanoparticles. **2010**.

(47) Fall, I., Doumèche, B., Abdellaoui, S., Rémond, C., Rakotoarivonina, H., & Ochs, M. (2024). based electrodes as a tool for detecting ligninolytic enzymatic activities. Bioelectrochemistry, 156, 108609.

(48) Cinti, S.; Cusenza, R.; Moscone, D.; Arduini, F. Paper-Based Synthesis of Prussian Blue Nanoparticles for the Development of Whole Blood Glucose Electrochemical Biosensor. *Talanta* **2018**, *187*, 59–64. https://doi.org/10.1016/j.talanta.2018.05.015.

(49) Cinti, S.; Proietti, E.; Casotto, F.; Moscone, D.; Arduini, F. Paper-Based Strips for the Electrochemical Detection of Single and Double Stranded DNA. *Anal. Chem.* **2018**, *90* (22), 13680–13686. https://doi.org/10.1021/acs.analchem.8b04052.

(50) Cinti, S.; Cinotti, G.; Parolo, C.; Nguyen, E. P.; Caratelli, V.; Moscone, D.; Arduini, F.; Merkoci, A. Experimental Comparison in Sensing Breast Cancer Mutations by Signal ON and Signal OFF Paper-Based Electroanalytical Strips. *Anal. Chem.* **2020**, *92* (2), 1674–1679. https://doi.org/10.1021/acs.analchem.9b02560.

(51) Moccia, M.; Caratelli, V.; Cinti, S.; Pede, B.; Avitabile, C.; Saviano, M.; Imbriani, A. L.; Moscone, D.; Arduini, F. Paper-Based Electrochemical Peptide Nucleic Acid (PNA) Biosensor for Detection of miRNA-492: A Pancreatic Ductal Adenocarcinoma Biomarker. *Biosensors and Bioelectronics* **2020**, *165*, 112371. https://doi.org/10.1016/j.bios.2020.112371.

(52) Cimmino, W.; Migliorelli, D.; Singh, S.; Miglione, A.; Generelli, S.; Cinti, S. Design of a Printed Electrochemical Strip towards miRNA-21 Detection in Urine Samples: Optimization of the Experimental Procedures for Real Sample Application. *Anal Bioanal Chem* **2023**, *415* (18), 4511–4520. https://doi.org/10.1007/s00216-023-04659-x.

(53) Roslan, N. A. F., Ab Rahim, R., Ralib, A. A. M., Za'bah, N. F., Nordin, A. N., Bashri, M. S. R., ... & Sugandi, G. (2021, August). Simulation of geometrical parameters of screen printed electrode (SPE) for electrochemical-based sensor. In 2021 IEEE Regional Symposium on Micro and Nanoelectronics (RSM) (pp. 137-140). IEEE.

CHAPTER 3. LC-HRMS APPROACHES FOR THE ACCURATE AND SUSTAINABLE MONITORING OF EMERGING NATURAL TOXIN

Liquid Chromatography coupled to High-Resolution Mass Spectrometry is a powerful tool for the accurate and sustainable monitoring of emerging natural toxins. It is particularly effective in discovering new toxins or toxin analogues, as well as known toxins in new geographical areas. Accuracy of LC-HRMS makes it suitable for both targeted and non-targeted screening, allowing for the detection of a wide range of toxins, including those that may not have been previously identified. The technology is reliable, specific, and selective, making it well-suited for the detection of emerging toxins.[1–4] However, the broad screening capabilities of LC-HRMS also bring new challenges. The number of analytes that can be detected is too large to process and verify manually, which is how it is typically completed for quantitative LC-MS/MS methods. Therefore, databases with target analytes and sufficient information as retention and/or fragmentation are needed.[5] When such a database is available, dereplication of known analytes of interest from the raw data can be rapid and automated. We applied this strategy in the analysis of different samples, thanks to the possibility to use the CyanoMetDB for revealing cyanotoxins and cyanometabolites, as novel approach that allows a faster and automated analysis.[5] Novel strategies are also evaluated in terms of early monitoring of palytoxin and its congeners. This study, which is still ongoing, aims to evaluate the efficiency of the SPATT as new, valuable, and sustainable technology for passive sampling of these toxins.[6] Four experimental works, discussed below, were carried out following these strategies:

1) The identification of marine toxins in mucilage from the 2021 North-Eastern Aegean Sea episode, in which an extensive preliminary screening of possible classes of toxins involved in the phenomenon was evaluated, leading to the identification of cyclic imines as the main class produced by the mucilage.

2) Untargeted LC-HRMS applied to microcystin-producing cyanobacterial cultures for the evaluation of the efficiency of chlorine-based treatments commonly used for water potabilization, in which the CyanoMetDB helped identify known and unknown cyanotoxins and cyanometabolites.

3) CyanoMetDB update and implementation: monitoring key metabolites from cyanobacterial blooms of *planktothrix* spp., which included the implementation and application of the mentioned database on cyanobacterial blooms of *planktothrix* spp.

4) Development of a solid-phase toxin adsorption method (SPATT) based on cross-linked cyclodextrins for monitoring palytoxin and its congeners, in which SPATT technology was investigated as a novel early monitoring and decontamination tool applied to passive adsorption of palytoxin and its congeners.

3.1 IDENTIFICATION OF MARINE TOXINS IN MUCILAGE FROM THE 2021 NORTH-EASTERN AEGEAN SEA EPISODE

3.1.1 Introduction

Eutrophication and global warming have led to an increase in algal blooms worldwide. In some marine environments, these blooms come with the secretion of substantial amounts of extracellular mucilaginous-type organic matter produced by diatoms, bacteria, and dinoflagellates.[7,8] A related episode, with an intense mucilage formation was observed in the Sea of Marmaras in June 2021,[9] followed by a similar event in the North-Eastern Aegean Sea in the summer 2021. Mucilage samples collected from the Aegean Sea were the object of a study in collaboration with the Institute of Nanomaterial and Nanoscience, NCSR 'Demokritos.' Mucilage is recognized as a carrier of numerous microorganisms and a substrate for microbial colonization, including pathogenic forms.[10] These episodes are global, with the Mediterranean Sea experiencing several incidents, the most severe in the northern Adriatic Sea during the 1990s. The Adriatic Sea episodes covered large areas, both coastal and offshore. Mucilage events have also occurred along Greek, Spanish, and Italian coasts, impacting mostly the economy and tourism.[9,11,12] During mucilage incidents, the presence of various phytoplankton species are reported, but there is limited information on the occurrence of marine toxins in mucilage matter. Toxins produced by marine microalgae can accumulate in shellfish or finfish and reach humans through the food web, causing serious illnesses. Liquid chromatography coupled to tandem mass spectrometry (LC-MS/MS) has been widely used for toxin detection, and High-Resolution Mass Spectrometry (HRMS) untargeted approaches have become valuable for identification in environmental and food matrices. In the 2021 North-Eastern Aegean Sea episode, the class of toxins primarily involved

were cyclic imines (CIs), specifically the neurotoxin Pinnatoxin G (PnTX-G), detected and confirmed through LC-HRMS/MS experiments, in 5 out of the 7 samples analyzed.

Pinnatoxins are a group of marine toxins that belong to the larger class of CIs, which were first discovered in the mid-1990s. PnTXs were initially identified in the digestive glands of bivalves from the *Pinna* genus; they are produced by the dinoflagellate *Vulcanodinium rugosum*, which has been found in water samples from various locations including the Mediterranean lagoons in France, Japan, New Zealand, Australia, and France.[13,14] The discovery followed shellfish poisoning incidents in China and Japan, where the adductor muscle of *P. attenuata* is commonly used in sushi. Since the 1990s, various PnTX structural variants (PnTX A-H and PnTX 7-methyl ester; Figure III.1) have been identified. All PnTXs feature a 7-membered cyclic imine unit spiro-linked to a cyclohexene moiety within a 27-membered carbocyclic backbone, characterized by spiroketal systems and different functional groups at C21, C22, C28, and C33 (Figure III.1).[15]

Different strains of *V. rugosum* produce PnTX E-H, while PnTX A-C and PnTX-D are considered derivatives of PnTX-G and PnTX E-F, respectively, resulting from hydrolytic and oxidative transformations in shellfish. The toxic profile of *V. rugosum* varies among strains, leading to different PnTX profiles in contaminated bivalves, depending on the algal strains encountered by filter feeding organisms.[14] Acute toxicity studies reveal that PnTXs rank among the most toxic CI sub-groups, displaying the highest toxicity through oral administration and intraperitoneal (IP) injection. Noteworthy variations in toxicity exist among PnTX analogues. In mouse studies on IP administration, an initial study in 2001 indicated that PnTX-B and -C were the most toxic congeners, with a 1:1 mixture displaying an LD99 of 22.0 μg/Kg. More recent

assessments revealed the following LD50 values: PnTX-F (12.7 μg/Kg), PnTX-G (48.0 μg/Kg), PnTX-E (57.0 μg/Kg), PnTX-H (67.0 μg/Kg), and PnTX-A (114.8 μg/Kg).[16,17]

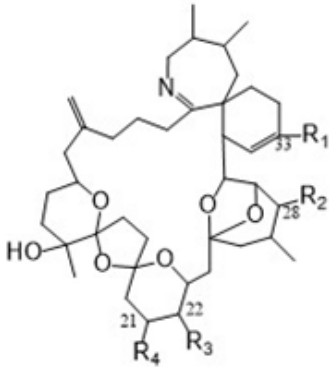

	$[M+H]^+$ *m/z*	R_1	R_2	R_3	R_4
PnTX-A	712.4419	—CO_2H	OH	H	H
PnTX-B (36*S*), -C (36*R*)	741.4685	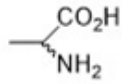	OH	H	H
PnTX-D	782.4838	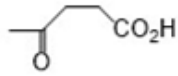	H	OH	CH_3
PnTX-E	784.4994	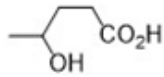	H	OH	CH_3
PnTX-F	766.4889	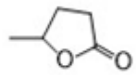	H	OH	CH_3
PnTX-G	694.4677		OH	H	H
PnTX-H	708.4834		H	OH	CH_3
PnTX-7-methyl ester	798.5151	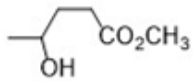	H	OH	CH_3
PtTX-A	831.4824	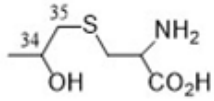	OH	H	H
PtTX-B (34*R*), -C (34*S*)	831.4824	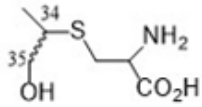	OH	H	H

Figure III.1. Planar structure and exact mass of PnTXs and PtTXs.

The Portimines, a significant class of marine toxins, are the smallest sub-group of cyclic imines (CIs) and consist of three secondary metabolites known as protamine A, protamine B, and kabirimine (Figure III.2). These toxins were isolated from the marine benthic dinoflagellate *Vulcanodinium rugosum*. Portimines are polycyclic ether toxins containing a cyclic imine moiety, and they are part of the larger group of marine lipophilic toxins (MLTs) originating from seawater phytoplankton, specifically dinoflagellates. Alongside other CIs such as spirolides (SPXs), gymnodimines (GYMs), pinnatoxins (PnTXs), and pteriatoxins (PtTXs), portimines have been detected in algae and mussels, contributing to the understanding of the diversity of marine biotoxins. The discovery of CIs, including portimines, has expanded the knowledge of marine toxins and their potential impact on marine ecosystems and human health. The name "portimine" originates from Portodonium honu, an initial name given to the dinoflagellate *V. rugosum*, while "kabirimine" is named after Kabira Bay, the location in Okinawa where the microalgal strain producing it was originally harvested (Figure III.2).[15,18,19]

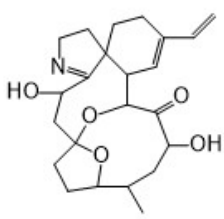

	$[M+H]^+$ *m/z*
Portimine A	402.2275

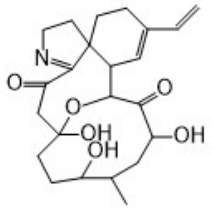

	$[M+H]^+$ *m/z*
Portimine B	418.2224

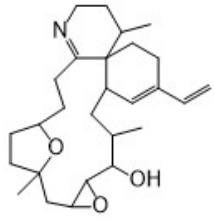

	$[M+H]^+$ *m/z*
Kabirimine	428.3159

Figure III.2. Planar structure and exact mass of $[M+H]^+$ ion of Portimines.

Acute toxicity studies revealed that portimine A is one of the least potent CI since a LD50 = 1570 μg/Kg was measured by IP injection in mice. On the other hand, portimine A exhibited a remarkable activity as antiproliferative agent and its cytotoxicity in cancer cells was about 100-fold higher than that observed for PnTX-F. The anticancer mechanism of portimine A lies into the ability to induce apoptotic death in Jurkat T-lymphoma cells through caspase-3 activation.[20] Moreover, this biological activity, never reported for any of the marine natural products so far, configured portimine A as potent antifungal agent. Portimine B displayed the same anticancer activity of portimine A, even if it was less potent, while kabirimine exhibited antiviral activity against the respiratory syncytial virus (RSV).[19–21] The presence of these toxins was studied in the frame of the International Agreement Type A between National Centre for Scientific Research "Demokritos" (Athens, Greece) and University of Napoli Federico II, following the emergency related to the extraordinary presence of mucilage that first surrounded the Turkish coasts and then the beaches of Limnos Island during the month of June 2021, using a combination of tandem MS/MS and HRMS-based techniques.

3.1.2 Experimental section

Mucilage samples were collected from multiple coastal sites of Limnos Island, North Aegean Sea, Greece, during the episode, in July 2021 (Table 1, Figure III.3). Detection and quantification of potentially toxic microalgae and microalgae associated with mucus production was carried out by applying a method based on EN 15204:2006.[22] Additionally, samples (5 mL) were centrifuged to separate the seawater from the phytoplankton pellet. The pellets were extracted with 5 mL of pure methanol in a sonication bath for 15 min. The extracts were evaporated to dryness under a nitrogen stream and re-dissolved in

500 μL of methanol. After sampling conducted in duplicate in 7 different coastal areas of the Island, one batch of samples was frozen (-24ºC) and shipped to MarBioTox laboratories together with methanol extracts obtained at NCSR "Demokritos" (Athens). The activities carried out at MarBioTox group involved the extraction of the batch of samples sent to us, with a mixture of MeOH\$H_2O$ 8:2, in order to extract even more hydrophilic toxins. The extraction procedure started with the separation of the biomass from the water by centrifugation; then each weighed sample (~5 g) was firstly extracted by adding 15 mL of MeOH\$H_2O$ 8:2, sonicated in ice bath for 5min, centrifugated at 5000 rpm for 10 min and collection of the supernatant. The phytoplankton samples were extracted in the same way for a second cycle (2^{nd} extraction) and a third time with only methanol, to obtain a final volume of 45mL. Each sample was evaporated to dryness under nitrogen steam and using a rotary evaporator, reconstituted in 500 μL of MeOH, sonicated and filtered through 0.45 μm centrifugal filters and transferred to vials for analysis.

Table 1. Description of marine phytoplankton samples.

Sample ID	**Sample Details** (see figure III.3a)	**Sampling Date**
1a	Site 1	25/6/2021
2a	Site 2	25/6/2021
3a	Site 3	25/6/2021
4a	Site 4	26/6/2021
5a	Site 5	26/6/2021
6a	Site 6	26/6/2021
7a	Site 7	26/6/2021

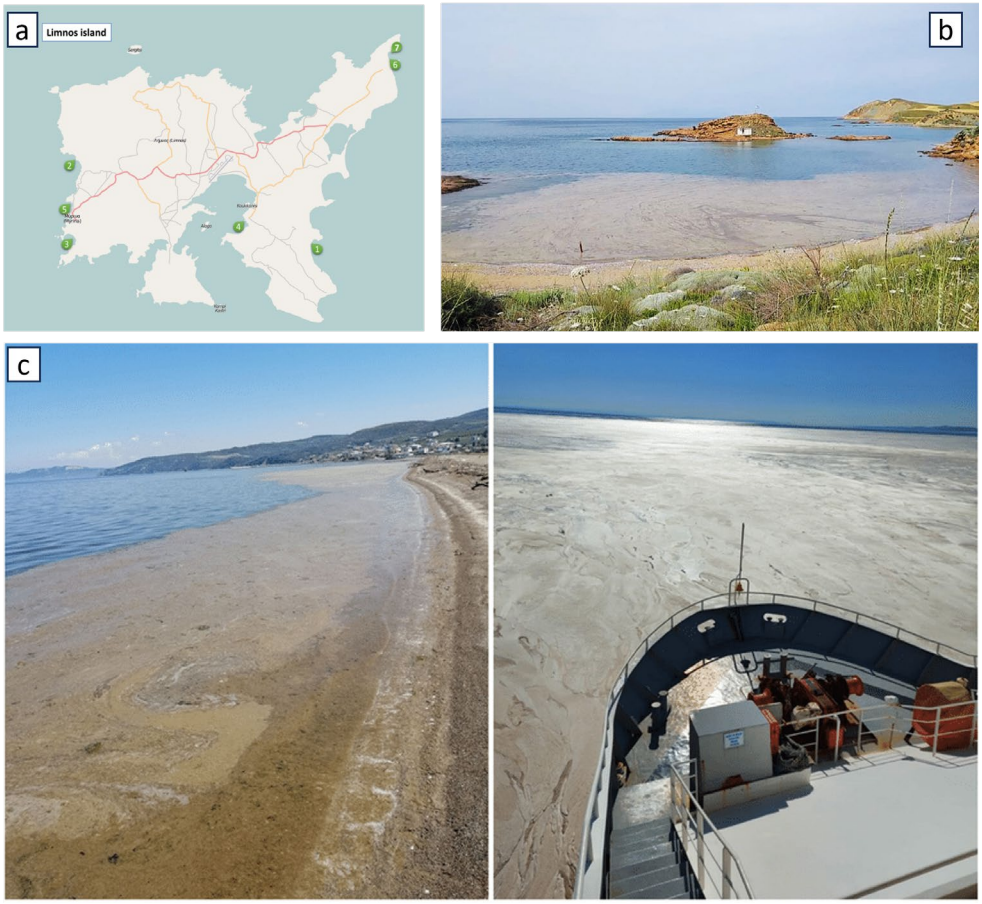

Figure III.3. a) Map of Limnos Island, Greece, with indication of sampling sites, b) mucilage spread on beaches of Limnos Island, c) mucilage spread on Turkish coasts.

Investigation for the presence of a wide number of marine toxins belonging to the classes of Pinnatoxins (PnTXs), Gymnodimines (GYMs), Yessotoxins (YTXs), Pectenotoxins (PTXs), Prorocentrolides, Azaspiracids (AZAs), Spirolides (SPXs), Okadaic acid and Dinophysitoxin analogues (OAs & DTXs), Palytoxins (PLTXs) and Palytoxin-like compounds (OVTXs), Paralytic Shellfish Poisoning Toxins (PSPs), Portimines and other toxins (i.e., Domoic acid, Spiro-prorocentrimine and Kabirimine) was carried out by LC-MS/MS and LC-HRMS. LC-MS/MS analysis was carried out at Demokritos, with a triple

quadrupole mass spectrometer (TSQ Discovery Max, Thermo) in multiple reaction monitoring mode (MRM). LC-HRMS analysis was carried out at MarBioTox UniNa laboratories, with an LTQ-Orbitrap XL^{TM} FTMS, (Thermo) in full scan HRMS^{n} (n= 1,2) and data depending on acquisition (DDA) mode. Electrospray ionization in positive mode was used in both cases. Chromatographic separation was achieved as reported in literature.[15]

Liquid chromatography–high resolution mass spectrometry (LC-HRMS) on LTQ-Orbitrap XL^{TM} FTMS

LC-HRMS analyses were carried out on a hybrid linear ion trap LTQ Orbitrap XL™ Fourier Transform Mass Spectrometer (FTMS) equipped with an ESI ION MAX™ source coupled with a Dionex Ultimate 3000 quaternary HPLC system (Thermo-Fisher, San Jose, CA, USA). LC separation was achieved at room temperature on a HyperClone BDS C8 column 50 × 2.0 mm, 13 Å, 3 μm (Phenomenex, USA). Mobile phases were water (A) and 95% acetonitrile/water (B) both added of 2 mM ammonium formate and 50 mM formic acid. A chromatographic separation was performed through the following gradient: 10% B as starting conditions, 10–100% B in 10 min, and 100% B for 5 min; re-equilibration time was 9 min. The flow rate was 0.2 mL/min and injection volumes were 5 μL. The source setting used were the following: capillary temperature 300 °C, sheath gas 38 and auxiliary gas 26.5 (arbitrary units), spray voltage 4.5 kV, capillary voltage 47 V, and tube lens voltage 170 V. Full scan spectra were recorded at resolving power (RP) 60,000 (FWHM at m/z 400) in the range m/z 400–1200. Higher-energy collisional dissociation (HCD) and Collision Induced Dissociation (CID) experiments were acquired at RP 30,000 (FWHM at m/z 400), collision energy (CE) 65% and 40%, respectively, isolation width 2 m/z, activation Q 0.250, and activation time 30 ms. Data dependent

acquisition (DDA) experiments were designed as follows: 5 scan events were set up with scan event 1 being the HR full-scan experiment in the range m/z 300–1500, whereas the other scan events were $HRMS^2$ acquisitions fragmenting the 4 most intense ions observed across the m/z range applied in the full-scan experiment. The identification and quantitation of PnTX-G, in the extracts, was possible thanks to the availability in our laboratory of the PnTX-G standard (certified reference material (CRM) from the Institute of Biotoxin Metrology, National Research Council of Canada (NRCC, Halifax, Canada)). Extracted Ion Chromatograms (XICs) were obtained by selecting the monoisotopic $[M+H]^+$ ion of each compound searched: m/z 712.4419 for PnTX-A, m/z 694.4677 for PnTX-G, m/z 508.3421 for GYM-A, and m/z 692.4521 for 13desMeSPX-C, with a mass tolerance of 5 ppm. Elemental formulae were calculated on the monoisotopic peak of the ion cluster through Thermo Xcalibur software v2.2 SP1.48 (Thermo Fisher, San Josè, CA, USA).

3.1.3 Results and discussion

Detection of potentially toxic microalgae and microalgae associated with mucus production

High cell concentrations of the dinoflagellate *Gonyaulax fragilis* and diatoms from the genus *Cylindrotheca* were revealed in all the samples. These microorganisms are linked to the creation of substantial mucous masses in the sea. Additionally, potentially toxic planktonic and benthic microalgae were identified, albeit in lower abundances. Notably, the species *Vulcanodinium* cf. *rugosum*, a recognized producer of Pinnatoxin and Portimine, was among the detected microalgae.[23]

Identification of marine toxins in mucilage from North Aegean Sea

After a first screening that revealed the dominant presence of CIs, the first objective was to confirm the presence of the neurotoxin Pinnatoxin G (PnTX-G) in the samples extracted in Greece, using LC-HRMS (Figure III.4). The application of the LC-HRMS method allowed this confirmation in 5 out of 7 planktonic samples analyzed, considering its retention time, its exact mass (HRMS), and its fragmentation pattern (HR-MS/MS), fully consistent with that observed for a certified reference material of PnTX-G. The quantification, in the extracts, was possible thanks to the availability of the PnTX-G standard in our laboratory and ranged from <0.05 to 1.24 µg/L (Table 2). Portimine A was also detected in the same planktonic samples.

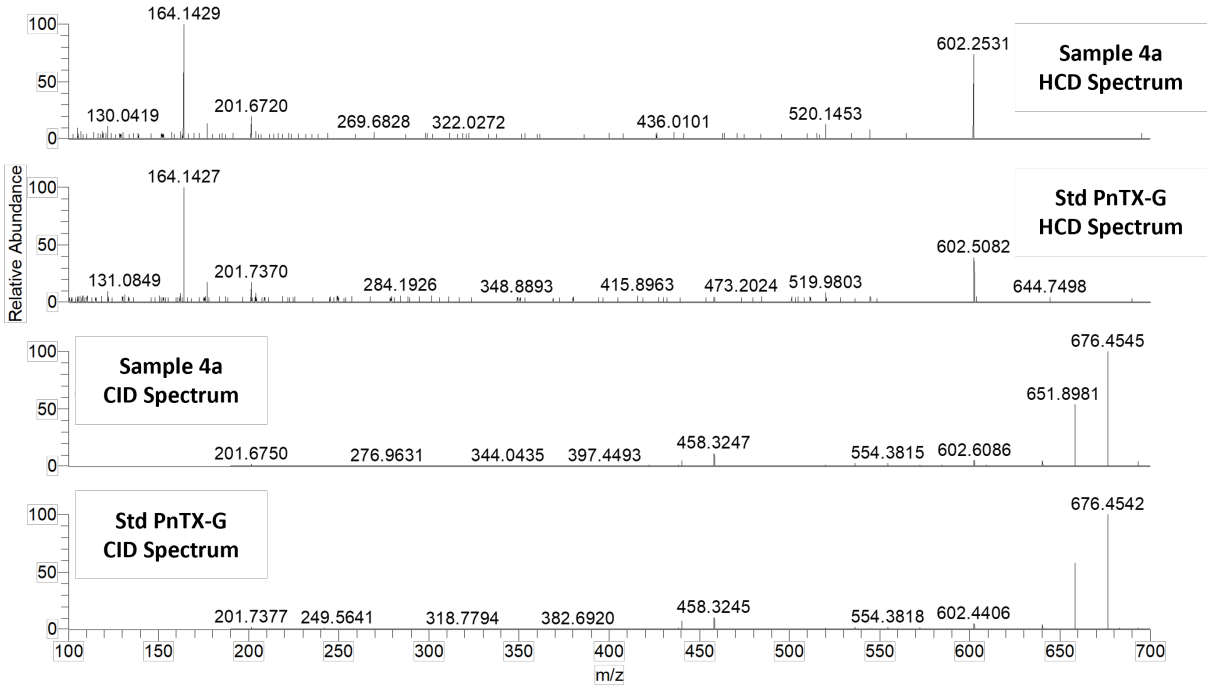

Figure III.4. Comparison between the fragmentation spectra obtained in HCD and CID mode for PnTX-G from the sample 4a and the PnTX-G standard solution (8 ng/mL).

PnTX-G was confirmed by comparing the full scan spectrum and the fragmentation pattern contained in the HCD and CID spectra associated to the peak eluting at 12.6 min in the samples with those of the standard (Figure III.4). The first fragmentation mode was used to confirm the presence of a cyclic imines diagnostic fragment at *m/z* 164.1429 ($C_{11}H_{18}N^+$), the second one with the purpose to definitively confirm the toxin through the study of its fragmentation pattern. PnTX-G was confirmed in the same way also in the extracts obtained in Italy.

Table 2. Summary of results for PnTX-G in Greek and Italian samples.

Sample ID (Greek extracts)	**Concentration of PnTX-G in the extract (ng/mL)**	**Concentration of PnTX-G in wet sample (ng/g)**
1a	nd	nd
2a	1.9	0.2
3a	4.1	0.4
4a	8.8	0.9
5a	1.4	0.1
6a	12.4	1.2
7a	nd	nd

	Concentration of PnTX-G in the extract (ng/mL)	**Concentration of PnTX-G in wet sample (ng/g)**
1a	nd	nd
2a	9.2	0.8
3a	26.1	2.5
4a	22.2	1.7
5a	10.2	1.0
6a	26.3	2.6
7a	nd	nd

Identification of Portimine A in 3 samples was achieved based on the presence of the characteristic MRM transitions on the LC-MS/MS system and confirmed by LC-HRMS^n fragmentations of the $[M + H]^+$ ion at *m/z* 402.2275 ($C_{23}H_{32}NO_5^+$) (Figure III.5).

It was not possible to quantify this toxin due to the absence of a reference standard. None of the other target toxins were detected in planktonic samples collected during the mucilage event.

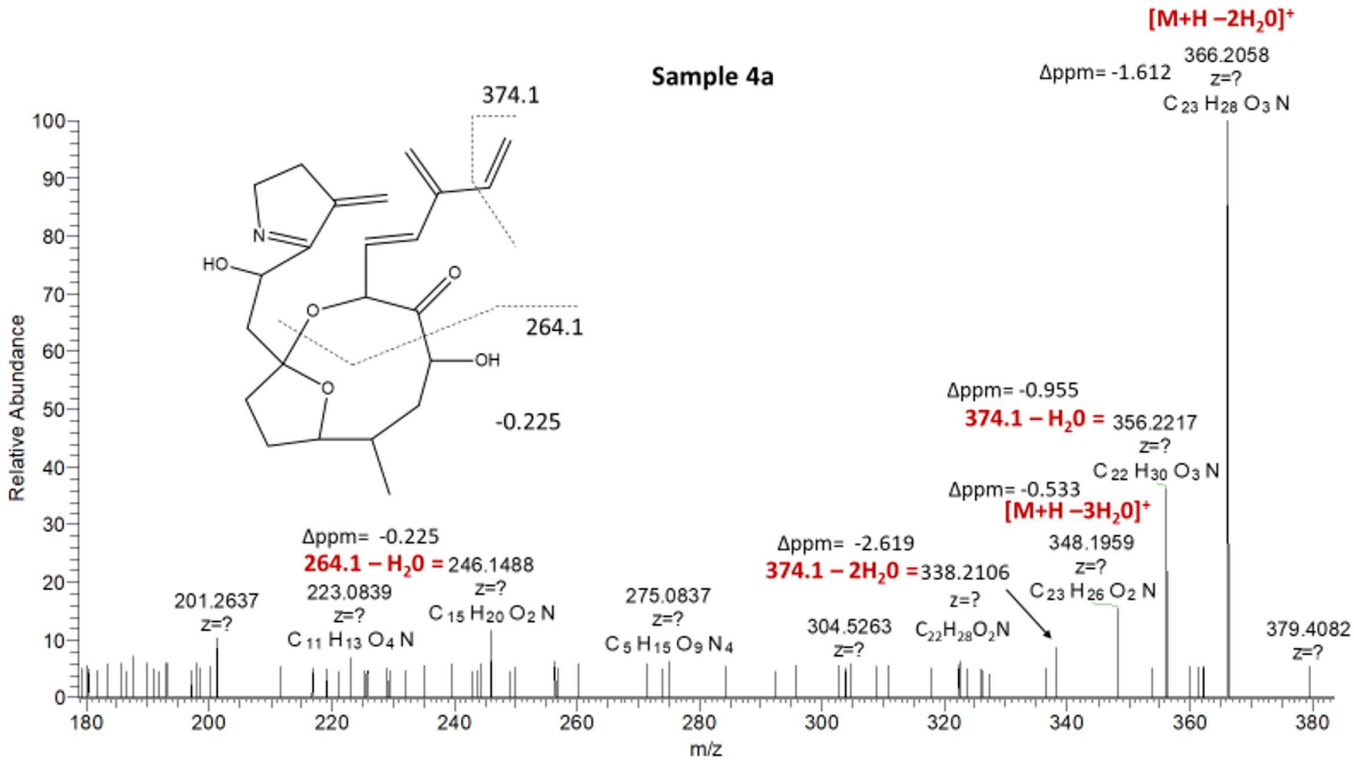

Figure III.5. Confirmation of Portimine A by interpretation of MS^2 CID spectra fragmentation of the ion at *m/z* 384.20 @CID20 $[M + H – H_2O]^+$, Sample 4a.

3.1.4 Conclusions

This study marks the inaugural exploration of a diverse array of marine toxins during a Mediterranean mucilage incident. Notably, the presence of Pinnatoxin G (PnTX-G) and Portimine A, have been reported for the first time in this context. The significance of these findings underscores the necessity for continued and in-depth investigations into the prevalence of toxins during mucilage events in the Aegean Sea. Such inquiries are imperative for a comprehensive understanding of the risks posed to both human health and the marine environment, considering also the economic and tourism aspects affected by mucilage events. For example, the proliferation of mucilage in the Sea of Marmara in 2021, attributed to pollution from wastewater and the resulting increase in phytoplankton, led to significant efforts to remove the mucilage and restore the marine environment. By unraveling the intricate dynamics of toxin occurrence in mucilage incidents, we can better assess and mitigate potential hazards in this vital ecosystem.

3.2 UNTARGETED LC-HRMS APPLIED TO MICROCYSTIN-PRODUCING CYANOBACTERIAL CULTURES FOR THE EVALUATION OF THE EFFICIENCY OF CHLORINE-BASED TREATMENTS COMMONLY USED FOR WATER POTABILIZATION

3.2.1 Introduction

Cyanobacteria represent major constituents of phytoplankton in aquatic ecosystems, contributing to 20-30% of the global primary production.[24] Under certain environmental conditions (e.g., high nutrient levels, water temperature, and light intensity), cyanobacteria can massively proliferate giving rise to harmful cyanobacterial blooms. Several studies highlight a close correlation between climate changes and the increasing magnitude, frequency and duration of cyanobacterial blooms.[25] Additionally, many cyanobacteria genera such as *Microcystis* and *Planktothrix* produce toxic metabolites (i.e., cyanotoxins) characterized by different chemical structures and mechanisms of action.[26] Microcystins (MCs) are one of the most studied cyanotoxins,[27] which exert hepatotoxic effects by targeting liver cells and inducing the inhibition of protein phosphatases, and may also act as tumor promoters. Among the more than 300 known MCs variants,[5] MC-LR - containing leucine and arginine in positions 2 and 4 - is considered the most common and toxic one (LD_{50} i.p. injection = 50 and 160-300 μg kg^{-1} for MC-LR and other MCs variants). Nonetheless, different and less-studied bioactive metabolites are produced by cyanobacteria, such as other peptides, e.g., cyanopeptolins and cyanopeptolin-type peptides (CPtps), which comprise more than 230 cyclic hexapeptides containing a β-lactone ring and featuring a characteristic 3-amino-6-hydroxy-2-piperidone (Ahp) moiety.[28] Despite cyanopeptides may occur in freshwater at concentrations similar to those reported for the well-studied MCs,[29] they have been poorly investigated from

both a chemical and a toxicological stand point. Cyanopeptides should not be neglected during water surveillance as a potential (eco)toxicity has recently emerged, due to a general inhibition effect on enzymes (proteases, trypsin, chymotrypsin, aminopeptidase among others) in micro- to nanomolar range and toxic effects in the same range of MCs when tested in biological assays.[30] In routine analyses, liquid chromatography coupled to mass spectrometry (LC-MS) is employed in targeted screening of selected cyanotoxins, whose reference standards are available, while no information can be easily obtained for other unknown cyanometabolites. More recently, approaches based on the untargeted analysis using LC-high resolution mass spectrometry (LC-HRMS), together with an ever-growing comprehensive database of cyanobacterial metabolites, have been successfully used for toxic profile determination of bloom material and cultured strains.[2,30,31]

In the perspective of the global safe management of drinking water supplies, cyanobacteria monitoring in water bodies for human consumption is a priority, and national regulations are in place to prevent the risks associated with cyanotoxins' exposure.[32] For instance, in Europe, the EU 2020/2184 directive includes MC-LR among the contaminants to be monitored.

Cyanobacteria may negatively affect the efficiency of drinking water treatment plants (DWTPs), in which several methods are employed, typically including coagulation, flocculation, sedimentation, filtration, and final disinfection.[33] Cyanobacteria biomass can cause filtration-clogging action or the increasing coagulant and flocculants demand, as well as the overloading of other downstream processes such as absorption on activated carbons,[33,34] or lead to the presence of cells and toxins within DWTPs or in finished water if cyanobacteria breakthrough occurs.[35–37] Even overcoming the difficulties arising from the presence of cyanobacterial biomass, the dispersed cyanobacteria cells can

negatively affect DWTPs. Evidence of cyanobacterial cells' accumulation, survival and even growth in the settling sludges arising in the water treatment chain have been reported. This phenomenon can cause cell damages, thus determining the increase of dissolved toxins' concentration in the water under treatment.[33] Another common step in water treatment is the pre-oxidation of raw water using oxidant disinfectants, specifically added to inactivate or kill waterborne pathogens.[38] Because of their relatively low costs, ready-availability, and wide-spectrum applications, chlorinated oxidants (chlorine dioxide, sodium hypochlorite, chloramines) are the most used disinfectants in DWTPs. However, pre-oxidation of raw water poses concerns about the chlorinated oxidants-driven formation of disinfection by-products (DBPs) such as carcinogenic trihalomethanes.[39] Furthermore, when toxic cyanobacteria are present, pre-oxidation may cause cell lysis and consequently extracellular toxin release.[34,40] Despite that, data suggested that pre-oxidation prior to flocculation and sedimentation may favour the removal of algal and cyanobacterial cells.[41] Accordingly, the use of low doses of oxidants during pre-oxidation (< 2.0 mg L^{-1}) of raw water has been suggested to achieve the inactivation of cells without causing lyses resulting in toxin release. In this complex scenario, is noteworthy that a pre-oxidation step may be required by national laws (i.e., in Italy; Italian Legislative Decree, 152/2006) and consequently, a careful evaluation of the related benefits and risks should be done. The present study aims to investigate the effects of low-dosed chlorinated oxidants commonly employed in DWTPs, i.e., sodium hypochlorite and chlorine dioxide, on cultures of the toxic cyanobacterium Microcystis aeruginosa. The effects of the oxidants on cell viability and on intra- and extra-cellular toxin content were assessed (Figure III.6). In this frame, metabolites produced by *M. aeruginosa* were explored by

analysing cultures before and after the treatments by an untargeted LC-HRMS approach.

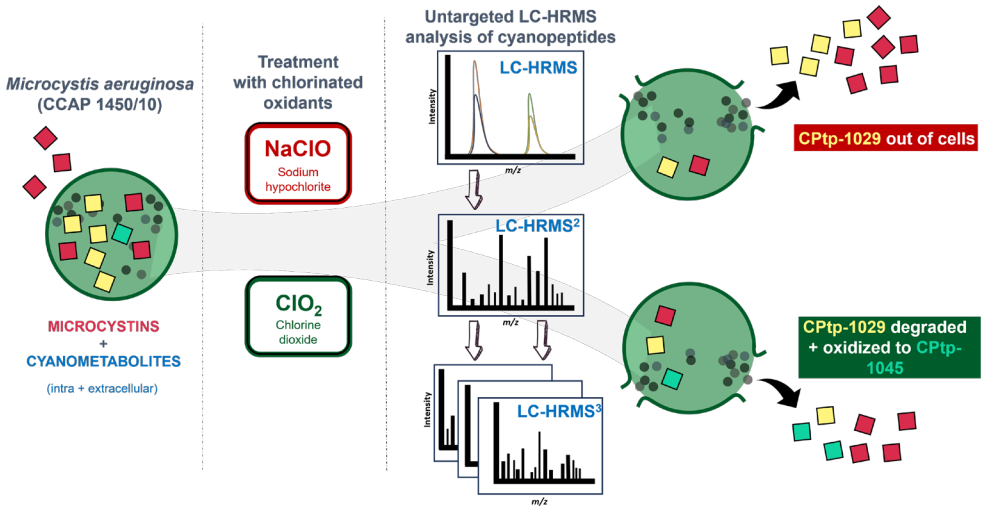

Figure III.6. Untargeted LC-HRMS applied to microcystin-producing cyanobacterial cultures for the evaluation of the efficiency of chlorine-based treatments commonly used for water potabilization.

3.2.2 Experimental section

Chemicals

All reagents, solvents, and chemical standards used were of analytical grade or higher. HPLC grade solvents (water, acetonitrile, methanol) and formic acid (reagent grade, ≥99.5%) used for LC-HRMS analyses were from Merck KGaA (Darmstadt, Germany). Chlorine dioxide stock solution of 146 mg L^{-1} (ClO_2) was prepared ready-to-use by the water treatment Company (Romagna Acque – Società delle Fonti S.p.A.), within a dedicated reactor by combining hydrochloric acid (33%) and sodium chlorite (25%), and the concentration was determined spectrophotometrically at λ = 445 nm. A commercial solution of sodium hypochlorite 15% (NaClO) was purchased ready-made (Società Chimica Bussi S.p.A.). Both oxidants were accordingly dosed for preliminary tests and for

oxidation experiments to obtain a final concentration in the range 0.1-2.0 mg L^{-1}. Sodium thiosulfate 1% (w/v) was prepared by dissolving 1 g of sodium thiosulphate in 100 mL of distilled water. Certified Reference Material (CRM) of MC-LR (10.3 µg mL^{-1}), [Dha^7]MC-LR (9.4 µg mL^{-1}), and MC-RR (10.1 µg mL^{-1}) were purchased from the National Research Council of Canada (Halifax, Canada).

Cyanobacterial strain and culture conditions

M. aeruginosa (CCAP 1450/10) was obtained from the Culture Collection of Algae and Protists (Scottish Marine Institute, Oban, UK) and grown in 0.2 L glass flasks in BG11 medium,[42] at a temperature of 20 ± 1 °C, light intensity 90-120 µmol m^{-2} s^{-1}, with a photoperiod of 16:8 h light:dark. Cultures were scaled-up at the same growing conditions for subsequent experiments using chlorinated oxidants. Prior to oxidation experiments, pH was adjusted to 7.0 ± 0.5 with hydrochloric acid (1.0 M).

Application of chlorinated oxidants on M. aeruginosa cultures for EC50 evaluation

Cultures of *M. aeruginosa* at exponential growth phase were diluted with demineralized water to reach a cell density of 300 × 10^6 cell L^{-1}. The two chlorinated oxidants, ClO_2 and NaClO, were preliminarily applied at increasing concentrations in the range of 0.0-4.0 mg L^{-1} (treatment time 1 h), to assess the maximum observed effect on the cyanobacterial photosynthetic efficiency. Then, a narrower range of concentrations for each oxidant (0.0-2.0 mg L^{-1} and 0.0-1.0 mg L^{-1} for ClO_2 and NaClO, respectively), was chosen to treat cultures (n = 3). After 1 h and 24 h of each treatment, aliquots of each sample (3 mL) were dark-adapted for 15-20 min and subsequently analysed by a pulse amplitude-modulated fluorometer, model 101-PAM (H. Walz, Effeltrich, Germany). The

photosynthetic efficiency was measured in terms of maximum and effective quantum yield of photosystem II (ΦPSII and Φ'PSII, respectively), and the half maximal effective concentration (EC_{50}) of the two chlorinated oxidants upon both ΦPSII and Φ'PSII was determined by fitting dose-response curves into a log-logistic model, using fluorometer's settings and calculations previously described.[43]

Oxidation experiment

M. aeruginosa cultures were scaled up to 10 L and collected at the exponential growth phase. The high cell density culture was gently mixed and divided into 0.5 L glass flasks for a total of 21 replicates (n = 3, for both control and each treatment). Before the oxidation experiment, each flask was diluted with demineralized water to reach a final cell density of 120×10^6 cell L^{-1}. Solutions of the chlorinated oxidants NaClO or ClO_2 were directly added to each flask to obtain a final dose of 0.5 mg L^{-1}, which was chosen based on the previously calculated EC_{50}. For ClO_2, a higher dose of 2.0 mg L^{-1} was also tested. Each combination of oxidant and dose was tested with a treatment time of 1 and 3 h versus controls. The oxidation experiments were conducted at room temperature in semi-dark conditions, to avoid direct exposure to light, and the flasks were gently mixed every 30 min. At the end of each exposure time, sodium thiosulfate solution (1% w/v) was added to quench the chemical oxidation.

Effect of the oxidants on cyanobacterial cells

The potential of each oxidant to inactivate and remove cyanobacterial cells was estimated by measuring photosynthetic efficiency and cell density, respectively. Sample aliquots (5 mL) were taken from each replicate to determine the maximum quantum yield of PSII as previously described. Remaining samples

were preserved with Lugol's iodine solution for subsequent cell enumeration using an inverted light microscope at 320x magnification (ZEISS Axiovert 100). The removal of cells following the oxidation treatments was calculated as percentage (%) compared to the number of cells in the control (von Sperling et al., 2020).[44]

Toxins extraction

Immediately after the addition of sodium thiosulfate, each replicate (controls and treatments with NaClO (0.5 mg L^{-1}) 1h, NaClO (0.5 mg L^{-1}) 3h, ClO_2 (0.5 mg L^{-1}) 1h, ClO_2 (0.5 mg L^{-1}) 3h, ClO_2 (2.0 mg L^{-1}) 1h, ClO_2 (2.0 mg L^{-1}) 3h was centrifuged (6500 × g, 10 min) to separate water from cyanobacterial biomass, from now on referred to as extracellular and intracellular fraction, respectively. Each extracellular fraction was extracted by solid phase extraction (SPE) using Oasis HBL cartridges (Waters, Milford, MA, USA), following the procedure described in Kaloudis et al. (2013).[45] The obtained eluates were evaporated under a gentle nitrogen stream until dryness. Each intracellular fraction was extracted according to an optimized protocol for fresh material.[46] Briefly, 1.5 mL of 75% aqueous methanol (v/v) was added to each test tube containing cyanobacterial biomass, vortexed, and sonicated in an ultrasonic bath for 15 min. The sonicated samples were then centrifuged (2550×g, 10 min at room temperature) and the supernatants collected. The procedure was repeated a second time using the same solvent mixture, and a third time using n-butanol. The resulting three supernatants were combined and dried under a gentle nitrogen stream. Dried samples were kept at -20°C until LC-HRMS analyses. Each extracellular and intracellular dried fraction was reconstituted with 500 µL of 20% aqueous methanol and analysed by LC-HRMS.

Untargeted LC-HRMS analyses of cyanotoxins and other cyanobacterial metabolites

LC–HRMS analyses were carried out using an Ultimate 3000 quaternary system coupled to a hybrid linear ion trap LTQ–Orbitrap XLTM Fourier transform MS equipped with an ESI ION MAX source (Thermo-Fisher, San José, USA) using LC-HRMS conditions reported in Varriale et al., (2023).[2] In particular, a chromatographic separation was performed through the following gradient: from 10 to 40% B in 10 min, 40 to 100% B in 5 min and 100% B for 5 min. Re-equilibration time was 8 min. Extracted ion chromatograms (XICs) were obtained from HR full-scan MS spectra by selecting the exact masses of $[M+H]^+$ and/or $[M+2H]^{2+}$ ions of all known MCs (±5 ppm) reported in CyanoMetDB,[5] (Supplementary information available at https://doi.org/10.5281/zenodo.7922070). For the suspected MC variants, precursor ions were selected for targeted $HRMS^2$ experiments in collision induced dissociation (CID) and higher energy collisional dissociation (HCD) modes (isolation width 2.0 *m/z*, activation Q 0.250, and activation time 30 ms) using a normalized collision energy of 40% (HCD) or 30% (CID). Identification of unknown cyanometabolites was carried out by DDA experiments, by setting up 9 scan events, with scan event 1 being a HR full-scan MS (range *m/z* 400–1200), and the other 8 scan events being $HRMS^2$ (CID or HCD) of the 8 most intense ions observed in the full-scan MS spectrum. Threshold value of MS^2 acquisition was set as 500 (intensity units). Elemental formulae were calculated based on the mass of the mono-isotopic peak of each ion cluster using Xcalibur v2.2 SP1.48 (Thermo-Fisher) with a mass tolerance of 3–5 ppm.

Quantitation of MCs and cyanopeptolin-type peptides

Each reconstituted intracellular fraction (1:10 dilution in 20% aqueous methanol) and extracellular fraction (1:100 dilution in 20% aqueous methanol) was analysed by LC–HRMS. Cyanotoxins detected in the samples were MCs containing a single Arg residue and, based on evidence reported by Varriale et al. (2023), quantitation was performed using MC-LR CRM as a reference and assuming similar molar response for all the other variants. Matrix interference on ionization of MC-LR CRM was negligible so, a matrix-free external standard calibration curve of MC-LR (15.6, 31.3, 62.5, 125, 250, 500, 1250 ng mL^{-1}) in methanol–water (1:4, v/v) was prepared from MC-LR CRM stock solution and analyzed by LC–HRMS. Quantitation was accomplished by comparing manually integrated XIC areas of each MC to the MC-LR CRM injected under the same experimental conditions (Table 3). The instrumental limit of quantitation (LOQ) measured for MC-LR was 5 ng mL^{-1} and, based on extraction efficiency data reported by Christophoridis et al., 2018 and Kaloudis et al., 2013 (extraction recoveries from biomass and water in the ranges 91-154% and 70-120%, respectively), the method LOQ for MCs in biomass and water were 0.042 fg $cell^{-1}$ and 0.01 μg L^{-1}, respectively. Quantitative estimation of the two new cyanopeptolin-type peptides, CPtp-1029 at *m/z* 1030.5246 and CPtp-1045 at *m/z* 1046.5222, was accomplished following the same approach. Finally, total toxin content was calculated as the sum of each intracellular and relevant extracellular fraction.

Table 3. Microcystins (MCs) and their dihydroxy and/or monochloro-hydroxy products formed through reaction with chlorine at the conjugated double bonds of Adda residue. X and Z represent variable L-amino acids at position-2 and -4. Exact masses, elemental compositions (for $[M+H]^+$ ions) and retention times of MC variants and their degradation products detected in the cyanobacterial intracellular and extracellular fractions.

Microcystin (MC-XZ)	**$[M+H]^+$, *m/z***	**Rt (min)**	**Elemental Formula**
MC-LR	995.5571	15.9	$C_{49}H_{75}O_{12}N_{10}^+$
[Dha^7]MC-LR	981.5412	16.0	$C_{48}H_{73}O_{12}N_{10}^+$
MC-LF	986.5250	16.2	$C_{52}H_{72}O_{12}N_7^+$
[D-Asp^3]MC-LF	972.5087	16.1	$C_{51}H_{70}O_{12}N_7^+$
MC-LY	1002.5197	15.4	$C_{52}H_{72}O_{13}N_7^+$
[D-Asp^3]MC-LY	988.5045	15.2	$C_{51}H_{70}O_{13}N_7^+$
Dihydroxy-MC-LR	1029.5542	13.4	$C_{49}H_{77}O_{14}N_{10}^+$
Monochloro-hydroxy-MC-LR	1047.5265	14.3	$C_{49}H_{76}ClO_{13}N_{10}^+$
Dihydroxy-[Dha^7]MC-LR	1015.5459	17.0	$C_{48}H_{75}O_{14}N_{10}^+$
Monochloro-hydroxy-[Dha^7]MC-LR	1033.5077	14.6	$C_{48}H_{74}ClO_{13}N_{10}^+$
Dihydroxy-MC-LF	1020.5288	14.7	$C_{52}H_{74}O_{14}N_7^+$
Monochloro-hydroxy-MC-LF	1038.4949	12.3	$C_{52}H_{73}ClO_{13}N_7^+$
Dihydroxy-[D-Asp^3]MC-LF	1006.5132	14.9	$C_{51}H_{72}O_{14}N_7^+$
Monochloro-hydroxy-[D-Asp^3]MC-LF	1024.4793	11.2	$C_{51}H_{71}ClO_{13}N_7^+$
Monochloro-hydroxy-MC-LY	1054.4899	11.3	$C_{52}H_{73}ClO_{14}N_7^+$
Dihydroxy-[D-Asp^3]MC-LY	1022.5081	14.6	$C_{51}H_{72}O_{15}N_7^+$
Monochloro-hydroxy-[D-Asp^3]MC-LY	1040.4742	11.2	$C_{51}H_{71}ClO_{14}N_7^+$

Effect of the oxidants on toxin content

The changes in toxin content of each treated sample versus the control were evaluated as percent toxin variation, i.e., ΔTox(%), and calculated as follows:

$$\Delta Tox(\%)=(1-(C_{low}/C_{high}))\times 100$$

Where C_{low} and C_{high} were the lowest and the highest toxin concentration measured between control and treated samples for each replicate, respectively.

Data analysis

Data analysis was performed on PAST version 4.11 for the comparison of the main evaluated parameters (i.e., cell or toxin concentrations) among the different

treatments. EC_{50} dose-response curves were generated on R version 4.2.0 (R Core Team, 2022). Data homogeneity was evaluated with Levene's test for homoskedasticity and was transformed accordingly prior to further investigation. The effect of the different treatments on the photosynthetic activity, the number of cells and percent removal, the toxin content and the percent variation were examined by analysis of variance (ANOVA) and Tukey's test for post-hoc comparisons was used when differences were significant ($p < 0.05$).

3.2.3 Results and discussion

Photosynthetic efficiency of M. aeruginosa cells treated with oxidants

A preliminary assessment of the effect of the chlorinated oxidants NaClO and ClO_2 on the photosynthetic efficiency of *M. aeruginosa* is reported in Figure III.7. Increasing doses of each oxidant led to a gradual inhibition of the maximum and effective quantum yields of PSII, resulting in values below 20% at the highest tested doses. For both oxidants, a significant reduction than control (ANOVA, $p < 0.05$) was obtained for all concentrations above 0.4 mg L^{-1}, regardless of the treatment time (1 h or 24 h).

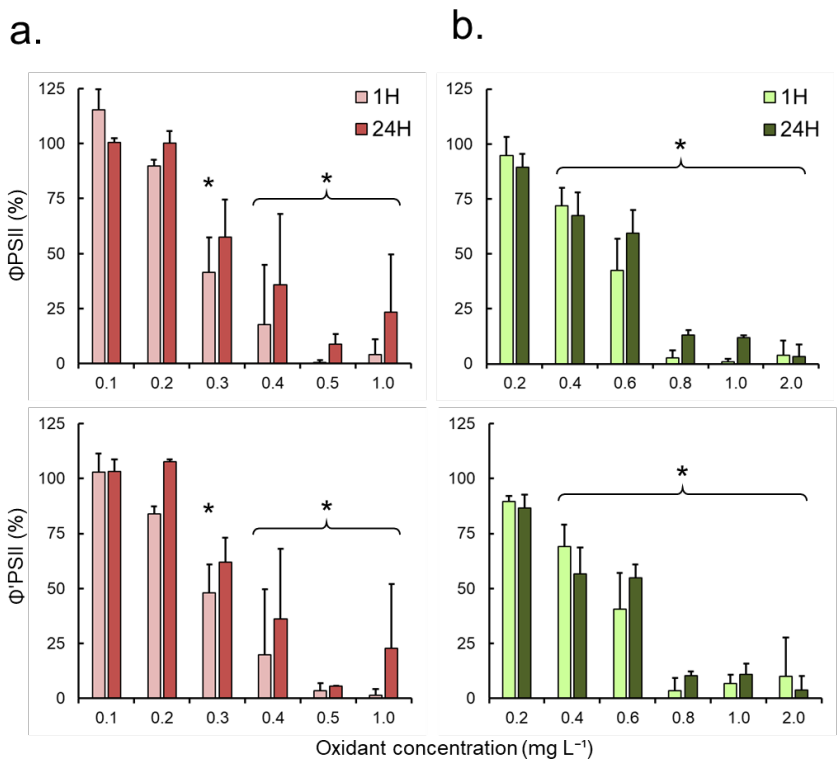

Figure III.7. Photosynthetic activity (%) of *M. aeruginosa* cells treated with increasing doses of the chlorinated oxidants NaClO (a, red) and ClO_2 (b, green), after 1 h and 24 h of treatment time. Values are expressed as percent inhibition of the maximum quantum yield (ΦPSII (%), upper graphs) and of the effective quantum yield (Φ'PSII (%), bottom graphs) with respect to the control. Significant differences compared to control are indicated with asterisks (ANOVA, $p < 0.05$).

The EC_{50} values (i.e., oxidant concentration needed to achieve a 50% inhibition of both maximum and effective quantum yields of PSII) obtained were almost two-fold higher for ClO_2-treated samples than for NaClO-treated ones, i.e. 0.50-0.59 vs 0.28-0.34 mg L^{-1}, respectively, indicating how the two oxidants affect differently the cyanobacterial cells. EC_{50} values slightly increased after 24 h compared to 1 h, likely as a result of the higher photosynthetic activity observed after 24 h of treatment with both oxidants (Figure III.7). This evidence suggests

that the damages upon the photosynthetic apparatus of *M. aeruginosa* caused by the chlorinated oxidants were reversible at the tested doses.

Removal of cells and inhibition of photosynthetic efficiency following the oxidation experiment

Based on preliminary investigations, *M. aeruginosa* cultures were treated with each oxidant at specific doses and times (i.e., 0.5 mg L^{-1} for 1 and 3 h, and 2.0 mg L^{-1} only for ClO_2), and the effects on the cell viability were evaluated in terms of cell density and photosynthetic activity, obtained from the maximum quantum yield of PSII (Figure III.8). During the oxidation experiment, the number of cells (Figure III.8a) remained unchanged after the NaClO treatment i.e., 121×10^6 vs $129\text{-}131\times10^6$ cell L^{-1} for control and NaClO treatment, respectively (ANOVA, $p > 0.05$), as also indicated by the negative values of percent removal of cells (– 6-8%), and by the calculated ratio among the cell density in treated cultures and in controls that was near to 1. The cell density significantly decreased only for ClO_2 treatments (32-46%, ANOVA, $p < 0.05$), with a major effect at the highest tested dose (2.0 mg L^{-1}) without differences among treatment times (cell density in the range $65\text{-}81\times10^6$ cell L^{-1}, Figure III.8a). The photosynthetic efficiency of the cyanobacterium both in terms of maximum (Figure III.8b) and effective quantum yield was inhibited by both oxidants compared to controls, resulting in a residual activity below 20% (ANOVA, $p < 0.05$).

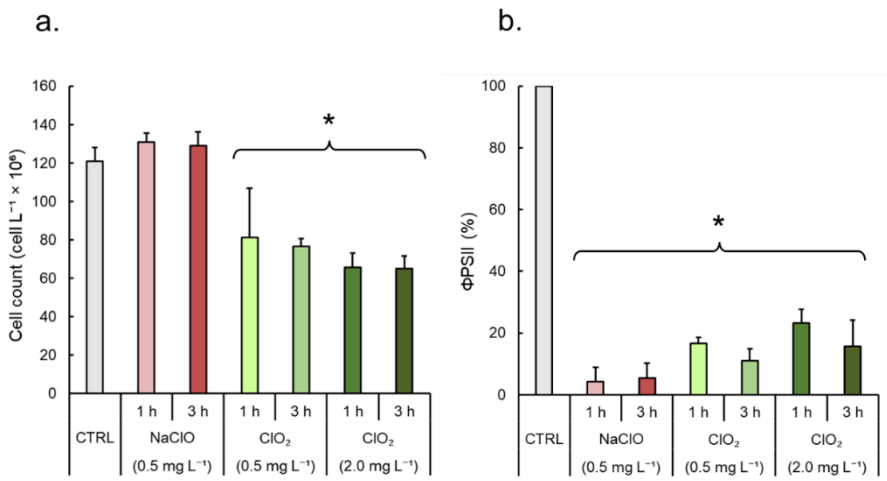

Figure III.8. Effect of NaClO and ClO_2 tested at 0.5 and 2.0 mg L^{-1} on cells of *M. aeruginosa* during the oxidation experiment, a) number of cells (cell × 10^6 L^{-1}), and b) photosynthetic activity calculated from maximum quantum yields (ΦPSII (%)).

Toxin profile by LC-HRMS

The intracellular and extracellular fractions resulting from the centrifugation of each culture (controls and treated ones) were analysed by LC-HRMS to first evaluate the toxin profile of the tested strain (Figure III.9). An array of microcystins, all featuring a single Arg at position-2, were detected in both *M. aeruginosa* controls and treated cultures. The number of Arg residues is a key structural feature influencing the ionization behaviour of MCs, particularly MCs containing 1-Arg (e.g., MC-LR) form predominantly $[M+H]^+$ ions and so quantitation can be accomplished using MC-LR standard assuming a similar molar response for all the variants. MC-LR and its analogue containing a dehydroalanine in position 7, [Dha^7]-MC-LR, were found to be the two dominant variants representing 18.0% and 5.7% of the intracellular toxin fraction, respectively, followed by MC-LY (1.3%), MC-LF (1.2%), [D-Asp^3]MC-LY (0.4%) and [D-Asp^3]MC-LF (0.1%). A similar trend was observed for the extracellular fraction (Figure III.9), although the toxin levels were markedly

higher than in the biomass. MC-LR and [Dha^7]MC-LR concentrations detected in the extracellular fraction were three- (69 vs 20 µg L^{-1}) and eight-fold (49 vs 6 µg L^{-1}) higher compared to the intracellular toxin content, respectively. In samples subjected to both treatments, trace levels of MCs oxidized products (dihydroxy and monochloro-hydroxy MCs, have been also detected. This suggested that chlorine treatments, at the low doses here tested (≤ 2 mg L^{-1}), only slightly promote MCs decomposition into the oxidized products. In addition to MCs, the presence of a new compound at *m/z* 1030.5246 eluting at 12.82 min emerged in the analysed samples, predominantly present in the biomass control sample. Unlike the other toxins, this compound was retained inside the cells (81 vs 2 µg L^{-1}) accounting for 71.4% of the total intracellular toxin content (Figure III.9). The HR full scan MS spectrum (Figure III.10) associated to the extracted ion chromatogram (XIC) of the ion at *m/z* 1030.5246 revealed the presence of a very intense in-source fragment due to the loss of a water molecule (at *m/z* 1012.5134), as well as $[M+Na]^+$ and $[M+K]^+$ adduct ions at *m/z* 1052.5052 and 1068.4785, respectively. The cross-checked interpretation of elemental formulae of all the protonated, in-source fragment, and adduct ions for the new compound, that we named cyanopeptolin-type peptide-1029 (CPtp-1029), allowed to assign it the elemental composition $C_{52}H_{71}O_{13}N_9$ (with the $[M+H]^+$ ion at *m/z* 1030.5246, $C_{52}H_{72}O_{13}N_9^+$ RDB = 21.5, Δ = 0.185 ppm). An oxidized derivative of CPtp-1029 at *m/z* 1046.5222 was also identified as a minor constituent of *M. aeruginosa* biomass (2%, Figure III.9), whereas in the extracellular fraction it was present only in traces (0.1%). The assigned molecular formula, $C_{52}H_{71}O_{14}N_9$ (with the $[M+H]^+$ ion at *m/z* 1046.5222, $C_{52}H_{72}O_{14}N_9^+$ RDB = 21.5, Δ = 2.748 ppm), contained one O atom more than CPtp-1029, likely a hydroxyl functionality, thus it was named cyanopeptolin-type peptide-1045 (CPtp-1045).

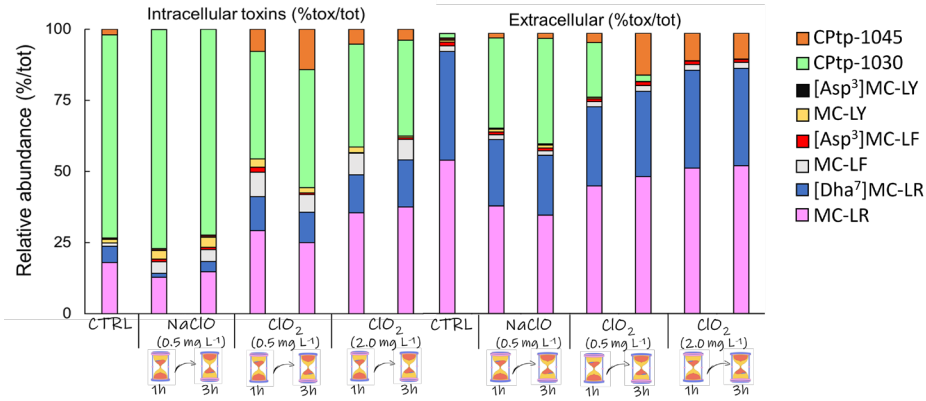

Figure III.9. Relative abundances of MCs variants and metabolites in *M. aeruginosa* cultures treated with NaClO and ClO_2 expressed as percentage on the total toxin content (µg L^{-1}) and divided for intracellular and extracellular fractions. CPtp-1029 = cyanopeptolin-type peptide-1029, CPtp-1045 = cyanopeptolin-type peptide-1045.

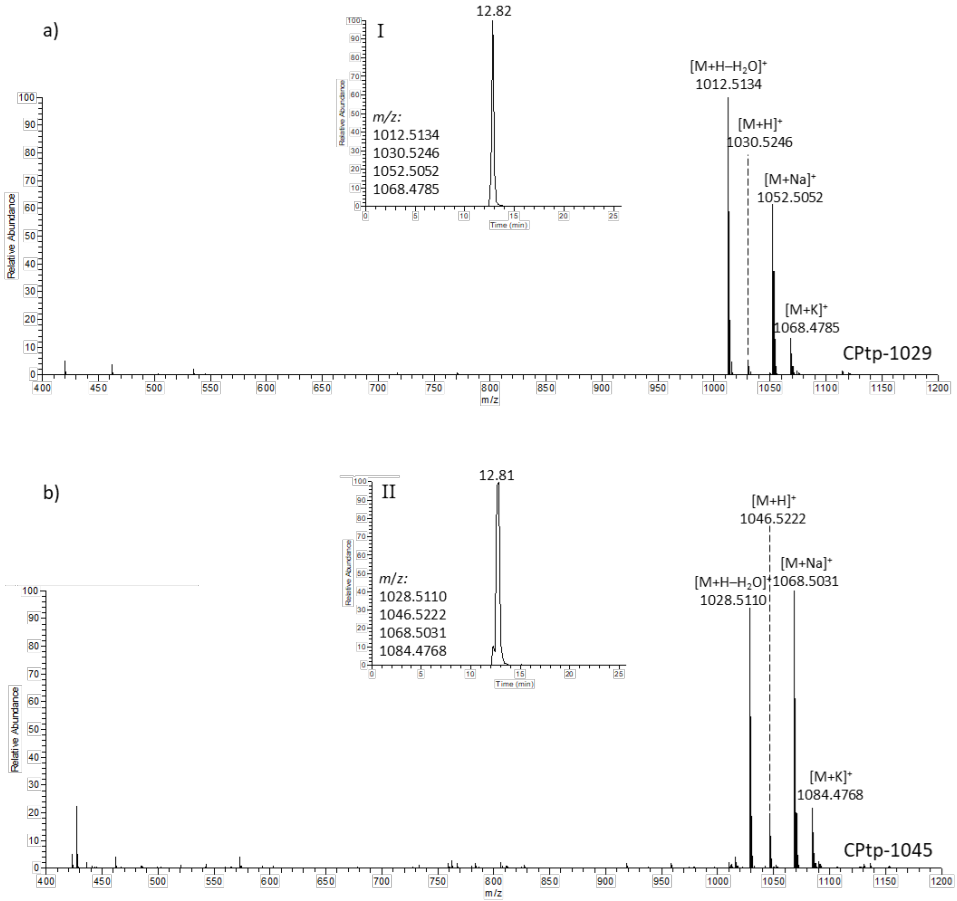

Figure III.10. HR full-scan MS spectra of the new compound, a) cyanopeptolin-type peptide-1029 (CPtp-1029) in the control sample, and b) its oxidized analogue (CPtp-1045) in treated sample. Inset I: Extracted ion chromatogram (XIC) obtained by summing the $[M+H]^+$, $[M+H-H_2O]^+$, $[M+Na]^+$ and $[M+K]^+$ ions for CPtp-1029. Inset II: XIC obtained by summing the $[M+H]^+$, $[M+H-H_2O]^+$, $[M+Na]^+$ and $[M+K]^+$ ions for CPtp-1045.

Multiple stage MS in structural characterization of the new cyanopeptolins

LC-HRMS^n (n = 2, 3) experiments were performed by fragmenting the main in-source $[M+ H-H_2O]^+$ precursor ion at *m/z* 1012.5134 in both CID (Figure III.11a) and HCD (Figure III.12a) modes generating different, and complementary, diagnostic product ions. The analysis of the CID HRMS^2 fragmentation pattern revealed the presence of a fragment at *m/z* 420.1914 corresponding to one of the

conserved structural motifs of CPtps ([Ahp^3+Phe^4+NMeTyr^5+H−H_2O]$^+$). An in-depth MS-based structural investigation provided for the identification of each single residue contained in the compound by observing diagnostic product ions (1-2 residues) in the HRMS^{2,3} spectra, including the neutral loss of individual residues from the precursor ion. Successively, the cross-interpretation of oligopeptide product ions (3–5 residues) in the HRMS^{2,3} spectra allowed to infer the position of each residue in the cyclic structure. Particularly, the presence of NMeTyr, Choi, Phe and hydroxyPro residues was indicated by their immonium ions at *m/z* 150.0913 ($C_9H_{12}ON^+$, Δ = – 0.270 ppm), *m/z* 140.1069 ($C_8H_{14}ON^+$, Δ = –0.647 ppm), *m/z* 120.0807 ($C_8H_{10}N^+$, Δ = −0.632 ppm), and *m/z* 70.0649 ($C_4H_8N^+$, Δ = −3.223 ppm), respectively. A Leu/Ile (indistinguishable based on MS evidence) was detected through the product ion at *m/z* 899.4313 ($C_{46}H_{59}O_{11}N_8^+$, Δ = +1.689 ppm) due to the neutral loss of $C_6H_{11}ON$ (113.0821 Da) from the precursor ion. Product ions at *m/z* 243.1129 ($C_{14}H_{15}O_2N_2^+$, Δ = +0.394) and 215.1179 ($C_{13}H_{15}ON_2^+$, Δ = +0.048 ppm) indicated the sequence Ahp+Phe as well as the fragment ion at *m/z* 296.1600 ($C_{14}H_{22}O_4N_3^+$ Δ = −1.630 ppm) revealed the sequence Choi+Gln. The presence of the characteristic product ion at *m/z* 420.1914 pointing out the sequence Ahp^3+Phe^4+NMeTyr^5 in combination with a fragment ion at *m/z* 717.3604, corresponding to the sequence [Choi^1+Gln^2+Ahp^3+Phe^4+NMeTyr^5+H−H_2O]$^+$ allowed to locate Choi^1+Gln^2. A Leu/Ile at position^6, a HydroxyPro^7 and Ala^8 were suggested by: i) a product ion at *m/z* 770.4078 corresponding to [Gln^2+Choi^1+Ala^8+Hyp^7+Leu/Ile^6+NMeTyr^5+H]+ and ii) a product ion at *m/z* 462.2343 corresponding to the neutral loss of Ahp^3+Phe^4+NMeTyr^5+Leu/Ile^6 from the precursor ion. HRMS^3 experiments carried out by further fragmenting the main product ions at *m/z* 770.4078, 462.2343, 717.3604 provided additional evidence of the amino acids sequence. As for CPtp-1045, HRMS^2 spectrum

showed a fragment at *m/z* 166.0866 versus the fragment at *m/z* 150.0913 obtained for CPtp-1029 suggesting a N-methyl hydroxy Tyr (versus N-methyl Tyr) at position-5. All the assignments for CPtp-1029 and CPtp-1045 are schematized in Table 4 and 5, respectively.

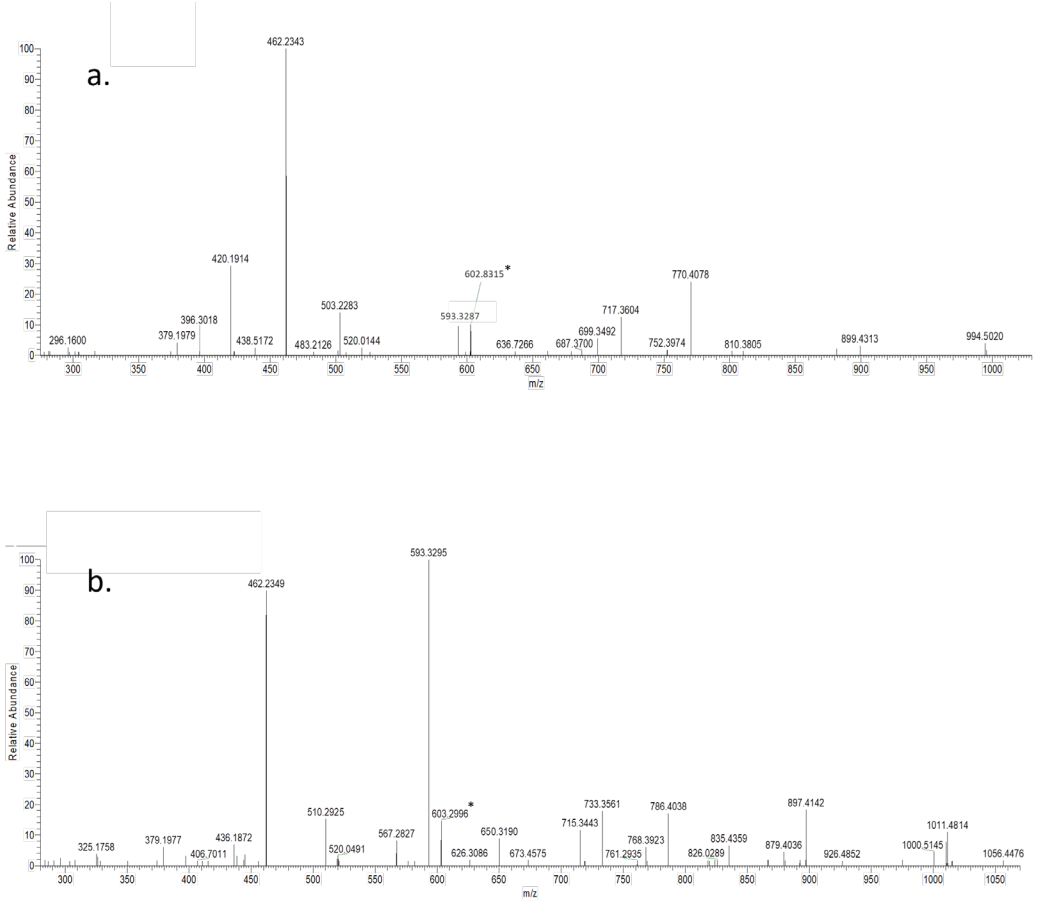

Figure III.11. CID HRMS^2 spectra acquired by selecting as precursor the $[M+H–H_2O]^+$ ion of a) CPtp-1029 at *m/z* 1012.5134 and b) CPtp-1045 at *m/z* 1028.5110. Collision energy, CE = 40%. ***** = Noise.

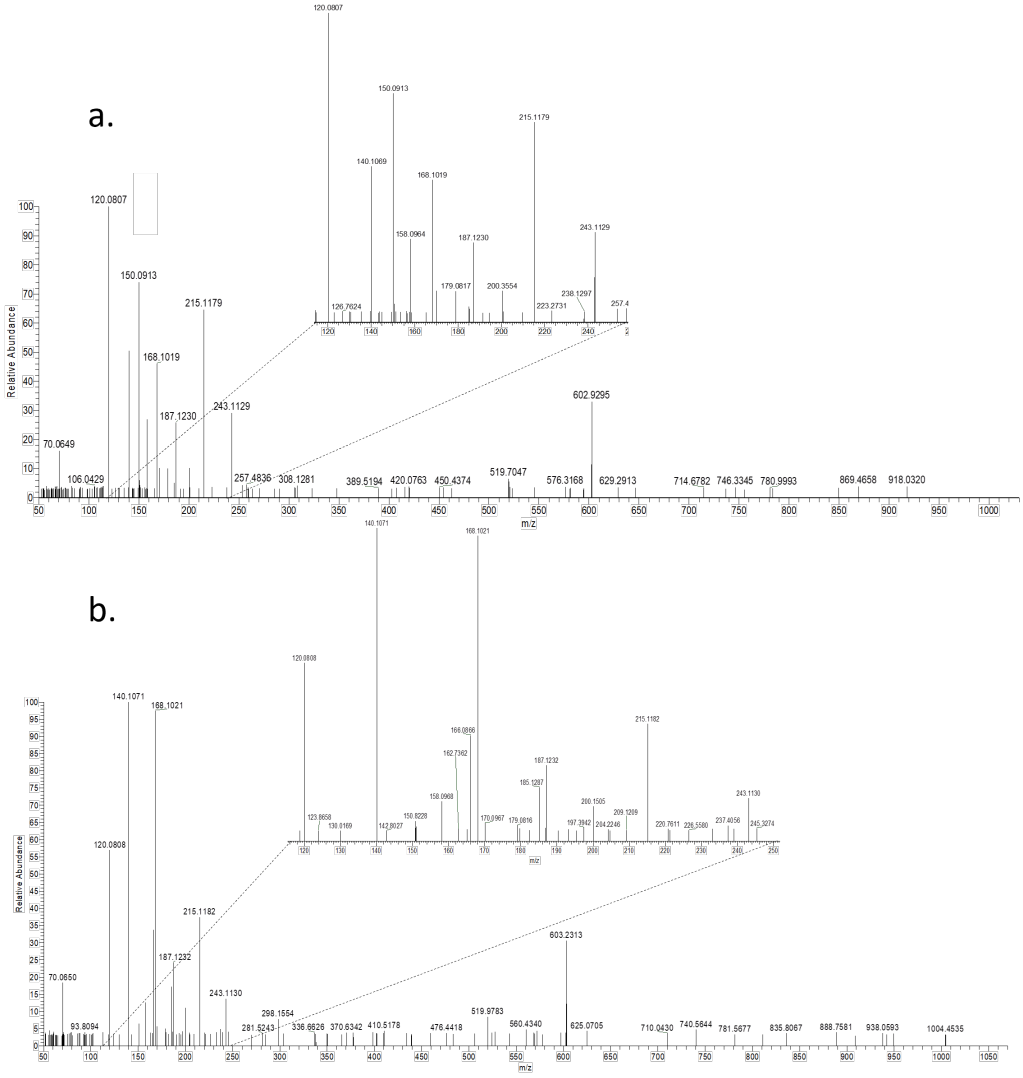

Figure III.12. HCD HRMS^2 spectra acquired by selecting as precursor the $[M+H–H_2O]^+$ ion of a) CPtp-1029 at *m/z* 1012.5134 and b) CPtp-1045 at *m/z* 1028.5110. Collision energy, CE = 40%. * = Noise.

Table 4. Assignment of product ions detected in CID and HCD spectra of cyanopeptolin-type peptide-1029 (CPtp-1029) precursor ion at *m/z* 1012.5.

	m/z	Formula	Sequence	Neutral loss
$[M+H]^+$	1030.5246	$C_{52}H_{72}O_{13}N_9^+$	$[Choi^1+Gln^2+Ahp^3+Phe^4+NMeTyr^5+Leu/Ile^6+Hyp^7+Ala^8+H]^+$	
$[M+H-H_2O]^+$	1012.5134	$C_{52}H_{70}O_{12}N_9^+$	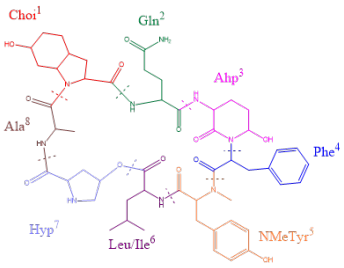	H_2O
	995.4904	$C_{52}H_{67}O_{12}N_8^+$		H_2O+NH_3
	994.5020	$C_{52}H_{68}O1_1N_9^+$		$2H_2O$
CID	899.4313	$C_{46}H_{59}O_{11}N_8^+$	$[Hyp^7+Ala^8+Choi^1+Gln^2+Ahp^3+Phe^4+NMeTyr^5+H-H_2O]^+$	Leu/Ile^6+H_2O
	881.4190	$C_{46}H_{57}O_{10}N_8^+$	$[Hyp^7+Ala^8+Choi^1+Gln^2+Ahp^3+Phe^4+NMeTyr^5+H-2H_2O]^+$	Leu/Ile^6+2H_2O
	770.4078	$C_{38}H_{56}O_{10}N_7^+$	$[Gln^2+ Choi^1+Ala^8+Hyp^7+Leu/Ile^6+NMeTyr^5+H]^+$	Ahp^3+Phe^4
	752.3974	$C_{38}H_{54}O_9N_7^+$	$[Gln^2+ Choi^1+Ala^8+Hyp^7+Leu/Ile^6+NMeTyr^5+H-H_2O]^+$	$Ahp^3+Phe^4+H_2O$
	717.3604	$C_{38}H_{49}O_8N_6^+$	$[Choi^1+Gln^2+Ahp^3+Phe^4+NMeTyr^5+H-H_2O]^+$	$Leu/Ile^6+Hyp^7+Ala^8+H_2O$
	699.3492[b]	$C_{38}H_{47}O_7N_6^+$	$[Choi^1+Gln^2+Ahp^3+Phe^4+NMeTyr^5+H-2H_2O]^+$	$Leu/Ile^6+Hyp^7+Ala^8+2H_2O$
	593.3287	$C_{28}H_{45}O_8N_6^+$	$[Gln^2+ Choi^1+Ala^8+Hyp^7+Leu/Ile^6+H-H_2O]^+$	$Ahp^3+Phe^4+NMeTyr^5+H_2O$
	503.2283	$C_{28}H_{31}O_5N_4$	$[Gln^2+Ahp^3+Phe^4+NMeTyr^5+H-CO-NH_2-H_2O]^+$	$Leu/Ile^6+Hyp^7+Ala^8+ Choi^1+CO+NH_2+H_2O$
	462.2343[a]	$C_{22}H_{32}O_6N_5^+$	$[Gln^2+ Choi^1+Ala^8+Hyp^7+H]^+$	$Ahp^3+Phe^4+NMeTyr^5+Leu/Ile^6$
	420.1914[b]	$C_{24}H_{26}O_4N_3^+$	$[Ahp^3+Phe^4+NMeTyr^5+H-H_2O]^+$	$Choi^1+Gln^2+Leu/Ile^6+Hyp^7+Ala^8+H_2O$
	296.1600[a,c]	$C_{14}H_{22}O_4N_3^+$	$[Choi^1+Gln^2+H]^+$	$Ahp^3+Phe^4+NMeTyr^5+Leu/Ile^6+Hyp^7+Ala^8$
HCD	308.1281	$C_{19}H_{18}O_3N^+$	$[Phe^4+NMeTyr^5+H-H_2O]^+$	$Choi^1+Gln^2+Ahp^3+Leu/Ile^6+Hyp^7+Ala^8+H_2O$
	243.1129	$C_{14}H_{15}O_2N_2^+$	$[Ahp^3+Phe^4+H-H_2O]^+$	$Choi^1+Gln^2+NMeTyr^5+Leu/Ile^6+Hyp^7+Ala^8+H_2O$
	215.1179	$C_{13}H_{15}ON_2^+$	$[Ahp^3+Phe^4+ H-CO-H_2O]^+$	$Choi^1+Gln^2+NMeTyr^5+Leu/Ile^6+Hyp^7+Ala^8+CO+H_2O$
	187.1230	$C_{12}H_{15}N_2^+$	$[Ahp^3+Phe^4+ H-2CO-H_2O]^+$	$Choi^1+Gln^2+NMeTyr^5+Leu/Ile^6+Hyp^7+Ala^8+2CO+H_2O$
	168.1019[c]	$C_9H_{14}O_2N^+$	$[Choi^1$ (immonium ion)$+CO+H]^+$	$Gln^2+Ahp^3+Phe^4+NMeTyr^5+Leu/Ile^6+Hyp^7+Ala^8$
	150.0913	$C_9H_{12}ON^+$	$[NMeTyr^5+H]^+$	$Choi^1+Gln^2+Ahp^3+Leu/Ile^6+Hyp^7+Ala^8$
	140.1069[c]	$C_8H_{14}ON^+$	$[Choi^1$ (immonium ion)$+H]^+$	$Gln^2+Ahp^3+Phe^4+NMeTyr^5+Leu/Ile^6+Hyp^7+Ala^8$
	120.0807	$C_8H_{10}N^+$	$[Phe^4$ (immonium ion)$+H]^+$	$Choi^1+Gln^2+Ahp^3+NMeTyr^5+Leu/Ile^6+Hyp^7+Ala^8$
	70.0649	$C_4H_8N^+$	$[Hyp^7$ (immonium ion)$+H]^+$	$Choi^1+Gln^2+Ahp^3+Phe^4+NMeTyr^5+Leu/Ile^6+Ala^8$

[a]Fragment confirmed also in LC-HRMS^3 experiment, precursor ion at *m/z* 770.4078; [b]Fragment confirmed also in LC-HRMS^3 experiment, precursor ion at *m/z* 717.3604; [c]Fragment confirmed also in LC-HRMS^3 experiment, precursor ion at *m/z* 462.2343.

Table 5. Assignment of product ions detected in CID and HCD LC-HRMS^{2,3} spectra of cyanopeptolin-type peptide-1045 (CPtp-1045) precursor ion at *m/z* 1046.5.

CPtp-1045	*m/z*	Formula	Sequence	Neutral loss
$[M+H]^+$	1046.5222	$C_{52}H_{72}O_{14}N_9^+$	$[Choi^1+Gln^2+Ahp^3+Phe^4+NMeTyrOH^5+Leu/Ile^6+Hyp^7+Ala^8+H]^+$	
$[M+H-H_2O]^+$	1028.5110	$C_{52}H_{70}O_{13}N_9^+$	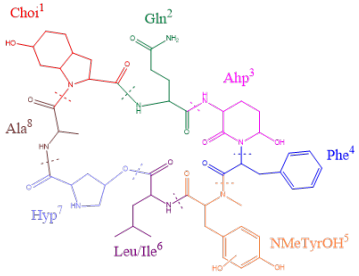	H_2O
	1011.4814	$C_{52}H_{67}O_{13}N_8^+$		H_2O+NH_3
	1010.4989	$C_{52}H_{68}O_{12}N_9^+$		$2H_2O$
CID	897.4142	$C_{46}H_{57}O_{11}N_8^+$	$[Hyp^7+Ala^8+Choi^1+Gln^2+Ahp^3+Phe^4+NMeTyr^5+H-2H_2O]^+$	Leu/Ile^6+2H_2O
	786.4038	$C_{38}H_{56}O_{11}N_7^+$	$[Gln^2+ Choi^1+Ala^8+Hyp^7+Leu/Ile^6+NMeTyr^5+H]^+$	Ahp^3+Phe^4
	768.3923	$C_{38}H_{54}O_{10}N_7^+$	$[Gln^2+ Choi^1+Ala^8+Hyp^7+Leu/Ile^6+NMeTyr^5+H-H_2O]^+$	$Ahp^3+Phe^4+H_2O$
	733.3561	$C_{38}H_{49}O_9N_6^+$	$[Choi^1+Gln^2+Ahp^3+Phe^4+NMeTyrOH^5+H-H_2O]^+$	$Leu/Ile^6+Hyp^7+Ala^8+H_2O$
	715.3443	$C_{38}H_{47}O_8N_6^+$	$[Choi^1+Gln^2+Ahp^3+Phe^4+NMeTyrOH^5+H-2H_2O]^+$	$Leu/Ile^6+Hyp^7+Ala^8+2H_2O$
	593.3295	$C_{28}H_{45}O_8N_6^+$	$[Gln^2+ Choi^1+Ala^8+Hyp^7+Leu/Ile^6+H-H_2O]^+$	$Ahp^3+Phe^4+NMeTyrOH^5+H_2O$
	519.2243	$C_{28}H_{31}O_6N_4^+$	$[Gln^2+Ahp^3+Phe^4+NMeTyrOH^5+H-CO-NH_2-H_2O]^+$	$Leu/Ile^6+Hyp^7+Ala^8+Choi^1+CO+NH_2+H_2O$
	462.2349	$C_{22}H_{32}O_6N_5^+$	$[Gln^2+ Choi^1+Ala^8+Hyp^7+H]^+$	$Ahp^3+Phe^4+NMeTyrOH^5+Leu/Ile^6$
	436.1872	$C_{24}H_{26}O_5N_3^+$	$[Ahp^3+Phe^4+NMeTyrOH^5+H-H_2O]^+$	$Choi^1+Gln^2+Leu/Ile^6+Hyp^7+Ala^8+H_2O$
	296.1616[a]	$C_{14}H_{22}O_4N_3^+$	$[Choi^1+Gln^2+H]^+$	$Ahp^3+Phe^4+NMeTyrOH^5+Leu/Ile^6+Hyp^7+Ala^8$
HCD	243.1130	$C_{14}H_{15}O_2N_2^+$	$[Ahp^3+Phe^4+H-H_2O]^+$	$Choi^1+Gln^2+NMeTyrOH^5+Leu/Ile^6+Hyp^7+Ala^8+H_2O$
	215.1182	$C_{13}H_{15}ON_2^+$	$[Ahp^3+Phe^4+H-CO-H_2O]^+$	$Choi^1+Gln^2+NMeTyrOH^5+Leu/Ile^6+Hyp^7+Ala^8+CO+H_2O$
	187.1232	$C_{12}H_{15}N_2^+$	$[Ahp^3+Phe^4+H-2CO-H_2O]^+$	$Choi^1+Gln^2+NMeTyrOH^5+Leu/Ile^6+Hyp^7+Ala^8+2CO+H_2O$
	168.1021[a]	$C_9H_{14}O_2N^+$	$[Choi^1$ (immonium ion)$+CO+H]^+$	$Gln^2+Ahp^3+Phe^4+NMeTyrOH^5+Leu/Ile^6+Hyp^7+Ala^8$
	166.0866	$C_9H_{12}O_2N^+$	$[NMeTyrOH^5+H]^+$	$Choi^1+Gln^2+Ahp^3+Leu/Ile^6+Hyp^7+Ala^8$
	140.1071[a]	$C_8H_{14}ON^+$	$[Choi^1$ (immonium ion)$+H]^+$	$Gln^2+Ahp^3+Phe^4+NMeTyrOH^5+Leu/Ile^6+Hyp^7+Ala^8$
	120.0808	$C_8H_{10}N^+$	$[Phe^4$ (immonium ion)$+H]^+$	$Choi^1+Gln^2+Ahp^3+NMeTyrOH^5+Leu/Ile^6+Hyp^7+Ala^8$
	70.0650	$C_4H_8N^+$	$[Hyp^7$ (immonium ion)$+H]^+$	$Choi^1+Gln^2+Ahp^3+Phe^4+NMeTyrOH^5+Leu/Ile^6+Ala^8$

[a]Fragment confirmed also in LC-HRMS^3 experiments, precursor ion at *m/z* 462.2343.

Effects of pre-oxidation on cyanopeptides content

Toxin levels in treated sample

Toxin content in *M. aeruginosa* cultures after the addition of each chlorinated oxidant and the resulting percent variation compared to controls (ΔTox(%)) is reported in Figure III.13. Toxin levels of the intracellular fraction were markedly lower in treated samples than in the controls, regardless of the oxidant used, the dose and the treatment time (Figure III.13a.; ANOVA, $p < 0.05$). The percent variation of intracellular toxins between controls and ClO_2-treated cultures was significantly higher compared to NaClO-treated cultures, being 99 vs 93%, respectively (Figure III.13b.; ANOVA, $p < 0.05$). Nonetheless, the simultaneous increase of extracellular toxins released in water was observed for treated cultures compared to controls. Specifically, a two-fold increase for NaClO-treated cultures was observed (Figure III.13a; ANOVA, $p < 0.05$), whereas for ClO_2 no significant effects were reported at the same low dose (0.5 mg L-1, ANOVA, $p > 0.05$). Only the highest dose of ClO_2 led to a decrease in extracellular toxin contents, which resulted in the actual effective treatment for the toxins removal (Figure III.13b; ΔTox 18-21%, ANOVA, $p < 0.05$). As for total toxin content (intracellular plus extracellular fractions), the concentration was significantly reduced compared to the controls only for cultures treated with the highest dose of ClO_2, regardless of the treatment time (ANOVA, $p < 0.05$). Similar trends were observed for toxin concentrations expressed per number of cells, with minor differences due to the reduced cell density in ClO_2-treated samples.

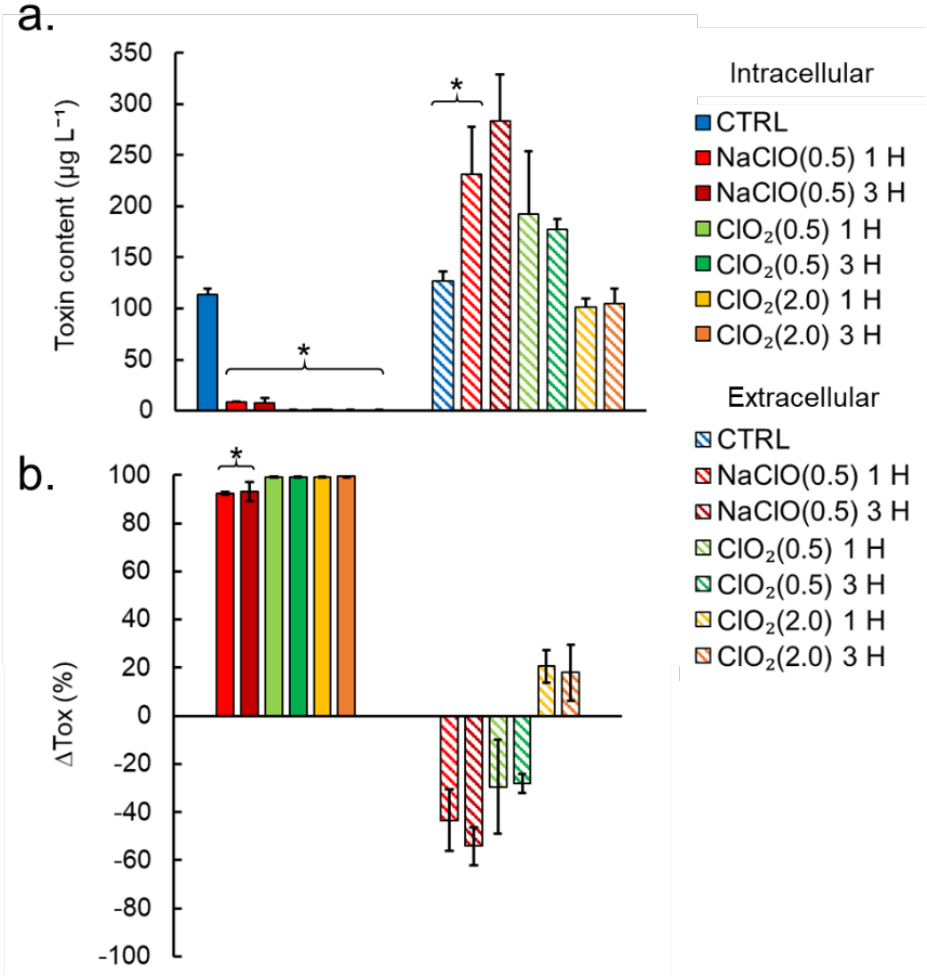

Figure III.13. Toxins' content in *M. aeruginosa* cultures (n = 3) treated with ClO_2 and NaClO and percent variation of their content compared to controls in each fraction, measured by LC-HRMS, i.e., intracellular (filled columns) and extracellular (striped columns); a) toxin content per volume (µg L^{-1}) and b) relative percent variation ΔTox(%).

Content variation of microcystins and of cyanopeptolin-type peptides

The percent variation of each toxin and CPtps between controls and each treatment for the intracellular and extracellular fractions, i.e., ΔTox(%), is reported in Figure III.14. Regardless of the treatment used, both MC variants and

the new CPtp-1029 were removed from the cells, although the extent of the removal was generally higher for ClO_2- than NaClO-treated cultures, especially for MC-LY and MC-LF and their [Asp^3]-analogues (Figure III.14). CPtp-1029 was particularly affected by all treatments, both in intracellular and extracellular fractions, turning into its oxidized derivative. In NaClO-treated cultures, CPtp-1029 accounted for 72-76% of *M. aeruginosa* intracellular fraction profile, whereas in ClO_2-treated cultures its relative intracellular abundance decreased to 33-41%. In extracellular fractions, CPtp-1029 concentration increased following oxidant treatments compared to the controls, especially when using NaClO (2 vs 80-100 μg L^{-1}, respectively). Thus, the percent variation of CPtp-1029 content resulted negative and about –100% for NaClO treatment compared to controls (Figure III.14). The overall results suggest that CPtp-1029 was not degraded in the biomass by NaClO but released in water likely due to cell damage, hence accounting for 32-37% of the extracellular fraction. Conversely, in ClO_2-treated cultures, the relative abundance of CPtp-1029 in extracellular fraction decreased to 19% after 1 h of treatment at the lowest dose (0.5 mg L^{-1}), whereas dropped to near 1% in all the other conditions. The actual removal of CPtp-1029 from water was only achieved at the highest ClO_2 dose (ΔTox 85-93%, Figure III.14). A simultaneous increase in the abundance of the oxidized derivative, CPtp-1045, was observed in the extracellular fraction, especially after the addition of ClO_2. This effect was particularly evident when comparing the residual extracellular concentration of the two CPtps following the treatment with ClO_2 at the lowest dose; after 1 h, CPtp-1029 was still present in relatively high amounts and CPtp-1045 was less abundant (31 and 8 μg L^{-1}, respectively). After 3 h an opposite trend emerged, as the concentration of the CPtp-1029 drastically decreased while its oxidized derivative increased (4 and 27 μg L^{-1}, respectively).

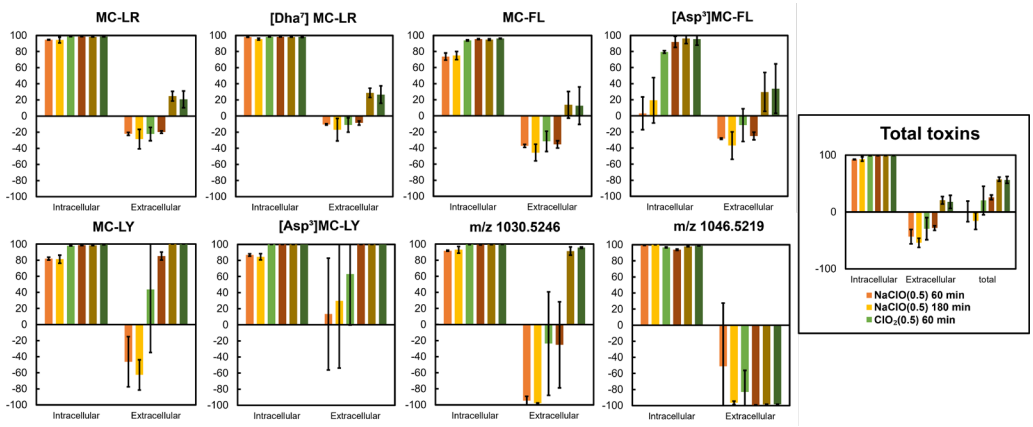

Figure III.14. Percent variation of each toxin variants (ΔTox(%)) after oxidation treatments with NaClO and ClO_2 in intracellular (filled columns) and extracellular (striped columns) fractions based on toxin concentrations per volume (μg L^{-1}).

The use of both oxidants, ClO_2 and NaClO, led to the inhibition of the photosynthetic activity of *M. aeruginosa*, in agreement with previous observations.[47,48] The results obtained herein showed how NaClO affected cell viability at markedly lower doses compared to ClO_2 (0.5 vs 0.8 mg L^{-1}). While ClO_2 remains as a dissolved gas in the solution when added to water, NaClO dissociates forming HClO, that can permeate the negatively charged cyanobacterial cells, causing damage at the membrane and intracellular levels. Additionally, at the tested doses, chosen in the range of EC_{50} values (i.e., 0.4-0.6 mg L^{-1} for ClO_2 and 0.3-0.4 mg L^{-1} for NaClO), the photosynthetic activity of *M. aeruginosa* firstly decreased following short-term treatment of 1 h, but slightly increased after 24 h. This evidence may indicate that the cultures treated with low doses of both oxidants were likely experiencing a temporary stress, rather than structural damages, since treated cells were able to partially recover their photosynthetic capacity after 1 day. While overdosing with oxidants (> 2 mg L^{-1}) may lead to various issues, including the formation of DBPs (Table 3), increase of turbidity and dissolved organic carbon, toxin and taste-and-odour compounds release,[33,41] soft-chlorination could shift the community composition in natural

assemblages leading to the persistence of some species less-susceptible to the oxidation.[49] Other studies have investigated how chlorinated oxidants differently affect cyanobacteria (i.e., cellular integrity, cells density, viability, toxin content), both in cultures [34,47–49] and natural-occurring blooms,[50,51] emphasizing how different test conditions and organisms can be differently affected by the treatments. The release of intracellular toxins into water and the simultaneous increase of their extracellular concentration were previously observed, suggesting that the rate of toxin degradation into nontoxic dihydroxy or monochloro-hydroxy derivatives, could be slower than its release due to oxidation-driven cellular damage.[52] Although noxious DBPs - collectively known as trihalomethanes and haloacetic acids - are outside the scope of this study, evidence exists that water chlorination using NaClO may lead to their formation because of reaction with natural organic matter.[39] Using ClO_2 is generally considered safer than other chlorinated oxidants because it does not form trihalomethanes, but in alkaline conditions it may react with OH^- in solution to form ClO^{2-} and ClO^{3-}, or other DBPs of health concerns whose formation depletes ClO^2 for oxidation of cyanotoxins.[53] Therefore, although better results in toxin removal were here obtained when using the highest dose of ClO^2 (2.0 mg L^{-1}), overdosing should be further discouraged. Additionally, the low concentrations of MCs oxidized products found in the present study agreed with the results by Kull et al. (2004) describing the effective oxidation of MCs occurring only at high ClO_2 concentrations (107 mg L^{-1}).[54]

Oxidation may act differently on each MC variant depending both on the amino acid residues and operational conditions. The reactivity of free chlorine is expected to be lower for MCs containing relatively unreactive aliphatic amino acids (e.g., MC-LA containing both leucine and alanine), and higher for those variants having amino acids with aromatic rings (e.g., MC-YR). Similarly, during

the here-set oxidation experiment, the major removal effect was observed for MC-LY and MC-LF variants, each containing amino acids with an aromatic ring (Y = tyrosine, F = phenylalanine). To the best of our knowledge, no studies on the effects of chlorinated oxidants on cyanopeptolin-type peptides have been conducted so far, whose presence have emerged thanks to the untargeted LC-HRMS approach here used. While the potential (eco)toxicity of CPtps has still not been investigated, toxic effects of purified extracts of similar metabolites (i.e., cyanopeptolins) have emerged when tested on model organisms; for instance reduced reproduction and lifespan, together with affected valvular integrity was observed in the nematode *Caenorhabditis elegans*,[55] whereas neurotoxic effects have emerged in zebrafish embryos.[56] Noteworthy, cyanopeptolins and MCs concentrations found in freshwaters are often comparable.[29] Most of the epidemiological studies on cyanotoxins focused on the potential exposure to well-known MCs, while the inclusion of less studied cyanobacterial peptides, such as CPtps, could give new insights especially when observing symptoms not ascribable to the presence of other known toxins. Furthermore, potential risks associated with the co-occurrence of multiple cyanometabolite classes may boost a synergistic toxic effect that has not been investigated so far. Thus, the implementation of untargeted LC-HRMS methods able to investigate the whole cyanometabolite profile appears desirable to guarantee human and animal safety.

3.2.4 Conclusions

The chlorinated oxidants NaClO and ClO_2 were able to inactivate *M. aeruginosa* cells at a low dose of 0.5 mg L^{-1}. High toxin removal from cyanobacterial cells and simultaneous increase in water was observed for both oxidants, suggesting possible cell damage, while a longer treatment time resulted not effective. While ClO_2 degraded cyanobacterial cells and total toxins, NaClO possibly stimulated

the extracellular toxin release, without an effective removal. Untargeted LC-HRMS led to identify two new cyanopeptolin-type peptides, CPtp-1029 and its oxidation derivative, CPtp-1045, with the latter increasing in extracellular fraction after oxidation treatment, especially when using ClO_2. These findings suggest that the toxicological risks associated with the presence of CPtps in the pre-oxidized drinking water should not be neglected. The choice of the oxidant to be used during raw water pre-treatment for potabilization purposes, as well as its dose and treatment time, should be taken into consideration. Since the success of a specific treatment highly depends on several environmental conditions (e.g., pH, temperature, organic matter), it is difficult to establish what the best pre-oxidation practice might be. The use of lower (< 2 mg L^{-1}) oxidant doses may limit treatment costs, while maintaining the benefits of using pre-oxidation before subsequent downstream potabilization processes and avoiding the excessive release of intracellular organic matter, including cyanotoxins and other unknown metabolites such as CPtps. Finally, major efforts should be put into understanding the fate of such compounds at downstream processes in DWTPs and their potential presence in finished water.

3.3 CYANOMETDB UPDATE AND IMPLEMENTATION: MONITORING KEY METABOLITES FROM CYANOBACTERIAL BLOOMS OF *PLANKTOTHRIX* SPP.

3.3.1 Introduction

Harmful cyanobacterial blooms, which frequently contain toxic secondary metabolites, are reported in aquatic environments around the world. More than two thousand cyanobacterial secondary metabolites have been reported from diverse sources over the past fifty years.[57–59] The study of cyanobacterial secondary metabolites presents two major challenges: the availability of analytical methods capable of detecting and identifying a broad range of compounds, and the lack of a publicly available list of known metabolites, including chemical structure information. A key hurdle is the lack of a universally accepted bioinformatics platform within the cyanobacterial research community. While commercial databases of secondary metabolites exist, they are only accessible to paying customers (e.g., Antibase, MarinLit, The Dictionary of Natural Products). Several open access databases are available, but they often have limitations in terms of the number of cyanobacterial metabolites or parameters listed (e.g., ALGALTOX List, NORINE database, Handbook of Marine Natural Products).[60–62] A comprehensive, publically-accessible database detailing these secondary metabolites would facilitate research into their occurrence, functions, and toxicological risks. In this context, from 2019, I participated to an international project, in the curation (continuous updating) and implementation (inclusion of $HRMS^2$ spectra) of the CyanoMetDB, a highly curated, flat-file, openly-accessible database of cyanobacterial secondary metabolites that contains >2010 cyanobacterial metabolites and 99 structurally related compounds, which aims to facilitate: (1) the detection and dereplication

of known cyanobacterial toxins and secondary metabolites; (2) identification of novel natural products from cyanobacteria; (3) the research on biosynthesis of cyanobacterial secondary metabolites, including substructure searches; and (4) the investigation of their abundance, persistence, and toxicity in natural environments.[5] The dataset includes microcytsins, cyanopeptolins, other depsipeptides, anabaenopeptins, microginins, aeruginosins, cyclamides, cryptophycins, saxitoxins, spumigins, microviridins, and anatoxins among other metabolite classes. In particular, at the current stage of the project, for 350 compounds MS^2 reference spectra have been measured and acquired from samples sent by all the contributors to the work and the data processing for the quality check is ongoing (DOI: 10.5281/zenodo.7922070).[5,30] CyanoMetDB is also integrated into other platforms, such as MetFrag, which allows for in silico predicted fragmentation mass spectrometry, and adds annotation content such as natural product taxonomy and chemical classes[63] and Mass Bank, where all mass spectra can be deposited and searchable by everyone.[64] The database is continuously updated, with the 2023 release available in various formats, including XLSX and CSV, for different workflow requirements. The group of Dr. Elisabeth Janssen from the Department of Environmental Chemistry of the Swiss Federal Institute of Aquatic Science and Technology (EAWAG) is the main proponent of the project, and they hosted me at their laboratories in the frame of the International Agreement Type B between Eawag (Swiss) and Department of Pharmacy of the University of Napoli Federico II, thanks to the winning of a scholarship for PhD mobility (DM 442/2020 - a.a 2022/2023). In addition, in order to strengthen and speed up the interpretation of the amount of data generated through a single LC-HRMS analysis, data processing is required to facilitate studies of identification and dereplication of emerging toxins and bioactive metabolites (known and new ones) in different matrices (fresh or salt

water, microalgal field or culture biomass samples, marine foods such as mollusks and fish, etc.).[2] Tools that can be used for the analysis and processing of data are several; in particular, during the visiting period at Eawag, I learnt how to proceed with the suspect screening by using Skyline, an open-source software designed for targeted proteomics and metabolomics data analysis. Developed by the MacCoss Lab at the University of Washington, it runs on Microsoft Windows and supports raw data formats from multiple mass spectrometric instruments.[65,66] Other tools include MetFrag (https://msbi.ipb-halle.de/MetFrag/), a online platform that allows to annotate the compounds present in the sample under investigation by comparing the list of transitions obtained from the $HRMS^2$ experiment with what is in the database, previously uploaded.[63] In this context, the use of Mass Bank (https://massbank.eu/MassBank/) can facilitate the confirmation of toxins whose $HRMS^2$ spectra are uploaded on the platform. At the same time new analogues can be more easily characterized, by comparing common fragments.[64] During my visiting period at Eawag, this workflow was successfully applied to the comparative analysis between samples of *Planktothrix rubescens*, already present at Eawag, and Italian *Planktothrix rubescens* and *P. agardhii* samples.

Cyanobacteria from the genus *Planktothrix* commonly found in freshwater environments, are known to produce a diverse array of metabolites, some of which have significant ecological and health implications.[57,67] Microcystins, anatoxins, saxitoxins, and other secondary metabolites are among the key compounds produced by *Planktothrix* during cyanobacterial blooms. Understanding the metabolism of *Planktothrix* and the production of these metabolites is crucial for effective monitoring, risk assessment, and management strategies to safeguard water quality and mitigate the impact of cyanobacterial blooms on both the environment and public health.[67] *Planktothrix rubescens*, also

known as *Oscillatoria rubescens*, is a colonial freshwater cyanobacterium. It is considered an indicator of increased trophic levels in a lake, as it blooms abundantly when there is a lot of organic and/or inorganic material available, depleting oxygen in the water and causing the disappearance of zooplankton. This species is commonly referred to as "red algae" due to its red colour, which is attributed to a specific photosynthetic pigment, phycoerythrin. The species is known to produce anatoxins (ATXs), cylindrospermopsin (CYN) and microcystins (MCs).[57,68] *Planktothrix agardhii* is another species of cyanobacteria that is regularly involved in the occurrence of cyanotoxins in lakes and reservoirs. This species is dominant in many eutrophic lakes and can produce hepatotoxic microcystins.[67,69] The mass appearance of *Planktothrix* species is often associated with the occurrence of toxins, mainly microcystins, in addition to many secondary metabolites, which can affect the functioning of the entire ecosystem.

3.3.2 Experimental section

Planktothrix spp. samples

Table 6 and 7 report the isolated strains and the biomass from lake samples analyzed at Eawag, respectively (#8 *Planktothrix rubescens* from Eawag, #1 *Planktothrix rubescens* from UniNa and #1 *Planktothrix agardhii* from UniNa and #15 isolates from lake Zürich).

Table 6. Isolated strains from Eawag and UniNa.

Nr	Species	Names	Origin	Culture grown at
1 (Eawag)	*Planktothrix rubescens*	NIVA-CYA 617 9707	Lake Zürich, Switzerland, 1997	Eawag
2 (Eawag)	*Planktothrix rubescens*	NIVA-CYA 619 CCAP 1460/15 BC Pla 9725	Lake Zürich, Switzerland, 1997	Eawag
3 (Eawag)	*Planktothrix rubescens*	NIVA-CYA 622 CCAP 1460/17 BC Pla 9743	Lake Zürich, Switzerland, 1997	Eawag
4 (Eawag)	*Planktothrix rubescens*	NIVA-CYA 622 CCAP 1460/17 BC Pla 97112	Lake Zürich, Switzerland, 1997	Eawag
5 (Eawag)	*Planktothrix rubescens*	NIVA-CYA 623 CCAP 1459/40 BC Pla 9303	Lake Zürich, Switzerland, 1993	Eawag
6 (Eawag)	*Planktothrix rubescens*	NIVA-CYA 624 CCAP 1459/41 BC Pla 9316	Lake Zürich, Switzerland, 1993	Eawag
7 (Eawag)	*Planktothrix rubescens*	no info	no info	Eawag
8 (Eawag)	*Planktothrix rubescens*	no info	no info	Eawag
9 (UniNa)	*Planktothrix agardhii*	CCAP 1059/16	Blelham Tarn, Cumbria, England, UK	University of Bologna, Italy
10 (UniNa)	*Planktothrix rubescens*	CCAP 1059/22	Blelham Tarn, Cumbria, England, UK	University of Bologna, Italy

Table 7. Lake samples from Lake Zürich.

Nr	Lake Name, Country	Dominating species	Sample dates
1 (Eawag)	Lake Zürich, Switzerland	Planktothrix rubescens	2019-2022, different months

LC-HRMS Analysis

LC–HRMS analyses were carried out using an UHPLC (Dionex UltiMate3000 RS pump, Thermo Fischer Scientific) coupled to a Orbitrap Exploris 240 equipped with an H-ESI source (Thermo-Fisher, San José, USA). A Kintetex column (2.6µm C18, 100× 2.1 mm, Phenomenex, Torrance, USA) provided of a guard column, kept at 40 °C, was used. Flow was set at 0.255 mL min-1 with water (eluent A) and methanol (eluent B), both acidified with formic acid (0.1%). Chromatographic gradient was: 4% B in 3 min, 4–30% B in 4 min, 30-70% B for 23 min 70-100% B for 8.5 min and 4% for 6.5 min. Injection volume was 20 µL. Resolving power was set at 120,000 (FWHM at *m*/*z* 400). Positive ions HR full-scan MS spectra were acquired in the range *m*/*z* 100–1200. The following source settings were used: spray voltage 3.5 kV, ion transfer tube temperature 320°C, sheath gas 40 and auxiliary gas 10 (arbitrary units), vaporizer temperature 275°C. Data-dependent high-resolution product ion spectra were obtained by normalized collision energies for HCD of 15%, 30%, 45% at a resolving power of 17,500 triggering data-dependent $HRMS^2$ acquisition using CyanoMetDB.[30]

Suspect screening work-flow

Suspect screening was performed with Skyline 22.2 (MacCoss Lab Software) for $[M+H]^+$ protonated ions. The so called "transition list" used to generate an initial list of suspects was obtained from CyanoMetDB in the range *m/z* 450-1350, imported as a CSV file to Skyline.[5] Subsequently, the acquired raw data was imported as results and a CSV file report was obtained. This is an initial suspect list that was further thinned by filtering the list based on mass error (±5 ppm), accurate isotope pattern (Skyline idotp value ≥0.95), and removal of duplicates. The filtered list obtained was loaded back into Skyline, and for each compound found in each sample, evaluation of the relevant HRMS spectrum was performed,

then confirmed considering the complete fragmentation information obtained from the relevant HRMS^2 spectrum. Extracted ion chromatograms (XICs) were obtained from the HR full-scan MS spectra by selecting the exact masses of $[M+H]^+$ and $[M+2H]^{2+}$ ions of all known MCs (±5 ppm).

3.3.3 Preliminary results

Suspect screening analysis

The suspect screening analysis was carried out using the Skyline Software 22.2 (MacCoss Lab Software), importing the CyanoMetDB transition list in the range *m*/*z* 450-1350, as a CSV file. After that all the samples analysed in the same conditions, are imported as raw data, together with a blank and a calibration curve obtained as standard mix of several cyanotoxins and isolated cyanometabolites available at Eawag (Figure III.15).

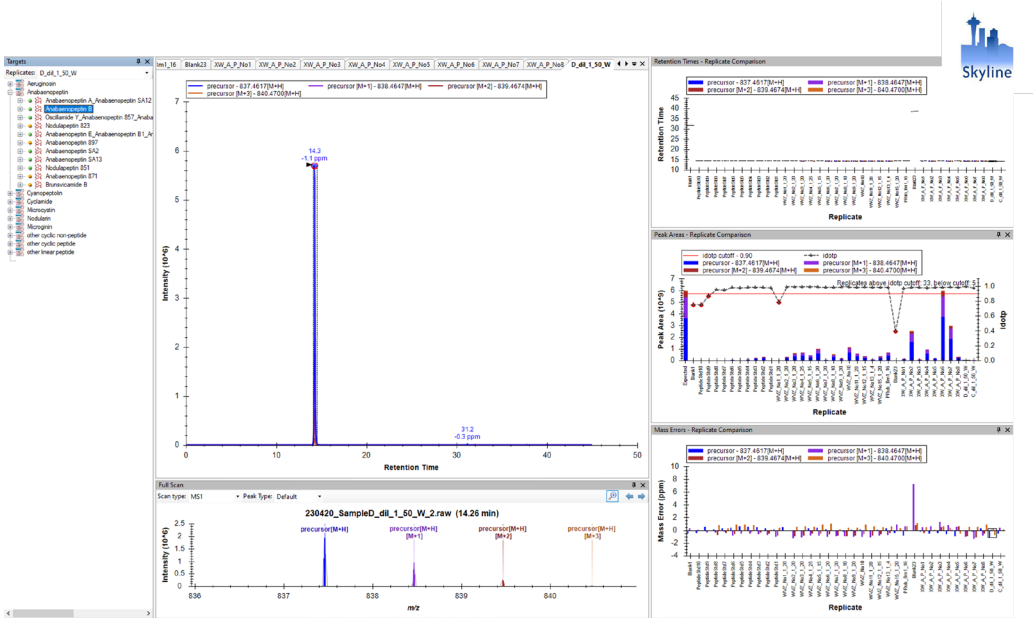

Figure III.15. Skyline interface showed for Anabaenopeptin B.

From the suspect screening analysis (MS^1), it is emerged that *Planktothrix rubescens* strains were dominated by the presence of microcystins and anabenopeptins, in good agreement with data reported in literature (Figure III.16a). *Planktothrix agardhii*, on the other hand, presented quite a different profile in terms of the microcystins found, which nevertheless represent the largest percentage of the cyanobacterial profile (Figure III.16b). The main difference between the *P. rubescens and agardhii* was, actually, the absence of [Dha^7]MC-RR in *P. agardhii* toxin profile. Moreover, *P. rubescens* samples featured richer profiles in terms of cyanobacteria secondary metabolites than the analysed *P. agardhii* one.

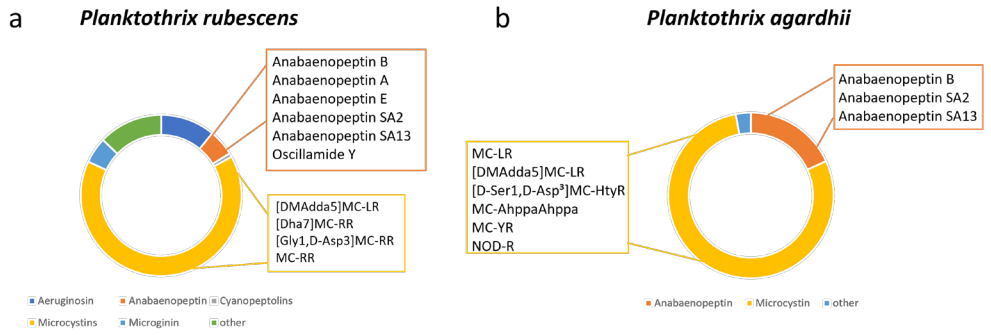

Figure III.16. Toxic profiles emerged from the suspect screening analysis through Skyline of a) *P. rubescens* (UniNa sample) and b) *P. agardhii* (UniNa sample). The principal differences in terms of detected microcystins and anabaenopeptins are reported in the squares.

After the suspect screening analysis, the results obtained needs to be confirmed. To achieve this, each suspect from the obtained suspect list will be annotated through the use of MetFrag and MassBank. MetFrag allows the annotation of the compounds present in the samples, comparing the transition list obtained from the $HRMS^2$ experiments with the one uploaded from the database (CyanoMetDB). In this way, considering all the isomers, the candidate molecules

are obtained, and the programme gives a score depending on the number of corresponding peaks. The programme makes possible to display the part of the molecule corresponding to each attributed fragment.

3.3.4 Conclusions

This ongoing activity have the aim is to understand how metabolically different samples can be, in terms of their constituent species, when they come from different backgrounds. In addition, the development of a workflow to be applied methodologically for the analysis of cyanobacterial samples would make the analysis of these samples faster and more efficient.

3.4 DEVELOPMENT OF A SOLID-PHASE TOXIN ADSORPTION (SPATT) METHOD BASED ON CROSS-LINKED CYCLODEXTRINS FOR MONITORING PALYTOXIN AND ITS CONGENERS

3.4.1 Introduction

The detection of algal blooms and biotoxin contamination in a timely manner is crucial for ensuring consumer safety, managing commercial growing areas, and preventing the harvesting of contaminated products. In recent years, there has been a shift towards using chemical testing methods to evaluate toxin contamination levels in shellfish, moving away from older methods that relied on mouse bioassays, which were deemed unreliable, expensive, and ethically questionable.[70–72] Newly developed performance-based methods, validated and demonstrated to be effective, have gained approval from regulatory authorities, even if they don't strictly adhere to a universally accepted protocol (e.g., European Communities Commission decision 2002/225/EC).[73] Although direct quantification of toxin levels in shellfish flesh remains the ultimate means of determining product suitability for marketing and consumption, routine testing for early contamination warnings in shellfish poses various challenges. These challenges include: (1) the difficulty and expense associated with obtaining and preparing samples (sampling, transport, shucking, and extraction) for analysis; (2) variations in toxin affinities among different shellfish species and biochemical transformations within shellfish tissues that may produce numerous toxin derivatives; and (3) frequent matrix problems within extracts and assays, combined with slow and relatively insensitive analyses.

Passive samplers are being considered as an early warning tool for predicting shellfish contamination or as a supplementary method in monitoring programs. They offer several advantages, including simplicity, low cost, minimal matrix

effects during resin analysis, and the ability to integrate spatial and temporal responses. However, challenges such as determining optimal deployment times, saturation limits, lack of calibration and standardization, and the need for a better understanding of their correlation with toxin contents must be addressed. It's also important to note that passive samplers can only monitor dissolved toxins, not those associated with particulate matter.[74–76] Research and development in this area are ongoing, and passive samplers show promise as a valuable tool in the detection of contaminants in shellfish and other environmental monitoring applications.[76] Nevertheless, they find valuable application in environmental monitoring and research, providing insights into Harmful Algal Blooms (HABs) such as geographical and temporal distribution, environmental persistence, and toxin dynamics.[6] MacKenzie introduced the concept of Solid-phase Adsorption Toxin Tracking (SPATT) in 2004,[77] involving the passive adsorption of toxins onto porous synthetic resins for subsequent extraction and analysis. These resins, enclosed in various frames, are deployed into the water column to adsorb toxins released by toxic microalgae.

Diaion® HP-20 is the most commonly used adsorbent substrate in passive samplers for both microalgae cultures and field studies.[76,78,79] In contrast to this resin's toxin adsorption, cyclodextrins (CDs) capture organic compounds through supramolecular interactions, displaying different affinity, kinetics, and saturation behaviours. Cyclodextrins are cyclic glucose oligomers forming a conical structure with a hydrophobic internal cavity and hydrophilic external rims. Their glucose unit count (e.g., 6 in α-CD, 7 in β-CD, and 8 in γ-CD) determines cavity size, enabling the inclusion of diverse organic molecules based on size, shape, and polarity.[80–82] Used in drug delivery and biosensors, CDs have been recently applied in marine toxin tracking by M. Campas et al., for the monitoring of

Prorocentrum lima cultures and deployed them in harbor waters during a *Dinophysis sacculus* bloom. [6]

Considering that palytoxin is among the most potent non-protein marine toxins known to date,[83] the necessity of an early warning of *Ostreopsis* proliferations turns out to be crucial to facilitate management and protect human health. SPATT technology can be a new, valuable, and sustainable method for passive sampling of palytoxin and ovatoxins.

In our study, several insoluble cyclodextrin polymers (β/γ-CD-hexamethylene diisocyanate (β/γ-CD-HDI), β/γ-CD-epichlorohydrin (β/γ-CD-EPI), and Diaion® HP-20 as control) have been exposed in both powder form and placed into the SPATT unit, to palytoxin standard solution and then to *O*. cf. *ovata* pellet extracts and suspension to evaluate the recovery yields of palytoxin and ovatoxins after being captured by cyclodextrins, extracted and finally analysed by LC-HRMS.

3.4.2 Experimental section

Small scale experiments

50 mg of cyclodextrin (β-epichlorohydrin (β-EPI), γ-epichlorohydrin (γ-EPI), β/γ - hexamethylene diisocyanate (HDI-A, HDI-B) and Comercial Diaion® (HP-20), as a control) in two replicates were added into Eppendorf tubes and spiked firstly, with 1 mL of Palytoxin standard solution 200 ng/mL in sterile seawater (Wako Chemicals GmbH, Neuss, Germany) and then with an equivalent content of OVTX-a from *O.* cf. *ovata* pellet extract and incubated overnight.

The *O.* cf. *ovata* strains (CBA 3318, CBA3320, CBA3321, CBA3322) were isolated in September 2020 in Passetto, Ancona and analyzed for toxin content in March 2021. The pellet extraction was carried out following the procedure described in the Chapter 2,[84] in order to determinate the toxin profile of each

strain, through the LC-HRMS method described in Chapter 2. A new CBA3318 strain was analyzed in April 2022 (Table 8).

β-CD-HDI, γ-CD-HDI, β-CD-EPI and γ-CD-EPI were synthesized as reported by Campas et al., in 2021 [6] while Diaion® HP-20 Supelco resin was obtained from VidraFoc (Barcelona, Spain). Certified reference material of Palytoxin (10 μg/mL in 1:1 EtOH/H_2O) was obtained from Wako Chemicals GmbH (Neuss, Germany).

The procedure consisted in covering the CD powder with the PLTX spiked sterile seawater (spiking concentration 200ng PLTX/mL) or with the *O.* cf. *ovata* extract or cell suspension and incubating for 4 hours for β-CD-HDI, γ-CD-HDI and 2 hours for Diaion®. Samples were then centrifuged for 10 min at 8000 rpm and the supernatant, and the resins were preserved in the fridge. A control sample (n=2), consisted in 1mL of has been prepared, in order to have a control sample for the elution of the obtained supernatant through Solid Phase Extraction (SPE) procedure, described in the chapter 2.[85] The extraction of PLTX and OVTXs from the resins consisted in the following steps:

a) 1 mL of the extracting mixture was added, vortexed, and incubated for 1.5h.

b) Samples were centrifuged for 10 min at 8000 rpm and the supernatant was transferred into an Eppendorf.

c) A second sequential extraction was performed adding 1 mL of the extracting mixture into the Eppendorf containing the CDs, vortexed and centrifuged again for 10 min at 8000 rpm; the supernatant resulted from the second extraction was kept separate from the first one.

d) An aliquot of 0.2 mL was taken for LC-HRMS analysis.

All incubation steps were performed under agitation on a mixing wheel (450 rpm) at room temperature.

Table 8. *O*.cf. *ovata* strains whose extracts and suspensions are used in CDs experiments.

***O*. cf. *ovata* Samples**	**Cell N°**	**Year of the LC-HRMS analysis**
CBA3318_1	1000000	2022
CBA3318_2	1000000	2022
CBA3318	1041000	2021
CBA3320	1051000	2021
CBA3321	1031000	2021
CBA3322	1091000	2021

Scale-up of the system

Passive sampling disks were constructed by placing 1 g of β-CD-HDI, β-CD-EPI, γ-CD-HDI, γ-CD-EPI and Diaion® HP-20 between two layers of 1-µm nylon mesh (Sefar Maissa S.A.U., Cardedeu, Barcelona, Spain), clipped between two cylindrical PVC rings (4-cm diameter) (Figure III.17).

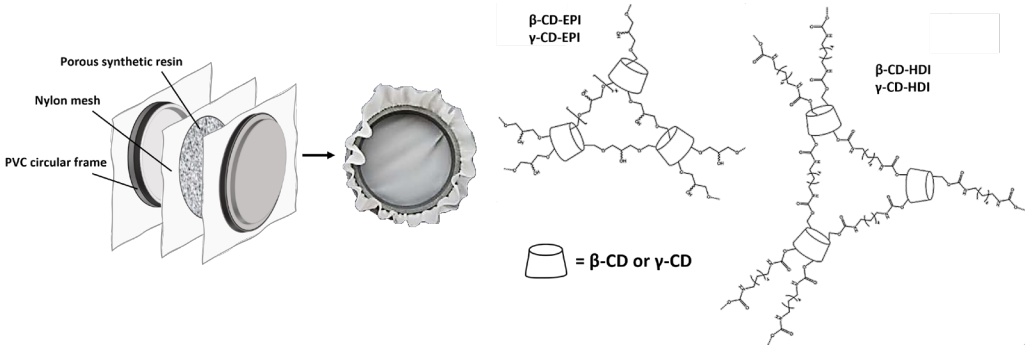

Figure III.17. Description of the SPATT unit constructed with 1g of each CD.

The scale up from 1 mL to 1L system was achieved by spiking 900 mL of seawater, previously filtered, with a concentration equivalent to 10^5 cells (10

mL), contained in the cell suspension and in the extract of the CBA3318 strain (2022) and proceeding with the incubation with the different SPATTs, under agitation, taking care to keep the SPATT vertical. After incubation, each SPATT was broken with the help of a cutter and the respective resin was decanted into a 50 mL falcon so that it could be extracted. The extraction was made with 20 mL of the extracting mixture for two times, as optimized in the small-scale experiments. Each extraction 1 was dried at rotavapor and redissolved in 1 mL of methanol 50%. The concentration step was evaluated also for a standard solution of palytoxin (20 mL as the extract), at a similar concentration of the OVTX-a spiked in the seawater, dried at rotavapor, and redissolved in 1 mL of WE 1:1. The remaining seawater was also analyzed through the SPE procedure, described before. Each 900 mL of seawater were loaded on a SPE cartridge (SPE Oasis HLB LP, 500 mg, 6cc) to assess how much OVTX-a, in the case of the experiment with the extracts, and how much PLTX, in the case of the experiment with the standard solution, was not captured by SPATT but remaining in the seawater.

Liquid chromatography–high resolution mass spectrometry (LC-HRMS) on LTQ-Orbitrap XL™ FTMS

LC-HRMS analyses were carried out on a hybrid linear ion trap LTQ Orbitrap XL™ Fourier Transform Mass Spectrometer (FTMS) equipped with an ESI ION MAX™ source coupled with a Dionex Ultimate 3000 quaternary HPLC system (Thermo-Fisher, San Jose, CA, USA). LC separation was achieved on a Kinetex 2.6 µm, 100Å, 100 x 2.1 mm (Phenomenex, Torrance, CA, USA) HPLC column, eluted at a flow rate of 0.2 mL/min at room temperature with water (A) and acetonitrile-water 95:5 (v/v) both containing acetic acid 30 mM. The optimized gradient is the following: (t) 0 min, 20% B; t 10 min, 100%B; t 15, 100%B; t 16,

20%B; t 17 20%B; re-equilibration time was 10 min. The MS parameters were spray voltage 4.8 kV, capillary temperature 360 °C, capillary voltage 36 V, sheath gas 60 and auxiliary gas 21 (arbitrary units), and tube lens voltage 100 V. Full-scan spectra were acquired in the m/z range 800-1400 at resolving power (RP) 60,000 (FWHM at m/z 400). The full-scan XIC of each toxin was obtained by selecting the exact mass of the mono-isotopic an the most intense peak of the $[M+H+Ca]^{3+}$ ion cluster. Elemental formulae were assigned with Thermo Xcalibur software v2.2 SP1.48 (Thermo Fisher, San Josè, CA, USA) within a mass tolerance of 5 ppm. Regarding quantification, the main limitation so far encountered is represented by the lack of reference and certified reference material (RM and CRM) for OVTXs. The latter hinders (i) the measurement of the toxicological properties of toxins and thus the assessment of actual risk to human health, (ii) the interlaboratory validation of analytical and biological detection methods, and (iii) the accurate quantification of toxins present in different matrices. Currently, the only available standard is the PLTX standard (uncertified; FUJIFILM Wako, Japan), while no certified reference material has been produced. The main reasons lie in (i) the slow growth of dinoflagellates when used as a biological source and (ii) the lack of optimized procedures to isolate OVTX produced in high yields and degrees of purity.

3.4.3 Preliminary results

Small scale experiments

The study began with the optimization of the most appropriate solvent mixture to be used to extract PLTX standard from cyclodextrins after incubation and consequently understand the capacity of cyclodextrins to capture this type of compound.

Several extraction mixtures were tested, methanol-water 80% + 0.1% of acetic acid, methanol-ACN-water 4:4:2 + 0.1% of acetic acid, ACN-water 80% + 0.1% of acetic acid and methanol-water 80%, and 80% methanol-water solution with 0.1% acetic acid was found to be the best alternative. Under these conditions, the best cyclodextrins tested were β/γ-CD-HDI followed by the control Diaion® and β/γ-CD-EPI (Figure III.18a). Consequently, the incubation time related to the contact between the resin and the PLTX standard contained in seawater, was optimized. It was tested between 1, 2 and 4 hours. 4 hours gave the higher recovery yields on the β/γ-CD-HDI and 2 hours for the Diaion® (Figure III.18b).

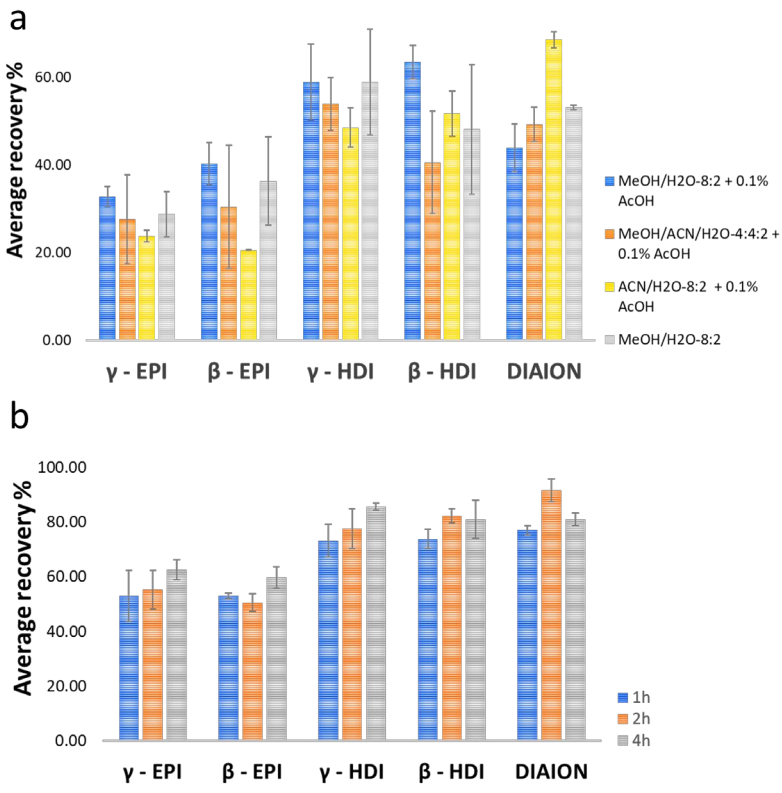

Figure III.18. Optimization of a) extraction mixtures evaluated among 1) methanol-water 80% + 0.1% of acetic acid, 2) methanol-ACN-water 4:4:2 + 0.1% of acetic acid, 3) ACN-water 80% + 0.1% of acetic acid and 4) methanol-water 80%, b) incubation time evaluated among 1, 2 and 4 hours.

Once these parameters were optimized, we moved on the incubation of the *Ostreopsis* strain, in the form of both, a methanolic extract and a cell suspension in seawater. The toxin profile of the new strain CBA3318 (2022) was obtained through LC-HRMS analysis and was dominated by the presence of ovatoxin-a followed by -b, -d and -e and by isobaric palytoxin (Table 9; Figure III.19).

Table 9. Quantification of OVTXs in *O.* cf. *ovata* CBA3318 (2022) extract.

OVTXs	[pg/cell]	%
OVTX-a	28.27	55.21
OVTX-b	14.15	27.64
OVTX-c	2.37	4.64
OVTX-d/e	6.20	12.11
ISO-PLTX	0.21	0.41
Total OVTXs content	51.21	100

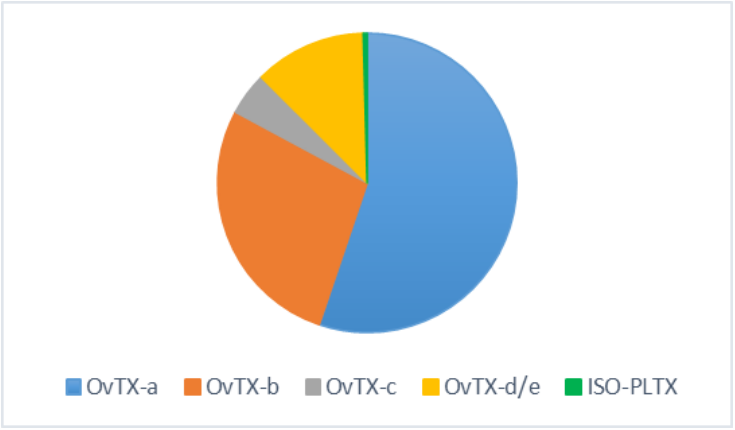

Figure III.19. Toxin profile of *O.* cf. *ovata* CBA3318 (2022) extract.

The quantification of the others *O.* cf. *ovata* CBA strains, extracted in 2021, gave similar results in terms of OVTX-a content, so they are comparable to the 2022 CBA3318 and they can be used for the following experiments.

3.4.4 Next step: scale-up of the system

Considering that *Ostreopsis* cf. *ovata* cell concentration in the seawater representing a risk for bathers and beach goers, the Italian Ministry of Health released some guidelines to manage the risk associated to *O. ovata* blooms during recreational activities. In particular, the alert stage starts when the density in the water column is equal to 10^4 cells/L.[86] *O. ovata* extract and *O. ovata* cell suspension in seawater at a concentration of 10^4 cells, corresponding to the alert stage, is selected to scale-up the system from 1 to 900mL of seawater. From the preliminary results obtained in the small-scale experiments, on cyclodextrins essentially in powder form, the next step involves scaling up the system from the small scale to the actual SPATT system. This consists in incubating the SPATT, in 900mL of previously filtered seawater, with a cell extract amount of 10^4 *O. ovata* cells/L. These experiments concern optimizing the incubation time required for the SPATT to capture toxins in the water. In fact, the possible presence of toxins not absorbed, but remaining in the water, is tested by means of a previously optimized SPE procedure for seawater.[85] First results obtained, shown that a larger amount of toxin remains in the water (~30/40 %) while a smaller percentage manages to be adsorbed and then extracted by the SPATT (~10/20 %), so it seems necessary to continue optimizing and implementing the system by testing different incubation times and then proceed with the active test of the SPATT system in seawater during a natural bloom of *Ostreopsis* cf. *ovata* or in mesocosm with an *Ostreopsis* cf. *ovata* culture.

References

(1) De Girolamo, A.; Lippolis, V.; Pascale, M. Overview of Recent Liquid Chromatography Mass Spectrometry-Based Methods for Natural Toxins Detection in Food Products. *Toxins* **2022**, *14* (5), 328. https://doi.org/10.3390/toxins14050328.

(2) Varriale, F.; Tartaglione, L.; Zervou, S.-K.; Miles, C. O.; Mazur-Marzec, H.; Triantis, T. M.; Kaloudis, T.; Hiskia, A.; Dell'Aversano, C. Untargeted and Targeted LC-MS and Data Processing Workflow for the Comprehensive Analysis of Oligopeptides from Cyanobacteria. *Chemosphere* **2023**, *311*, 137012. https://doi.org/10.1016/j.chemosphere.2022.137012.

(3) Dom, I.; Biré, R.; Hort, V.; Lavison-Bompard, G.; Nicolas, M.; Guérin, T. Extended Targeted and Non-Targeted Strategies for the Analysis of Marine Toxins in Mussels and Oysters by (LC-HRMS). *Toxins* **2018**, *10* (9), 375. https://doi.org/10.3390/toxins10090375.

(4) Klijnstra, M. D.; Faassen, E. J.; Gerssen, A. A Generic LC-HRMS Screening Method for Marine and Freshwater Phycotoxins in Fish, Shellfish, Water, and Supplements. *Toxins* **2021**, *13* (11), 823. https://doi.org/10.3390/toxins13110823.

(5) Jones, M. R.; Pinto, E.; Torres, M. A.; Dörr, F.; Mazur-Marzec, H.; Szubert, K.; Tartaglione, L.; Dell'Aversano, C.; Miles, C. O.; Beach, D. G.; McCarron, P.; Sivonen, K.; Fewer, D. P.; Jokela, J.; Janssen, E. M.-L. CyanoMetDB, a Comprehensive Public Database of Secondary Metabolites from Cyanobacteria. *Water Research* **2021**, *196*, 117017. https://doi.org/10.1016/j.watres.2021.117017.

(6) Campàs, M.; Rambla-Alegre, M.; Wirén, C.; Alcaraz, C.; Rey, M.; Safont, A.; Diogène, J.; Torréns, M.; Fragoso, A. Cyclodextrin Polymers as Passive Sampling Materials for Lipophilic Marine Toxins in Prorocentrum Lima Cultures and a Dinophysis Sacculus Bloom in the NW Mediterranean Sea. *Chemosphere* **2021**, *285*, 131464. https://doi.org/10.1016/j.chemosphere.2021.131464.

(7) Hallegraeff, G. M.; Anderson, D. M.; Belin, C.; Bottein, M.-Y. D.; Bresnan, E.; Chinain, M.; Enevoldsen, H.; Iwataki, M.; Karlson, B.; McKenzie, C. H.; Sunesen,

I.; Pitcher, G. C.; Provoost, P.; Richardson, A.; Schweibold, L.; Tester, P. A.; Trainer, V. L.; Yñiguez, A. T.; Zingone, A. Perceived Global Increase in Algal Blooms Is Attributable to Intensified Monitoring and Emerging Bloom Impacts. *Commun Earth Environ* **2021**, *2* (1), 1–10. https://doi.org/10.1038/s43247-021-00178-8.

(8) *Climate warming may increase algal blooms caused by sediment nutrient release in lakes – management must adapt*. https://environment.ec.europa.eu/news/climate-warming-may-increase-algal-blooms-caused-sediment-nutrient-release-lakes-management-must-2023-01-18_en (accessed 2024-01-14).

(9) KARADURMUŞ, U.; SARI, M. Marine Mucilage in the Sea of Marmara and Its Effects on the Marine Ecosystem: Mass Deaths. *Turkish Journal of Zoology* **2022**, *46* (1), 93–102. https://doi.org/10.3906/zoo-2108-14.

(10) Tas, S.; Kus, D.; Yilmaz, I. N. Temporal Variations in Phytoplankton Composition in the Northeastern Sea of Marmara: Potentially Toxic Species and Mucilage Event. *Mediterranean Marine Science* **2020**, *21* (3), 668–683. https://doi.org/10.12681/mms.22562.

(11) Giani, M.; Rinaldi, A.; Degobbis, D. Mucilages in the Adriatic and Tyrrhenian Sea: An Introduction. *Science of The Total Environment* **2005**, *353* (1), 3–9. https://doi.org/10.1016/j.scitotenv.2005.09.006.

(12) Deserti, M.; Cacciamani, C.; Chiggiato, J.; Rinaldi, A.; Ferrari, C. R. Relationships between Northern Adriatic Sea Mucilage Events and Climate Variability. *Science of The Total Environment* **2005**, *353* (1), 82–88. https://doi.org/10.1016/j.scitotenv.2005.09.009.

(13) Lamas, J. P.; Arévalo, F.; Moroño, Á.; Correa, J.; Muñíz, S.; Blanco, J. Detection and Spatio-Temporal Distribution of Pinnatoxins in Shellfish from the Atlantic and Cantabrian Coasts of Spain. *Toxins* **2019**, *11* (6), 340. https://doi.org/10.3390/toxins11060340.

(14) Hort, V.; Bastardo-Fernández, I.; Nicolas, M. Exploration of Vulcanodinium Rugosum Toxins and Their Metabolism Products in Mussels from the Ingril Lagoon

Hotspot in France. *Marine Drugs* **2023**, *21* (8), 429. https://doi.org/10.3390/md21080429.

(15) Varriale, F.; Tartaglione, L.; Cinti, S.; Milandri, A.; Dall'Ara, S.; Calfapietra, A.; Dell'Aversano, C. Development of a Data Dependent Acquisition-Based Approach for the Identification of Unknown Fast-Acting Toxins and Their Ester Metabolites. *Talanta* **2021**, *224*, 121842. https://doi.org/10.1016/j.talanta.2020.121842.

(16) Sosa, S.; Pelin, M.; Cavion, F.; Hervé, F.; Hess, P.; Tubaro, A. Acute Oral Toxicity of Pinnatoxin G in Mice. *Toxins* **2020**, *12* (2), 87. https://doi.org/10.3390/toxins12020087.

(17) Chain (CONTAM), E. P. on C. in the F. Scientific Opinion on Marine Biotoxins in Shellfish – Cyclic Imines (Spirolides, Gymnodimines, Pinnatoxins and Pteriatoxins). *EFSA Journal* **2010**, *8* (6), 1628. https://doi.org/10.2903/j.efsa.2010.1628.

(18) Seo, N.; Jo, H. Y.; Lee, S. G.; Kim, H. J.; Oh, M. J.; Kim, Y. S.; Ro, S.; Jeon, Y. J.; An, H. J. An Enhanced LC-MRM-MS Platform for Sensitive and Simultaneous Quantification of Cyclic Imines in Shellfish. *Journal of Chromatography B* **2023**, *1229*, 123883. https://doi.org/10.1016/j.jchromb.2023.123883.

(19) Selwood, A. I.; Wilkins, A. L.; Munday, R.; Shi, F.; Rhodes, L. L.; Holland, P. T. Portimine: A Bioactive Metabolite from the Benthic Dinoflagellate Vulcanodinium Rugosum. *Tetrahedron Letters* **2013**, *54* (35), 4705–4707. https://doi.org/10.1016/j.tetlet.2013.06.098.

(20) Tang, J.; Li, W.; Chiu, T.-Y.; Martínez-Peña, F.; Luo, Z.; Chong, C. T.; Wei, Q.; Gazaniga, N.; West, T. J.; See, Y. Y.; Lairson, L. L.; Parker, C. G.; Baran, P. S. Synthesis of Portimines Reveals the Basis of Their Anti-Cancer Activity. *Nature* **2023**, *622* (7983), 507–513. https://doi.org/10.1038/s41586-023-06535-1.

(21) Fribley, A. M.; Xi, Y.; Makris, C.; Alves-de-Souza, C.; York, R.; Tomas, C.; Wright, J. L. C.; Strangman, W. K. Identification of Portimine B, a New Cell Permeable Spiroimine That Induces Apoptosis in Oral Squamous Cell Carcinoma.

ACS Med. Chem. Lett. **2019**, *10* (2), 175–179. https://doi.org/10.1021/acsmedchemlett.8b00473.

(22) *UNI EN 15204:2006 - UNI Ente Italiano di Normazione*. https://store.uni.com/uni-en-15204-2006 (accessed 2024-01-15).

(23) Aráoz, R.; Barnes, P.; Séchet, V.; Delepierre, M.; Zinn-Justin, S.; Molgó, J.; Zakarian, A.; Hess, P.; Servent, D. Cyclic Imine Toxins Survey in Coastal European Shellfish Samples: Bioaccumulation and Mode of Action of 28-O-Palmitoyl Ester of Pinnatoxin-G. First Report of Portimine-A Bioaccumulation. *Harmful Algae* **2020**, *98*, 101887. https://doi.org/10.1016/j.hal.2020.101887.

(24) de la Cruz, A. A.; Chernoff, N.; Sinclair, J. L.; Hill, D.; Diggs, D. L.; Lynch, A. T. Introduction to Cyanobacteria and Cyanotoxins. In *Water Treatment for Purification from Cyanobacteria and Cyanotoxins*; John Wiley & Sons, Ltd, 2020; pp 1–35. https://doi.org/10.1002/9781118928677.ch1.

(25) Huisman, J.; Codd, G. A.; Paerl, H. W.; Ibelings, B. W.; Verspagen, J. M. H.; Visser, P. M. Cyanobacterial Blooms. *Nat Rev Microbiol* **2018**, *16* (8), 471–483. https://doi.org/10.1038/s41579-018-0040-1.

(26) Buratti, F. M.; Manganelli, M.; Vichi, S.; Stefanelli, M.; Scardala, S.; Testai, E.; Funari, E. Cyanotoxins: Producing Organisms, Occurrence, Toxicity, Mechanism of Action and Human Health Toxicological Risk Evaluation. *Arch Toxicol* **2017**, *91* (3), 1049–1130. https://doi.org/10.1007/s00204-016-1913-6.

(27) Wang, J.; Zhang, S.; Mu, X.; Hu, X.; Ma, Y. Research Characteristics on Cyanotoxins in Inland Water: Insights from Bibliometrics. *Water* **2022**, *14* (4), 667. https://doi.org/10.3390/w14040667.

(28) McDonald, K.; Renaud, J. B.; Pick, F. R.; Miller, J. D.; Sumarah, M. W.; McMullin, D. R. Diagnostic Fragmentation Filtering for Cyanopeptolin Detection. *Environmental Toxicology and Chemistry* **2021**, *40* (4), 1087–1097. https://doi.org/10.1002/etc.4941.

(29) Beversdorf, L. J.; Weirich, C. A.; Bartlett, S. L.; Miller, T. R. Variable Cyanobacterial Toxin and Metabolite Profiles across Six Eutrophic Lakes of

Differing Physiochemical Characteristics. *Toxins* **2017**, *9* (2), 62. https://doi.org/10.3390/toxins9020062.

(30) Janssen, E. M.-L.; Jones, M. R.; Pinto, E.; Dörr, F.; Torres, M. A.; Rios Jacinavicius, F.; Mazur-Marzec, H.; Szubert, K.; Konkel, R.; Tartaglione, L.; Dell'Aversano, C.; Miglione, A.; McCarron, P.; Beach, D. G.; Miles, C. O.; Fewer, D. P.; Sivonen, K.; Jokela, J.; Wahlsten, M.; Niedermeyer, T. H. J.; Schanbacher, F.; Leão, P.; Preto, M.; D'Agostino, P. M.; Baunach, M.; Dittmann, E.; Reher, R. S75 | CyanoMetDB | Comprehensive Database of Secondary Metabolites from Cyanobacteria, 2023. https://doi.org/10.5281/zenodo.7922070.

(31) Kust, A.; Řeháková, K.; Vrba, J.; Maicher, V.; Mareš, J.; Hrouzek, P.; Chiriac, M.-C.; Benedová, Z.; Tesařová, B.; Saurav, K. Insight into Unprecedented Diversity of Cyanopeptides in Eutrophic Ponds Using an MS/MS Networking Approach. *Toxins* **2020**, *12* (9), 561. https://doi.org/10.3390/toxins12090561.

(32) Moreira, C.; Vasconcelos, V.; Antunes, A. Cyanobacterial Blooms: Current Knowledge and New Perspectives. *Earth* **2022**, *3* (1), 127–135. https://doi.org/10.3390/earth3010010.

(33) Jalili, F.; Moradinejad, S.; Zamyadi, A.; Dorner, S.; Sauvé, S.; Prévost, M. Evidence-Based Framework to Manage Cyanobacteria and Cyanotoxins in Water and Sludge from Drinking Water Treatment Plants. *Toxins* **2022**, *14* (6), 410. https://doi.org/10.3390/toxins14060410.

(34) Zamyadi, A.; Fan, Y.; Daly, R. I.; Prévost, M. Chlorination of Microcystis Aeruginosa: Toxin Release and Oxidation, Cellular Chlorine Demand and Disinfection by-Products Formation. *Water Research* **2013**, *47* (3), 1080–1090. https://doi.org/10.1016/j.watres.2012.11.031.

(35) Mohamed, Z. A. Breakthrough of Oscillatoria Limnetica and Microcystin Toxins into Drinking Water Treatment Plants – Examples from the Nile River, Egypt. *Water SA* **2016**, *42* (1), 161–165. https://doi.org/10.4314/wsa.v42i1.16.

(36) Pazouki, P.; Prévost, M.; McQuaid, N.; Barbeau, B.; de Boutray, M.-L.; Zamyadi, A.; Dorner, S. Breakthrough of Cyanobacteria in Bank Filtration. *Water Research* **2016**, *102*, 170–179. https://doi.org/10.1016/j.watres.2016.06.037.

(37) Rose, A. K.; Fabbro, L.; Kinnear, S. Cyanobacteria Breakthrough: Effects of Limnothrix Redekei Contamination in an Artificial Bank Filtration on a Regional Water Supply. *Harmful Algae* **2018**, *76*, 1–10. https://doi.org/10.1016/j.hal.2018.04.010.

(38) Betancourt, W. Q.; Rose, J. B. Drinking Water Treatment Processes for Removal of Cryptosporidium and Giardia. *Veterinary Parasitology* **2004**, *126* (1), 219–234. https://doi.org/10.1016/j.vetpar.2004.09.002.

(39) Mazhar, M. A.; Khan, N. A.; Ahmed, S.; Khan, A. H.; Hussain, A.; Rahisuddin; Changani, F.; Yousefi, M.; Ahmadi, S.; Vambol, V. Chlorination Disinfection By-Products in Municipal Drinking Water – A Review. *Journal of Cleaner Production* **2020**, *273*, 123159. https://doi.org/10.1016/j.jclepro.2020.123159.

(40) Zhang, H.; Dan, Y.; Adams, C. D.; Shi, H.; Ma, Y.; Eichholz, T. Effect of Oxidant Demand on the Release and Degradation of Microcystin-LR from Microcystis Aeruginosa during Oxidation. *Chemosphere* **2017**, *181*, 562–568. https://doi.org/10.1016/j.chemosphere.2017.04.120.

(41) Qi, J.; Ma, B.; Miao, S.; Liu, R.; Hu, C.; Qu, J. Pre-Oxidation Enhanced Cyanobacteria Removal in Drinking Water Treatment: A Review. *Journal of Environmental Sciences* **2021**, *110*, 160–168. https://doi.org/10.1016/j.jes.2021.03.040.

(42) Stanier, R. Y.; Kunisawa, R.; Mandel, M.; Cohen-Bazire, G. Purification and Properties of Unicellular Blue-Green Algae (Order Chroococcales). *Bacteriological Reviews* **1971**, *35* (2), 171–205. https://doi.org/10.1128/br.35.2.171-205.1971.

(43) Pichierri, S.; Pezzolesi, L.; Vanucci, S.; Totti, C.; Pistocchi, R. Inhibitory Effect of Polyunsaturated Aldehydes (PUAs) on the Growth of the Toxic Benthic Dinoflagellate Ostreopsis Cf. Ovata. *Aquatic Toxicology* **2016**, *179*, 125–133. https://doi.org/10.1016/j.aquatox.2016.08.018.

(44) Sperling, M. von; Verbyla, M. E.; Oliveira, S. M. A. C. *Assessment of Treatment Plant Performance and Water Quality Data: A Guide for Students, Researchers and Practitioners*; IWA Publishing, 2020.

(45) Kaloudis, T.; Zervou, S.-K.; Tsimeli, K.; Triantis, T. M.; Fotiou, T.; Hiskia, A. Determination of Microcystins and Nodularin (Cyanobacterial Toxins) in Water by LC–MS/MS. Monitoring of Lake Marathonas, a Water Reservoir of Athens, Greece. *Journal of Hazardous Materials* **2013**, *263*, 105–115. https://doi.org/10.1016/j.jhazmat.2013.07.036.

(46) Christophoridis, C.; Zervou, S.-K.; Manolidi, K.; Katsiapi, M.; Moustaka-Gouni, M.; Kaloudis, T.; Triantis, T. M.; Hiskia, A. Occurrence and Diversity of Cyanotoxins in Greek Lakes. *Sci Rep* **2018**, *8* (1), 17877. https://doi.org/10.1038/s41598-018-35428-x.

(47) Li, X.; Chen, S.; Zeng, J.; Song, W.; Yu, X. Comparing the Effects of Chlorination on Membrane Integrity and Toxin Fate of High- and Low-Viability Cyanobacteria. *Water Research* **2020**, *177*, 115769. https://doi.org/10.1016/j.watres.2020.115769.

(48) Zhou, S.; Shao, Y.; Gao, N.; Li, L.; Deng, J.; Zhu, M.; Zhu, S. Effect of Chlorine Dioxide on Cyanobacterial Cell Integrity, Toxin Degradation and Disinfection by-Product Formation. *Science of The Total Environment* **2014**, *482–483*, 208–213. https://doi.org/10.1016/j.scitotenv.2014.03.007.

(49) Moradinejad, S.; Glover, C. M.; Mailly, J.; Seighalani, T. Z.; Peldszus, S.; Barbeau, B.; Dorner, S.; Prévost, M.; Zamyadi, A. Using Advanced Spectroscopy and Organic Matter Characterization to Evaluate the Impact of Oxidation on Cyanobacteria. *Toxins* **2019**, *11* (5), 278. https://doi.org/10.3390/toxins11050278.

(50) Greenstein, K. E.; Zamyadi, A.; Glover, C. M.; Adams, C.; Rosenfeldt, E.; Wert, E. C. Delayed Release of Intracellular Microcystin Following Partial Oxidation of Cultured and Naturally Occurring Cyanobacteria. *Toxins* **2020**, *12* (5), 335. https://doi.org/10.3390/toxins12050335.

(51) Ye, B.; Cang, Y.; Li, J.; Zhang, X. Advantages of a ClO2/NaClO Combination Process for Controlling the Disinfection by-Products (DBPs) for High Algae-Laden

Water. *Environ Geochem Health* **2019**, *41* (3), 1545–1557. https://doi.org/10.1007/s10653-018-0231-8.

(52) Ding, J.; Shi, H.; Timmons, T.; Adams, C. Release and Removal of Microcystins from *Microcystis* during Oxidative-, Physical-, and UV-Based Disinfection. *Journal of Environmental Engineering* **2010**, *136* (1), 2–11. https://doi.org/10.1061/(ASCE)EE.1943-7870.0000114.

(53) Sorlini, S.; Gialdini, F.; Biasibetti, M.; Collivignarelli, C. Influence of Drinking Water Treatments on Chlorine Dioxide Consumption and Chlorite/Chlorate Formation. *Water Research* **2014**, *54*, 44–52. https://doi.org/10.1016/j.watres.2014.01.038.

(54) Kull, T. P. J.; Backlund, P. H.; Karlsson, K. M.; Meriluoto, J. A. O. Oxidation of the Cyanobacterial Hepatotoxin Microcystin-LR by Chlorine Dioxide: Reaction Kinetics, Characterization, and Toxicity of Reaction Products. *Environ. Sci. Technol.* **2004**, *38* (22), 6025–6031. https://doi.org/10.1021/es0400032.

(55) Lenz, K. A.; Miller, T. R.; Ma, H. Anabaenopeptins and Cyanopeptolins Induce Systemic Toxicity Effects in a Model Organism the Nematode Caenorhabditis Elegans. *Chemosphere* **2019**, *214*, 60–69. https://doi.org/10.1016/j.chemosphere.2018.09.076.

(56) Faltermann, S.; Zucchi, S.; Kohler, E.; Blom, J. F.; Pernthaler, J.; Fent, K. Molecular Effects of the Cyanobacterial Toxin Cyanopeptolin (CP1020) Occurring in Algal Blooms: Global Transcriptome Analysis in Zebrafish Embryos. *Aquatic Toxicology* **2014**, *149*, 33–39. https://doi.org/10.1016/j.aquatox.2014.01.018.

(57) Baumann, H. I.; Jüttner, F. Inter-Annual Stability of Oligopeptide Patterns of Planktothrix Rubescens Blooms and Mass Mortality of Daphnia in Lake Hallwilersee. *Limnologica* **2008**, *38* (3), 350–359. https://doi.org/10.1016/j.limno.2008.05.010.

(58) Gkelis, S.; Lanaras, T.; Sivonen, K. Cyanobacterial Toxic and Bioactive Peptides in Freshwater Bodies of Greece: Concentrations, Occurrence Patterns, and

Implications for Human Health. *Marine Drugs* **2015**, *13* (10), 6319–6335. https://doi.org/10.3390/md13106319.

(59) Mazur-Marzec, H.; Kaczkowska, M. J.; Blaszczyk, A.; Akcaalan, R.; Spoof, L.; Meriluoto, J. Diversity of Peptides Produced by Nodularia Spumigena from Various Geographical Regions. *Marine Drugs* **2013**, *11* (1), 1–19. https://doi.org/10.3390/md11010001.

(60) Sorokina, M.; Steinbeck, C. Review on Natural Products Databases: Where to Find Data in 2020. *J Cheminform* **2020**, *12* (1), 20. https://doi.org/10.1186/s13321-020-00424-9.

(61) Le Manach, S.; Duval, C.; Marie, A.; Djediat, C.; Catherine, A.; Edery, M.; Bernard, C.; Marie, B. Global Metabolomic Characterizations of Microcystis Spp. Highlights Clonal Diversity in Natural Bloom-Forming Populations and Expands Metabolite Structural Diversity. *Frontiers in Microbiology* **2019**, *10*.

(62) van Santen, J. A.; Jacob, G.; Singh, A. L.; Aniebok, V.; Balunas, M. J.; Bunsko, D.; Neto, F. C.; Castaño-Espriu, L.; Chang, C.; Clark, T. N.; Cleary Little, J. L.; Delgadillo, D. A.; Dorrestein, P. C.; Duncan, K. R.; Egan, J. M.; Galey, M. M.; Haeckl, F. P. J.; Hua, A.; Hughes, A. H.; Iskakova, D.; Khadilkar, A.; Lee, J.-H.; Lee, S.; LeGrow, N.; Liu, D. Y.; Macho, J. M.; McCaughey, C. S.; Medema, M. H.; Neupane, R. P.; O'Donnell, T. J.; Paula, J. S.; Sanchez, L. M.; Shaikh, A. F.; Soldatou, S.; Terlouw, B. R.; Tran, T. A.; Valentine, M.; van der Hooft, J. J. J.; Vo, D. A.; Wang, M.; Wilson, D.; Zink, K. E.; Linington, R. G. The Natural Products Atlas: An Open Access Knowledge Base for Microbial Natural Products Discovery. *ACS Cent. Sci.* **2019**, *5* (11), 1824–1833. https://doi.org/10.1021/acscentsci.9b00806.

(63) Ruttkies, C.; Schymanski, E. L.; Wolf, S.; Hollender, J.; Neumann, S. MetFrag Relaunched: Incorporating Strategies beyond in Silico Fragmentation. *Journal of Cheminformatics* **2016**, *8* (1), 3. https://doi.org/10.1186/s13321-016-0115-9.

(64) Horai, H.; Arita, M.; Kanaya, S.; Nihei, Y.; Ikeda, T.; Suwa, K.; Ojima, Y.; Tanaka, K.; Tanaka, S.; Aoshima, K.; Oda, Y.; Kakazu, Y.; Kusano, M.; Tohge, T.; Matsuda,

F.; Sawada, Y.; Hirai, M. Y.; Nakanishi, H.; Ikeda, K.; Akimoto, N.; Maoka, T.; Takahashi, H.; Ara, T.; Sakurai, N.; Suzuki, H.; Shibata, D.; Neumann, S.; Iida, T.; Tanaka, K.; Funatsu, K.; Matsuura, F.; Soga, T.; Taguchi, R.; Saito, K.; Nishioka, T. MassBank: A Public Repository for Sharing Mass Spectral Data for Life Sciences. *Journal of Mass Spectrometry* **2010**, *45* (7), 703–714. https://doi.org/10.1002/jms.1777.

(65) Adams, K. J.; Pratt, B.; Bose, N.; Dubois, L. G.; St. John-Williams, L.; Perrott, K. M.; Ky, K.; Kapahi, P.; Sharma, V.; MacCoss, M. J.; Moseley, M. A.; Colton, C. A.; MacLean, B. X.; Schilling, B.; Thompson, J. W. Skyline for Small Molecules: A Unifying Software Package for Quantitative Metabolomics. *J. Proteome Res.* **2020**, *19* (4), 1447–1458. https://doi.org/10.1021/acs.jproteome.9b00640.

(66) MacLean, B.; Tomazela, D. M.; Shulman, N.; Chambers, M.; Finney, G. L.; Frewen, B.; Kern, R.; Tabb, D. L.; Liebler, D. C.; MacCoss, M. J. Skyline: An Open Source Document Editor for Creating and Analyzing Targeted Proteomics Experiments. *Bioinformatics* **2010**, *26* (7), 966–968. https://doi.org/10.1093/bioinformatics/btq054.

(67) Tonk, L.; Visser, P. M.; Christiansen, G.; Dittmann, E.; Snelder, E. O. F. M.; Wiedner, C.; Mur, L. R.; Huisman, J. The Microcystin Composition of the Cyanobacterium Planktothrix Agardhii Changes toward a More Toxic Variant with Increasing Light Intensity. *Applied and Environmental Microbiology* **2005**, *71* (9), 5177–5181. https://doi.org/10.1128/AEM.71.9.5177-5181.2005.

(68) Komárek, J. Planktic Oscillatorialean Cyanoprokaryotes (Short Review According to Combined Phenotype and Molecular Aspects). In *Phytoplankton and Equilibrium Concept: The Ecology of Steady-State Assemblages*; Naselli-Flores, L., Padisák, J., Dokulil, M. T., Eds.; Developments in Hydrobiology; Springer Netherlands: Dordrecht, 2003; pp 367–382. https://doi.org/10.1007/978-94-017-2666-5_30.

(69) Lenard, T.; Poniewozik, M. Planktothrix Agardhii versus Planktothrix Rubescens: Separation of Ecological Niches and Consequences of Cyanobacterial Dominance

in Freshwater. *International Journal of Environmental Research and Public Health* **2022**, *19* (22), 14897. https://doi.org/10.3390/ijerph192214897.

(70) Free, C. M.; Moore, S. K.; Trainer, V. L. The Value of Monitoring in Efficiently and Adaptively Managing Biotoxin Contamination in Marine Fisheries. *Harmful Algae* **2022**, *114*, 102226. https://doi.org/10.1016/j.hal.2022.102226.

(71) Bodero, M.; Gerssen, A.; Portier, L.; Klijnstra, M. D.; Hoogenboom, R. L. A. P.; Guzmán, L.; Hendriksen, P. J. M.; Bovee, T. F. H. A Strategy to Replace the Mouse Bioassay for Detecting and Identifying Lipophilic Marine Biotoxins by Combining the Neuro-2a Bioassay and LC-MS/MS Analysis. *Marine Drugs* **2018**, *16* (12), 501. https://doi.org/10.3390/md16120501.

(72) Reverté, L.; Soliño, L.; Carnicer, O.; Diogène, J.; Campàs, M. Alternative Methods for the Detection of Emerging Marine Toxins: Biosensors, Biochemical Assays and Cell-Based Assays. *Marine Drugs* **2014**, *12* (12), 5719–5763. https://doi.org/10.3390/md12125719.

(73) *2002/225/EC: Commission Decision of 15 March 2002 Laying down Detailed Rules for the Implementation of Council Directive 91/492/EEC as Regards the Maximum Levels and the Methods of Analysis of Certain Marine Biotoxins in Bivalve Molluscs, Echinoderms, Tunicates and Marine Gastropods (Text with EEA Relevance) (Notified under Document Number C(2002) 1001)*; 2002; Vol. 075. http://data.europa.eu/eli/dec/2002/225/oj/eng (accessed 2024-01-15).

(74) Vincent-Hubert, F.; Wacrenier, C.; Morga, B.; Lozach, S.; Quenot, E.; Mège, M.; Lecadet, C.; Gourmelon, M.; Hervio-Heath, D.; Le Guyader, F. S. Passive Samplers, a Powerful Tool to Detect Viruses and Bacteria in Marine Coastal Areas. *Frontiers in Microbiology* **2021**, *12*.

(75) Stewart, M.; Cameron, M.; McMurtry, M.; Sander, S.; Benedict, B.; Graham, L.; Hosie, M.; Green, T. Development of Passive Sampling Devices for Bioavailable Contaminants of Current and Emerging Concern: Waitemata Harbour Case Study. *New Zealand Journal of Marine and Freshwater Research* **2016**, *50* (4), 526–548. https://doi.org/10.1080/00288330.2016.1181662.

(76) Kudela, R. M. Chapter Eleven - Passive Sampling for Freshwater and Marine Algal Toxins. In *Comprehensive Analytical Chemistry*; Diogène, J., Campàs, M., Eds.; Recent Advances in the Analysis of Marine Toxins; Elsevier, 2017; Vol. 78, pp 379–409. https://doi.org/10.1016/bs.coac.2017.08.006.

(77) MacKenzie, L.; Beuzenberg, V.; Holland, P.; McNabb, P.; Selwood, A. Solid Phase Adsorption Toxin Tracking (SPATT): A New Monitoring Tool That Simulates the Biotoxin Contamination of Filter Feeding Bivalves. *Toxicon* **2004**, *44* (8), 901–918. https://doi.org/10.1016/j.toxicon.2004.08.020.

(78) Fux, E.; Bire, R.; Hess, P. Comparative Accumulation and Composition of Lipophilic Marine Biotoxins in Passive Samplers and in Mussels (M. Edulis) on the West Coast of Ireland. *Harmful Algae* **2009**, *8* (3), 523–537. https://doi.org/10.1016/j.hal.2008.10.007.

(79) Roué, M.; Darius, H. T.; Chinain, M. Solid Phase Adsorption Toxin Tracking (SPATT) Technology for the Monitoring of Aquatic Toxins: A Review. *Toxins* **2018**, *10* (4), 167. https://doi.org/10.3390/toxins10040167.

(80) Syeda, S. E. Z.; Nowacka, D.; Khan, M. S.; Skwierawska, A. M. Recent Advancements in Cyclodextrin-Based Adsorbents for the Removal of Hazardous Pollutants from Waters. *Polymers* **2022**, *14* (12), 2341. https://doi.org/10.3390/polym14122341.

(81) Wacławek, S.; Krawczyk, K.; Silvestri, D.; Padil, V. V. T.; Řezanka, M.; Černík, M.; Jaroniec, M. Cyclodextrin-Based Strategies for Removal of Persistent Organic Pollutants. *Advances in Colloid and Interface Science* **2022**, *310*, 102807. https://doi.org/10.1016/j.cis.2022.102807.

(82) Okasha, A. T.; Abdel-Khalek, A. A.; Alenazi, N. A.; AlHammadi, A. A.; Al Zoubi, W.; Alhammadi, S.; Ko, Y. G.; Abukhadra, M. R. Progress of Synthetic Cyclodextrins-Based Materials as Effective Adsorbents of the Common Water Pollutants: Comprehensive Review. *Journal of Environmental Chemical Engineering* **2023**, *11* (3), 109824. https://doi.org/10.1016/j.jece.2023.109824.

(83) Pelin, M.; Sosa, S.; Tubaro, A. Palytoxins: Toxicological Profile. In *Marine and Freshwater Toxins*; Gopalakrishnakone, P., Haddad Jr., V., Tubaro, A., Kim, E., Kem, W. R., Eds.; Toxinology; Springer Netherlands: Dordrecht, 2016; pp 129–145. https://doi.org/10.1007/978-94-007-6419-4_19.

(84) Tartaglione, L.; Dello Iacovo, E.; Mazzeo, A.; Casabianca, S.; Ciminiello, P.; Penna, A.; Dell'Aversano, C. Variability in Toxin Profiles of the Mediterranean Ostreopsis Cf. Ovata and in Structural Features of the Produced Ovatoxins. *Environ. Sci. Technol.* **2017**, *51* (23), 13920–13928. https://doi.org/10.1021/acs.est.7b03827.

(85) Tartaglione, L.; Dell'Aversano, C.; Mazzeo, A.; Forino, M.; Wieringa, A.; Ciminiello, P. Determination of Palytoxins in Soft Coral and Seawater from a Home Aquarium. Comparison between Palythoa- and Ostreopsis-Related Inhalatory Poisonings. *Environ. Sci. Technol.* **2016**, *50* (2), 1023–1030. https://doi.org/10.1021/acs.est.5b05469.

(86) Funari, E.; Manganelli, M.; Testai, E. Ostreospis Cf. Ovata Blooms in Coastal Water: Italian Guidelines to Assess and Manage the Risk Associated to Bathing Waters and Recreational Activities. *Harmful Algae* **2015**, *50*, 45–56. https://doi.org/10.1016/j.hal.2015.10.00.

CHAPTER 4. NOVEL ARCHITECTURE IN THE FIELD OF ELECTROCHEMICAL SENSORS AND BIOSENSORS

The field of electrochemical sensors and biosensors has witnessed a surge in innovation, driven by advancements in materials science, nanotechnology, and bioengineering. Novel architectures are being developed to enhance the sensitivity, specificity, and versatility of sensors, making them invaluable for applications in healthcare, environmental monitoring, and various industries.[1–4] One of the key developments in this area is the integration of microelectronics and nanotechnology into sensor design.[5,6] This has led to the creation of micro and nanoscale devices, mainly represented by screen-printed electrodes (SPE), which can provide near-molecular scale sensitivity.[1] In this context, a strategy deeply investigated in this dissertation, consists in the development of novel integrated devices that can exploit several advantages. Starting from a classical three electrode configuration printed on polyester and then combined with filter paper, we exploited the advantages of filter paper as tool for storing reagents, treat real matrices and preconcentrate the analyte of interest.[7–10] Consequently, we exploited the advantages of filter paper when used both as substrate for printing and as integration for treating complex matrices Moving on, we proceeded with the characterization and application of total new sustainable polymers used to realize novel bio-based electroanalytical (bio)sensors. Finally, we integrated our devices in a glove for in situ monitoring of pesticides. In addition, many modern electrochemical sensors and biosensors are based on electrodes chemically modified in order to improve their analytical performance.[11] A strategy for increasing the performance and selectivity of electrochemical (bio)sensors is the use of nanostructured materials such as metallic nanoparticles,[12] carbon-based nanomaterials (carbon black and

graphene), carbon coatings,[13] membranes, and even some conductive polymers.[14] These nanostructures provide a high surface area, facilitating efficient electron transfer and improving the sensitivity of the (bio)sensors.[15,16] Surface modifications can lead to proper immobilization of biorecognition elements, improvement of the signal-to-noise ratio, enhanced sensitivity, and prevention of non-specific binding. The engineered nanomaterials provide higher electrical conductivity, have nanoscale size, can be used to amplify desired signals, and are compatible with biological molecules.[16] Moreover, the incorporation of nanomaterials in biosensors allows for easy enzyme immobilization, which can enhance the reuse and recycle of enzymes.[17] The use of nanomaterials may lead to increased biosensor performance due to their increased surface-to-volume ratio, chemical activity, mechanical strength, electrocatalytic properties, and enhanced diffusivity. However, it's important to note that while these strategies can significantly enhance the performance of electrochemical (bio)sensors, they also present challenges. Therefore, further research and development are needed to fully realize the potential of these strategies in the field of electrochemical sensing. Four experimental works, discussed below, were carried out following these strategies:

1) The development of an integrated paper-polyester electrochemical platform was applied to Nickel detection in cosmetic products, in which the advantages of integrating a robust polyester screen-printed sensor with filter paper as tool for storing reagents, treat real matrices and preconcentrate the analyte of interest, were exploited.

2) The development of an all-in paper-based 2D configuration for electrochemical and facile detection of paracetamol in wastewaters, in which the investigated platform is totally printed on paper.

3) The characterization and application of porous PHBV-based bacterial polymers to realize novel bio-based electroanalytical (bio)sensors, as novel bio substrates for printing.

4) The development of a glove-integrated enzyme inhibition-based screen-printed biosensor, for the detection of pesticides directly on fruit peels.

4.1 PAPER-POLYESTER INTEGRATION: ELECTROCHEMICAL PLATFORM FOR FAST NICKEL DETECTION IN COSMETICS

4.1.1 Introduction

A variety of chemicals are commonly used in cosmetic products as ingredients or preservatives, including heavy metals, such as lead (Pb), cadmium (Cd), nickel (Ni), arsenic (As) and mercury (Hg), often used in cosmetics for blocking ultraviolet light or colouring pigments.[18] Cosmetic products are regulated for health and safety, but there are concerns regarding the presence of harmful chemicals, including heavy metals, in these products; some metals, exceed specific concentrations, can cause serious safety issues such as skin troubles and allergies. Although absorption of metals from cosmetics through the skin is rather low,[19] these elements may accumulate in the skin and internal organs, where they can cause toxic effects. Numerous cases of topical, mainly allergic contact dermatitis, and systemic effects caused by exposure to metals present in cosmetics have been reported.[20–25] Among these, nickel is one of the most common allergens responsible for contact dermatitis, because it is found everywhere in the environment. High exposure to nickel can cause serious health effects, such as contact dermatitis or eczema. Some types of nickel (in the form of oxides, sulphides and soluble nickel compounds (primarily nickel sulphate and nickel chloride) are also considered to be carcinogenic.[26] Clinically, nickel allergy occurs when nickel-containing products are in direct and prolonged contact with the skin, leading to releasing nickel ions (to be) absorbed through the skin causing and starting an allergenic effect.[27] The symptoms of nickel allergy occur up to 48 h after exposure to the products containing this metal, however very often the skin lesions appear immediately. The symptoms persist about 2–4 weeks and they are located in a place directly contact of skin with

allergen. The result for sensitive skin is the allergic contact dermatitis.[28,29] Due to the harmfulness of metals to human health, their content in cosmetic products is prohibited or restricted by the regulations of some countries, but in many countries, there are no regulations in this regard.[18] The European Regulations describe over 1200 toxic substances whose presence are prohibited in cosmetic products. Among them, there are metals particularly dangerous for human health, such as Pb, Cd, As, Ni and Hg.[30] These are detected in different types of cosmetics currently available on the market (colored cosmetics, products for face and body care, hair cosmetics, herbal cosmetics, etc.), in some cases in dangerous concentrations.[31] In this context, the importance of nickel allergy proves introduced in 1994 in the European Union Directive 94/27/EC,[32] laying down the conditions for the nickel-containing products which are in direct and prolonged contact with the skin. Regulation 1223/2009 and Directive 76/768 / EEC prohibit the use of nickel and its salts as ingredients in cosmetics while allowing traces of metals in the form of impurities.[18] EU does not indicate limits for the presence of nickel in cosmetics, but the recommended tolerance limit is 1 ppm (1 mg/kg). The cosmetic companies that carry out these tests label their products with the words "nickel testing" and the test result, eg. << 0.00001%. This indication on the product packaging shows that the cosmetics have been tested and the results obtained are below detectable limits. This does not completely rule out the possibility of an allergic reaction, but it does indicate that the risk is considerably low. Therefore, it is important to measure the exact amount of metal in cosmetic products. In general, the quantification of nickel in cosmetics occurs through the use of traditional techniques, such as wet chemical analysis (e.g. gravimetric, titrimetric, colorimetric, etc.), inductively coupled plasma/mass spectrometry (ICP/MS) and Inductively coupled plasma—optical emission spectrometry (ICP-OES), or atomic absorption spectroscopy (AAS).[33] These operations are often

difficult due to the presence of many organic and inorganic materials such as oils, polymers, waxes, polyols, surfactants, and metal powders which give an important matrix effect. Moreover, transportation of samples to the laboratory and sample pretreatment using additional chemicals and filtration can significantly increase the overall time of analysis and cause analyte loss. Nickel determination is officially recognized by a test method known as EN 1811 and subsequent updates, in which nickel determination takes place by atomic absorption spectroscopy or any other appropriate technique (e.g. ICP-MS or ICP-OES).[32] In contrast to current standard techniques, as already said, electrochemical methods offer the possibility for miniaturization and construction of portable analysers that can be used for real-time analysis in the field. Considering the spread of this type of allergy among the population and the predominant use of cosmetic products (from detergents, body creams to make-up products), use portable and easy-to-use devices, which allow a quick and accurate detection of nickel above the permitted limits, could represent a valid and effective alternative for the protection of human health.

Different approaches have been reported for nickel electrochemical sensing in several matrices using dimethylglyoxime (DMG) in different way, as a selective Ni(II) chelating agent.[34–36] In contrast to some other metals (e.g. Cu, Pb, Fe), electrochemical determination of Ni(II) is complicated and usually suffers from low electrochemical signals and irreversible reduction at very negative potential. Baldwin et al. firstly described a voltammetric method for the determination of traces of nickel ions, preconcentrated selectively on the surface of a chemically modified electrode (CME) based on dimethylglyoxime (DMG) – containing carbon paste, with a limit of detection (LOD) of 0.05 μM in ammonium standard solution.[37] Similar, the group of Wang et al., developed disposable complexing sensor strips for trace nickel by doping the screen – printed carbon ink with ligand

DMG and the subsequently microfabrication of a thick – film. With a short accumulation period of 30s they reached a LOD of 5 µg/L for Nickel in buffer solution and 13 µg/L in river water samples.[38] Sensitivity of Ni(II) determination has been increased using also, for example, a cation exchanger Dowex 50 W by Gonzalez et al.; in this case, the ion exchanger was incorporated into the Nujol – graphite base paste and with 12 min of accumulation and 5 min of deposition, nickel was quantified until 0.005 µg/L in buffer solution and 5 µg/L in mineral and tap water.[39] Ferancova et al., modified commercial screen – printed electrodes with DMG in Nafion (DMG – N/SPE) for the determination of Ni(II) in mine site discharge waters. LOD was calculated of 0.03 mg/L in standard solution and lower than 0.1 mg/L for on-site monitoring in discharge water.[40] In addition to these electrochemical application for determining nickel ions, in the recent years the use of paper-based substrates has been applied towards the detection of metals, including nickel ions. Various approaches have been reported focusing on different architectures, both considering the configuration and the experimental setup. For instance, Whatman filter paper No. 4, acrylic lacquer and copper ions were used to detect nickel ions down to 0.5 ppm in jewellery waste samples, using a paper-based screen-printed electrode.[41] Another kind of paper-based support, namely hydrophobic photographic paper, has been used in combination with the more sophisticated inkjet-printing approach to produce a platform for nickel detection. In this case the authors prepared a mixture containing nafion, dimethylglyoxime, carbon black, silver nanoparticles to detect nickel ions in water samples.[42] The adoption of paper-based substrates has been also reported with the aim to store the reagents, not only related to the detection of nickel ions in combination with printed electrodes, e.g. arsenic determination in white wine, silver in river, mercury in tap water, cadmium and lead in mussels, enzymatic activity in serum etc.[8,9,43] However, with relationship

to nickel determination some examples have been reported in literature: Pokpas and colleagues combined a chromatographic paper-based disk with a commercial DropSens carbon screen-printed electrode. They loaded the buffer solution, DMG and Hg within the structure of paper-based disk, being released at the moment of measurements. Recovery studies of nickel ions in real water samples were performed, and the authors conclude that the Hg still exhibited superior detection performance over the Hg-free platform.[44] Following this concept, the group of Henry developed different approaches to combine the use of paper-based support to monitor metal ions. A Janus electrochemical paper-based analytical device was designed to contain four independent channels and working electrodes, to conduct square-wave anodic stripping voltammetry and square-wave cathodic stripping voltammetry for simultaneous detection of Ni, Cd, Pb, Cu, and Fe. The device was applied towards airborne particulate matter that was collected using ultrasonic personal aerosol samplers and then digested using microwave assisted digestion.[45] The next step was also focused on the combination of colorimetric and electrochemical detection of multi-metals, where paper-based preconcentration was combined with a portable heater. The method was applied to the electrochemical determination of Pb and Cd, and to the colorimetric determination of Fe and Ni in samples of drinking water, tap water, pond water, and wastewater.[46]

Although various examples have been reported to electrochemically and colorimetrically detect nickel ions, also through paper-based platforms, the development of electrochemical sensors for the detection of nickel in cosmetics is lacking, despite the increasing importance of this market and the regulations around these products. As a consequence, in this work, carried out in collaboration with the group of prof. Laneri of the Pharmacy Department of Federico II University of Naples, we propose the development and optimization

of a screen-printed electrode (SPE) coupled to a mm-diameter paper-based disk for fast, simple, and low-cost determination of Ni (II) at concentrations consistent with the allowable in cosmetics, using DMG as a metal complexing agent, avoiding time-consuming procedures. In particular we exploited the use of a chromatographic paper combined with a printed electrochemical strip, taking advantage, for the first time, of a 2D mixed polyester – filter paper device for Ni (II) ions detection in cosmetics. The sensitive detection of nickel ions has been achieved by employing polyester to realize the printed electrochemical strips and filter paper principally for store all the reagents necessary for carrying out the assay and allow the treatment of complex matrices as cosmetic ones.[47,48] The method developed has allowed to work with small amount of sample (microliters level) in which the combination of two different supports, polyester and filter paper, represents an alternative more suitable for application with the required flexibility and resistance are required (in particular with respect to those alumina and ceramic-based electrodes); in fact, polyester gives the advantage to obtain a more robust and sensitive platform that fit well with a domestic use of the device. Moreover, it should be noted that, only the reported architecture is capable to merge the sensibility of plastic-based device (detecting nickel ions) and the storing capacity of chromatographic paper (store reagents, remove interferences, preconcentrate matrix).

4.1.2 Experimental section

Fully printed hybrid platform

Electrodes were home produced on a flexible polyester film as substrate. The three-electrode were manually screen-printed as described in Chapter 2. The semicircle pattern was designed with Adobe Illustrator, and it has been printed onto a chromatographic paper (Whatman No. 1) with a solid-ink printer (Xerox

8580). The wax - printed paper has been cured in the oven for 1 min at a temperature of 100°C. The process is essential to facilitate the permeation of wax - based ink through the paper, creating a completely insulated hydrophilic area where the samples can be added.[7]

Nickel determination

The electroanalytical technique adopted to measure Ni (II) was the Differential pulse voltammetry (DPV). In particular, 0.1 M ammonium buffer solution, pH = 8.0, was used as working solution and the method parameters have been optimized as follows: after an accumulation time in open circuit of 3 min, the measurement was carried out in a range potential from -0.5 to -1.4 V, with an E step of 0.01 V, E pulse of 0.2 V, t pulse of 0.02 s and scan rate of 0.1 V s^{-1}. The determination with the hybrid polyester - filter paper device consists of: (1) adding all the reagents (ammonium buffer and DMG) and samples inside the wax paper disk in contact with the plastic-based electrode, (2) waiting 3 min at open circuit conditions and (3) release and analysis at the printed strips, as shown in Figure IV.1.

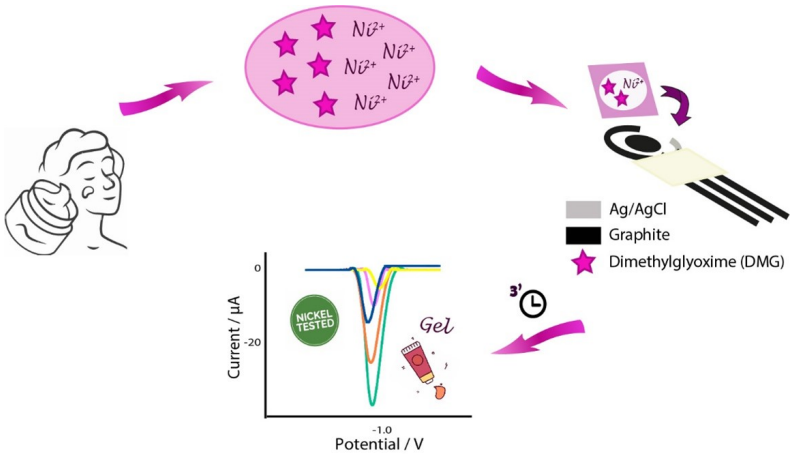

Figure IV.1. Schematic representation for the development of the hybrid polyester - filter paper platform to detect nickel ions in cosmetic products.

Cosmetics formulations

Different formulations, including a cream and gel, were prepared. At the end, 100 g of each formulation was spiked with different amount of $NiCl_2$ to obtain positive controls. In addition, the same formulations were analyzed in absence of nickel. Regarding to the cream, it contained two phases: Phase O (oil phase) polyglyceryl-3 methylglucose 5.0%, cetyl alcohol 2.5%, and isopropylmiristate 2.5%, and Phase W (water phase) containing water (89.6%), carbomer (0.1%), 5-Chloro-2-methyl-4-isothiazolin-3-one, 2-Methyl-4-isothiazolin-3-one (0.3%). All components used to produce the cream were bought from ACEF (Fiorenzuola D'Arda, Italy). The cream was produced by energetically shaking the two phases at 70°C using a Silverson L5M-A Laboratory Mixer (SBL, Shanghai, China), cooled in an ice bath, and adding the preservant and $NiCl_2$ solution at room temperature. The pH was calculated using a Crison GPL20 pH-Meter (Crison, Barcelona, Spain) (5.5) and viscosity (27.995–28.365 mPa; L4, 20 rpm) were tested using a Visco Basic Plus rheometer (Fungilab, Barcelona, Spain). The gel was prepared by dissolving 1 g of Carbomer 340 with 93g of water and following the addition of glycerol (4g) and neutralized at pH=5 with 2 M NaOH. When the gel preparation was finished, it was spiked with chosen level of nickel.

ICP-MS measurements

Concentrated nitric (UpA) and hydrochloric (UpA) acids, and certified stock standard solutions were purchased from Romil. Standard solutions of nickel were prepared in 3% nitric acid at five different concentrations, (0, 1, 10, 50 and 100 ppb). Samples were mineralized as follows: 250 microliters were transferred into a 7 mL Pyrex. Concentrated nitric acid and hydrochloric acid were added to each sample (in the ratio of 1:3). The reaction was conducted for 16 h at temperature of 90°C. The samples after digestion were diluted to 15 mL in milli-Q water and

were transferred into an ICP-MS vial for the analysis. Measurement have been performed with an Agilent 7700 ICP-MS instrument (Agilent Technologies) equipped with a frequency-matching radio frequency (RF) generator and 3rd generation Octapole Reaction System (ORS3) operating with helium gas in ORF. The following parameters were used: RF power: 1550 W, plasma gas flow: 14 L/min; carrier gas flow: 0.99 L/min; He gas flow: 4.3 mL/min. 103Rh was used as an internal standard (final concentration: 50 ppb).

4.1.3 Results and discussion

Optimization of the experimental parameters

First optimization was focused on the selection of the substrate for printing the conductive strips. Office paper (80 g/m2, Fabriano, Italy) and polyester were chosen to conduct this evaluation. As shown in Figure IV.2, same electrode configuration was printed on the two substrates, two microliters of 10 mM ethanolic dimethylglyoxime have been added in the buffer solution (ammonium buffer 0.1 M, pH = 8), and determination was performed using a 100 µM standard solution of nickel ions.

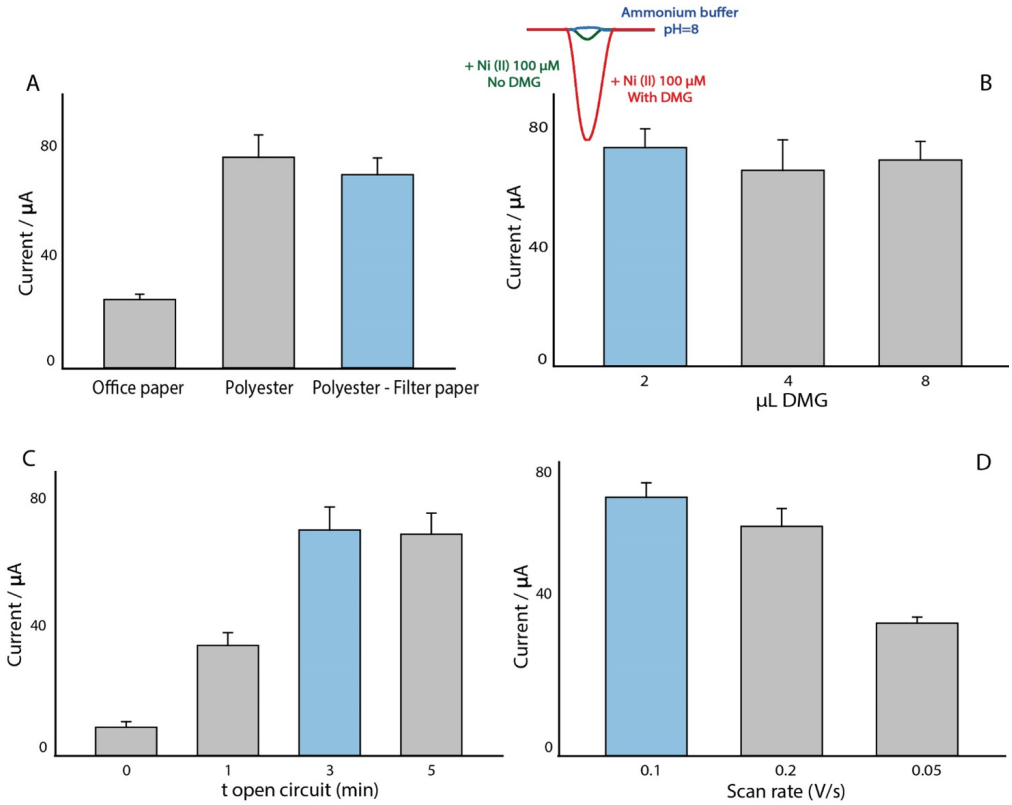

Figure IV.2. A) Choice of the substrate (polyester, office paper compared with the 2D configuration polyester-filter paper), B) Evaluation of the amount of 10 mM ethanolic DMG to be added to complex Ni (II), C) open circuit time optimization between 0 and 5 min and D) scan rate of the pulsed voltammetry (0.05, 0.1, 0.2 V/s). Each vertical bar is the results of 3 different polyester-filter paper devices. All the electrochemical measurements for optimization were performed in ammonium buffer 0.1 M, pH = 8, using a standard solution of $NiCl_2$ 100µM.

The choice of the substrate should reflect the final application of the analytical device, and plastic-based one would be more suitable for application where flexibility and resistance are required. Polyester provides the advantage to obtain a more robust and sensitive platform that fits well with a domestic use of the device. On the other hand, paper-based ones could represent a good compromise between sustainability and sensitivity. However, as shown in Figure IV.2A, the sensitivity obtained using at the office paper-based electrodes resulted low within

the same experimental conditions. This could be due to the porosity of office paper that leads to a decrease of the availability of DMG on the working electrode to form the detected complex. In addition, a novel configuration in which the more sensitive polyester substrate is successfully coupled with a waxed filter paper disk, was tested in order to obtain a multi-task device able of managing complex matrices, such as the cosmetic ones. As shown in Figure IV.2A the sensitivity achieved with this new configuration is comparable to that on the traditional plastic-based electrode with the advantages of (1) store reagents (ammonium buffer solution and DMG), (2) treat real matrix (cosmetic products) and (3) pre-concentrate nickel ions. After having selected the flexible polyester-based substrate, the experimental setup has been optimized, by investigating the effect of DMG volume, the time in open circuit needed and the scan rate of the pulsed voltammetry, as reported in Figure IV.2B, C and D, respectively. Previous studies of DMG and its complexation reaction with nickel have shown that slightly basic pH values between 8.0 and 9.0 represents optimum conditions for accumulation of this metal.[49] After the establishment of the Ni-DMG complex, nickel is reduced onto the carbon electrode. It should be noted that in absence of DMG (inset of Figure IV.2B), the signal due to nickel is evidently lower than that in the presence of the complexing agent. What has been observed is that an amount of DMG higher than 2 μL (comprising 4 and 8 μL) had not produced a significative improvement in terms of recorded current (that depends on the nickel that is reduced at the working electrode surface): as a consequence of this, an amount of 2 μL of 10 mM ethanolic DMG was chosen as the optimal compromise between sensitivity and amount of reagents. According to the work reported by Ferancová and colleagues,[40] an accumulation step is required for Ni(II) determination based on complexation by DMG. This step was performed at open circuit conditions (no potential was applied) and tested at 1, 3 and 5 min,

and the results were compared with the absence of this time, as shown in Figure IV.2C. Ni (II) was accumulated on the carbon electrode in ammonium buffer solution (pH 8.0) prior to measurement and the absorption showed a plateau after 3 min, which was chosen as the best alternative between sensitivity and measurement time. Finally, the scan rate of the pulsed technique has been considered, and, in the range comprised between 0.05 and 0.1 V/s, 0.1V/s has represented the optimal choice to obtain a sensitive signal and satisfactory repeatability (Figure IV.2D).

Analytical performance

Subsequently to the optimization of the experimental parameters, the integrated polyester-filter paper device has been tested for determination of nickel ions within the 0–100 µM range in standard solution as reported in following Figure IV.3.

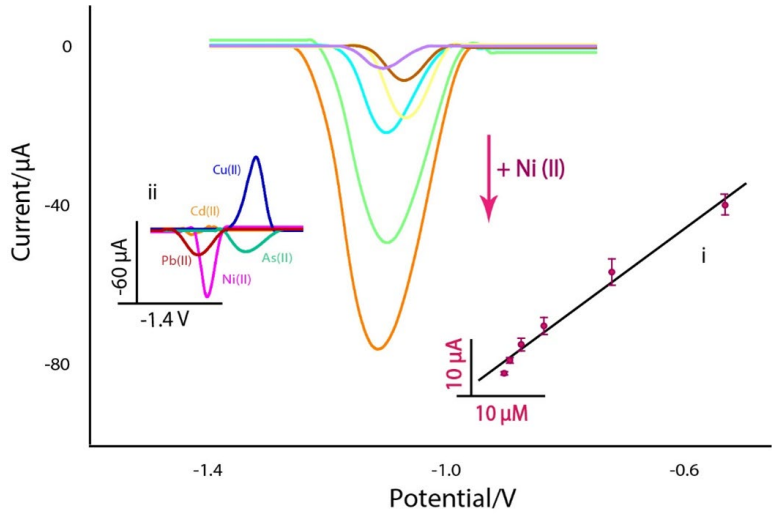

Figure IV.3. Recorded DPV from 2 to 100 µM of Ni (II) complexed with DMG in 0.1 M ammonium buffer, pH = 8.0, using the polyester – filter paper integrated platform. Inset i: calibration curve in a linear range up to 100 µM (n = 4). Inset ii: measurements of Nickel (pink) in presence of copper (blue), cadmium (orange), arsenic (green) and lead (red) at 20 µM concentration level in 0.1 M ammonium buffer, pH = 8.0.

Experimental parameters: t open circuit: 3 min, E begin: -0.5 V, E end: -1.4 V, E step: 0.01 V, E pulse: 0.2 V, t pulse: 0.02 s, Scan rate: 0.1 V/s.

As shown in inset i of Figure IV.3, a linear correlation has been obtained between the height of the current peaks and the concentration of nickel ions. The relationship is described by the following equation, $y = 0.60 x + 10$, $r^2=0.97$ (where y represents the current difference between nickel and the blank, and x represents the nickel level expressed in μM), and each point on the curve is the result of four replicates using different electrodes. LOD calculated as 3σB/slope (σB represents the standard deviation calculated for blank measurements, slope is the slope of the calibration curve), resulted equal to ca. 2 μM and the limit of quantification, LOQ, has resulted equal to ca. 6 μM, with a relative standard deviation (RSD) of 9% (calculated on four replicates). As reported in the inset ii of Figure IV.3, the signal due to interfering species have been evaluated using the same experimental conditions. In particular, measurements of solution containing ca. 20 μM of copper, lead, cadmium, and arsenic ions, demonstrating the absence of significative signals in the at the potential for nickel determination. As reported in literature, the stability constant of DMG complex with nickel is much higher than that of other metals.[50,51] However, even if the signal is not flat for the metals that have been tested, it should be noted that the peak potential due to the reduction of nickel is different from the others and, specifically to cosmetics, the concentration of other metals are very low (for this experiments very high concentrations have been interrogated).

By comparing these analytical results with those obtained by analyzing nickel at different electrochemical platforms and matrices (e.g. tap water, wastewater, fuel, particulate matter, pond water etc.) it should be noted that it represents the first application towards matrices used in cosmetic industry.[42,44–46,52,53] In fact, the use of portable analytical systems like the one developed, has not been yet

applied towards the analysis in complex matrices such as gels and creams. It should be highlighted how the combination of polyester/chromatographic paper allows to reduce tasks for end-user, avoiding the use of complex and time-consuming procedures that reduce the portability of the systems, e.g. use of external heating blocks, microwave digestions etc. In fact, even if the analytical performance as the detection limit obtained at the different printed electrochemical systems appear roughly the same, i.e. ppb range, the approach herein reported provides a new route to develop an all-in-one method, faster and more user friendly. The possibility to use external paper-based disk reduces all the tasks that are associated to the preconcentration of nickel ions and in particular the addition of buffer solution that is necessary to carry out the assay. With this architecture, the measurement can be exploited using a single-shot platform, especially in presence of real samples as the cosmetic ones.

Application to cosmetics

The analytical applicability and efficacy of the developed electrochemical sensor for the determination of nickel ions has been demonstrated by applying it to the determination of nickel ions in cosmetic products. More specifically, the integrated system was tested firstly onto a cream and a synthetic gel, diluted 1 to 10 in the ammonium buffer solution, and then spiked with different amount of the nickel solution in order to evaluate the linearity of the method in these two complex matrices. A potential issue is given by the presence of many organic and inorganic materials such as oils, polymers, waxes, polyols, and surfactants which give an important matrix effect of suppression of the signal (and they can also interfere with printed inks). A possible strategy to limit this possibility is represented by using porous filter paper in combination with the traditional polyester electrode, thus reducing the gross interferences. However, it should be

noted that for the present study, an all-in-one approach has been adopted. The cream/gel sample, diluted 1 to 10 in ammonium buffer solution at pH = 8.0, has been drop casted onto the chromatographic paper disk and not on the polyester support where the electrodes are printed. Briefly, a chromatographic paper-based substrate has been used to load all reagents together: diluted placebo (cream/gel) sample and DMG were drop casted onto the same spot and the solution is allowed to dry at room temperature. Then a specific concentration of the nickel solution was added and, after 3 min in open circuit, measurement is performed with the use of the optimized parameters. Consequently, cream and gel samples has been spiked with nickel ions level up to 100 µM (Figure IV.4).

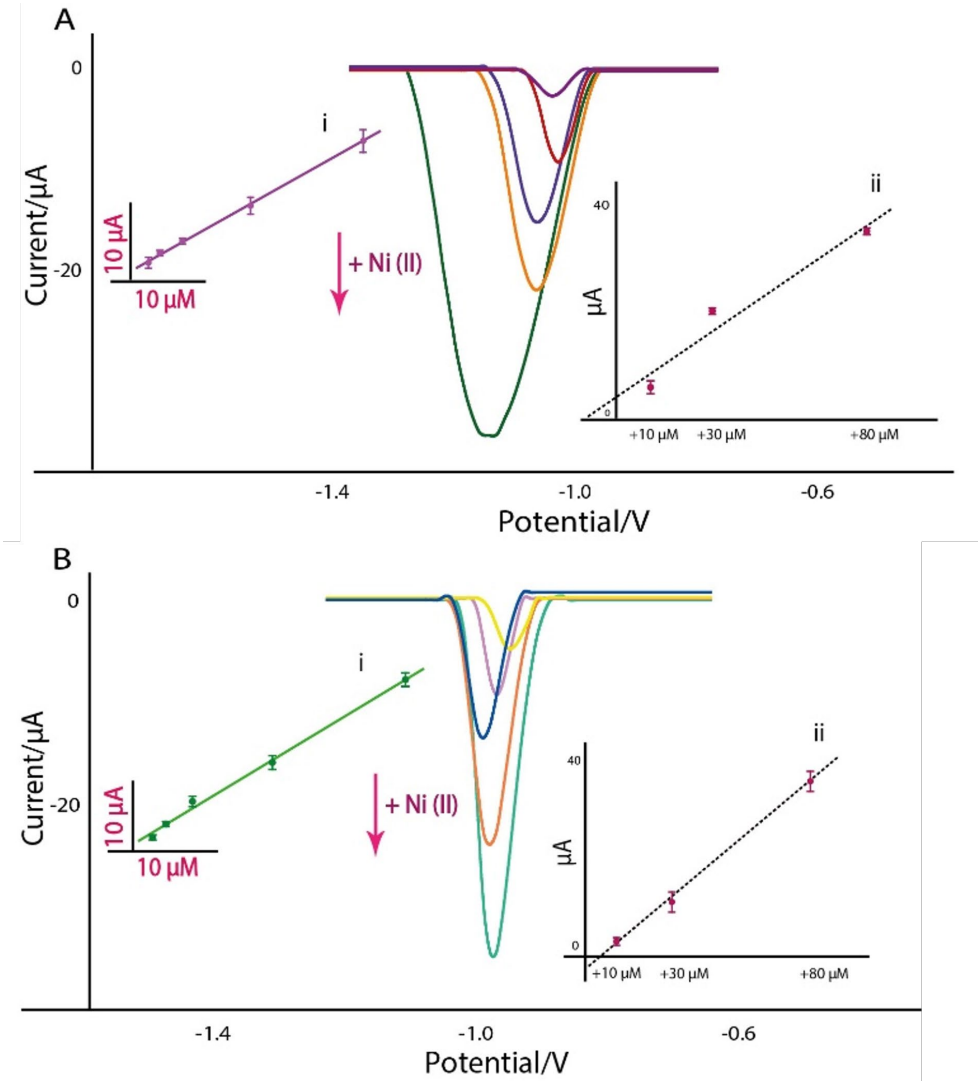

Figure IV.4. DPV recorded performing in A) placebo cream sample diluted 1:10 and spiked with different concentration of nickel solution and B) placebo gel sample diluted 1:10 and spiked with different concentration of nickel solution, in presence of DMG, using all-in-one polyester – filter paper platform. Inset i A: calibration curve for cream in a linear range up to 100 µM (n=4). Inset i B: calibration curve for gel in a linear range up to 100 µM (n=4). Inset ii A: recovery studies in presence of 10 µM spiked cream sample. Inset ii B: recovery studies in presence of 10 µM spiked gel sample.

As shown in inset i of Figure IV.4A and B, a good linearity has been obtained for cream and gel samples, in the range comprised between 5 and 100 µM: it should

be noted a good agreement between them, and a decrease of the slope if compared with the results that have been obtained in standard solution. The relationship is described by the following equation, $y = 0.324x + 2.8$, $r^2=0.985$ for the cream and $y = 0.358x + 2$ $r^2=0.991$ for the gel. LODs were calculated equal to 4 and 5 µM in cream and gel, respectively. After having evaluated the absence of nickel in these matrices, recoveries studies have been carried out, using the standard addition method, starting from a concentration of 10 µM, obtaining 100 and 97% recovery for cream and gel, respectively (inset ii of Figure IV.4A and B). Due to the complexity of these matrices, the sensitivity was different in comparison with measurements carried out in standard solution, but the use of polyester – filter paper platform for filtering gross impurities and the adoption of standard addition method, produced satisfactory recoveries. In addition, the satisfactory accuracy of the reported polyester – filter paper architecture has been confirmed by comparing the results obtained with the standard addition method on the two spiked cosmetic samples, with those obtained by ICP-MS, and the results have been reported in Table 10.

Table 10. Recoveries and comparison with measurements on ICP-MS.

Sample	**Spiked level**		**Recovery**
Cream	10 µM		100%
Gel	10 µM		97%
Sample	**ICP-MS measure**	**SPE measure**	**Accordance (ICP-MS/SPE)**
Cream	22 µM	20 µM	92%
Gel	14 µM	15 µM	93%

Moreover, the hybrid polyester-filter paper platform was also tested for the analysis of two available commercial cosmetic products (Yves Rocher hand cream and Teva Gambe fresh gel), as shown in Figure IV.5.

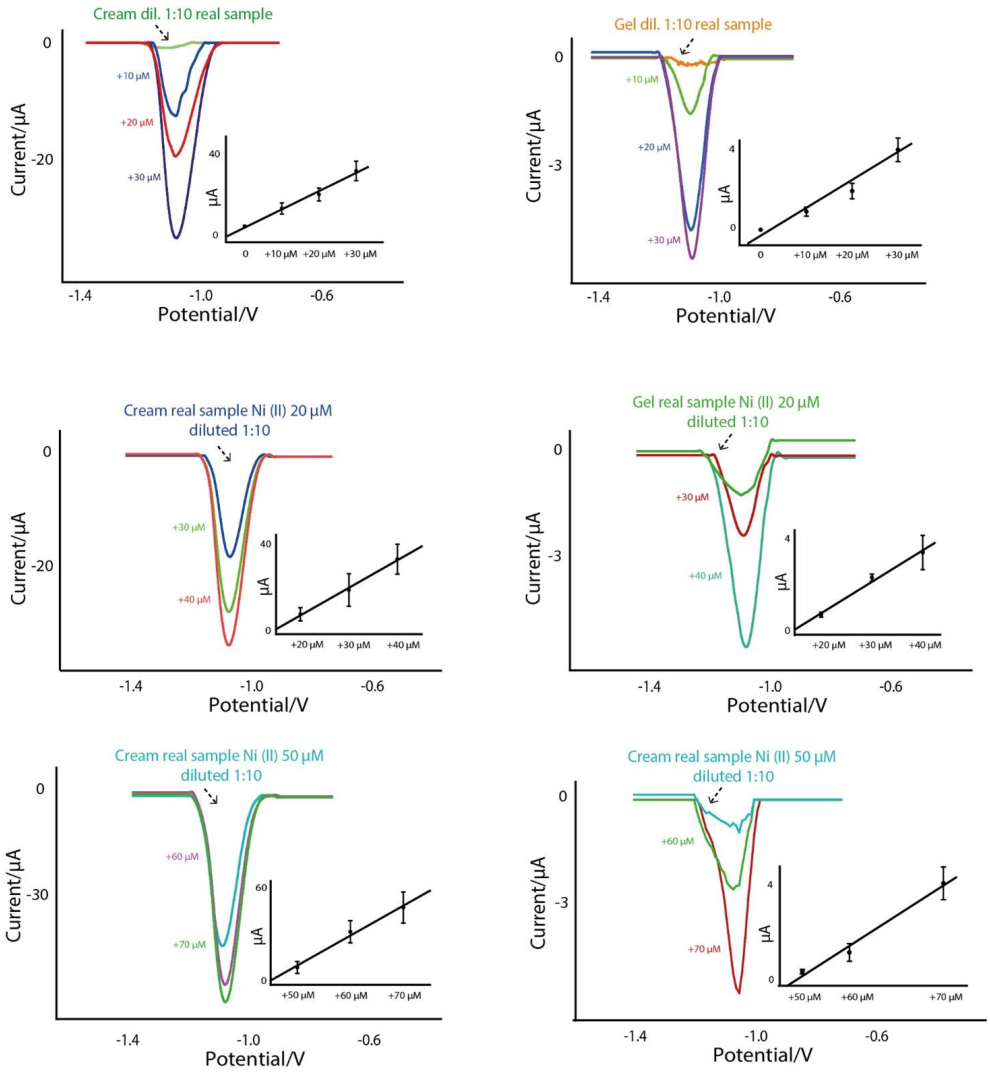

Figure IV.5 Application of the hybrid polyester - filter paper platform on the analysis of two real cosmetic samples on the market, a hand cream, and a gel. A) diluted 1 to 10 cream sample in presence of DMG (first line) and after three additions of Ni (II) solution (10, 20, 30 µM); B, C) curves recorded at two different nickel ions concentrations (20 and 50 µM) for commercial cream. D) diluted 1:10 gel sample in presence of DMG (first line) and after three additions of Ni (II) solution (10, 20, 30 µM); E, F) curves recorded at two different nickel ions concentrations (20 and 50 µM) for commercial gel.

After having evaluated that the content of nickel in these "nickel tested" products was lower than LOD of the developed methods, both the cream and gel samples

were spiked with different amount of nickel in order to evaluate the applicability of this methods towards commercial cosmetics. The samples were analysed in presence of 20 and 50 μM of nickel. It should be noted that the presence of this complex matrix has produced a decrease of the sensitivity due to the presence of different species like co-existing metal ions, oils, polymers, and surfactants, more for the commercial gel matrix than the commercial cream.[54,55]

4.1.4 Conclusions

In this work, for the first time a simple combination between flexible screen-printed electrode and porous waxed filter paper has been successfully proposed for the detection of nickel ions in cosmetic products. In particular, it has been demonstrated how the adoption of a small and low-cost filter paper-based disk has been able to lower the tasks required for the treatment and measurements of these samples. The effect of external porous substrate has been also exploited for storing reagents, adding complexing agents, and sampling. The humble architectures reported in this work allowed to detect nickel ions down to micromolar range in both standard, cream and gel samples. The system has been satisfactorily compared with ICP-MS measurements, thus demonstrating the good accuracy of the proposed approach. The utilization of traditional polyester substrates in electroanalysis can be empowered by the combination with porous and sustainable materials like filter paper. This offers to represent the basis for the development of novel user-friendly architectures for improving decentralized analysis by non-specialists.

4.2 ALL-IN PAPER-BASED 2D CONFIGURATION: ELECTROCHEMICAL AND FACILE DETECTION OF PARACETAMOL IN WASTEWATERS

4.2.1 Introduction

In recent years, environmental science has faced increasing challenges from emerging contaminants, diverse substances impacting ecosystems and human health.[56–58] The term "emerging contaminants" includes pharmaceuticals, personal care products, pesticides, and industrial chemicals.[59–62] These substances often evade traditional water treatment, and due to recent recognition, their full environmental and health implications are not fully understood.[63–65]

Urban and industrial wastewater serves as a crucial case study for managing substances from human activities, industrial processes, and agriculture, raising concerns about the effectiveness of current water monitoring and treatment.[59,61,64,66] Monitoring and research efforts aid regulatory authorities in informed decision-making about managing potential risks.[67,68] Pharmaceuticals have emerged as contaminants, infiltrating aquatic ecosystems and challenging traditional water quality concepts. Despite being designed to improve human well-being, pharmaceuticals contribute to a new environmental challenge. Improper disposal, incomplete metabolization, and inefficient removal during water treatment led to pharmaceutical compounds entering wastewater.[69–71] Conventional water treatment struggles to effectively remove pharmaceuticals, posing concerns for long-term impacts on wastewater quality and habitats. Since 2020, UNESCO listed human pharmaceuticals as emerging contaminants, addressing their detection and elimination in Goal 6 of the 2030 Agenda for Sustainable Development.[69,72–74]

Paracetamol, or acetaminophen, is available over-the-counter and widely used as analgesic globally, known for relieving pain and reducing fever.[75]

The presence of pharmaceuticals in the environment, including paracetamol, results from incomplete removal during wastewater treatment and improper disposal of medications; consequently, these compounds may persist in treated effluent, entering surface waters. Recent studies have reported paracetamol detection in European water streams at concentrations up to 65 ppb, raising concerns about potential ecological consequences for aquatic organisms, long-term exposure, development of resistance, and human exposure through water consumption.[76–78] However, many countries have no specific regulation for the discharge limit of paracetamol, in particular close to the pharmaceutical factories.[79]

Enhancements in wastewater treatment, public awareness on medication disposal, and advances in analytical techniques can improve the monitoring of pharmaceutical contaminants in water sources. Analyzing water samples for specific pharmaceutical compounds is a common approach in monitoring. The choice of analytical method depends on factors like the targeted pharmaceuticals, required sensitivity, and the sample type. These include titrimetric, [80] chemiluminescent,[81] high performance-liquid chromatography,[82] liquid chromatography,[83] liquid chromatography-mass spectroscopy, [84] capillary electrophoresis ,[85] UV–Vis spectrometry ,[86] flow and batch injection analysis.[87,88] Commonly, these techniques are costly, complicated, time taking process and operated by highly skilled technicians. Incidentally, electrochemical methods provide a simple, rapid, selective detection with low-cost of systems and eco-friendly. Electrochemical sensors and biosensors are promising tools for in situ monitoring of paracetamol in water systems like wastewater.[89] These devices offer advantages such as real-time monitoring, high sensitivity, and the potential

for miniaturization, making them suitable for on-site applications.[7,8,90,91] Different approaches have been reported for paracetamol electrochemical sensing in several matrices thanks to its electroactivity at solid electrodes. P. A. Raymundo-Pereira et al., reports an electrochemical method using carbon SPEs pretreated with sulfuric acid solution, able to detect simultaneously the hydroquinone, paracetamol and estradiol in tap water in range between 0.1 and 0.8 μM.[91] Moreover, in the work of N. Karikalan et al., the electrochemical properties of paracetamol at the screen printed carbon were investigated at the bare screen printed carbon electrode (BSPCE) and its electrochemistry was studied in various pHs, confirming that the mechanism of the electro-oxidation of paracetamol was not stable in strong acidic and strong alkaline media, while it is stable in intermediate pHs due to its dimerization.[7,8,89–92] Wan-Yu Su et al., reports electrocatalytic oxidation of paracetamol at screen-printed electrode (SPE) modified with electrogenerated poly(3,4-ethylenedioxythiophene) (PEDOT) film obtaining a limit of detection of 1.39 μM.[93] These examples prove that advancements in analytical techniques continue to contribute to the development of more sensitive, selective, and efficient methods for monitoring pharmaceuticals as emerging contaminants in the environment. On the other hand, few examples are reported about the use of sustainable and green substrates for producing electrochemical sensors (Electrochemical paper-based analytical devices, ePADs) able to detect paracetamol in environmental matrices. Among these materials, paper is a valid alternative to the classic polyester because it is biodegradable, biocompatible, besides being convenient and easy to use.[94,95] Utilizing paper-based substrates, in particular when filter paper is used for manufacturing analytical strips, allow the preloading and preconcentration of reagents into the device due to its porous nature; moreover, the integration with paper allows to collect and filter real samples in order to avoid further treatments

of the samples. Specifically, the effective integration of the paper-based platform, straightforward manufacturing process, and customizable features enabled the creation of a self-contained platform, able to store all required reagents for the assay, process the sample by eliminating significant interferences, and display the results within minutes.

In literature are reported several examples of ePADs for paracetamol electrochemical determination in pharmaceutical, biological, and food matrices.[96-100] However, there are few examples regarding the detection of paracetamol in wastewater or environmental matrices in general. Table 11 summarized the comparison of our device with other PADs for detecting paracetamol in several matrices.

Table 11. Comparative table between of our device and other PADs for detecting paracetamol in several matrices.

Electrode	Substrate	Technique	LOD	Application	Ref
Dual electrode detectors pencil-drawn	Whatman n°1 chromatographic paper based fluidic channels	CV and CA	6µM	Tablets of Efferalgan drug	96
AuNP-PGA/SWCNT electrode	Nafion-modified nitrocellulose membrane	CV and DPV	15µM	Pill-type pharmaceutical samples	97
GPT/WPE (ink composed of nail polish and graphite)	Waterproof paper	CV and DPV	$5.4*10^{-8}$M	Pharmaceuticals samples and saliva, urine, and sweat samples	98
ePADs using graphite pencil	Vegetal paper	SWV	298µM	Whiskey	99
Fully PoP-drawn PADs	Filter paper	DPV	20.5µM	Gin sample spiked with paracetamol	100
Paper-based 2D configuration	Whatman n°1 chromatographic paper	DPV	0.7µM	Wastewater samples	This work

Leveraging the advantages of electrochemical detection and the simplicity of paper substrates, these sensors offer a promising solution for real-time and environmentally sustainable monitoring.[9,101,102]

Considering that, the aim of this work was to develop a paper-based device capable of electrochemically detecting paracetamol *in situ*, quickly and easily, without the need for pre-treatment of the test sample. The answer to these needs appeared consistent in the integration of our paper-based electrochemical devices coupled to a 2D paper-based channel, allowing the possibility of autonomously treat real samples, and representing a starting point towards the decentralized analysis of emerging pollutants.

4.2.2 Experimental section

Materials and apparatus

Paracetamol, PBS tablets (140 mM NaCl, 10 mM phosphate buffer, 3 mM KCl), and potassium chloride were purchased from Sigma-Aldrich (St. Louis, MO, USA). All solutions were prepared in Milli-Q water. 0.1 M potassium chloride was employed as supporting electrolyte and all measurements were performed at room temperature. Incoming and outgoing water from drinking water treatment plants were purchased by Acea Elabori Group (Rome, Italy). Conductive inks (Ag/AgCl and graphite) were acquired from Acheson (Italy). Whatman No.1 chromatography paper was purchased from Merck (Italy). Scotch adhesive tape was purchased in the local market. Adobe Illustrator was used to design the wax pattern of both the testing area of the paper-based screen-printed electrode and paper-based channel. A solid ink printer, namely, ColorQube 8580 from Xerox (USA) was used to print the hydrophobic layer of wax onto paper-based substrates. All the electrochemical measurements were carried out with the use of a portable potentiostat, EmStat3 (PalmSens, The Netherlands), connected to a

laptop. Currents were recorded and displayed on a laptop by using the software PSTrace 5.9.

Fully printed paper-based platform

The final pattern of the paper-based device was drawn on Adobe Illustrator and wax-printed onto a Whatman No. 1 chromatographic paper. Then, waxed paper was cured in an oven at 100 °C for 1 min, allowing the wax to diffuse through the paper, producing a hydrophobic layer all around the hydrophilic testing area. This step was very important to define the testing area and confine the solution in the delimitated electrochemical cell area, avoiding its diffusion toward the electrical contacts and affecting the readout.[102] After that, the three-electrode system was manually screen-printed onto the hydrophilic zone using a spatula and two masks, first one for the Ag/AgCl ink (Electrodag 477 SS), that was used to print the connections and the reference electrode, and the other one for the carbon ink (Electrodag 421), that was used to print the working and counter electrodes. After each printing step, the screen-printed electrodes (SPEs) were cured at 60 °C for 30 min. Thermally curing was necessary to make the printed ink stable for electrochemical measurements.[102] The diameter of the working electrode was 0.4 cm, the whole three-electrode system is ca. 2.5 cm (length) and 1 cm (width). Subsequently, the backside of the printing surface was covered with adhesive tape (without covering electrical connections) to prevent the solution leaking out. The complete platform consisted of a hydrophilic rectangular zone (microfluidic channel, 2.6 cm (length) x 0.2 cm (width)), connected to a hydrophilic semicircle zone (electrochemical cell, 1 cm diameter) where the electrodes were screen-printed as reported in the Figure IV.6.

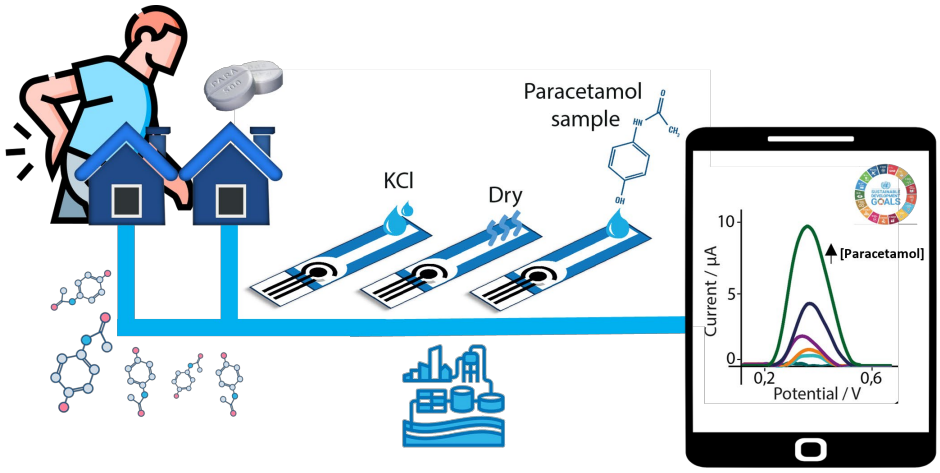

Figure IV.6 Paper-based 2D configuration for the electrochemical detection of paracetamol.

Paracetamol determination

Paracetamol was electrochemical oxidated to N-acetyl-p-benzoquinone-imine (NAPQI) within a quasi-reversible two-electron process at the electrode surface.[89,92] The electroanalytical technique adopted to measure paracetamol is the differential pulse voltammetry (DPV). In particular, 0.1 M potassium chloride was used as working solution and the technique parameters were optimized as follows: the measurement was carried out in a range potential from 0.0 V to 0.8 V, with an E step of 0.02 V, E pulse of 0.2 V, t pulse of 0.02 s and scan rate of 0.05 V/s. The final procedure to detect paracetamol within the 2D paper-based devices consisted in 1) pre-loaded the channel with a solution of potassium chloride and let dry, 2) adding the sample containing paracetamol at the edge of the strip, and finally 3) waited 1 minutes in order to let the sample re-dissolve KCl, mixing and reaching the working electrode surface for proceed with the measurement.

4.2.3 Results and Discussion

Optimization of the experimental set up

The first step of the optimization was focused on the selection of the substrate for printing the carbon screen-printed electrodes. The substrates tested were polyester and chromatographic paper as reported in Figure IV.7.

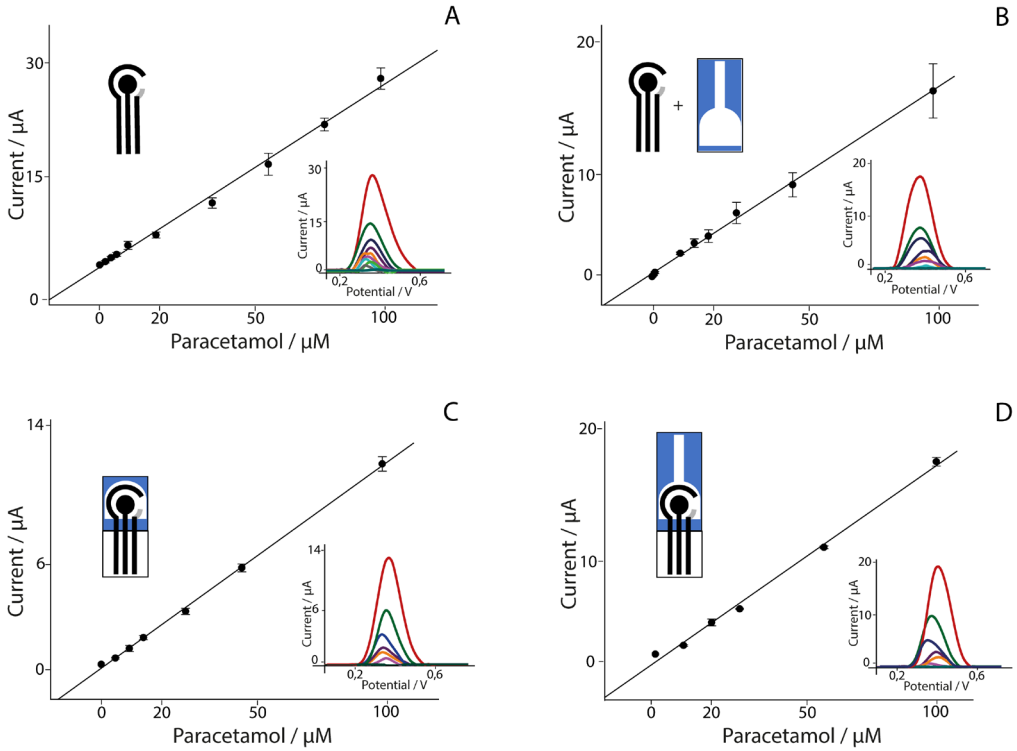

Figure IV.7. Choice of the substrate evaluated at increasing concentration of paracetamol (0-100µM) on A) polyester SPE, B) polyester SPE + filter paper strip, C) filter paper SPE, D) filter paper SPE + filter paper strip.

As shown Figures IV.7A and C the efficiency of the two substrates was evaluated for increasing levels of paracetamol in a range from 0 to 100 µM, obtaining a good linearity for both the substrate described by the following equations: $y=0.226x - 0.287$ ($r^2=0.988$) and $y=0.116x - 0.216$ ($r^2=0.997$) for polyester and chromatographic paper, respectively, where the y represents the anodic current

in microampere and x represents the concentration of paracetamol expressed in micromolar. The sensitivity resulted higher using the polyester substrate because in this case the solution is in direct contact with the electrode area, while when paper is used the solution needs to diffuse the porous structure of paper prior to arrive the electrode: as observed in prior study, this might affect the sensitivity of detection [9]. However, we proceeded with paper-based substrate because of the final goal to have an all-in-one and more sustainable platform. Prior to realize the fully integrated device, two other configurations were characterized, e.g, polyester-based SPE combined with an external paper-based channel, and a fully paper-based SPE and channel, as shown in Figures IV.7B and D. What is should be noted is that when the polyester is coupled to paper-based channel its sensitivity decreased, while the fully paper-based device still retained the initial sensitivity towards paracetamol. Once the effectiveness of the obtained configuration in detecting paracetamol was satisfactory, we tried to improve our system evaluating different parameters such as the length of the channels, the run time of the solution within the channel and the working volume of solution to be placed on the edge of the channel. As shown in Figure IV.8, different channel lengths were evaluated, namely 2.6, 4.8 and 6.0 cm.

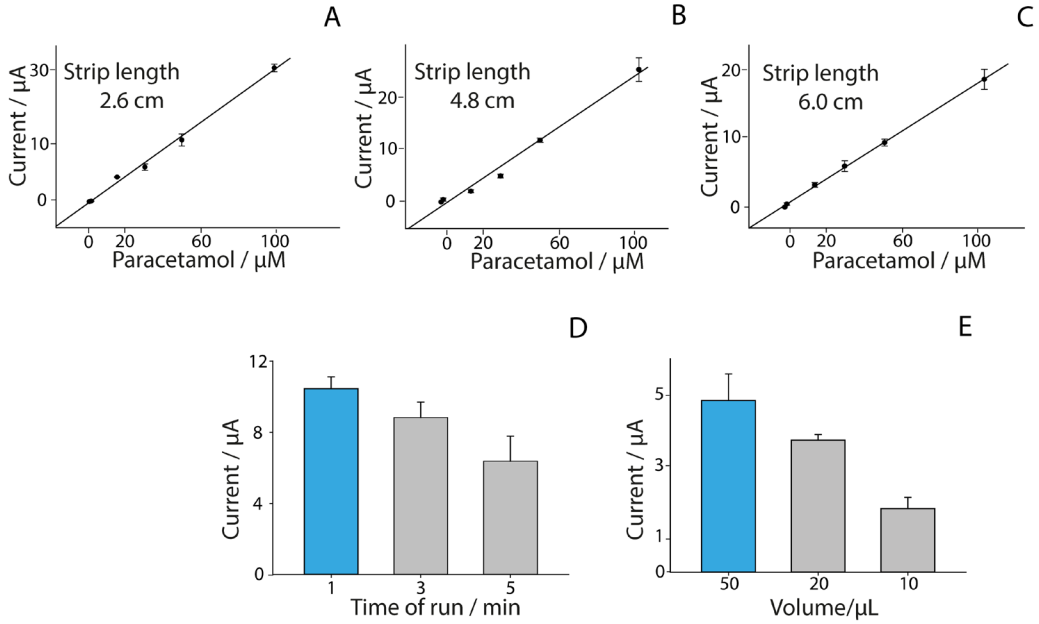

Figure IV.8. Optimization of the filter paper strip length: A) 2.6 cm, B) 4.8 cm and C) 6.0 cm, D) Optimization of the time of run of the drop on the filter paper strip tested at 1, 3, 5 minutes in presence of 30µM of paracetamol; E) Optimization of the volume of paracetamol solution to be placed onto the filter paper strip tested at 10, 20 and 50 µL in presence of 30µM of paracetamol.

As can be observed, the shortest strip gave the best results in terms of linearity and repeatability (n=3), even if the length did not affect the sensitivity significantly. Using the chosen configuration, both the run time (Figure IV.8D) and drop volume (Figure IV.8E) were evaluated. With regard to the run time, in a range comprised between 1 and 5 minutes, 1 minutes gave the highest signal, and this was combined with the choice of a drop volume of 50 µL of solution to perform the measurements.

Analytical performance

Subsequently to the optimization of the experimental parameters, the fully printed paper-based device was tested for determination of paracetamol within

the 0-50 µM range in 0.1 M KCl standard solution as reported in following Figure IV.9.

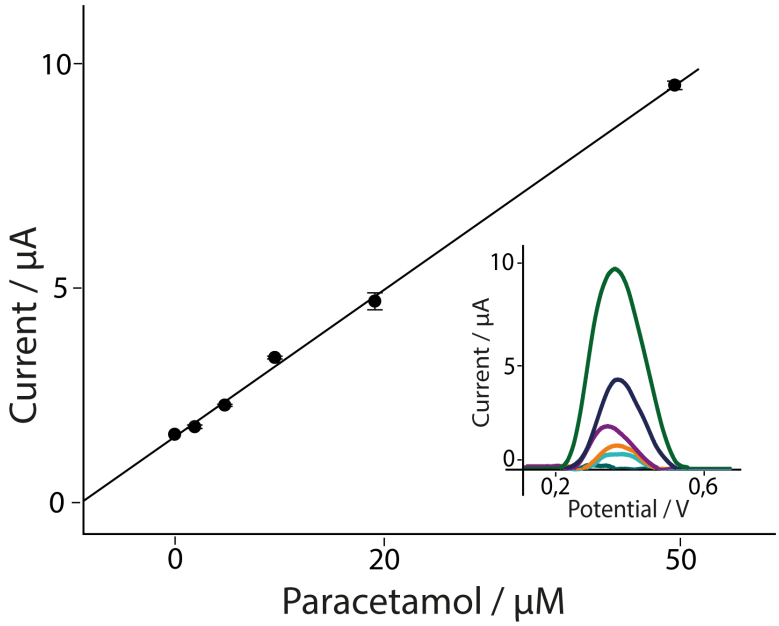

Figure IV.9. Calibration curve from 0 to 50 µM of paracetamol in 0.1 M KCl, using the fully paper-based platform. Inset i: recorded DPV in the range up to 50 µM (n = 3). Experimental parameters: E begin: 0.0 V, E end: 0.8 V, E step: 0.02 V, E pulse: 0.2 V, t pulse: 0.02 s, Scan rate: 0.05 V/s.

As shown in Figure IV.9, a linear correlation was obtained between the height of the current peaks and the concentration of paracetamol. The relationship is described by the following equation, $y = 0.14 x – 0.05$, $r^2=0.99$, and each point on the curve was the result of three replicates using different electrodes. The detection limit, calculated as 3σB/slope (σB represents the standard deviation calculated for blank measurements, slope is the slope of the calibration curve), was calculated equal to 0.7 µM and the limit of quantification resulted equal to ca. 2.1 µM, with a relative standard deviation (RSD) of 7% (calculated on three replicates).

Application to real samples analysis

The analytical applicability and efficacy of the final device was demonstrated by applying it to the determination of paracetamol in wastewater samples. More specifically, the integrated system was tested firstly at known concentrations of paracetamol in incoming and outgoing water, from drinking water treatment plants purchased by Acea Group. The samples were spiked with different amount of paracetamol solution in order to evaluate both the linearity of the method and the effects of the matrices. A potential issue was given by the presence of many interferents species which can give an important matrix effect of suppression of the signal (and they can also interfere with SPE). The incoming and outgoing samples, without any kind of pretreatment, was drop casted at the edge of the paper-based channel as above described. Briefly, a chromatographic paper-based substrate was used to load all reagents together: the wastewater sample spiked with wide levels of paracetamol (0-50 µM) was added on the paper-based strip and, after 1 minutes, measurement was performed with the use of the optimized parameters, as reported in Figure IV.10.

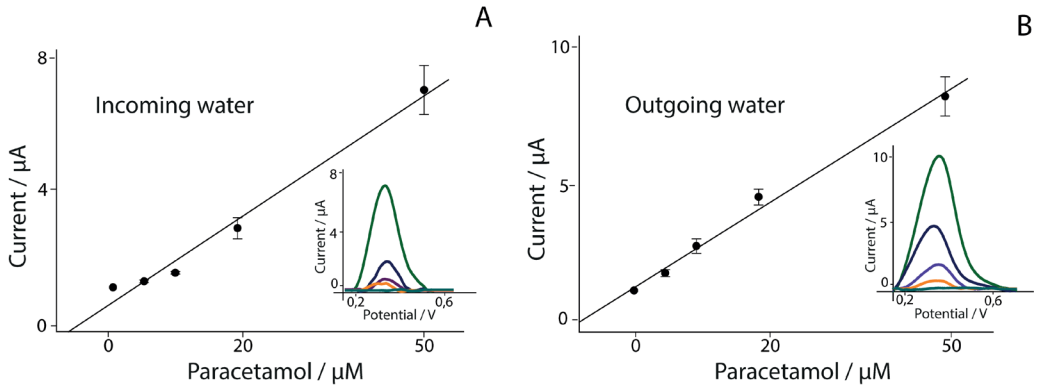

Figure IV.10. Application of the fully paper-based platform for the detection of paracetamol in incoming and outgoing wastewaters. A) Matrix effect evaluation at increasing concentrations (0-50 µM) of paracetamol added in an incoming water sample. B) Matrix effect evaluation at increasing concentrations (0-50 µM) of paracetamol added in an outgoing water sample. Experimental parameters: E begin: 0.0 V, E end: 0.8 V, E step: 0.02 V, E pulse: 0.2 V, t pulse: 0.02 s, Scan rate: 0.05 V/s.

As shown in Figures IV.10A and IV.10B, a good linearity was obtained both for incoming and outgoing wastewaters. It should be noted a good agreement between them, and a similar slope if compared with the results obtained in standard solution. The relationship was described by the following equation, $y = 0.18x - 0.66$, $r^2=0.97$ for the incoming water and $y = 0.17x + 0.16$, $r^2=0.98$ for the outgoing. The detection limit resulted equal to ca. 2 μM and 1.7 μM for incoming and outgoing wastewaters, respectively, confirming the good efficacy of this kind of architecture to handle complex environmental matrices such as wastewater, without a prior filtering of the sample because this step is already included in the configuration of the device.

Consequently, to improve the easiness of the system, exploiting the advantage of paper porosity to loads reagents, the potassium chloride was pre-loaded on the channel prior to analyze the solution. As shown in Figure IV.11, three different experimental setup were taken into account, namely:

a) Paracetamol in 0.1 M KCl solution

b) Pre-conditioning of the strip with 1M KCl solution, get dried and load of the paracetamol sample

c) Paracetamol in ultrapure water solution

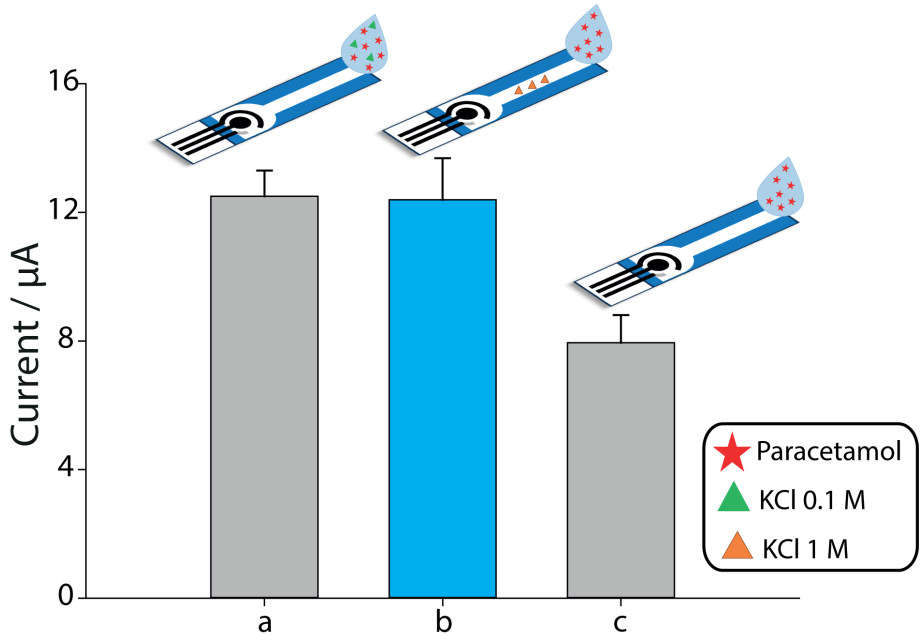

Figure IV.11. Pre-conditioning evaluation by comparing b) 1M KCl pre-conditioned filter paper strip (blue) with a) classical drop casting of paracetamol solution prepared in 0.1M KCl and c) paracetamol prepared in ultrapure water.

As showed in the figure IV.11, the pre-loading of 1 M KCl solution on the filter paper strip, gave similar results in terms of sensitivity and repeatability than the ones obtained with the classical drop-casting method of paracetamol prepared in 0.1 M KCl solution. In this way we are able to obtain a pre-conditioned strip, where it was possible to directly load the paracetamol sample prepared in ultrapure water. We also tried to load on the filter paper strip directly the paracetamol sample prepared in water, but the absence of the electrolyte solution caused a visible decrease of the current.

As the last characterization of the paper-based device, the recovery studies were carried out in presence of two paracetamol spiking of 10 and 50 µM, in both incoming and outgoing wastewaters. With the use of the standard addition method, recoveries of 92 and 94% were obtained in incoming wastewater,

respectively to 10 and 50 μM, while recoveries of 94 and 89% were obtained in outgoing wastewater, respectively to 10 and 50 μM.

4.2.4 Conclusions

In this work, an all-in-one paper-based portable device for the analysis of paracetamol in wastewaters was reported. In particular, a reagent-free platform was obtained merging a paper-based screen-printed electrode with a 2D paper-based channel. This approach not only simplifies the process for the end-user, but also offers a method that is easily transportable and low-cost. The optimized device was used specifically for the detection of paracetamol in wastewater, both incoming and outgoing, in collaboration with Acea Elabori. This strategy resulted in remarkably low detection limits of 0.7 μM in standard solution and ca. 2 μM in real samples. In fact, even if the analytical performance obtained at the paper base electrochemical systems appear roughly the same to what obtained with others analytical methods, the approach herein reported provides a new route to develop an all-in-one method, faster and more user-friendly. By loading the reagents necessary for the assay within the porous structure of the paper, it was possible to develop a sustainable and reagent-free device for the direct application on the site of interest. The method was applied towards wastewaters analysis and also the recoveries were characterized: in all the matrices tested, the recoveries of spiked solutions of paracetamol were comprised between 89 and 94%, highlighting the satisfactory accuracy of the device. These results represent a significant step towards more effective and accurate detection of paracetamol in wastewater, redefining the concept of environmental analysis, making it more accessible, affordable and sustainable.

4.3 NOVEL BIO SUBSTRATES FOR PRINTING: CHARACTERIZATION AND APPLICATION OF POROUS PHBV-BASED BACTERIAL POLYMERS TO REALIZE NOVEL BIO-BASED ELECTROANALYTICAL (BIO)SENSORS

4.3.1 Introduction

Since the United Nations published the 2030 Agenda for Sustainable Development in 2015,[103] sustainability represents the main direction towards the establishment of novel technologies, approaches and actions.[72] For instance, taking into account the Covid-19 pandemic, the development of economically sustainable point-of-care tests has improved indexes for social sustainability.[104] In particular, the research and development activities around the world of sensing devices and transducers is being characterized by an increasing and interdisciplinary rush towards the advance in a number of diverse themes ranging from materials, procedures, optimization strategies and applications,[105–109] and the establishment of novel disruptive technologies represents a common requirement for the sustainable enhancement of sensing performance and functionalities. Among the different sensors architectures, the electrochemical ones are characterized by a high level of simplicity, making them a reliable alternative to other techniques because of their possibility to analyze colored/turbid solutions, to be applied for continuous monitoring and to be prone for reagent-free settings.[110–112] The most sold worldwide device is the electrochemical glucose biosensor,[113] and literature contains various examples dealing with the use of decentralized printed electrodes for fatigue/stress monitoring through skin, liquid biopsy on chip and tools for precision agriculture to be adopted on crops cultivations.[114–117] However, the development of green sensing platforms plays a fundamental role for reducing the use of hazardous

reagents, and consequently to decrease the formation of undesired by-products which represent one of the main issue in the waste management/removal.[118,119] An estimated 86% of all plastic packaging is used only once before it is discarded, producing a stream of waste that persists in environment and releases harmful pollutants.[120] Electronic waste, abbreviated as E-waste, also represents significative environmental issue and the development of electrochemical strips is always looking at "greener" alternative to plastic-based platforms, including the use of biodegradable and sustainable materials.[10] Although the use of paper-based platforms has been demonstrated to be a valuable alternative to traditional plastic-based materials, it should be considered that the cost and the procedures associated with their production (depending on the purity and porosity) are not always advantageous. In fact, even if cellulose is an abundant, renewable, biodegradable and non-toxic polymer, its purification from plant fibers involves chemical treatments (e.g. extraction, bleaching).[121] The choice of utilizing polymer-based materials is very widespread thanks to their very wide range of mechanical/functional properties that together with their lightweight that makes these materials very appreciated in several technological fields, and the use of fully bio-based and biodegradable sustainable materials as the so-called bacterial polymers can represent an alternative.[122] Among those, polyhydroxyalkanoates (PHAs) are the most attractive due to their well-known outstanding biodegradability in open environment, biocompatibility and bioresorbability.[123] Typically, food and agricultural wastes are used as feedstock for the bioconversion process. Nevertheless, also biomasses obtained from degradation processes of industrial textile dyes or post-consumer agricultural polyethylene have been found suitable feedstocks for PHAs production.[124,125] The nature of the substrate and the bacterial strain are key factors in order to obtain different types of hydroxyalkanoic monomers, which can be employed by microorganisms

during the biosynthetic polymerization process. Nowadays, several different types of PHAs either homopolymer or copolymer can be produced.[126] In particular, the copolymer poly(3-hydroxybutyrate-co-3-hydroxyvalerate) (PHBV) has been recently studied extensively in different technological fields thanks to its advantageous malleability and processability. In particular, PHBV has been mainly used in biomedical applications thanks to its biocompatibility, but also as piezoelectric sensor, thermal- and humidity-triggered actuator, and for producing green electronics.[127–132] Depending on the specific need, PHBV can be customized with other materials, for instance, it can be made more hydrophilic following the addition of cellulose-based compounds.[133] With regards to the use of bacterial substrates for application in sensing, some examples have been reported in literature, even if are mainly based on the use of bacterial cellulose due to its mechanical properties, biocompatibility, and porous structure that are able to mimic the extracellular matrix of the skin. The group headed by Morales-Narvaez developed a plasmonic bacterial nanopaper-based device for the evaluation of uncontrolled UV exposure.[129] A similar platforms, based on luminescent macrofibers based on quantum-dots onto bacterial cellulose nanofibers was developed to evaluate pH and glucose, in both serum and saliva.[128] Silva et al. demonstrated the suitability of printing electrodes onto microbial nanocellulose produced by oxidative fermentation to detect lead, cadmium, uric acid and 17β-estradiol in sweat.[127] The group of Sgobbi demonstrated the use of bacterial cellulose to develop a sweat-lactate biosensors, printing conductive inks modified with Prussian Blue and lactate oxidase enzyme.[133] Although the use of bacterial nano- and micro-cellulose have been investigated for both colorimetric and electrochemical sensing, the use of PHBV related substrates has not been reported for this purpose.

In this paper, we deeply characterized both PHBV and a cellulose modified PHBV to be used as novel substrates to be applied in the (bio)sensor field. In particular, these two alternative substrates have been screen-printed with conductive inks to realize electrochemical strips. Their performance has been characterized and compared with the traditional polyester (the substrate that is mainly adopted for screen-printed manufacturing). The substrates have been characterized through different approaches, including morphological (scanning electron microscopy (SEM, not showed), contact angle, not showed), mechanical (tensile tests, not showed), electrochemical (cyclic voltammetry, chronoamperometry, impedance spectroscopy, showed below) and (bio)analytical (detection of iron ions and organophosphate pesticides, showed below). The diverse characterization methodologies have been able to highlight the potentiality of PHBV-based materials for future sustainable application in the electroanalytical field.

4.3.2 Experimental section

Preparation of dispersible MFC

The MFC aqueous suspension (as prepared) cannot be added directly to the polymeric solutions for miscibility reason. Also, the simple drying of the MFC suspension is not a viable option since it leads to MFC aggregation, which is difficult to redisperse in the polymeric solution. To overcome this problem, an aqueous PEO solution (10 wt%) was added to the aqueous MFC suspension and the solution was stirred at room temperature using an ULTRA-TURRAX® stirrer operating at 8500 rpm and sonicated for 1 h. The so-obtained PEO/MFC mixture was then freeze-dried by an Epsilon 2–4 LSCplus (Martin Christ GmbH). The very fast freezing and the water removed in supercritical conditions allows obtaining a composite material mainly constituted by MFC micro-fibrillated in

solid PEO. The prepared MFC-based material was then finely cryo-milled (using liquid nitrogen) by an IKA A10 basic.

Substrate preparation

Purified PHBV has been solubilized in $CHCl_3$, and casted in a petri dish (diameter 15 cm) and left dry overnight at room temperature under aspiration hood. Two substrate thicknesses have been prepared. Specifically, 0.8 g of PHBV have been dissolved in 15 mL of $CHCl_3$ to obtain a film with a thickness of approximately 50 μm, whereas 2.5 g of PHBV in 25 mL of $CHCl_3$ were used to obtain a substrate 150 μm thick. To improve the typical low hydrophilicity of the PHBV-based materials, 5 wt% (with respect to the polymer amount) of the prepared MFC has been added to the aforementioned PHBV/$CHCl_3$ solutions. The dispersion of the MFC in the polymeric solutions has been obtained by the combination of magnetic stirring and dip-sonication for about 5 h before casting the solution in the petri dish.

Fabrication of the electrochemical strips

To fabricate the electrochemical strips, serigraphy was adopted with an in-house experimental setup. Following the selection of the substrate (i.e. polyester, PHBV, PBHV/MFC) the three electrodes were manually screen-printed as described in chapter 2. After each step, the ink was cured for 30 min in the oven at 70 °C. The diameter of the working electrode was 4 mm.

Scanning electron microscopy

SEM analyses were performed by an Ultra Plus FESEM scanning electron microscope (Zeiss, Germany). Cut surfaces of all samples were mounted on stub

and gold-sputtered at 20 nm thickness with the HR208 Cressington sputter coater and analyzed at 5–10 kV with an SE2 detector as already reported.[134]

Electrochemical measurements

All the experiments have been carried out using screen-printed electrodes connected to a portable potentiostat (PalmSens 4) and all the measurements have been performed by covering the three electrodes (working, counter, reference) with a 100 μL drop of the working solution.

4.3.3 Results and discussion

Electrochemical characterization

Electrochemical impedance spectroscopy characterization

Electrochemical impedance spectroscopy was carried out at + 0.2 V in 0.1 M potassium chloride in the presence of 5 mM ferricyanide and the results are presented in Figure IV.12 In the complex plane plots (Figure IV.12a and inset) all the samples show a semicircle for high frequencies and a straight line at lower frequencies, with a slope below 45° for PHBV /MFC bottom side, PHBV /MFC top side and Polyester and above for PHBV bottom side and PHBV top side. The equivalent circuit used to fit the PHBV /MFC bottom side, PHBV /MFC top side and Polyester data is the typical Randles circuit (Figure IV.12b) composed by the cell resistance (RW) in series with the electrical double layer capacitance (CPEdl) and the charge transfer resistance (Rct), respectively in parallel. In series with the latter there is an open Warburg element (W), which describes the mass transfer of the system. For the hydrophobic samples (PHBV bottom/top side) the open Warburg element is replaced with the support capacity (CPEs), since the

hydrophobicity of the support slows down the mass transfer which is not observable.

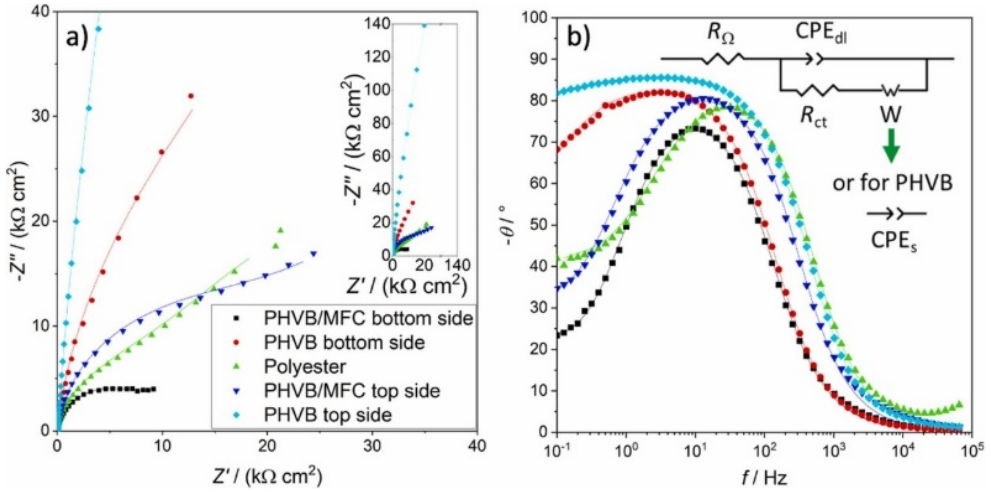

Figure IV.12. EIS complex plane (a, magnification in inset) and Bode phase (b) plots registered at 0.2 V in 5 mM ferricyanide solution. Equivalent circuits used to fit impedance data are presented as inset.

Another element that demonstrates that hydrophobicity does not favour electrochemical performances is the detection of the maximum impedance value for these latter samples, in the order PHBV top side > PHBV bottom side > Polyester and PHBV/MFC top side > PHBV/MFC bottom side. In all cases, instead of a pure capacity, a constant phase element is used, which reflects the presence of surfaces that are not perfectly homogeneous, which deviate from ideality, measured by a parameter, between 0.5 and 1.

The Bode graph of the phase is in line with the previous results: at low frequencies PHBV/MFC bottom side, PHBV/MFC top side and Polyester show points below 45°, while PHBV bottom side and PHBV top side above, confirming the presence of the open Warburg element or capacity, respectively. Furthermore, the trend is very similar for PHBV/MFC bottom side, PHBV/MFC top side and Polyester and for PHBV bottom side and PHBV top side. However,

at higher frequencies the Polyester trend is more similar to PHBV bottom side and PHBV top side. The results previously obtained are confirmed by the parameters derived from the fitting. The morphology of the support (bottom or top side) is fundamental in the formation of the electric double layer, as demonstrated by the similar CPEdl values for bottom and top side surfaces, respectively. These values are higher for the bottom side ones because the capacitor that is formed is more uniform. The results are also confirmed by the CPEs values. For the electrochemical performances, hydrophilicity plays a key role. In fact, the lowest Rct is for PHBV /MFC bottom side, with a value comparable to Polyester taken as a reference, followed by PHBV /MFC top side. Hydrophobic samples (PHBV ones) perform less, with better results for smooth substrate. Furthermore, the PHBV /MFC bottom side and PHBV /MFC top side samples are more performing than Polyester due to the lower resistance to mass transfer (RW), a phenomenon aided by the absorbency of the cellulose.

Cyclic voltammetry and chronoamperometry characterization

It should be considered that the choice of the substrates where the electrodes will be screen-printed may affect the electrochemical performance of the ultimate device. In fact, the adoption of porous materials, i.e. paper-based, could reduce the diffusion of the electrochemical species and thus making the device not appropriated for real application. To evaluate the effect of the different substrates on the effectiveness of the printed strips, cyclic voltammetry experiments have been carried out in presence of a 100-µL drop containing 5 mM ferricyanide dissolved in 0.1 M potassium chloride interrogating the scan rates, from 0.02 to 0.5 V/s (Figure IV.13).

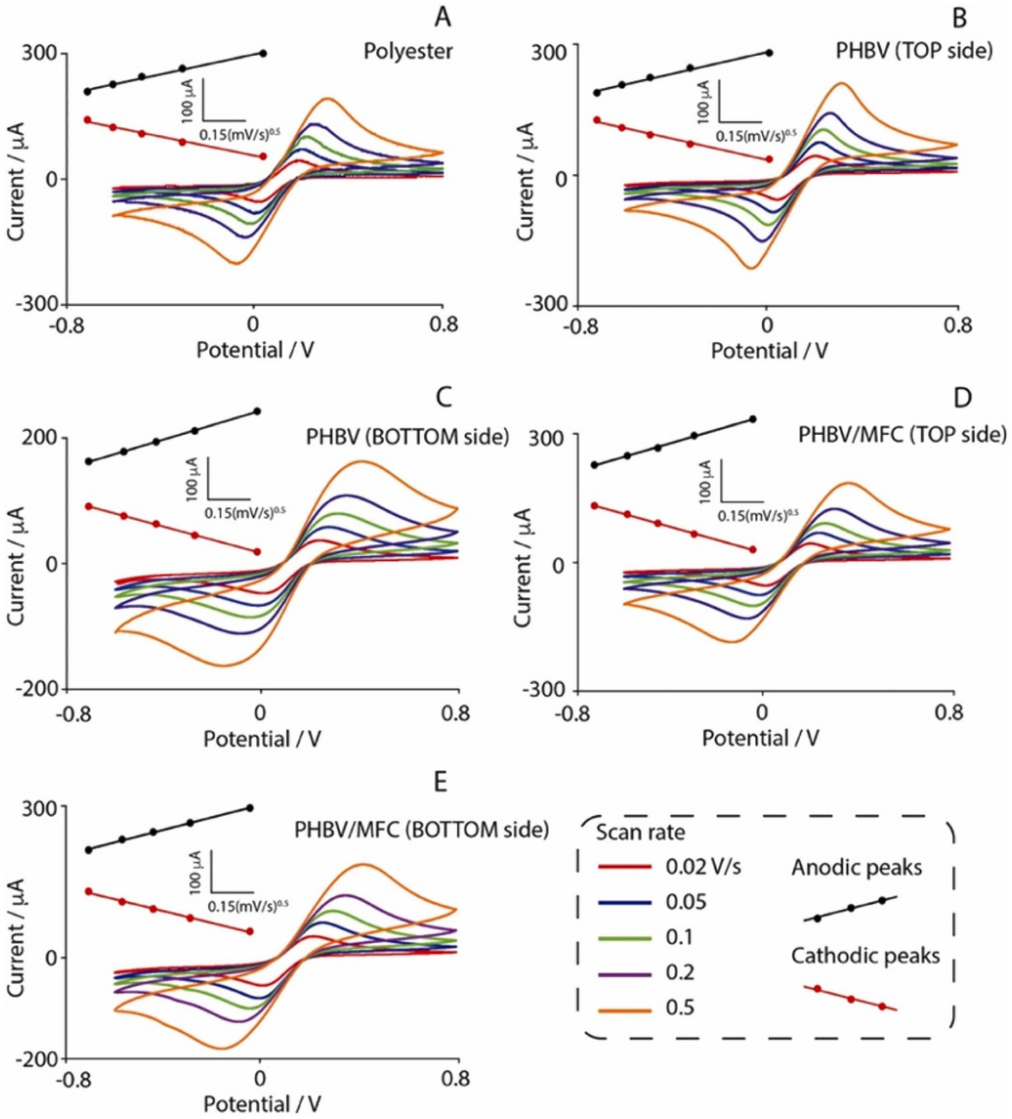

Figure IV.13. Cyclic voltammetric experiments of electrodes screen-printed onto A) polyester, B) PHBV (TOP side), C) PHBV (BOTTOM side), D) PHBV/MFC (TOP side) and E) PHBV/MFC (BOTTOM side). All the experiments have been carried out through the analysis of 100 mL drop of a solution containing 5 mM, using various scan rates, namely 0.02, 0.05, 0.1, 0.2 and 0.5 V/s. Inset: linearity among the intensity of the anodic (black curve) and cathodic (red curve) and the square root of the tested scan rates.

As is clearly visible, for all the substrates that were used to screen-print the strips, the cathodic and anodic voltammetric peaks resulted linear to the square root of

the scan rate, and this behaviour was consistent with a semi-infinite diffusion of the electroactive species at electrode surface, showing that reagents were able in diffusing and reaching the electrode area without any entrapment,[135,136] that might be observed in presence of porous substrates. The approximated slopes relative to the correlation existing between the anodic curves and the square root of the scan rate were calculated equal to ca. 238, 260, 200, 241 and 208 mA* $(s/mV)^{0.5}$ respectively to polyester, PHBV (TOP side), PHBV (BOTTOM side), PHBV/MFC (TOP side) and PHBV/MFC (BOTTOM side). Even if the PHBV/MFC displayed the presence of a cellulosic content, it was not relevant in affecting the semi-infinite diffusion of the model redox probe. No significant differences were observed within the experimental error, considering a 10–15% variation due to the manually scree-printing process. Moreover, for all the substrates tested, the ratio between the anodic current and the cathodic current was comprised in the 0.89–1.05 range. The substrates' performance was also tested after 50 bendings by carrying out a cyclic voltammetry in presence of 5 mM ferricyanide prior and after the bendings. A slight difference in the signal was observed after 50 repetitions: polyester and PHBV/MFC were consistent with a decrease of the signal less than 7%, while PHBV showed a decrease of ca.13%. A possibility could be ascribable to the presence of cellulose which allowed a major resistance to these stresses.

In addition with these investigation, in order to evaluate the diffusion of the redox probe at the different substrates, the diffusion coefficient (D) for ferricyanide was calculated using chronoamperometry experiments in absence and in presence of different concentrations of ferricyanide, namely 2, 4 and 8 mM, as reported in Figure IV.14.

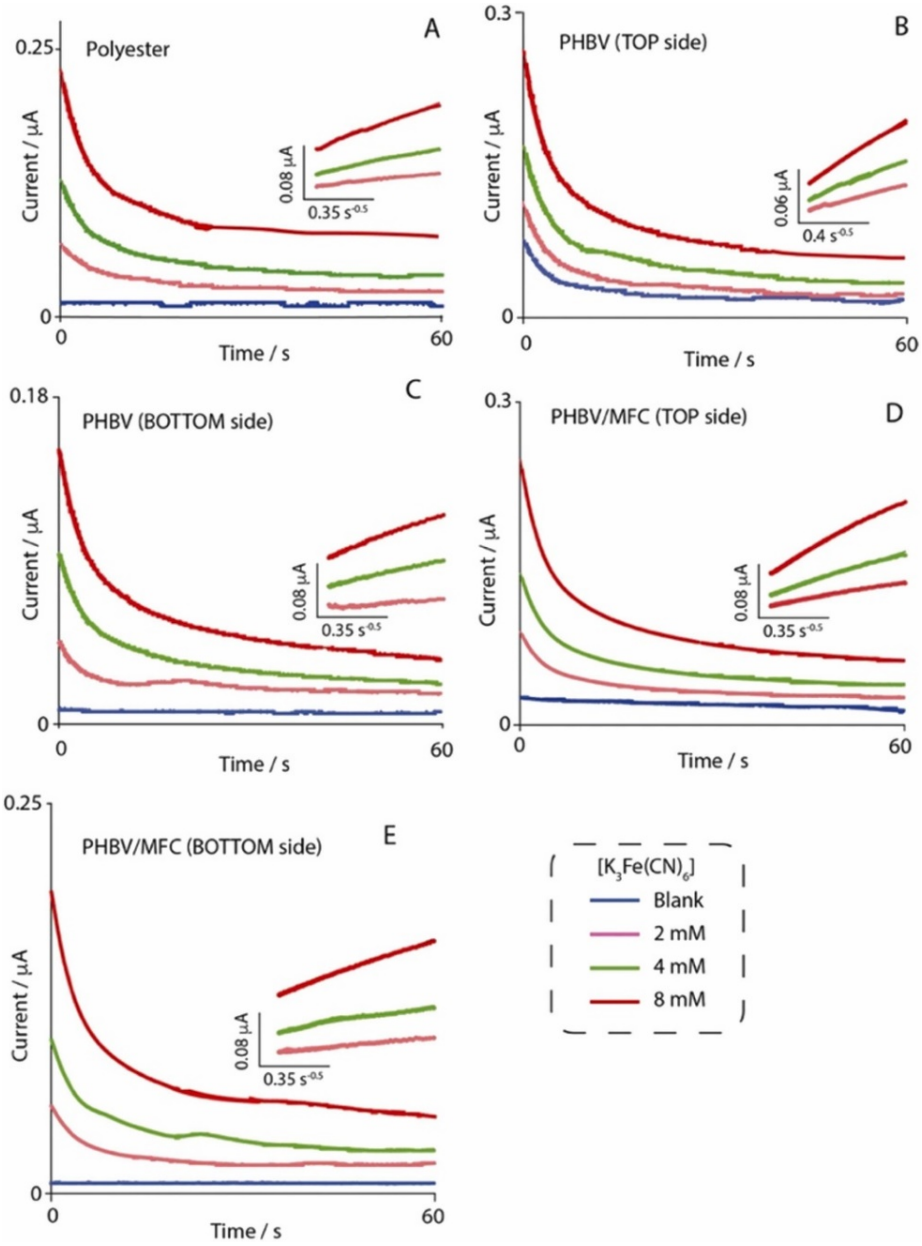

Figure IV.14. Chronoamperometry experiments carried out in a 100-mL drop of 0.1 M KCl in absence (blue line) and in presence of 2 (pink line), 4 (green line) and 8 mM (red line) of ferricyanide. A, B, C, D and E are relative to the use of, respectively, polyester, PHBV (TOP side), PHBV (BOTTOM side), PHBV/MFC (TOP side) and PHBV/MFC (BOTTOM side). Insets: show plots of I vs. $t^{0.5}$ obtained for the three different ferricyanide concentrations tested. All the measurements have been carried out by applying 0.4 V (vs. Ag/AgCl) for 60 s.

To estimate the diffusion coefficient of the redox specie in combination with the selected substrates, Cottrell equation was taken into account.[137] All the experiments were performed by screen-printing the same amount and type of graphite-based ink, and according to the Cottrell approximation, the sampled current resulting from a potential step decay to zero inversely proportional to the square root of time. As reported in Figure IV.14, the main images report chronoamperograms at three levels of ferricyanide concentration (plus the measurement carried out in 0.1 M KCl), while the insets are obtained by plotting the current vs. square root of time. If the slopes of these linear curves are plotted against the redox probe concentrations, the diffusion coefficient (D) for ferricyanide can be evaluated following the Cottrel equation. For all the tested substrates, the calculated diffusion coefficient for ferricyanide was ca. 10^5 cm^2/s and this appeared to be in good agreement with those reported in previous reports. What it should be noted is that, in the present experimental setup, the presence of cellulosic portion does not play a crucial role in hindering the diffusion of ions considering the species contained in the working solution diffuses through the bottom (where the electrodes are screen-printed). However, the roughness of the substrates often represents the first drawback while printing electrochemical device, due to a lower adhesion between the mask and the substrate; for this reason, the following studies have taken into account the "BOTTOM side" of each of the two PHBV-based materials in comparison with polyester.

Iron sensing and organophosphates biosensing

The analysis of metal ions is of high importance in the field of sensors, in fact, their presence gives indications for many purposes, from diagnostics to agriculture, through environment and industry. Among the metals and their sensing importance, iron ions represent a versatile target that is related to various

context: anemia affects a majority of individuals with advanced chronic kidney disease,[138] iron plays a fundamental role in the metabolism and growth of plants,[139] and the presence of iron in wastewater in industrial factories need to be carefully evaluated, such as the wastewater produced following manufacture of steel.[140] In this study, the three substrates have been compared towards the electrochemical detection of iron ions through the use of anodic stripping voltammetry. Briefly, the iron present in the working solution is initially electrodeposited on top of the working electrode and successively oxidized back in solution, and it produces a detectable signal (anodic peak) that is related to the amount of the ion present in the solution. The comparison among the three substrates has been carried out by analyzing iron ions in the ppm range, as showed in Figure IV.15.

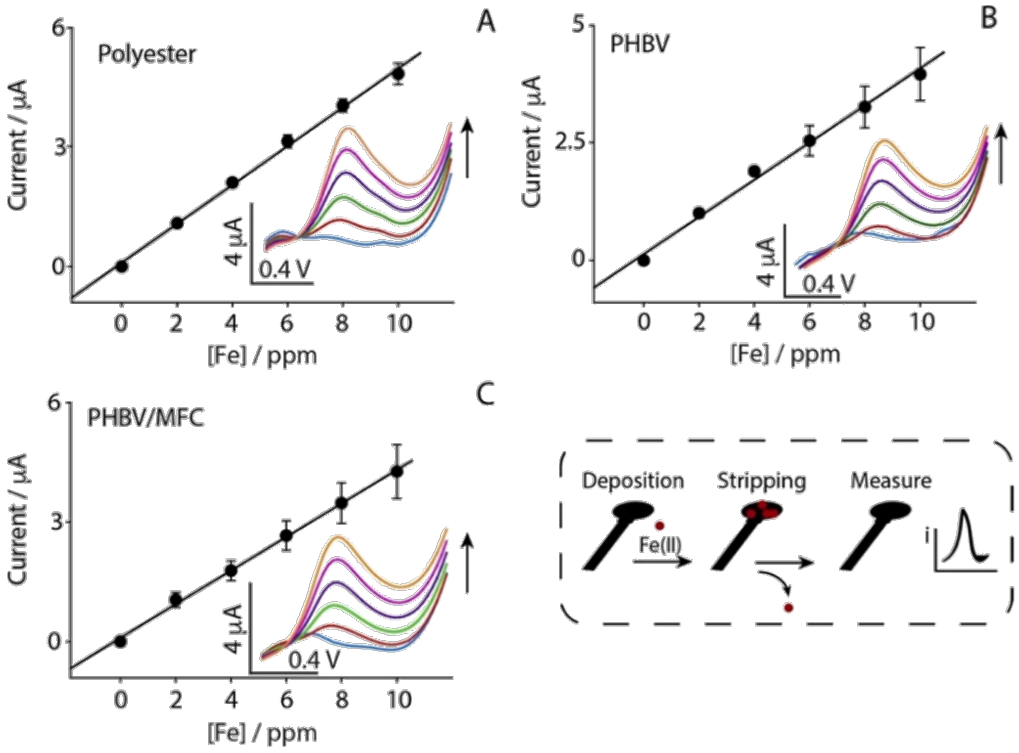

Figure IV.15. Stripping voltammograms for increasing Fe levels up to 10 ppm obtained onto electrodes that have been screen-printed on A) Polyester, B) PHBV and C)

PHBV/MFC. Corresponding calibration plot using linear sweep anodic stripping voltammetry (LS-ASV). Experimental conditions: 0.1 M hydrochloric acid, deposition potential at −1 V for 100 s, scan rate of 0.2 V/s. Low inset: mechanism for stripping detection of iron ions is reported.

As showed in Figure IV.15 all the substrates allowed a satisfactory detection of iron ions within the same range of concentrations. The equations describing the linear correlation among the current and the concentration have been approximated as follows, $y = 0.49x + 0.10$ (r^2 of 0.994), $y = 0.40x + 0{,}14$ (r^2 of 0.964), and $y = 0.42\ x + 0{,}09$ (R^2 of 0.953), relatively to polyester, PHBV and PHBV/MFC, respectively, where y represents the current difference between metal ion and the blank, and x represents the metal level expressed in ppm. A detection limit (LOD) was calculated following the equation LOD= 3*σb/slope (standard deviation of the blank)/ (slope of the curve), obtaining 90, 140 and 150 ppb, respectively to polyester, PHBV and PHBV/MFC. These results appear well-compared with other unmodified electrochemical architectures as the one reported by Prof. Compton group with a LOD of ca. 2 mM iron (110 ppb), which also included 20 min to remove the dissolved oxygen in solution.[141] Another paper reporting the electrochemical detection of iron ions was recently reported using commercial graphite-based screen-printed electrodes (DropSens) through the anodic stripping voltammetry in presence of o-phenanthroline, ferrocyanide and 240 s of accumulation: even if this method allowed to reach a LOD of ca. 4 ppb, it should be noted that the experimental setup was more complex with respect to an unmodified SPE platform.[142] Another system to compare was also represented by a carbon-based platform modified with a coating of carbon nanotubes and Nafion, and the linear sweep stripping voltammetry allowed a LOD of ca. 35 ppb of iron ions (using an accumulation of 4.5 min).[143] It should be noted that various electroanalytical architectures based on modified systems

have been reported for iron sensing, including gold nanoparticles, bismuth nanoparticles, graphene, carbon nanotubes, and Nafion. In addition to this, the PHBV-based screen-printed electrodes may represent a starting point for the construction of more sophisticated printed electroanalytical architectures. Even if the three tested substrates highlighted a similar sensitivity towards the detection of iron ions, it should be noted that the repeatability appeared slightly different.[144,145] The repeatability was calculated as the relative standard deviation (RSD), and while the polyester-based strips (Figure IV.15A) were characterized by a repeatability of ca. 7%, the RSD calculated for PHBV and PHBV/MFC was equal to 12% and 14%, respectively (RSD has been calculated on three replicates, using three different electrochemical strips for each kind of substrates tested). This slight difference could be attributed to production strategy of the PHBV-based substrates with respect to polyester: the layer of the PHBV-based materials, as reported in the SEM images, presented some morphological heterogeneity and this might lead to a slight source of variation in the final product. However, the results demonstrated the good performance of the novel substrates with detection limit in the ppb range.

In order to make the characterization of these substrates wider, an additional case of study has been interrogated. The substrates have been modified with Prussian Blue and butyrylcholinesterase enzyme to evaluate the presence of dichlorvos, as a model organophosphate inhibitor. The system has been obtained by drop casting 8 mL Prussian Blue nanoparticles (1 mg/mL) and 2 mL of butyrylcholinesterase enzyme (1 U/mL). In presence of the enzymatic substrate (butyrylthiocolione), one of the by-products of the reaction is the thiocholine that can be easily oxidized at the electrode surface via Prussian Blue. Instead, the presence of the inhibitor (which de-activate the enzyme) has the effect of

decreasing the enzymatic activity, thus producing less thiocholine with the results of having a lower oxidation current.[90] As reported in Figure IV.16, the organophosphate inhibitor has been measured at the three substrates ranging from 1 ppb to 1 ppm.

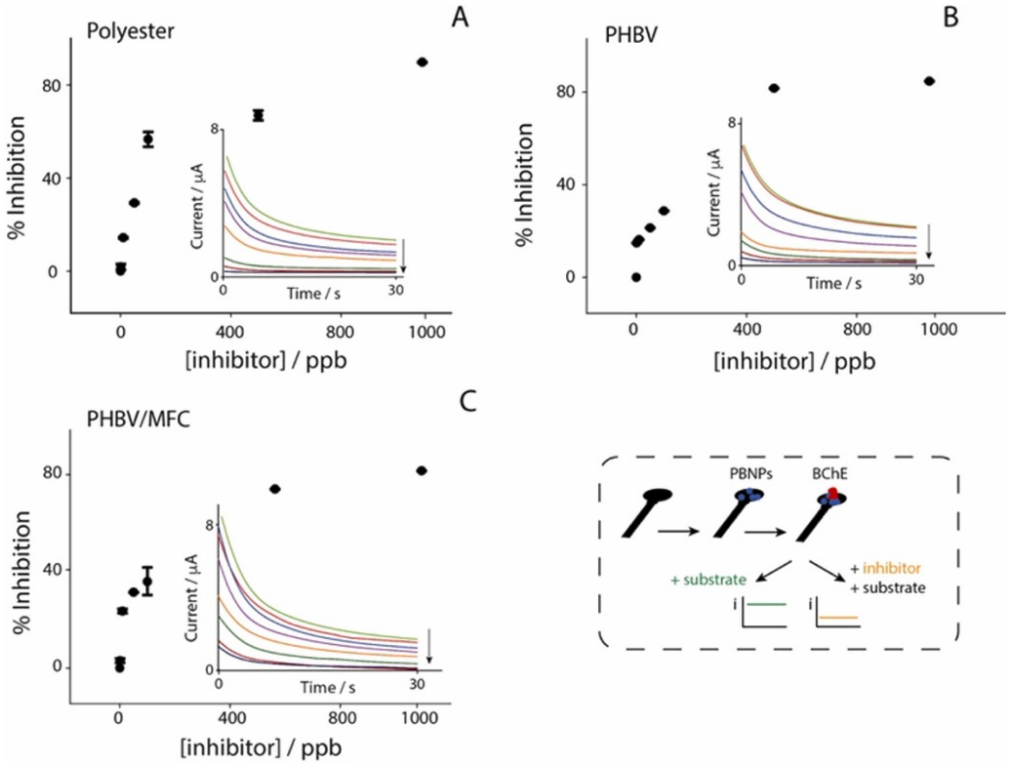

Figure IV.16. Chronoamperometric recordings obtained in the range between 1 ppb and 1 ppm of organophosphate inhibitor using A) polyester, B) PHBV and C) PBHV/MFC. The inset shows both the composition of the device and the electrochemical scheme on which the detection is based.

As reported, the intensity of the chronoamperometric curves were consistent with a decrease as the inhibitor concentration increases. The three tested platforms were challenged in presence of inhibitor, i.e. dichlorvos, from 1 ppb to 1000 ppm. As the concentration of substrate, a concentration of 10 mM was chosen to give a high current signal as the background. The calibration curves in the linear range, up to 100 ppb, were described by the following equations, $y = 0.54x + 3.1$,

$y = 0.24x + 11$, $y = 0.36x + 10$, respectively to polyester, PHBV, PHBV/MFC, where y represents the percentage of inhibition and x is the concentration of the inhibitor expressed in ppb, and the detection limit for each device was calculated to be equal 0.8, 0.4 and 0.5 ppb, respectively. With respect to other electrochemical inhibition-based biosensors for the determination of organophosphate pesticides, the results reported in terms of LOD appear in agreement within the concentration range of a paper-based printed electroanalytical system based on Prussian Blue Nanoparticles that produced a 3 ppb LOD,[146] a flexible cobaltphthalocyanine-based screen-printed electrode with a ca. 5ppb LOD,[147] an amperometric AChE-based screen-printed electrode modified with a mixture of silver nanowire-graphene-TiO_2 sol-gel-chitosan characterized by a LOD of ca. 2 ppb and also with the use of a different architecture based on the inhibition of choline oxidase based on poly(brilliant cresyl blue) films formed on multiwall-carbon nanotube, dichlorvos was detected down to ca. 0.5 ppb. In addition, the repeatability has been calculated on three measurements of 20 ppb standard solution, obtaining a value lower than 10% for all the substrates. However, the overall applicability of these new substrates looks promising, displaying satisfactory performance in presence of different species to be detected.

4.3.4 Conclusions

This work reported for the first time a complete characterization of novel materials based on PHBV to be used in electroanalytical sensing application. These so-called bacterial polymers are fully bio-based and biodegradable sustainable materials, and they might replace the use of plastic-based materials for realizing portable devices. PHBV and PHBV/MFC have been deeply investigated through the use of morphological, mechanical and electrochemical

approaches, and those have been compared with the gold standard in developing screen-printed electrodes, namely polyester. All the characterization studies have demonstrated the suitability of these substrates to be combined with the screen-printing process, highlighting the satisfactory performance. In particular, the novel materials have been applied to the determination of iron ions and organophosphate inhibitors in aqueous solutions demonstrating the good preliminary findings. The replacement of "old" material with sustainable alternatives is of pivotal importance, especially in the field of sensors and biosensors. The use of bio-based and biodegradable substrates, as the PHBV ones, opens to novel possibilities about the decentralization of portable devices. For instance, the growth of precision agriculture, where sensing devices are required to be in close contact with fruit, leaf, stem, soil etc. would be a perfect field of application for these bacterial polymers, which will be lowering the issue related to contamination and waste disposal, especially in remote areas.

4.4 ON-GLOVE APPLICATIONS: DEVELOPMENT OF AN ELECTROCHEMICAL BIOSENSOR FOR DETECTION OF PESTICIDES DIRECTLY ON FRUIT PEELS

4.4.1 Introduction

Climate change, anthropogenic pollution, land, and water exploitation affect the condition of ecosystems leading to environmental issues and human health consequences. In recent decades, environmental pollution has emerged as a core issue around the globe, posing concern for a multitude of specialists including eco-toxicologists, environmental biologists, eco-chemists, pathologists, and researchers from other fields.[148] The survival of many societies, and of the biological support systems of the planet, is at risk. In particular, one of the greatest challenges for the future is the conservation of global agricultural production, severely affected by the climate change and the exponential growth of the population, and it is reported as one of the bullet point in the 2030 agenda, established by the United Nations.[149] All efforts to ensure sustainable food production systems and implement smart agricultural practices that increase productivity and production while helping to maintain ecosystems are urgently needed. Agricultural systems around the world must become more productive and less wasteful. Sustainable agricultural practices and food systems, including both production and consumption, must be pursued from a holistic and integrated point of view. We can no longer look at food, livelihoods and the management of natural resources separately.[150] The importance of plants is well known: they are the first link in the food network, able to convert solar energy into chemical energy; they provide us with up to 80% of the food we eat, such as fruits, vegetables and legumes, and produce about 98% of atmospheric oxygen. Therefore, there is an urgent need to meet the demand for food and ensure

sustainable development of the agricultural sector. However, emerging plant diseases, caused by biological and environmental stressors, are straining crop productivity worldwide, such as pests and pathogens, that are affecting plant health and, consequently, the agricultural industry.[151] As a key factor in increasing agricultural production, pesticides have been used worldwide on crops because of their ability to eliminate plant pests and consequently, reduce labor intensity. There are many types of pesticides, classified considering their functional groups, in: carbamates, organochlorides, pyrethroids, organophosphates, and other substances.[152] On the other hand, their misuse also results in excessive pesticide residues in agricultural products, affecting consumers' food safety and harming human health. The total amount of pesticides applied to the environment amounts to millions of tons every year in the world causing serious pollution of the environment (in the soil, surface/water, atmosphere, etc.) and negative effects on the ecosystem.[153] Regulation (EC) No 396/2005 sets the maximum quantities of pesticide residues permitted in products of animal or vegetable origin intended for human or animal consumption at 0.01 ppm.[154] Considering that, it is necessary to implement early monitoring of the health conditions of crops through new technologies in order to increase agricultural productivity and reduce food losses, so as to guarantee food security and a sustainable development.[155] In addition, as demonstrated by the Covid-19 pandemic, the necessity of portable and wearable solutions for analyzing samples, from the medical to the environmental field, is growing day by day: an example is the development of "smart agriculture" or "precision agriculture", that has been attracting increasing attention due to its capability for using less to grow more, compared to traditional agricultural practices, improving the quality of the work environment.[156] Smart agriculture comprises a set of technologies that combines sensors, information systems, enhanced machinery, and informed

management to optimize production by accounting for variabilities and uncertainties within sustainable agricultural systems.[156,157] Among the several technologies, advanced sensing systems that monitor soil and plants health conditions and crop developments are of great importance because they collect and evaluate data, especially when crop growing conditions change in space and time, such as in case of plants diseases, weeds or pests; in this way, it is possible to make long-term spatial models that can be used to create an intelligent and sustainable agricultural system.[158] In addition, a system where sensing devices are required to be in close contact with fruit, leaf or soil, lowering the risk of contamination, waste disposal, especially in remote areas. In this scenario, the use of sensors and biosensors capable of detecting the state of health of crops has proved to be a useful strategy for optimizing agricultural production. Nowadays, traditional techniques, such as gas chromatography (GC), gas chromatography-mass spectrometer (GC-MS) and liquid chromatography-tandem mass spectrometry (LC-MS/MS), are still the main methods used for environmental monitoring, including pesticides, but they have some disadvantages, such as the complicated pre-treatment of the sample, high cost, time-consuming, and difficulty in realizing in-situ detection, that can't allow their application in precision agriculture.[159] Hence, economically viable and rapid analytical methods are required to assess the levels of the pesticides and other contaminants in real samples, and electroanalytical (bio)sensors represent an excellent alternative. Compared with the traditional detection techniques, they have many advantages: good sensitivity and accuracy, short response time, portability, low cost, low interference and small volume required.[160] The modification of the working area is usually performed by using the recognition elements, such as surfactants, polymers, in-/organic and metal–organic compounds, biomaterials, metal and semi-metallic nanoparticles, which can enhance the electrochemical performance

by improving the sensitivity and selectivity of the electrochemical sensor.[160,161] Moreover, the development of disposable and low-cost screen-printed electrode (SPE) allow to fabricate electrochemical sensors and biosensors that show higher capability, portability and versatility in comparison to the traditional electrode sensing system.[162] To date, the SPE-based sensors and biosensors have been widely applied in the fields of food safety,[163,164] environmental analysis[90,160,165] and clinical diagnosis,[166–168] where, the success of the blood glucose test strips (billion dollar per annum global market)[168], is the main example of how this kind of systems are promising to preserve human health and ecosystems.[13-22] Another step forward, is the development of wearable sensors, generally reported as electronic devices that can be incorporated into clothing or worn on the body for monitoring several health parameters;[169,170] they can be applied to plants due to their capability to continually track important physiological and pathological parameters in situ, also adding the opportunity to integrate remote communication and control. Plant wearables possess a great potential as precision agriculture tools, thanks to their ability to allow a simple, precise, and continuous monitor of plant health at large scale.[158,171–175] As example, in their work, Jae Joon Kim et al., proposed a vapor-deposited conducting polymer sensor, tattooed on plant leaves, used to perform on-site impedance analysis, which reveals ozone damage, even at low exposure levels. These vapor deposited polymer tattoos, PEDOT-Cl, are created using oxidative chemical vapor deposition and reached a limit of detection of about 10 ppm, which is lower than the estimated dose at which fruit yields suffer.[172] Moreover, Hossain et al, proposed a multiplexed, bioagent-free electrochemical sensor (leaf-FIT), which was fabricated on a flexible polyimide substrate using a screen-printing process to quantitatively monitor the levels of Salicylic acid (SA) in the leaves of a living plant in different stressed situations, obtaining a good correlation with the spectroscopic analysis.

The electrode was modified with a composite of copper-based metal-organic framework that selectively oxidized SA with a limit of detection of 11.3 μM.[173] Recently, another interesting application was conducted by Martins et al, that developed an electrochemical sensors on paper kraft, for the non-enzymatic detection of the fungicide carbendazim on the skin of apple and cabbage, obtaining a detection limit of 0.06 μM.[174] Zhao et al., focused their attention on the development of an electrochemical device for in-situ analysis of organophosphorus pesticide on crop surfaces; their three-electrode system was prepared via laser-induced graphene (LIG) technology and modified with organophosphorus hydrolase (OPH) and equipped with biocompatible semisolid electrolyte; in this way it can selectively capture and recognize methyl parathion down to micromolar range.[175] All these architectures require the sensor to be installed directly on the leaf, fruit, etc., so they can be invasive to the plant; in addition, they must necessarily be weatherproof and adaptable to different climatic conditions. Considering this sophisticated experimental setup, a good alternative could be to involve the farmer in this monitoring process, through the integration of a suitable and disposable biosensor in a glove, that can be easily worn by the farmer who can check the health of a tree, leaf or fruit, only by rubbing the specific surface. This sensor on-glove technology was applied by Barfidokht et al., for the on-site detection of fentanyl, through a glove-based sensor consists of flexible screen-printed carbon electrodes integrated on the fingertips, modified with multiwalled carbon nanotubes and a ionic liquid, able to oxidate fentanyl in both liquid and powder forms with a detection limit of 10 μM.[176] Moreover, Mishra et al., published a work about the development of a glove biosensor for on-site detection of nerve-agent compounds on suspicious surfaces and agricultural products. They developed the method for the detection of methyl parathion (MP) and methyl paraoxon (MPOx) as proof of concept of

the usefulness of this kind of devices.[177] Following this concept, our aim was to develop an electrochemical device that exploit the possibility to be integrated in a glove, combined with a portable electrochemical analyzer, able to detect organophosphorus pesticide on site, under the limits required, thanks to the immobilization of a specific enzyme on the electrode surface that allow a selective and sensible detection, so the farmer can act only on a specific plant and not impact the whole crop. In this work, we proposed a screen-printed electrochemical biosensor for the enzymatic detection of organophosphorus pesticides directly on fruits peels, only by scrubbing their surface. The system has been suitably modified by loading bio-hybrid nanosized probes (Prussian blue, carbon black, and butyrylcholinesterase enzyme) able to recognize and detect the organophosphorus pesticide: the presence of the inhibitor de-activate the enzyme, resulting in a decreasing of the enzymatic activity, thus producing a lower oxidation current.[90] The portable system was successfully applied for in situ quantification of Dichlorvos deposited at different levels on orange and apple peels. The advantages associated to this kind of system consist in the possibility of integrating the biosensor in a glove, combined with a portable electrochemical analyzer, that allows the quantification only by scrubbing the surface of the peels and proceeding with the electrochemical measurement. The device is low cost, disposable and can selectively detect organophosphorus pesticides even at low concentrations, down to nanomolar range, so it can be used as valuable tools for precision agriculture in decentralized monitoring settings (Figure IV.17).

4.4.2 Experimental section

Reagents and equipment

Butyrylcholinesterase (BuChE) from equine serum, butyrylthiocholine chloride, and MXC032 Analytical Standard have been bought from Merck, USA. Carbon black (CB) VXC72R powder and Prussian Blue have been provided by Cabot Corporation, Italy. All the measurement were carried out in phosphate buffer prepared dissolving a PBS tablet 140 mM NaCl at pH=7.0 (Merck, USA) in 1L of bi-distilled water. Electro-chemical measurements have been carried out with the use of a portable potentiostat, EmStat (3) (PalmSens, Netherlands) connected to a laptop.

Screen printed platform

Electrodes were in-house produced onto a flexible polyester film as substrate (HT5, Autostat). The adoption of polyester-based substrates for manufacturing electrochemical strips compared to paper-based ones allow creating more robust platforms to be applied in decentralized context. The three-electrode design was obtained as described in Chapter 2.

Strip Nanoengineering

The electrochemical printed strips have been modified with 4µL mixture composed of carbon black (CB), Prussian blue (PB), drop casted onto the working electrode area and let it dry; then the enzyme, BuChE, has been drop-cast at the optimized concentration and let dry.[90]

Pesticide Quantification

The level of pesticides is obtained by measuring the change of the BuChE activity in the presence of the inhibitor. Briefly, the working area of the electrode,

modified with the hybrid nanocomposite, is covered with the suitable volume of phosphate buffer containing the substrate (butyryltiocholine) and the inhibitor (Dichlorvos). After several minutes, the enzymatic activity is calculated by measuring the amount of the electroactive byproduct of the BuChE substrate, namely, thiocholine. The current recorded in the presence and in the absence of the inhibitor is used to calculate the inhibition degree that is proportional to the inhibitor concentration. A chrono-amperometric technique at 0.4 V (versus Ag/AgCl) is used to show the enzymatic activity; the intensity of the chronoamperograms, recorded in the presence of the inhibitor, highlights a decrease as the inhibitor concentration increases.

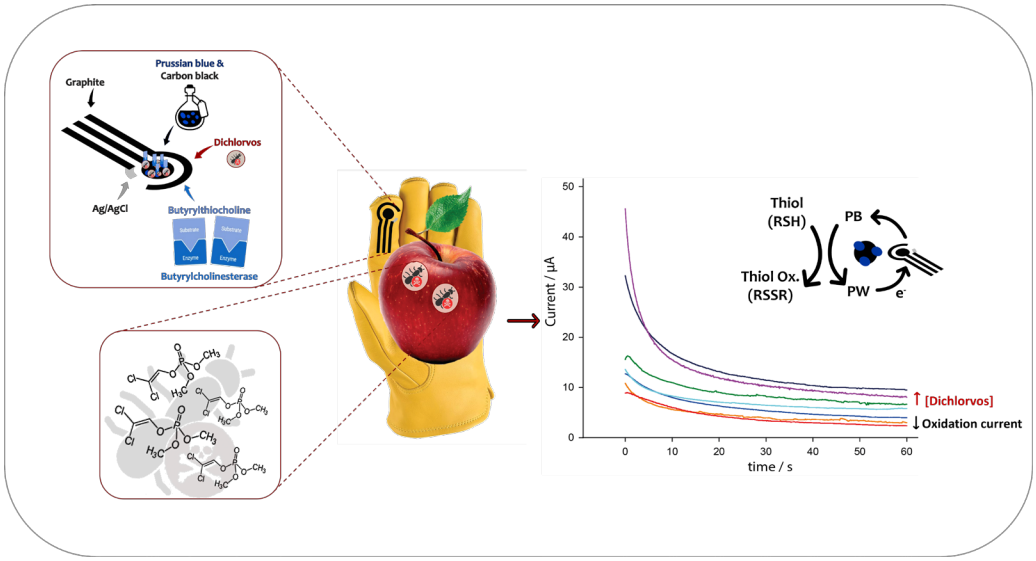

Figure IV.17. Schematic representation of the organophosphate pesticide's detection directly on fruit peels by using on-glove electrochemical strips, nanoengineered with the electrocatalyst (prussian blue), conductivity enhancer (carbon black), and sensing bioelement (BuChE), and the typical amperometric inhibition-based response at increasing concentrations of inhibitor.

4.4.3 Results and discussions

Evaluation of the experimental setup

The detection method of the organophosphorus pesticide is based on the irreversible inhibition of the Butyrylcholinesterase (BuChE) that hydrolyzes its substrate, butyrylcholine, giving byproducts butyric acid and choline. Unfortunately, both these products are not electroactive, and the enzymatic activity cannot be observed at the printed electrochemical device. For this reason, butyrylthiocholine has been chosen as the enzymatic substrate, giving byproducts butyric acid and thiocholine, an electroactive compound that can be easily electrochemically revealed.[175] This is possible thanks to the modification of the working electrode with a nanohybrid composite made with the combination of BuChE, PB, and CB: BuChE produces thiocholine, PB is sensitive to its oxidation at less interfering potential, and CB has the dual function of hosting the composite and improving conductivity. Thus, the biosensor has been optimized to obtain satisfactory sensitivity and repeatability. As shown in Figure IV.18a, b and c, several parameters were optimized: first, the constant potential applied during the chrono-amperometric measurement, set at 0.4 V, then the waiting time that allows the enzymatic reaction with the substrate and the inhibition time required for the pesticide to inhibit BuChE enzymatic activity, set respectively at three and five minutes. Successively, the concentrations of both BuChE (Figure IV.18d) and the substrate (Figure IV.19) have been taken into account, respectively. It is important to obtain the optimal condition to (1) have a good sensitivity, (2) evaluate future inhibition, and (3) reduce the costs. The nano-engineered platform has been first evaluated in the presence of different concentrations of BuChE (Figure IV.18d) in a range between 12.5 and 100 U mL^{-1} at the presence of a fixed amount of inhibitor (100 ppb), in order to obtain a good sensitivity and a high inhibition. The use of 100 U mL^{-1} of BuChE has

yielded the highest substrate conversion but the inhibition associated has been low and the sensitivity of the method will not be enough for inhibitor quantification; the best compromise in terms of BuChE amount and inhibition degree has been obtained by modifying the device with 25 U mL^{-1} of enzyme with a 70% inhibition in the presence of 100 ppb of Dichlorvos. After optimizing the amount of enzyme to be used, we proceed with the optimization of the substrate concentration: measurements have been performed using increasing concentration of butyrylthiocholine up to 20 mM. A typical Michaelis–Menten behavior has been observed. Considering that the difference between the responses due to 5, 10 and 20 mM of enzymatic substrate is negligible, 5 mM has been chosen as the minimum concentration of substrate to reach the Vmax and it has been selected for successive measurements in the presence of the inhibitor (Figure IV.19).

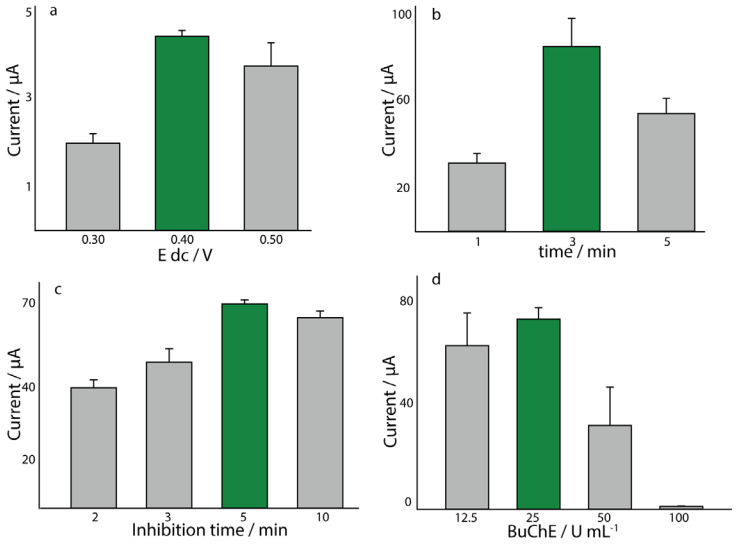

Figure IV.18. Optimization of the constant potential applied during the chrono-amperometry; b) Optimization of the enzymatic reaction waiting time; c) Optimization of the inhibition time; d) evaluation of the enzymatic activity between 12.5-100 U mL^{-1} BuChE in the presence of 5 mM substrate, with the use of the optimized parameters, at an applied potential of 0.4 V (versus Ag/AgCl), reaction time of 3 min.

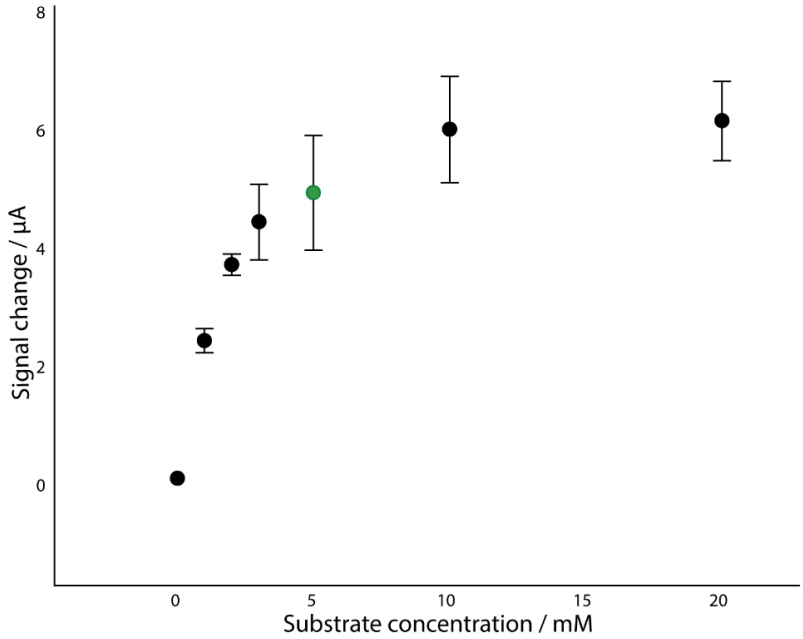

Figure IV.19. Calibration curve in the presence of various levels of enzymatic substrates, i.e., butyrylthiocholine, in the 0–20 mM range, at an applied potential of 0.4 V (versus Ag/AgCl), reaction time of 3 min, using 25 U mL^{-1} of BuChE.

Analytical features

After having optimized all the experimental parameters, a calibration curve has been obtained in the range between 0 and 100 ppb of Dichlorvos, using a phosphate buffer at pH=7 as working solution, as reported in Figure IV.20. The intensity of the chronoamperograms (Figure IV.20, inset i), recorded in the presence of the inhibitor, highlights a decrease as the inhibitor concentration increases. A linear trend is observed up to 20 ppb, while a dynamic interval is observed for higher levels of inhibitor. The calibration curve is described by the following equation: $y = 2.3x + 4.9$, where y represents the % of inhibition and x is the concentration of dichlorvos in ppb, with $r^2 = 0.971$. LOD calculated as 3σB/slope (σB represents the standard deviation calculated for blank

measurements, slope is the slope of the calibration curve in the linear range), resulted equal to ca. 1.3 nM (0.3 ppb). The repeatability has been calculated on four measurements of 20 ppb concentration of inhibitor, obtaining a value of 7%. It should be noted that all the measurements have been performed using one-shot platforms. The selectivity of the platform has been evaluated in the presence of common ions including toxic ones that could affect the enzymatic activity such as in the presence of nitrates, phosphates, potassium, sulphates, mercury, copper, cadmium and water. As reported in the Figure IV.20 inset ii, the % of inhibition calculated in presence of all these interfering species is negligible when compared with the inhibition obtained with the same concentration of the pesticide, demonstrating the absence of the interference of these compounds at the level evaluated (10 ppb – 1 ppm).

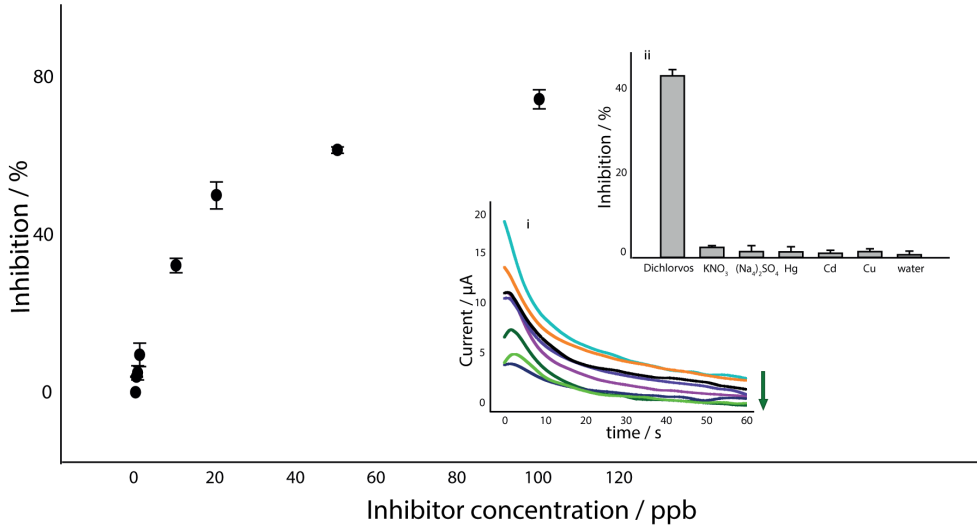

Figure IV.20. Calibration curve in the range between 0 and 100 ppb of inhibitor, using a phosphate buffer at pH=7 as working solution. Inset i) chronoamperometric recordings obtained in the range between 0 and 100 ppb of inhibitor. Inset ii) Selectivity studies conducted in presence of nitrates, phosphates, potassium, sulphates, mercury, copper, cadmium and water. Experimental conditions are the same as described in previous optimization studies.

Application on fruit peels

In order to evaluate the applicability of the new platform, the system was tested on real samples, taking into account the possibility of using this type of device directly in the field, where the farmer can check the presence and concentration (quali-quantitative analysis) of the pesticide easily by rubbing the fruit peel with the modified sensor, as described above, and inserted in a glove. We tested this system on two different fruit peels, apple and orange; the main problem associated with this architecture is that the rubbing can scratch the surface of the electrode, which, as a result, will be less performing. For this reason, we first tested the system "in solution," where the inhibitor was deposited and allowed to dry on the fruit peel, and then wetting the area again with bi-distilled water and rubbing the sensor on the drop (Figure IV.21a, b); then the system was also tested in a "dry" situation, where the sensor is rubbed directly on the fruit peel where the inhibitor was deposited and allowed to dry (Figure IV.21c, d). Chrono-amperometric measurement was then carried out by adding the solution containing the substrate. Meanwhile, the control experiments without pesticide were carried out under the same condition. As showed in Figure IV.21, the system works in both cases, with a limit of detection of 8nM and 40nM (2-10ppb) for the apple peel, tested in solution and dry (Figure IV.21a, c), respectively and with a LOD of 12 and 24nM (3-6 ppb) for the orange peel, tested in solution and dry (Figure IV.21b, d), respectively.

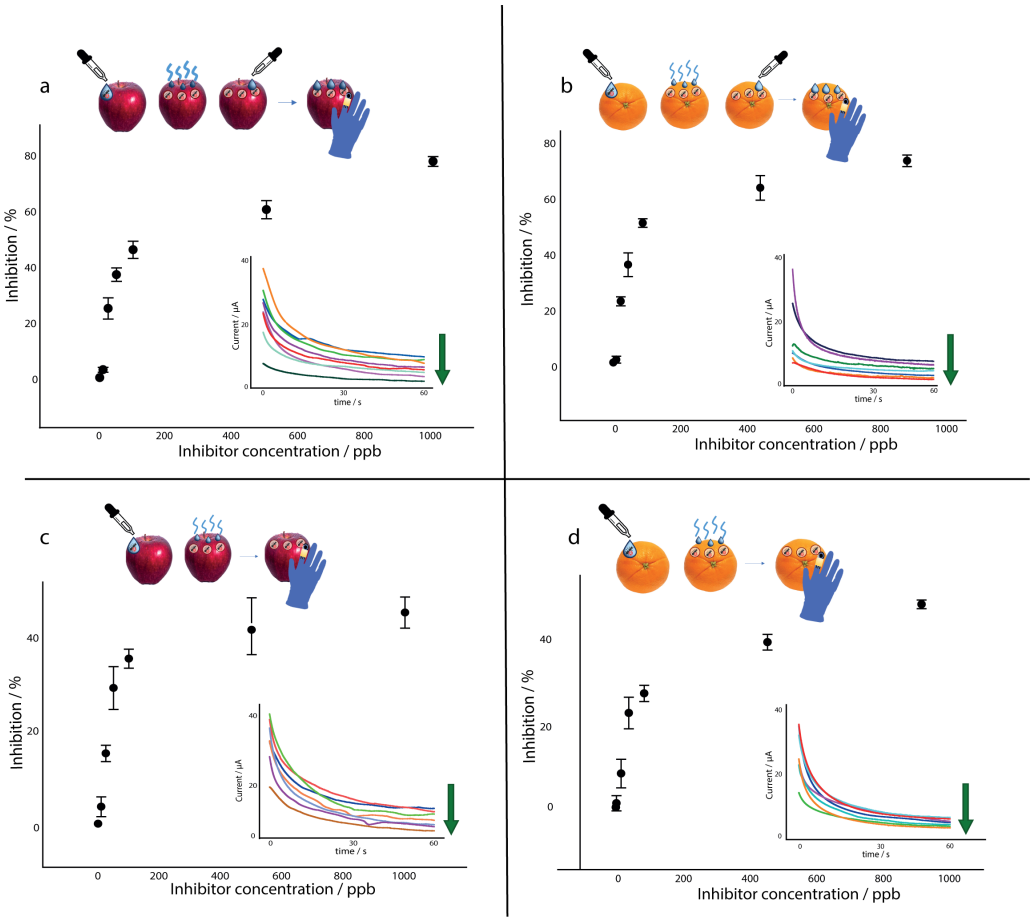

Figure IV.21. Calibration curves and chronoamperometric measurements obtained by testing the system on apple and orange peels. 4a) and 4b) biosensor rubbed "on drop" where the inhibitor was deposited and allowed to dry on apple and orange peels, and then wetting the area again with water and rubbing the sensor on the drop. 4c) and 4d) biosensor rubbed directly on the fruit peel where the inhibitor was deposited and allowed to dry. Experimental conditions are the same as described in previous optimization studies.

4.4.4 Conclusions

In this work, we developed a screen-printed electrochemical biosensor for enzymatic detection of organophosphorus pesticides directly on fruit peels, just by rubbing their surface. Taking into account the results obtained, the use of common materials such as a simple polyester substrate, suitably modified, proved to be a suitable architecture for the realization of a portable device for the

detection of organophosphate pesticides, which can be used for in situ analysis due to its strength and flexibility and easy integration into a glove. Dichlorvos was detected down to a nanomolar range in a few microliters of sample. The combination of the three-electrode configuration, printed on polyester with biomimetic (PB) catalysts, and the BuChE enzyme allowed accurate quantification of the target analyte. Two different fruit peels were analyzed, and satisfactory detection limits were achieved. The results obtained pave the way for on-glove technology, with which the farmer could perform rapid and accurate pesticide measurement and act only on specific fruits or leaves, without impacting the entire crop.

References

(1) Grieshaber, D.; MacKenzie, R.; Vörös, J.; Reimhult, E. Electrochemical Biosensors - Sensor Principles and Architectures. *Sensors* **2008**, *8* (3), 1400–1458. https://doi.org/10.3390/s80314000.

(2) Anchidin-Norocel, L.; Savage, W. K.; Gutt, G.; Amariei, S. Development, Optimization, Characterization, and Application of Electrochemical Biosensors for Detecting Nickel Ions in Food. *Biosensors* **2021**, *11* (12), 519. https://doi.org/10.3390/bios11120519.

(3) Perumal, V.; Hashim, U. Advances in Biosensors: Principle, Architecture and Applications. *Journal of Applied Biomedicine* **2014**, *12* (1), 1–15. https://doi.org/10.1016/j.jab.2013.02.001.

(4) Cui, F.; Yue, Y.; Zhang, Y.; Zhang, Z.; Zhou, H. S. Advancing Biosensors with Machine Learning. *ACS Sens.* **2020**, *5* (11), 3346–3364. https://doi.org/10.1021/acssensors.0c01424.

(5) Cinti, S.; Mazzaracchio, V.; Öztürk, G.; Moscone, D.; Arduini, F. A Lab-on-a-Tip Approach to Make Electroanalysis User-Friendly and de-Centralized: Detection of Copper Ions in River Water. *Analytica Chimica Acta* **2018**, *1029*, 1–7. https://doi.org/10.1016/j.aca.2018.04.065.

(6) Cinti, S.; Valdés-Ramírez, G.; Gao, W.; Li, J.; Palleschi, G.; Wang, J. Microengine-Assisted Electrochemical Measurements at Printable Sensor Strips. *Chem. Commun.* **2015**, *51* (41), 8668–8671. https://doi.org/10.1039/C5CC02222C.

(7) Miglione, A.; Spinelli, M.; Amoresano, A.; Cinti, S. Sustainable Copper Electrochemical Stripping onto a Paper-Based Substrate for Clinical Application. *ACS Meas. Au* **2022**. https://doi.org/10.1021/acsmeasuresciau.1c00059.

(8) Raucci, A.; Miglione, A.; Spinelli, M.; Amoresano, A.; Cinti, S. A Hybrid Screen-Printed Strip for Enhanced Electroanalysis towards Lead and Cadmium in Multi-Matrices. *Journal of The Electrochemical Society* **2022**, *169* (3), 037516. https://doi.org/10.1149/1945-7111/ac5c98.

(9) Ortone, V.; Matino, L.; Santoro, F.; Cinti, S. Merging Office/Filter Paper-Based Tools for Pre-Concentring and Detecting Heavy Metals in Drinking Water. *Chem. Commun.* **2021**, *57* (58), 7100–7103. https://doi.org/10.1039/D1CC02481G.

(10) Singh, S.; Wang, J.; Cinti, S. Review—An Overview on Recent Progress in Screen-Printed Electroanalytical (Bio)Sensors. *ECS Sens. Plus* **2022**, *1* (2), 023401. https://doi.org/10.1149/2754-2726/ac70e2.

(11) Fethi, A. Novel Materials for Electrochemical Sensing Platforms. *Sensors International* **2020**, *1*, 100035. https://doi.org/10.1016/j.sintl.2020.100035.

(12) Islam, T.; Hasan, M. M.; Awal, A.; Nurunnabi, M.; Ahammad, A. J. S. Metal Nanoparticles for Electrochemical Sensing: Progress and Challenges in the Clinical Transition of Point-of-Care Testing. *Molecules* **2020**, *25* (24), 5787. https://doi.org/10.3390/molecules25245787.

(13) Eivazzadeh-Keihan, R.; Bahojb Noruzi, E.; Chidar, E.; Jafari, M.; Davoodi, F.; Kashtiaray, A.; Ghafori Gorab, M.; Masoud Hashemi, S.; Javanshir, S.; Ahangari Cohan, R.; Maleki, A.; Mahdavi, M. Applications of Carbon-Based Conductive Nanomaterials in Biosensors. *Chemical Engineering Journal* **2022**, *442*, 136183. https://doi.org/10.1016/j.cej.2022.136183.

(14) Wooten, M. D. Electrochemical Sensors Based on Enzymes, Biopolymers and Nanoparticles. **2010**.

(15) Holzinger, M.; Le Goff, A.; Cosnier, S. Nanomaterials for Biosensing Applications: A Review. *Frontiers in Chemistry* **2014**, *2*.

(16) Anusha, J. R.; Arasu, M. V.; Al-Dhabi, N. A.; Raj, C. J. Nanomaterials in Electrochemical Biosensors and Their Applications. In *Emerging Nanomaterials for Advanced Technologies*; Krishnan, A., Ravindran, B., Balasubramanian, B., Swart, H. C., Panchu, S. J., Prasad, R., Eds.; Nanotechnology in the Life Sciences; Springer International Publishing: Cham, 2022; pp 487–516. https://doi.org/10.1007/978-3-030-80371-1_16.

(17) Kilic, N. M.; Singh, S.; Keles, G.; Cinti, S.; Kurbanoglu, S.; Odaci, D. Novel Approaches to Enzyme-Based Electrochemical Nanobiosensors. *Biosensors* **2023**, *13* (6), 622. https://doi.org/10.3390/bios13060622.

(18) Regulation (EC) No 1223/2009 of the European Parliament and of the Council of 30 November 2009 on Cosmetic Products. 151.

(19) Filon, F. L.; D'Agostin, F.; Crosera, M.; Adami, G.; Bovenzi, M.; Maina, G. In Vitro Absorption of Metal Powders through Intact and Damaged Human Skin. *Toxicology in Vitro* **2009**, *23* (4), 574–579. https://doi.org/10.1016/j.tiv.2009.01.015.

(20) Warley, M. A.; Blackledge, P.; O'Gorman, P. Lead Poisoning from Eye Cosmetic. *Br Med J* **1968**, *1* (5584), 117.

(21) Zemba, C.; Romaguaera, C.; Vilaplana, J. Allergic Contact Dermatitis from Nickel in an Eye Pencil. *Contact Dermatitis* **1992**, *27* (2), 116–116. https://doi.org/10.1111/j.1600-0536.1992.tb05224.x.

(22) Saxena, M.; Warshaw, E.; Ahmed, D. D. F. Eyelid Allergic Contact Dermatitis to Black Iron Oxide. *American Journal of Contact Dermatitis* **2001**, *12* (1), 38–39. https://doi.org/10.1053/ajcd.2000.18398.

(23) Özkaya, E.; Mirzoyeva, L.; Ötkür, B. Mercury-Induced Systemic Allergic Dermatitis Caused by 'White Precipitate' in a Skin Lightening Cream. *Contact Dermatitis* **2009**, *60* (1), 61–63. https://doi.org/10.1111/j.1600-0536.2008.01460.x.

(24) Travassos, A. R.; Bruze, M.; Dahlin, J.; Goossens, A. Allergic Contact Dermatitis Caused by Nickel in a Green Eye Pencil. *Contact Dermatitis* **2011**, *65* (5), 307–308. https://doi.org/10.1111/j.1600-0536.2011.01960.x.

(25) Dickenson, C. A.; Woodruff, T. J.; Stotland, N. E.; Dobraca, D.; Das, R. Elevated Mercury Levels in Pregnant Woman Linked to Skin Cream from Mexico. *American Journal of Obstetrics and Gynecology* **2013**, *209* (2), e4–e5. https://doi.org/10.1016/j.ajog.2013.05.030.

(26) Costa, M.; Salnikow, K.; Cosentino, S.; Klein, C. B.; Huang, X.; Zhuang, Z. Molecular Mechanisms of Nickel Carcinogenesis. *Environ Health Perspect* **1994**, *102* (Suppl 3), 127–130.

(27) Genchi, G.; Carocci, A.; Lauria, G.; Sinicropi, M. S.; Catalano, A. Nickel: Human Health and Environmental Toxicology. *Int J Environ Res Public Health* **2020**, *17* (3), 679. https://doi.org/10.3390/ijerph17030679.

(28) Saito, M.; Arakaki, R.; Yamada, A.; Tsunematsu, T.; Kudo, Y.; Ishimaru, N. Molecular Mechanisms of Nickel Allergy. *Int J Mol Sci* **2016**, *17* (2), E202. https://doi.org/10.3390/ijms17020202.

(29) Da Mata Perez, L.; França, A. T.; Zimmerman, J. R. Systemic Nickel Allergy Syndrome. *World Allergy Organization Journal* **2015**, *8* (1), A89–A89. https://doi.org/10.1186/1939-4551-8-S1-A89.

(30) Borowska, S.; Brzóska, M. M. Metals in Cosmetics: Implications for Human Health. *Journal of Applied Toxicology* **2015**, *35* (6), 551–572. https://doi.org/10.1002/jat.3129.

(31) Amry, M. A.; Al-Saikhan, F.; Ayoubi, A. Toxic Effect of Cadmium Found in Eyeliner to the Eye of a 21 Year Old Saudi Woman: A Case Report. *Saudi Pharmaceutical Journal* **2011**, *19* (4), 269–272. https://doi.org/10.1016/j.jsps.2011.05.002.

(32) *European Parliament and Council Directive 94/27/EC of 30 June 1994 Amending for the 12th Time Directive 76/769/EEC on the Approximation of the Laws, Regulations and Administrative Provisions of the Member States Relating to Restrictions on the Marketing and Use of Certain Dangerous Substances and Preparations*; 1994; Vol. 188. http://data.europa.eu/eli/dir/1994/27/oj/eng (accessed 2024-01-16).

(33) Cha, N.-R.; Lee, J.-K.; Lee, Y.-R.; Jeong, H.-J.; Kim, H.-K.; Lee, S.-Y. Determination of Iron, Copper, Zinc, Lead, Nickel and Cadmium in Cosmetic Matrices by Flame Atomic Absorption Spectroscopy. *Analytical Letters* **2010**, *43* (2), 259–268. https://doi.org/10.1080/00032710903325781.

(34) Ma, F.; Jagner, D.; Renman, L. Mechanism for the Electrochemical Stripping Reduction of the Nickel and Cobalt Dimethylglyoxime Complexes. *Anal. Chem.* **1997**, *69* (9), 1782–1784. https://doi.org/10.1021/ac961023s.

(35) Kokkinos, C.; Economou, A.; Raptis, I.; Speliotis, T. Disposable Mercury-Free Cell-on-a-Chip Devices with Integrated Microfabricated Electrodes for the Determination of Trace Nickel(II) by Adsorptive Stripping Voltammetry. *Analytica Chimica Acta* **2008**, *622* (1), 111–118. https://doi.org/10.1016/j.aca.2008.05.051.

(36) Tekenya, R.; Pokpas, K.; Jahed, N.; Iwuoha, E. I. Enhanced Specificity and Sensitivity for the Determination of Nickel(II) by Square-Wave Adsorptive Cathodic Stripping Voltammetry at Disposable Graphene-Modified Pencil Graphite Electrodes. *Analytical Letters* **2019**, *52* (2), 373–398. https://doi.org/10.1080/00032719.2018.1469139.

(37) Baldwin, R. P.; Christensen, J. Kai.; Kryger, Lars. Voltammetric Determination of Traces of Nickel(II) at a Chemically Modified Electrode Based on Dimethylglyoxime-Containing Carbon Paste. *Anal. Chem.* **1986**, *58* (8), 1790–1798. https://doi.org/10.1021/ac00121a042.

(38) Wang, J.; Nascimento, V. B.; Lu, J.; Park, D. S.; Angnes, L. Disposable Nickel Screen-Printed Sensor Based on Dimethylglyoxime-Containing Carbon Ink. *Electroanalysis* **1996**, *8* (7), 635–638. https://doi.org/10.1002/elan.1140080706.

(39) González, P.; Cortínez, V. A.; Fontán, C. A. Determination of Nickel by Anodic Adsorptive Stripping Voltammetry with a Cation Exchanger-Modified Carbon Paste Electrode. *Talanta* **2002**, *58* (4), 679–690. https://doi.org/10.1016/S0039-9140(02)00381-8.

(40) Ferancová, A.; Hattuniemi, M. K.; Sesay, A. M.; Räty, J. P.; Virtanen, V. T. Rapid and Direct Electrochemical Determination of Ni(II) in Industrial Discharge Water. *Journal of Hazardous Materials* **2016**, *306*, 50–57. https://doi.org/10.1016/j.jhazmat.2015.11.057.

(41) Nurak, T.; Praphairaksit, N.; Chailapakul, O. Fabrication of Paper-Based Devices by Lacquer Spraying Method for the Determination of Nickel (II) Ion in Waste Water. *Talanta* **2013**, *114*, 291–296. https://doi.org/10.1016/j.talanta.2013.05.037.

(42) Pokpas, K.; Jahed, N.; Bezuidenhout, P.; Smith, S.; Land, K.; Iwuoha, E. Nickel Contamination Analysis at Cost-Effective Silver Printed Paper-Based Electrodes

Based on Carbon Black Dimethylglyoxime Ink as Electrode Modifier: Original Scientific Paper. *Journal of Electrochemical Science and Engineering* **2022**, *12* (1), 153–164. https://doi.org/10.5599/jese.1173.

(43) Bagheri, N.; Cinti, S.; Nobile, E.; Moscone, D.; Arduini, F. Multi-Array Wax Paper-Based Platform for the Pre-Concentration and Determination of Silver Ions in Drinking Water. *Talanta* **2021**, *232*, 122474. https://doi.org/10.1016/j.talanta.2021.122474.

(44) Pokpas, K.; Jahed, N.; Iwuoha, E. Tuneable, Pre-Stored Paper-Based Electrochemical Cells (μPECs): An Adsorptive Stripping Voltammetric Approach to Metal Analysis. *Electrocatalysis* **2019**, *10* (4), 352–364. https://doi.org/10.1007/s12678-019-00516-7.

(45) Mettakoonpitak, J.; Volckens, J.; Henry, C. S. Janus Electrochemical Paper-Based Analytical Devices for Metals Detection in Aerosol Samples. *Anal. Chem.* **2020**, *92* (1), 1439–1446. https://doi.org/10.1021/acs.analchem.9b04632.

(46) Ninwong, B.; Ratnarathorn, N.; Henry, C. S.; Mace, C. R.; Dungchai, W. Dual Sample Preconcentration for Simultaneous Quantification of Metal Ions Using Electrochemical and Colorimetric Assays. *ACS Sens.* **2020**, *5* (12), 3999–4008. https://doi.org/10.1021/acssensors.0c01793.

(47) Yamada, K.; Citterio, D.; Henry, C. S. "Dip-and-Read" Paper-Based Analytical Devices Using Distance-Based Detection with Color Screening. *Lab Chip* **2018**, *18* (10), 1485–1493. https://doi.org/10.1039/C8LC00168E.

(48) Nantaphol, S.; Kava, A. A.; Channon, R. B.; Kondo, T.; Siangproh, W.; Chailapakul, O.; Henry, C. S. Janus Electrochemistry: Simultaneous Electrochemical Detection at Multiple Working Conditions in a Paper-Based Analytical Device. *ANAL. CHIM. ACTA* **2019**, *1056*, 88–95. https://doi.org/10.1016/j.aca.2019.01.026.

(49) Zhang, Z.-Q.; Liu, H.; Zhang, H.; Li, Y.-F. Simultaneous Cathodic Stripping Voltammetric Determination of Mercury, Cobalt, Nickel and Palladium by Mixed

Binder Carbon Paste Electrode Containing Dimethylglyoxime. *Analytica Chimica Acta* **1996**, *333* (1), 119–124. https://doi.org/10.1016/0003-2670(96)00241-3.

(50) Hu, C.; Wu, K.; Dai, X.; Hu, S. Simultaneous Determination of Lead(II) and Cadmium(II) at a Diacetyldioxime Modified Carbon Paste Electrode by Differential Pulse Stripping Voltammetry. *Talanta* **2003**, *60* (1), 17–24. https://doi.org/10.1016/S0039-9140(03)00116-4.

(51) Ali, S. Y.; Reddy, K. D.; Manna, A. K. Structural, Electronic, and Spectral Properties of Metal Dimethylglyoximato [M(DMG)2; M = Ni2+, Cu2+] Complexes: A Comparative Theoretical Study. *J. Phys. Chem. A* **2019**, *123* (42), 9166–9174. https://doi.org/10.1021/acs.jpca.9b06762.

(52) Segura, R.; Pradena, M.; Pinto, D.; Godoy, F.; Nagles, E.; Arancibia, V. Adsorptive Stripping Voltammetry of Nickel with 1-Nitroso-2-Napthol Using a Bismuth Film Electrode. *Talanta* **2011**, *85* (5), 2316–2319. https://doi.org/10.1016/j.talanta.2011.07.062.

(53) Takeuchi, R. M.; Santos, A. L.; Padilha, P. M.; Stradiotto, N. R. A Solid Paraffin-Based Carbon Paste Electrode Modified with 2-Aminothiazole Organofunctionalized Silica for Differential Pulse Adsorptive Stripping Analysis of Nickel in Ethanol Fuel. *Analytica Chimica Acta* **2007**, *584* (2), 295–301. https://doi.org/10.1016/j.aca.2006.11.069.

(54) Wang, W.; Bao, N.; Yuan, W.; Si, N.; Bai, H.; Li, H.; Zhang, Q. Simultaneous Determination of Lead, Arsenic, and Mercury in Cosmetics Using a Plastic Based Disposable Electrochemical Sensor. *Microchemical Journal* **2019**, *148*, 240–247. https://doi.org/10.1016/j.microc.2019.05.011.

(55) Zhong, Z.; Li, G. Current Trends in Sample Preparation for Cosmetic Analysis. *Journal of Separation Science* **2017**, *40* (1), 152–169. https://doi.org/10.1002/jssc.201600367.

(56) Hao, Y.; Liu, S.; Lu, Z.-N.; Huang, J.; Zhao, M. The Impact of Environmental Pollution on Public Health Expenditure: Dynamic Panel Analysis Based on Chinese

Provincial Data. *Environ Sci Pollut Res* **2018**, *25* (19), 18853–18865. https://doi.org/10.1007/s11356-018-2095-y.

(57) Khan, S.; Naushad, Mu.; Govarthanan, M.; Iqbal, J.; Alfadul, S. M. Emerging Contaminants of High Concern for the Environment: Current Trends and Future Research. *Environmental Research* **2022**, *207*, 112609. https://doi.org/10.1016/j.envres.2021.112609.

(58) Paszkiewicz, M.; Godlewska, K.; Lis, H.; Caban, M.; Białk-Bielińska, A.; Stepnowski, P. Advances in Suspect Screening and Non-Target Analysis of Polar Emerging Contaminants in the Environmental Monitoring. *TrAC Trends in Analytical Chemistry* **2022**, *154*, 116671. https://doi.org/10.1016/j.trac.2022.116671.

(59) Rathi, B. S.; Kumar, P. S.; Show, P.-L. A Review on Effective Removal of Emerging Contaminants from Aquatic Systems: Current Trends and Scope for Further Research. *Journal of Hazardous Materials* **2021**, *409*, 124413. https://doi.org/10.1016/j.jhazmat.2020.124413.

(60) Kumar, R.; Qureshi, M.; Vishwakarma, D. K.; Al-Ansari, N.; Kuriqi, A.; Elbeltagi, A.; Saraswat, A. A Review on Emerging Water Contaminants and the Application of Sustainable Removal Technologies. *Case Studies in Chemical and Environmental Engineering* **2022**, *6*, 100219. https://doi.org/10.1016/j.cscee.2022.100219.

(61) Prajapati, D.; Shah, M.; Yadav, A.; Panchal, J. A Critical Review on Emerging Contaminants: Origin, Discernment, and Remedies. *Sustain. Water Resour. Manag.* **2023**, *9* (3), 69. https://doi.org/10.1007/s40899-023-00853-y.

(62) Barber, L. B. 1.13 - Emerging Contaminants. In *Comprehensive Water Quality and Purification*; Ahuja, S., Ed.; Elsevier: Waltham, 2014; pp 245–266. https://doi.org/10.1016/B978-0-12-382182-9.00015-3.

(63) Puri, M.; Gandhi, K.; Kumar, M. S. Emerging Environmental Contaminants: A Global Perspective on Policies and Regulations. *Journal of Environmental Management* **2023**, *332*, 117344. https://doi.org/10.1016/j.jenvman.2023.117344.

(64) Wilkinson, J.; Hooda, P. S.; Barker, J.; Barton, S.; Swinden, J. Occurrence, Fate and Transformation of Emerging Contaminants in Water: An Overarching Review of the Field. *Environmental Pollution* **2017**, *231*, 954–970. https://doi.org/10.1016/j.envpol.2017.08.032.

(65) Lopez, B.; Ollivier, P.; Togola, A.; Baran, N.; Ghestem, J.-P. Screening of French Groundwater for Regulated and Emerging Contaminants. *Science of The Total Environment* **2015**, *518–519*, 562–573. https://doi.org/10.1016/j.scitotenv.2015.01.110.

(66) Ahmed, S. F.; Mofijur, M.; Nuzhat, S.; Chowdhury, A. T.; Rafa, N.; Uddin, Md. A.; Inayat, A.; Mahlia, T. M. I.; Ong, H. C.; Chia, W. Y.; Show, P. L. Recent Developments in Physical, Biological, Chemical, and Hybrid Treatment Techniques for Removing Emerging Contaminants from Wastewater. *Journal of Hazardous Materials* **2021**, *416*, 125912. https://doi.org/10.1016/j.jhazmat.2021.125912.

(67) Pereira, L. C.; de Souza, A. O.; Bernardes, M. F. F.; Pazin, M.; Tasso, M. J.; Pereira, P. H.; Dorta, D. J. A Perspective on the Potential Risks of Emerging Contaminants to Human and Environmental Health. *Environ Sci Pollut Res* **2015**, *22* (18), 13800–13823. https://doi.org/10.1007/s11356-015-4896-6.

(68) Lin, X.; Xu, J.; Keller, A. A.; He, L.; Gu, Y.; Zheng, W.; Sun, D.; Lu, Z.; Huang, J.; Huang, X.; Li, G. Occurrence and Risk Assessment of Emerging Contaminants in a Water Reclamation and Ecological Reuse Project. *Science of The Total Environment* **2020**, *744*, 140977. https://doi.org/10.1016/j.scitotenv.2020.140977.

(69) Samal, K.; Mahapatra, S.; Hibzur Ali, M. Pharmaceutical Wastewater as Emerging Contaminants (EC): Treatment Technologies, Impact on Environment and Human Health. *Energy Nexus* **2022**, *6*, 100076. https://doi.org/10.1016/j.nexus.2022.100076.

(70) Chaturvedi, P.; Shukla, P.; Giri, B. S.; Chowdhary, P.; Chandra, R.; Gupta, P.; Pandey, A. Prevalence and Hazardous Impact of Pharmaceutical and Personal Care Products and Antibiotics in Environment: A Review on Emerging Contaminants.

Environmental Research **2021**, *194*, 110664. https://doi.org/10.1016/j.envres.2020.110664.

(71) Valdez-Carrillo, M.; Abrell, L.; Ramírez-Hernández, J.; Reyes-López, J. A.; Carreón-Diazconti, C. Pharmaceuticals as Emerging Contaminants in the Aquatic Environment of Latin America: A Review. *Environ Sci Pollut Res* **2020**, *27* (36), 44863–44891. https://doi.org/10.1007/s11356-020-10842-9.

(72) Colglazier, W. Sustainable Development Agenda: 2030. *Science* **2015**, *349* (6252), 1048–1050. https://doi.org/10.1126/science.aad2333.

(73) Soergel, B.; Kriegler, E.; Weindl, I.; Rauner, S.; Dirnaichner, A.; Ruhe, C.; Hofmann, M.; Bauer, N.; Bertram, C.; Bodirsky, B. L.; Leimbach, M.; Leininger, J.; Levesque, A.; Luderer, G.; Pehl, M.; Wingens, C.; Baumstark, L.; Beier, F.; Dietrich, J. P.; Humpenöder, F.; von Jeetze, P.; Klein, D.; Koch, J.; Pietzcker, R.; Strefler, J.; Lotze-Campen, H.; Popp, A. A Sustainable Development Pathway for Climate Action within the UN 2030 Agenda. *Nat. Clim. Chang.* **2021**, *11* (8), 656–664. https://doi.org/10.1038/s41558-021-01098-3.

(74) Guppy, L.; Mehta, P.; Qadir, M. Sustainable Development Goal 6: Two Gaps in the Race for Indicators. *Sustain Sci* **2019**, *14* (2), 501–513. https://doi.org/10.1007/s11625-018-0649-z.

(75) Abdel Shaheed, C.; Ferreira, G. E.; Dmitritchenko, A.; McLachlan, A. J.; Day, R. O.; Saragiotto, B.; Lin, C.; Langendyk, V.; Stanaway, F.; Latimer, J.; Kamper, S.; McLachlan, H.; Ahedi, H.; Maher, C. G. The Efficacy and Safety of Paracetamol for Pain Relief: An Overview of Systematic Reviews. *Medical Journal of Australia* **2021**, *214* (7), 324–331. https://doi.org/10.5694/mja2.50992.

(76) Lee, W. J.; Goh, P. S.; Lau, W. J.; Ismail, A. F. Removal of Pharmaceutical Contaminants from Aqueous Medium: A State-of-the-Art Review Based on Paracetamol. *Arab J Sci Eng* **2020**, *45* (9), 7109–7135. https://doi.org/10.1007/s13369-020-04446-1.

(77) Parida, V. K.; Saidulu, D.; Majumder, A.; Srivastava, A.; Gupta, B.; Gupta, A. K. Emerging Contaminants in Wastewater: A Critical Review on Occurrence, Existing

Legislations, Risk Assessment, and Sustainable Treatment Alternatives. *Journal of Environmental Chemical Engineering* **2021**, *9* (5), 105966. https://doi.org/10.1016/j.jece.2021.105966.

(78) Agarwal, N. Paracetamol - A Contaminant of High Concern: Existence in Environment and Adverse Effect. *Pharmaceutical Drug Regulatory Affairs Journal* **2022**, *5*. https://doi.org/10.23880/pdraj-16000128.

(79) Koagouw, W.; Arifin, Z.; Olivier, G. W. J.; Ciocan, C. High Concentrations of Paracetamol in Effluent Dominated Waters of Jakarta Bay, Indonesia. *Marine Pollution Bulletin* **2021**, *169*, 112558. https://doi.org/10.1016/j.marpolbul.2021.112558.

(80) Burgot, G.; Auffret, F.; Burgot, J.-L. Determination of Acetaminophen by Thermometric Titrimetry. *Analytica Chimica Acta* **1997**, *343* (1–2), 125–128. https://doi.org/10.1016/S0003-2670(96)00613-7.

(81) Ruengsitagoon, W.; Liawruangrath, S.; Townshend, A. Flow Injection Chemiluminescence Determination of Paracetamol. *Talanta* **2006**, *69* (4), 976–983. https://doi.org/10.1016/j.talanta.2005.11.050.

(82) Baranowska, I.; Kowalski, B. The Development of SPE Procedures and an UHPLC Method for the Simultaneous Determination of Ten Drugs in Water Samples. *Water Air Soil Pollut* **2010**, *211* (1), 417–425. https://doi.org/10.1007/s11270-009-0310-7.

(83) Gioia, M. G.; Andreatta, P.; Boschetti, S.; Gatti, R. Development and Validation of a Liquid Chromatographic Method for the Determination of Ascorbic Acid, Dehydroascorbic Acid and Acetaminophen in Pharmaceuticals. *Journal of Pharmaceutical and Biomedical Analysis* **2008**, *48* (2), 331–339. https://doi.org/10.1016/j.jpba.2008.01.026.

(84) Lou, H.; Yuan, H.; Ruan, Z.; Jiang, B. Simultaneous Determination of Paracetamol, Pseudoephedrine, Dextrophan and Chlorpheniramine in Human Plasma by Liquid Chromatography–Tandem Mass Spectrometry. *Journal of Chromatography B* **2010**, *878* (7), 682–688. https://doi.org/10.1016/j.jchromb.2010.01.005.

(85) Zhao, S.; Bai, W.; Yuan, H.; Xiao, D. Detection of Paracetamol by Capillary Electrophoresis with Chemiluminescence Detection. *Analytica Chimica Acta* **2006**, *559* (2), 195–199. https://doi.org/10.1016/j.aca.2005.11.071.

(86) Sirajuddin; Khaskheli, A. R.; Shah, A.; Bhanger, M. I.; Niaz, A.; Mahesar, S. Simpler Spectrophotometric Assay of Paracetamol in Tablets and Urine Samples. *Spectrochimica Acta Part A: Molecular and Biomolecular Spectroscopy* **2007**, *68* (3), 747–751. https://doi.org/10.1016/j.saa.2006.12.055.

(87) Šatínský, D.; Neto, I.; Solich, P.; Sklenářová, H.; Conceição, M.; Montenegro, B. S. M.; Araújo, A. N. Sequential Injection Chromatographic Determination of Paracetamol, Caffeine, and Acetylsalicylic Acid in Pharmaceutical Tablets. *Journal of Separation Science* **2004**, *27* (7–8), 529–536. https://doi.org/10.1002/jssc.200301644.

(88) Quintino, M. S. M.; Araki, K.; Toma, H. E.; Angnes, L. Batch Injection Analysis Utilizing Modified Electrodes with Tetraruthenated Porphyrin Films for Acetaminophen Quantification. *Electroanalysis* **2002**, *14* (23), 1629–1634. https://doi.org/10.1002/elan.200290003.

(89) Karikalan, N.; Karthik, R.; Chen, S.-M.; Velmurugan, M.; Karuppiah, C. Electrochemical Properties of the Acetaminophen on the Screen-Printed Carbon Electrode towards the High Performance Practical Sensor Applications. *Journal of Colloid and Interface Science* **2016**, *483*, 109–117. https://doi.org/10.1016/j.jcis.2016.08.028.

(90) Cioffi, A.; Mancini, M.; Gioia, V.; Cinti, S. Office Paper-Based Electrochemical Strips for Organophosphorus Pesticide Monitoring in Agricultural Soil. *Environ. Sci. Technol.* **2021**, *55* (13), 8859–8865. https://doi.org/10.1021/acs.est.1c01931.

(91) Raymundo-Pereira, P. A.; Gomes, N. O.; Machado, S. A. S.; Oliveira, O. N. Simultaneous, Ultrasensitive Detection of Hydroquinone, Paracetamol and Estradiol for Quality Control of Tap Water with a Simple Electrochemical Method. *Journal of Electroanalytical Chemistry* **2019**, *848*, 113319. https://doi.org/10.1016/j.jelechem.2019.113319.

(92) Nematollahi, D.; Shayani-Jam, H.; Alimoradi, M.; Niroomand, S. Electrochemical Oxidation of Acetaminophen in Aqueous Solutions: Kinetic Evaluation of Hydrolysis, Hydroxylation and Dimerization Processes. *Electrochimica Acta* **2009**, *54* (28), 7407–7415. https://doi.org/10.1016/j.electacta.2009.07.077.

(93) Su, W.-Y.; Cheng, S.-H. Electrochemical Oxidation and Sensitive Determination of Acetaminophen in Pharmaceuticals at Poly(3,4-Ethylenedioxythiophene)-Modified Screen-Printed Electrodes. *Electroanalysis* **2010**, *22* (6), 707–714. https://doi.org/10.1002/elan.200900455.

(94) Dortez, S.; Crevillen, A. G.; Escarpa, A.; Cinti, S. Electroanalytical Paper-Based Device for Reliable Detection and Quantification of Sugars in Milk. *Sensors and Actuators B: Chemical* **2024**, *398*, 134704. https://doi.org/10.1016/j.snb.2023.134704.

(95) Faheem, A.; Cinti, S. Chapter 5 - Advanced Techniques for Manufacturing Paper-Based Microfluidic Analytical Devices. In *Microfluidic Biosensors*; Mak, W. C., Pui Ho, A. H., Eds.; Academic Press, 2023; pp 159–170. https://doi.org/10.1016/B978-0-12-823846-2.00009-2.

(96) Dossi, N., Toniolo, R., Piccin, E., Susmel, S., Pizzariello, A., & Bontempelli, G. (2013). Pencil-Drawn Dual Electrode Detectors to Discriminate Between Analytes Comigrating on Paper-Based Fluidic Devices but Undergoing Electrochemical Processes with Different Reversibility. Electroanalysis, 25(11), 2515-2522.

(97) Lee, S. H., Lee, J. H., Tran, V. K., Ko, E., Park, C. H., Chung, W. S., & Seong, G. H. (2016). Determination of acetaminophen using functional paper-based electrochemical devices. Sensors and Actuators B: Chemical, 232, 514-522.

(98) Camargo, J. R., Andreotti, I. A., Kalinke, C., Henrique, J. M., Bonacin, J. A., & Janegitz, B. C. (2020). Waterproof paper as a new substrate to construct a disposable sensor for the electrochemical determination of paracetamol and melatonin. Talanta, 208, 120458.

(99) Dias, A. A., Cardoso, T. M., Chagas, C. L., Oliveira, V. X., Munoz, R. A., Henry, C. S., ... & Coltro, W. K. (2018). Detection of analgesics and sedation drugs in

whiskey using electrochemical paper-based analytical devices. Electroanalysis, 30(10), 2250-2257.

(100) Pagkali, V., Stavra, E., Soulis, D., & Economou, A. (2021). Development of a high-throughput low-cost approach for fabricating fully drawn paper-based analytical devices using commercial writing tools. Chemosensors, 9(7), 178.

(101) Miglione, A.; Lorenzo, R. D.; Grumetto, L.; Spinelli, M.; Amoresano, A.; Laneri, S.; Cinti, S. An Integrated Electrochemical Platform Empowered by Paper for Fast Nickel Detection in Cosmetics. *Electrochimica Acta* **2022**, *434*, 141332. https://doi.org/10.1016/j.electacta.2022.141332.

(102) Cinti, S.; Moscone, D.; Arduini, F. Preparation of Paper-Based Devices for Reagentless Electrochemical (Bio)Sensor Strips. *Nature Protocols* **2019**, *14* (8), 2437–2451. https://doi.org/10.1038/s41596-019-0186-y.

(103) Europe, W. H. O. R. O. for. *The European Health Report 2021. Taking Stock of the Health-Related Sustainable Development Goals in the COVID-19 Era with a Focus on Leaving No One Behind*; World Health Organization. Regional Office for Europe, 2022.

(104) Pulia, M. S.; O'Brien, T. P.; Hou, P. C.; Schuman, A.; Sambursky, R. Multi-Tiered Screening and Diagnosis Strategy for COVID-19: A Model for Sustainable Testing Capacity in Response to Pandemic. *Annals of Medicine* **2020**, *52* (5), 207–214. https://doi.org/10.1080/07853890.2020.1763449.

(105) Lo Presti, D.; Zaltieri, M.; Bravi, M.; Morrone, M.; Caponero, M. A.; Schena, E.; Sterzi, S.; Massaroni, C. A Wearable System Composed of FBG-Based Soft Sensors for Trunk Compensatory Movements Detection in Post-Stroke Hemiplegic Patients. *Sensors* **2022**, *22* (4), 1386. https://doi.org/10.3390/s22041386.

(106) Parolo, C.; Sena-Torralba, A.; Bergua, J. F.; Calucho, E.; Fuentes-Chust, C.; Hu, L.; Rivas, L.; Álvarez-Diduk, R.; Nguyen, E. P.; Cinti, S.; Quesada-González, D.; Merkoçi, A. Tutorial: Design and Fabrication of Nanoparticle-Based Lateral-Flow Immunoassays. *Nat Protoc* **2020**, *15* (12), 3788–3816. https://doi.org/10.1038/s41596-020-0357-x.

(107) Turner, A. P. F. Perspective—An Age of Sensors. *ECS Sens. Plus* **2022**, *1* (1), 011601. https://doi.org/10.1149/2754-2726/ac5523.

(108) Weiss, C.; Carriere, M.; Fusco, L.; Capua, I.; Regla-Nava, J. A.; Pasquali, M.; Scott, J. A.; Vitale, F.; Unal, M. A.; Mattevi, C.; Bedognetti, D.; Merkoçi, A.; Tasciotti, E.; Yilmazer, A.; Gogotsi, Y.; Stellacci, F.; Delogu, L. G. Toward Nanotechnology-Enabled Approaches against the COVID-19 Pandemic. *ACS Nano* **2020**, *14* (6), 6383–6406. https://doi.org/10.1021/acsnano.0c03697.

(109) del Valle, M. Sensors as Green Tools in Analytical Chemistry. *Current Opinion in Green and Sustainable Chemistry* **2021**, *31*, 100501. https://doi.org/10.1016/j.cogsc.2021.100501.

(110) Mahato, K.; Wang, J. Electrochemical Sensors: From the Bench to the Skin. *Sensors and Actuators B: Chemical* **2021**, *344*, 130178. https://doi.org/10.1016/j.snb.2021.130178.

(111) Lu, S.-M.; Peng, Y.-Y.; Ying, Y.-L.; Long, Y.-T. Electrochemical Sensing at a Confined Space. *Anal. Chem.* **2020**, *92* (8), 5621–5644. https://doi.org/10.1021/acs.analchem.0c00931.

(112) Hernández-Rodríguez, J. F.; Rojas, D.; Escarpa, A. Electrochemical Sensing Directions for Next-Generation Healthcare: Trends, Challenges, and Frontiers. *Anal. Chem.* **2021**, *93* (1), 167–183. https://doi.org/10.1021/acs.analchem.0c04378.

(113) Turner, A. P. F. Biosensors: Sense and Sensibility. *Chem. Soc. Rev.* **2013**, *42* (8), 3184–3196. https://doi.org/10.1039/C3CS35528D.

(114) Faheem, A.; Cinti, S. Non-Invasive Electrochemistry-Driven Metals Tracing in Human Biofluids. *Biosensors and Bioelectronics* **2022**, *200*, 113904. https://doi.org/10.1016/j.bios.2021.113904.

(115) Grell, M.; Barandun, G.; Asfour, T.; Kasimatis, M.; Collins, A. S. P.; Wang, J.; Güder, F. Point-of-Use Sensors and Machine Learning Enable Low-Cost Determination of Soil Nitrogen. *Nat Food* **2021**, *2* (12), 981–989. https://doi.org/10.1038/s43016-021-00416-4.

(116) Gao, W.; Emaminejad, S.; Nyein, H. Y. Y.; Challa, S.; Chen, K.; Peck, A.; Fahad, H. M.; Ota, H.; Shiraki, H.; Kiriya, D.; Lien, D.-H.; Brooks, G. A.; Davis, R. W.; Javey, A. Fully Integrated Wearable Sensor Arrays for Multiplexed in Situ Perspiration Analysis. *Nature* **2016**, *529* (7587), 509–514. https://doi.org/10.1038/nature16521.

(117) Numan, A.; Singh, S.; Zhan, Y.; Li, L.; Khalid, M.; Rilla, K.; Ranjan, S.; Cinti, S. Advanced Nanoengineered—Customized Point-of-Care Tools for Prostate-Specific Antigen. *Microchim Acta* **2021**, *189* (1), 27. https://doi.org/10.1007/s00604-021-05127-y.

(118) Koel, M. Do We Need Green Analytical Chemistry? *Green Chem.* **2016**, *18* (4), 923–931. https://doi.org/10.1039/C5GC02156A.

(119) Nowak, P. M.; Wietecha-Posłuszny, R.; Pawliszyn, J. White Analytical Chemistry: An Approach to Reconcile the Principles of Green Analytical Chemistry and Functionality. *TrAC Trends in Analytical Chemistry* **2021**, *138*, 116223. https://doi.org/10.1016/j.trac.2021.116223.

(120) Li, T.; Zhang, J.; Schneiderman, D. K.; Francis, L. F.; Bates, F. S. Toughening Glassy Poly(Lactide) with Block Copolymer Micelles. *ACS Macro Lett.* **2016**, *5* (3), 359–364. https://doi.org/10.1021/acsmacrolett.6b00063.

(121) Dufresne, A. Nanocellulose: A New Ageless Bionanomaterial. *Materials Today* **2013**, *16* (6), 220–227. https://doi.org/10.1016/j.mattod.2013.06.004.

(122) Rehm, B. H. A. Bacterial Polymers: Biosynthesis, Modifications and Applications. *Nat Rev Microbiol* **2010**, *8* (8), 578–592. https://doi.org/10.1038/nrmicro2354.

(123) Chen, G.-Q.; Wu, Q. The Application of Polyhydroxyalkanoates as Tissue Engineering Materials. *Biomaterials* **2005**, *26* (33), 6565–6578. https://doi.org/10.1016/j.biomaterials.2005.04.036.

(124) Tamboli, D. P.; Gomare, S. S.; Kalme, S. S.; Jadhav, U. U.; Govindwar, S. P. Degradation of Orange 3R, Mixture of Dyes and Textile Effluent and Production of Polyhydroxyalkanoates from Biomass Obtained after Degradation. *International*

Biodeterioration & Biodegradation **2010**, *64* (8), 755–763. https://doi.org/10.1016/j.ibiod.2010.09.003.

(125) Nielsen, C.; Rahman, A.; Rehman, A. U.; Walsh, M. K.; Miller, C. D. Food Waste Conversion to Microbial Polyhydroxyalkanoates. *Microbial Biotechnology* **2017**, *10* (6), 1338–1352. https://doi.org/10.1111/1751-7915.12776.

(126) Sabbagh, F.; Muhamad, I. I. Production of Poly-Hydroxyalkanoate as Secondary Metabolite with Main Focus on Sustainable Energy. *Renewable and Sustainable Energy Reviews* **2017**, *72*, 95–104. https://doi.org/10.1016/j.rser.2016.11.012.

(127) Silva, R. R.; Raymundo-Pereira, P. A.; Campos, A. M.; Wilson, D.; Otoni, C. G.; Barud, H. S.; Costa, C. A. R.; Domeneguetti, R. R.; Balogh, D. T.; Ribeiro, S. J. L.; Oliveira Jr., O. N. Microbial Nanocellulose Adherent to Human Skin Used in Electrochemical Sensors to Detect Metal Ions and Biomarkers in Sweat. *Talanta* **2020**, *218*, 121153. https://doi.org/10.1016/j.talanta.2020.121153.

(128) Yao, J.; Ji, P.; Wang, B.; Wang, H.; Chen, S. Color-Tunable Luminescent Macrofibers Based on CdTe QDs-Loaded Bacterial Cellulose Nanofibers for pH and Glucose Sensing. *Sensors and Actuators B: Chemical* **2018**, *254*, 110–119. https://doi.org/10.1016/j.snb.2017.07.071.

(129) Francisco-Aldana, L.; Morales-Narváez, E. Plasmonic Colored Nanopaper: A Potential Preventive Healthcare Tool against Threats Emerging from Uncontrolled UV Exposure. *J. Phys. Photonics* **2019**, *1* (4), 04LT01. https://doi.org/10.1088/2515-7647/ab41aa.

(130) Sun, X.; Mei, C.; French, A. D.; Lee, S.; Wang, Y.; Wu, Q. Surface Wetting Behavior of Nanocellulose-Based Composite Films. *Cellulose* **2018**, *25* (9), 5071–5087. https://doi.org/10.1007/s10570-018-1927-8.

(131) Bon, S. B.; Chiesa, I.; Degli Esposti, M.; Morselli, D.; Fabbri, P.; De Maria, C.; Morabito, A.; Coletta, R.; Calamai, M.; Pavone, F. S.; Tonin, R.; Morrone, A.; Giorgi, G.; Valentini, L. Carbon Nanotubes/Regenerated Silk Composite as a Three-Dimensional Printable Bio-Adhesive Ink with Self-Powering Properties. *ACS Appl.*

Mater. Interfaces **2021**, *13* (18), 21007–21017. https://doi.org/10.1021/acsami.1c03288.

(132) De Maria, C.; Chiesa, I.; Morselli, D.; Ceccarini, M. R.; Bittolo Bon, S.; Degli Esposti, M.; Fabbri, P.; Morabito, A.; Beccari, T.; Valentini, L. Biomimetic Tendrils by Four Dimensional Printing Bimorph Springs with Torsion and Contraction Properties Based on Bio-Compatible Graphene/Silk Fibroin and Poly(3-Hydroxybutyrate-Co-3-Hydroxyvalerate). *Advanced Functional Materials* **2021**, *31* (52), 2105665. https://doi.org/10.1002/adfm.202105665.

(133) Gomes, N. O.; Carrilho, E.; Machado, S. A. S.; Sgobbi, L. F. Bacterial Cellulose-Based Electrochemical Sensing Platform: A Smart Material for Miniaturized Biosensors. *Electrochimica Acta* **2020**, *349*, 136341. https://doi.org/10.1016/j.electacta.2020.136341.

(134) Bagheri, N.; Mazzaracchio, V.; Cinti, S.; Colozza, N.; Di Natale, C.; Netti, P. A.; Saraji, M.; Roggero, S.; Moscone, D.; Arduini, F. Electroanalytical Sensor Based on Gold-Nanoparticle-Decorated Paper for Sensitive Detection of Copper Ions in Sweat and Serum. *Anal. Chem.* **2021**, *93* (12), 5225–5233. https://doi.org/10.1021/acs.analchem.0c05469.

(135) Streeter, I.; Wildgoose, G. G.; Shao, L.; Compton, R. G. Cyclic Voltammetry on Electrode Surfaces Covered with Porous Layers: An Analysis of Electron Transfer Kinetics at Single-Walled Carbon Nanotube Modified Electrodes. *Sensors and Actuators B: Chemical* **2008**, *133* (2), 462–466. https://doi.org/10.1016/j.snb.2008.03.015.

(136) Cinti, S.; Talarico, D.; Palleschi, G.; Moscone, D.; Arduini, F. Novel Reagentless Paper-Based Screen-Printed Electrochemical Sensor to Detect Phosphate. *Analytica Chimica Acta* **2016**, *919*, 78–84. https://doi.org/10.1016/j.aca.2016.03.011.

(137) Compton, R. G.; Banks, C. E. *Understanding Voltammetry (Third Edition)*; World Scientific, 2018.

(138) Batchelor, E. K.; Kapitsinou, P.; Pergola, P. E.; Kovesdy, C. P.; Jalal, D. I. Iron Deficiency in Chronic Kidney Disease: Updates on Pathophysiology, Diagnosis, and Treatment. *Journal of the American Society of Nephrology* **2020**, *31* (3), 456. https://doi.org/10.1681/ASN.2019020213.

(139) *ROLE OF IRON IN PLANT GROWTH AND METABOLISM*. https://www.jstage.jst.go.jp/article/ras/3/0/3_1/_article (accessed 2024-01-17).

(140) Sun, W.; Xu, X.; Lv, Z.; Mao, H.; Wu, J. Environmental Impact Assessment of Wastewater Discharge with Multi-Pollutants from Iron and Steel Industry. *Journal of Environmental Management* **2019**, *245*, 210–215. https://doi.org/10.1016/j.jenvman.2019.05.081.

(141) Lu, M.; Compton, R. G. Voltammetric Determination of Iron(III) in Water. *Electroanalysis* **2013**, *25* (5), 1123–1129. https://doi.org/10.1002/elan.201200661.

(142) Ustabasi, G. S.; Pérez-Ràfols, C.; Serrano, N.; Díaz-Cruz, J. M. Simultaneous Determination of Iron and Copper Using Screen-Printed Carbon Electrodes by Adsorptive Stripping Voltammetry with o-Phenanthroline. *Microchemical Journal* **2022**, *179*, 107597. https://doi.org/10.1016/j.microc.2022.107597.

(143) Silva, J. J.; Paim, L. L.; Stradiotto, N. R. Simultaneous Determination of Iron and Copper in Ethanol Fuel Using Nafion/Carbon Nanotubes Electrode. *Electroanalysis* **2014**, *26* (8), 1794–1800. https://doi.org/10.1002/elan.201400136.

(144) Lin, M.; Han, H.; Pan, D.; Zhang, H.; Su, Z. Voltammetric Determination of Total Dissolved Iron in Coastal Waters Using a Glassy Carbon Electrode Modified with Reduced Graphene Oxide, Methylene Blue and Gold Nanoparticles. *Microchim Acta* **2015**, *182* (3), 805–813. https://doi.org/10.1007/s00604-014-1391-6.

(145) Hu, X.; Pan, D.; Lin, M.; Han, H.; Li, F. Graphene Oxide-Assisted Synthesis of Bismuth Nanosheets for Catalytic Stripping Voltammetric Determination of Iron in Coastal Waters. *Microchim Acta* **2016**, *183* (2), 855–861. https://doi.org/10.1007/s00604-015-1733-z.

(146) Cinti, S.; Minotti, C.; Moscone, D.; Palleschi, G.; Arduini, F. Fully Integrated Ready-to-Use Paper-Based Electrochemical Biosensor to Detect Nerve Agents. *Biosensors and Bioelectronics* **2017**, *93*, 46–51. https://doi.org/10.1016/j.bios.2016.10.091.

(147) Cinti, S.; Neagu, D.; Carbone, M.; Cacciotti, I.; Moscone, D.; Arduini, F. Novel Carbon Black-Cobalt Phthalocyanine Nanocomposite as Sensing Platform to Detect Organophosphorus Pollutants at Screen-Printed Electrode. *Electrochimica Acta* **2016**, *188*, 574–581. https://doi.org/10.1016/j.electacta.2015.11.069.

(148) Hao, Y.; Liu, S.; Lu, Z.-N.; Huang, J.; Zhao, M. The Impact of Environmental Pollution on Public Health Expenditure: Dynamic Panel Analysis Based on Chinese Provincial Data. *Environ Sci Pollut Res* **2018**, *25* (19), 18853–18865. https://doi.org/10.1007/s11356-018-2095-y.

(149) Cf, O. Transforming Our World: The 2030 Agenda for Sustainable Development. *United Nations: New York, NY, USA* **2015**.

(150) Food and Agriculture: Key to Achieving the 2030 Agenda for Sustainable Development. *FOOD AND AGRICULTURE*.

(151) Lo Presti, D.; Di Tocco, J.; Massaroni, C.; Cimini, S.; De Gara, L.; Singh, S.; Raucci, A.; Manganiello, G.; Woo, S. L.; Schena, E.; Cinti, S. Current Understanding, Challenges and Perspective on Portable Systems Applied to Plant Monitoring and Precision Agriculture. *Biosensors and Bioelectronics* **2023**, *222*, 115005. https://doi.org/10.1016/j.bios.2022.115005.

(152) Intisar, A.; Ramzan, A.; Sawaira, T.; Kareem, A. T.; Hussain, N.; Din, M. I.; Bilal, M.; Iqbal, H. M. N. Occurrence, Toxic Effects, and Mitigation of Pesticides as Emerging Environmental Pollutants Using Robust Nanomaterials – A Review. *Chemosphere* **2022**, *293*, 133538. https://doi.org/10.1016/j.chemosphere.2022.133538.

(153) Nicolopoulou-Stamati, P.; Maipas, S.; Kotampasi, C.; Stamatis, P.; Hens, L. Chemical Pesticides and Human Health: The Urgent Need for a New Concept in Agriculture. *Frontiers in Public Health* **2016**, *4*.

(154) *EU legislation on MRLs*. https://food.ec.europa.eu/plants/pesticides/maximum-residue-levels/eu-legislation-mrls_en (accessed 2023-08-17).

(155) *World Agriculture towards 2030/2050: The 2012 Revision*; Alexandratos, N., Bruinsma, J., Eds.; ESA Working Papers 12-03; 2012. https://doi.org/10.22004/ag.econ.288998.

(156) Stafford, J. V. Implementing Precision Agriculture in the 21st Century. *Journal of Agricultural Engineering Research* **2000**, *76* (3), 267–275. https://doi.org/10.1006/jaer.2000.0577.

(157) Zhang, N.; Wang, M.; Wang, N. Precision Agriculture—a Worldwide Overview. *Computers and Electronics in Agriculture* **2002**, *36* (2), 113–132. https://doi.org/10.1016/S0168-1699(02)00096-0.

(158) Yin, H.; Cao, Y.; Marelli, B.; Zeng, X.; Mason, A. J.; Cao, C. Soil Sensors and Plant Wearables for Smart and Precision Agriculture. *Advanced Materials* **2021**, *33* (20), 2007764. https://doi.org/10.1002/adma.202007764.

(159) Li, B.; Sun, P.; Zhen, J.; Gong, W.; Zhang, Z.; Jia, W.; Liang, G.; Pan, L. pH-Controlled UV−Vis Sensing Strategy for Indirect, Rapid Detection of Paraoxon Based on Molecular Form Conversion. *Sensors and Actuators B: Chemical* **2021**, *348*, 130715. https://doi.org/10.1016/j.snb.2021.130715.

(160) Hayat, A.; Marty, J. L. Disposable Screen Printed Electrochemical Sensors: Tools for Environmental Monitoring. *Sensors* **2014**, *14* (6), 10432–10453. https://doi.org/10.3390/s140610432.

(161) Singh, S.; Wang, J.; Cinti, S. Review—An Overview on Recent Progress in Screen-Printed Electroanalytical (Bio)Sensors. *ECS Sens. Plus* **2022**, *1* (2), 023401. https://doi.org/10.1149/2754-2726/ac70e2.

(162) Liang, G.; He, Z.; Zhen, J.; Tian, H.; Ai, L.; Pan, L.; Gong, W. Development of the Screen-Printed Electrodes: A Mini Review on the Application for Pesticide Detection. *Environmental Technology & Innovation* **2022**, *28*, 102922. https://doi.org/10.1016/j.eti.2022.102922.

(163) Mahmudiono, T.; Olegovich Bokov, D.; Abdalkareem Jasim, S.; Kamal Abdelbasset, W.; Dinora M. Khashirbaeva. State-of-the-Art of Convenient and Low-Cost Electrochemical Sensor for Food Contamination Detection: Technical and Analytical Overview. *Microchemical Journal* **2022**, *179*, 107460. https://doi.org/10.1016/j.microc.2022.107460.

(164) Kuswandi, B.; Hidayat, M. A.; Noviana, E. Paper-Based Electrochemical Biosensors for Food Safety Analysis. *Biosensors* **2022**, *12* (12), 1088. https://doi.org/10.3390/bios12121088.

(165) Arduini, F.; Cinti, S.; Scognamiglio, V.; Moscone, D.; Palleschi, G. How Cutting-Edge Technologies Impact the Design of Electrochemical (Bio)Sensors for Environmental Analysis. A Review. *Analytica Chimica Acta* **2017**, *959*, 15–42. https://doi.org/10.1016/j.aca.2016.12.035.

(166) Singh, S.; Miglione, A.; Raucci, A.; Numan, A.; Cinti, S. Towards Sense and Sensitivity-Based Electrochemical Biosensors for Liquid Biopsy-Based Breast Cancer Detection. *TrAC Trends in Analytical Chemistry* **2023**, *163*, 117050. https://doi.org/10.1016/j.trac.2023.117050.

(167) Miglione, A.; Raucci, A.; Amato, J.; Marzano, S.; Pagano, B.; Raia, T.; Lucarelli, M.; Fuso, A.; Cinti, S. Printed Electrochemical Strip for the Detection of miRNA-29a: A Possible Biomarker Related to Alzheimer's Disease. *Anal. Chem.* **2022**, *94* (45), 15558–15563. https://doi.org/10.1021/acs.analchem.2c03542.

(168) Calabria, D.; Lazzarini, E.; Pace, A.; Trozzi, I.; Zangheri, M.; Cinti, S.; Difonzo, M.; Valenti, G.; Guardigli, M.; Paolucci, F.; Mirasoli, M. Smartphone-Based 3D-Printed Electrochemiluminescence Enzyme Biosensor for Reagentless Glucose Quantification in Real Matrices. *Biosensors and Bioelectronics* **2023**, *227*, 115146. https://doi.org/10.1016/j.bios.2023.115146.

(169) Kim, J.; Jeerapan, I.; Imani, S.; Cho, T. N.; Bandodkar, A.; Cinti, S.; Mercier, P. P.; Wang, J. Noninvasive Alcohol Monitoring Using a Wearable Tattoo-Based Iontophoretic-Biosensing System. *ACS Sens.* **2016**, *1* (8), 1011–1019. https://doi.org/10.1021/acssensors.6b00356.

(170) Ferreira, P. C.; Ataíde, V. N.; Silva Chagas, C. L.; Angnes, L.; Tomazelli Coltro, W. K.; Longo Cesar Paixão, T. R.; Reis de Araujo, W. Wearable Electrochemical Sensors for Forensic and Clinical Applications. *TrAC Trends in Analytical Chemistry* **2019**, *119*, 115622. https://doi.org/10.1016/j.trac.2019.115622.

(171) Di Tocco, J.; Lo Presti, D.; Massaroni, C.; Cinti, S.; Cimini, S.; De Gara, L.; Schena, E. Plant-Wear: A Multi-Sensor Plant Wearable Platform for Growth and Microclimate Monitoring. *Sensors* **2023**, *23* (1), 549. https://doi.org/10.3390/s23010549.

(172) Kim, J. J.; Fan, R.; Allison, L. K.; Andrew, T. L. On-Site Identification of Ozone Damage in Fruiting Plants Using Vapor-Deposited Conducting Polymer Tattoos. *Science Advances* **2020**, *6* (36), eabc3296. https://doi.org/10.1126/sciadv.abc3296.

(173) Hossain, N. I.; Noushin, T.; Tabassum, S. Leaf-FIT: A Wearable Leaf Sensor for In-Situ and Real-Time Monitoring of Plant Phytohormones. In *2021 IEEE Sensors*; 2021; pp 1–4. https://doi.org/10.1109/SENSORS47087.2021.9639842.

(174) Martins, T. S.; Machado, S. A. S.; Oliveira, O. N.; Bott-Neto, J. L. Optimized Paper-Based Electrochemical Sensors Treated in Acidic Media to Detect Carbendazim on the Skin of Apple and Cabbage. *Food Chemistry* **2023**, *410*, 135429. https://doi.org/10.1016/j.foodchem.2023.135429.

(175) Zhao, F.; He, J.; Li, X.; Bai, Y.; Ying, Y.; Ping, J. Smart Plant-Wearable Biosensor for in-Situ Pesticide Analysis. *Biosensors and Bioelectronics* **2020**, *170*, 112636. https://doi.org/10.1016/j.bios.2020.112636.

(176) Barfidokht, A.; Mishra, R. K.; Seenivasan, R.; Liu, S.; Hubble, L. J.; Wang, J.; Hall, D. A. Wearable Electrochemical Glove-Based Sensor for Rapid and on-Site Detection of Fentanyl. *Sensors and Actuators B: Chemical* **2019**, *296*, 126422. https://doi.org/10.1016/j.snb.2019.04.053.

(177) Mishra, R. K.; Hubble, L. J.; Martín, A.; Kumar, R.; Barfidokht, A.; Kim, J.; Musameh, M. M.; Kyratzis, I. L.; Wang, J. Wearable Flexible and Stretchable Glove Biosensor for On-Site Detection of Organophosphorus Chemical Threats. *ACS Sens.* **2017**, *2* (4), 553–561. https://doi.org/10.1021/acssensors.7b00051.

CHAPTER 5. ADDITIONAL FINDINGS

As additional part of my doctoral studies, the development of novel electrochemical sensors and biosensors was applied also in the field of human health monitoring. Biosensors are particularly useful in healthcare for the diagnosis and monitoring of diseases due to their sensitivity, specificity, and potential for miniaturization and integration into portable devices for point-of-care applications.[1] Considering the tight interconnection between emerging contaminants and human health, a paper-based electrochemical sensor for copper detection in serum samples was developed. The system was basically very similar to the one that we developed for nickel detection but with the advantages of using paper as substrate for the electrodes production. Also in this case the system was integrated with filter paper in order to achieve a rapid preconcentration and making the platform adaptable to real matrix scenarios.[2] A paper-based architecture was also applied in the forensic field for nitrite ions detection.[3] In addition, a total new architecture was thought in order to combine the electrochemical measurements with lateral flow immunoassays (LFIAs), named electrochemical LFIA (eLFIA).[4] This was based on gold nanoparticles dissolution and detection and was successfully applied towards the detection of prostate-specific antigen (PSA). Moreover, I spent three months at the Electroanalysis and (Bio)Electrochemical sensors group (GEBE), of the Analytical Chemistry Department of the Universidad Complutense of Madrid, where I focused on electrochemical immunosensing based on the modification of the electrode surface with functionalized magnetic beads.[5] The system was applied towards the detection of collagen as biomarker in colorectal cancer samples.[6] Finally, the development of a printed electrochemical strip for the detection of miRNA-29A as possible biomarker related to Alzheimer's disease,

is quickly presented. In this case the strategies for developing electrochemical biosensors based on the immobilization at the electrode surface of specific nucleic acids were exploited and applied, in particular, towards the detection of microRNAs (miRNAs), small noncoding RNAs, recently highlighted for their promising role as biomarkers for early diagnosis.[7] All these applications fall within the ASSURED (Affordable, Sensitive, Specific, User-friendly, Rapid and robust, Equipment-free, and Deliverable) criteria, that are essential for ensuring that diagnostic devices are suitable for use in resource-limited settings, where access to traditional laboratory facilities may be limited. Recently, a revised version of the criteria, known as REASSURED, has been proposed. REASSURED encompasses key criteria such as real-time connectivity, ease of specimen collection, affordability, sensitivity, specificity, user-friendliness, rapid and reliable performance, equipment-free operation, and deliverability to those in need. The REASSURED criteria aim to address the evolving landscape of diagnostic technologies, including the integration of digital technology and mobile health (m-health), to strengthen the efficiency of health care systems and improve patient outcomes. These criteria are crucial for guiding the development, validation, and regulation of point-of-care tests for various applications, including human healthcare and infectious disease diagnostics.

5.1 SUSTAINABLE COPPER ELECTROCHEMICAL STRIPPING ONTO A PAPER-BASED SUBSTRATE FOR CLINICAL APPLICATION

The electroanalytical field has exploited great advantages in using paper-based substrates, even if the word "paper" might be general. In fact, the mainly adopted paper-based substrates are often chromatographic and office ones. They are characterized by the following main features (and drawbacks): chromatographic paper is well-established for storing reagents/ treating samples, but the sensitivity compared to traditional screen-printed ones is lower (due to porosity), while office paper represents a sustainable alternative to plastic (with similar sensitivity), but its porosity is not enough to load reagents.[8] To overcome the limitations that might arise due to the adoption of a type of individual paper-based substrate, herein, we describe for the first time the development of a two-dimensional merged paper-based device for electrochemical copper ion detection in serum. Copper (Cu) is as an essential metal playing a crucial role in various biochemical reactions as a co-factor of many metalloenzymes and in physiological regulations. Although copper ions are mainly bound to serum proteins, from a clinical perspective the determination of copper in its unbound form is of particular interest because of its high toxicity. In this work, we report a novel configuration to produce an integrated all-in-one electrochemical device, in which no additional working medium has to be added by the end user and the sensitivity can be tuned by rapid preconcentration on porous paper, with the advantage of making the platform adaptable to real matrix scenarios. The novel architecture has been obtained by combining office paper to screen-print a sustainable and robust electrochemical strip and a chromatographic disk to (1) store the reagents, (2) collect real samples, and (3) preconcentrate the analyte of interest (Figure V.1). The novel sensing platform has allowed us to obtain a detection limit for copper ions down to 4 ppb in all the solutions that have been

investigated, namely, standard solutions and serum, and a repeatability of ca. 10% has been obtained. Inductively coupled plasma-mass spectrometry measurements confirmed the satisfactory correlation.[2]

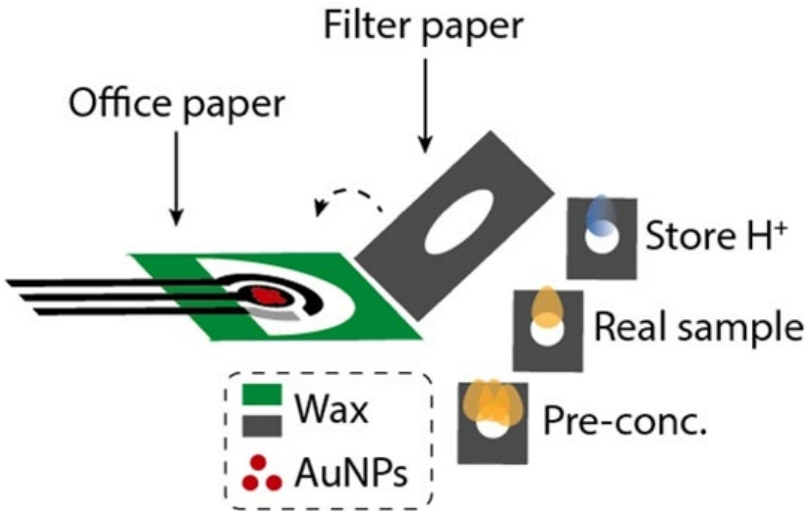

Figure V.1. Schematic representation of the combination between office paper and chromatographic paper to obtain a synergic platform.

5.2 TECHNICAL EVALUATION OF PAPER-BASED ELECTROCHEMICAL STRIP TO MEASURE NITRITE IONS IN FORENSIC FIELD

Nitrite is a compound used as a food additive for its preservative action and coloring capability, as well as an industrial agent for its antifreezing action and for preventing corrosion, and it is also used as a pharmaceutical in cyanide detoxification therapy. However, nitrite also has potential health risks. It can cause methemoglobinemia, a condition where an abnormal amount of methemoglobin is produced, reducing the oxygen-carrying capacity of the blood; maternal exposure to nitrates and nitrites may increase the risk of pregnancy complications such as anemia, threatened abortion/premature labor and nitrite, combined with secondary amines, can lead to the formation of carcinogenic nitrosamines.[9] Furthermore, nitrite has been used as a lethal agent in cases of suicide and murder due to its high toxicity and easy availability. Sodium nitrite is a powerful oxidizing agent that can cause hypotension, limit oxygen transport, and lead to death.

In this work, in collaboration with Department of Diagnostics and Public Health of University of Verona, we developed an electrochemical paper-based device for selectively determining nitrite in complex biofluids, such as blood, cadaveric blood, vitreous humor, serum, plasma, and urine. The approach was validated in terms of the linearity of response, selectivity, and sensitivity, and the accuracy of the determination was verified by comparing the results with a chromatographic instrumental method. A linear response was observed in the micromolar range; the sensitivity of the method expressed as the limit of detection, was 0.4 μM in buffer measurements. The simplicity of use, the portability of the device, and the performance shown make the approach suitable for detecting nitrite in complex biofluids, including contexts of forensic interest, such as murders or suicides in

which nitrite is used as a toxic agent (Figure V.2). Limits of detection of ca. 1, 2, 4, 5, 3, and 4 µM were obtained in vitreous humor, urine, serum and plasma, blood, and cadaveric blood, also highlighting a satisfactory accuracy comprised between 91 and 112%.[3]

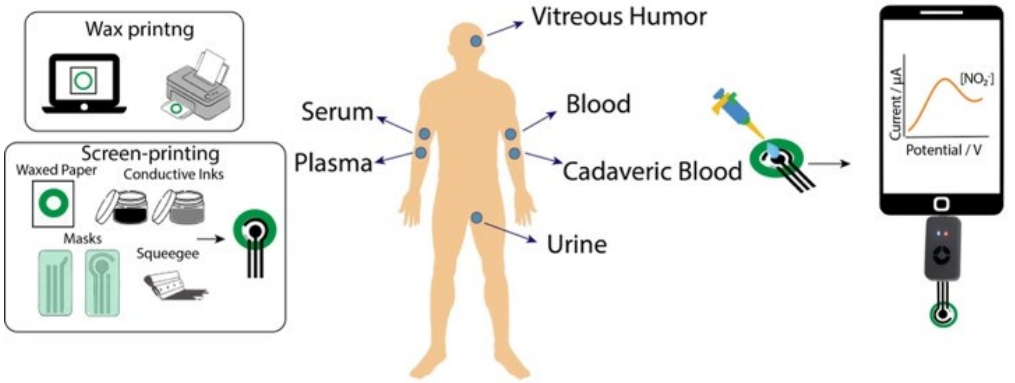

Figure V.2. Schematic representation of the manufacture of the electrochemical strip based onto office paper (wax printing and screen printing), for the determination of nitrites in various biological matrices.

5.3 GOLD NANOPARTICLES-BASED LATERAL FLOW IMMUNOASSAY FOR PROSTATE SPECIFIC ANTIGEN COLORIMETRIC AND ELECTROCHEMICAL DETECTION

COVID-19 pandemic highlighted lateral flow immunoassay (LFIA) strips as the most known point-of-care (POC) devices enabling rapid and easy detection of bio- or chemical relevant markers in a simple and low-cost way by non-specialized users. However, these test strips rarely provide the quantitative detection of biomarkers in clinical samples.[10–13] Alternatively, electrochemical-based diagnostics, especially known for diabetes care, enables quantitative detection in immunoassays. Electrochemical transduction is attractive to be integrated into LFIAs due to its simplicity, high sensitivity, fast signal generation, and cost-effectiveness. In particular, the advantages associated with use of screen-printed electrodes (SPEs) consist in very small sample volumes used, improved performance, unlike optically based detection where miniaturized system can lead to poorer sensitivity.[4] Moreover, the electrochemical performance can be further improved through developing signal tracer in similar manners achievable for naked-eye detection, such as utilizing gold nanoparticles (AuNPs) that remains a gold standard in LFA that allows detection of the color change by naked eyes. enables quantitative determination of biomarkers.[14] From an analytical point perspective, the combination of the two approaches might be representing a step forward for the POC world. In this work, developed together the group of Prof. Anfossi, from the University of Turin, LFIA strip has been combined with an electrochemical transduction, yielding an electrochemical LFIA (eLFIA) (Figure V.3). As proof-of-concept, the detection of prostate-specific antigen has been carried out by combining printed-electrochemical strip with the traditional LFIA tests. The electrochemical detection has been based on the measurement of the Au ions produced from the dissolution of the gold

nanoparticles previously captured on the test line. The analytical performance obtained at LFIA and eLFIA were compared, highlighting how the use of differential pulse voltammetry allowed for a lower detection limit, respectively 0.38 and 0.15 ng/mL, but increasing the time of analysis. Although the correlation between the two architectures confirmed the satisfactory agreement of outputs, this technical note has been thought to provide the reader a fair statement with regards the strength and drawbacks about combining the two (apparently) competitor devices in diagnostics field, namely LFIA and electrochemical strips.

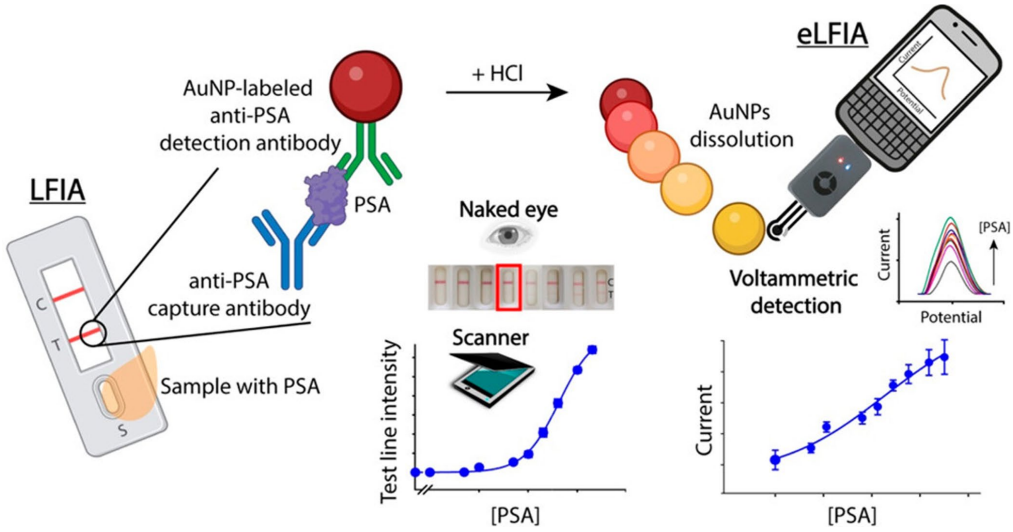

Figure V.3. Experimental setup of eLFIA architecture which includes: LFIA visualization, cutting of the test line, AuNPs dissolution in pre-acidified vials, and smartphone-based electrochemical detection.

5.4 IMMUNOSENSING PLATFORM FOR ELECTROCHEMICAL DETECTON OF COLLAGEN 1α IN COLORECTAL CANCER SAMPLES

Electrochemical immunosensors are advanced analytical tools that leverage the specificity of antibody-antigen interactions and the sensitivity of electrochemical detection to identify and quantify specific analytes. The antibody–antigen immunoreaction can directly produce electrical charges for the quantitative analysis of target molecules. Electrochemical transducers have attracted huge attention in constructing immunosensors due to the advantages of inexpensive cost, good compatibility with miniature and portable electrical readers, and ease of large-scale electrode production. Electrochemical immunosensors provide good selectivity and sensitivity when using a variety of signal probes, including enzymes, redox mediators, and nanomaterials, for amplifying immunoreaction results.[15,16] Using magnetic beads (MBs) allows producing relatively fast and simple electrochemical magneto-immunosensors, with the advantages of concentrate the target analyte from the sample, increasing the sensitivity of the detection and obtain easy separation and washing steps, streamlining the assay procedure.[17,18] During my period abroad, at the GEBE group of the analytical chemistry department of the Universidad Complutense of Madrid, we developed an electrochemical immunosensor based on functionalized magnetic microbeads, for the sensitive detection of Collagen type I alpha 1 (COL1A1), in different colorectal cancer samples. COL1A1 is highly expressed in various cancers and regulates various cellular processes, including cell proliferation, metastasis, apoptosis, and cisplatin resistance. COL1A1 is also associated with cancer progression and prognosis; elevated COL1A1 expression is associated with poor prognosis in cancer patients.[6] A selective capture antibody was used to build up a sandwich-immunosensor, based on carboxylic acid-modified magnetic beads

(HOOC-MBs). A biotinylated antibody, then conjugated with horseradish peroxidase (HRP) were used as detector antibody for the target protein. Amperometric detection at -0.20 V (vs. an Ag pseudo-reference electrode) was performed using single screen-printed carbon.

electrodes and the H_2O_2/hydroquinone (HQ) system. The measured variation in the cathodic current was directly proportional to the concentration of target protein (Figure V.4). The developed bioplatforms exhibit a good selectivity and sensitivity providing limits of detection (LOD) values of 15 pg/mL for COL1A1. Several clinical and biological samples have been tested, confirming the reliability of the developed immunosensor and its potential to early detect at lower concentration this important biomarker in colorectal cancer patients.

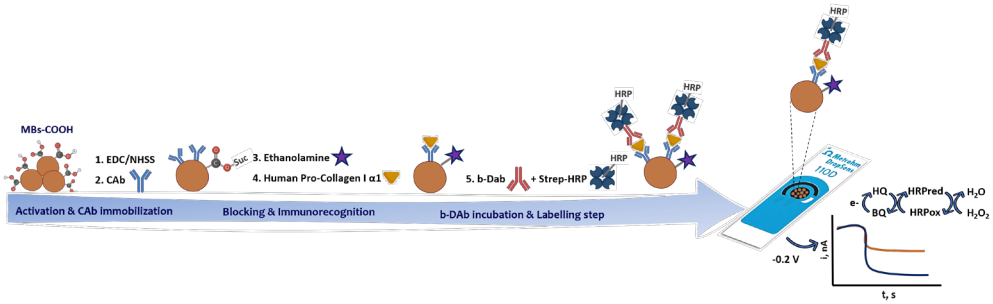

Figure V.4. Schematic display of the fundamentals involved in the immunosensing platforms developed for the amperometric determination of Collagen type I alpha 1.

5.5 PRINTED ELECTROCHEMICAL STRIP FOR THE DETECTION OF miRNA-29a: A POSSIBLE BIOMARKER RELATED TO ALZHEIMER'S DISEASE

The development of electrochemical strips, as extremely powerful diagnostic tools, has received much attention in the field of sensor analysis and, in particular, the detection of nucleic acids in complex matrixes is a hot topic in the electroanalytical area, especially when directed toward the development of emerging technologies, for the purpose of facilitating personal healthcare.[19–21] One of the major diseases for which early diagnosis is crucial is represented by Alzheimer's disease (AD). AD is a progressive neurodegenerative disease, and it is the most common cause of dementia worldwide. In this context, microRNAs (miRNAs), which are small noncoding RNAs, have recently been highlighted for their promising role as biomarkers for early diagnosis. In particular, miRNA-29 represents a class of miRNAs known to regulate pathogenesis of AD.[22,23] In this work, carried out in collaboration with the group of prof. Pagano from the Pharmacy Department of Federico II University of Naples, we developed an electrochemical printed strip for the detection of miRNA-29a at low levels. The architecture was characterized by the presence of gold nanoparticles (AuNPs) and an antimiRNA-29a probe labeled with a redox mediator, the methylene blue (MB). The novel analytical tool has been characterized with microscale thermophoresis and electrochemical methods, and it has been optimized by selection of the most appropriate probe density to detect low target concentration (Figure V.5). The present tool was capable to detect miRNA-29a both in standard solution and in serum, respectively, down to 0.15 and 0.2nM. The platform highlighted good repeatability (calculated as the relative standard deviation) of ca.10% and satisfactory selectivity in presence of interfering species. This work has the objective to open a way for the study and possible early diagnosis of a

physically and socially devastating disease such as Alzheimer's. The results demonstrate the suitability of this approach in terms of ease of use, time of production, sensitivity, and applicability.[7]

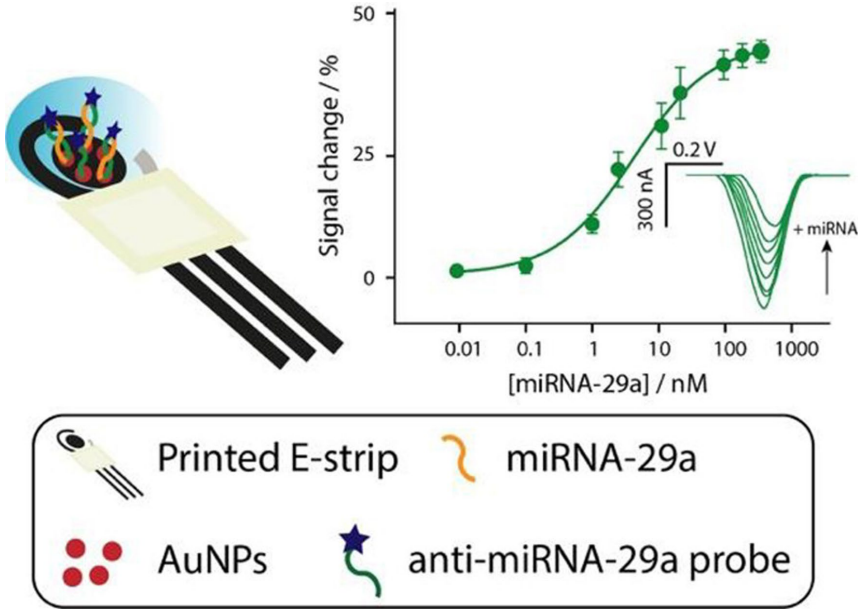

Figure V.5. Schematic representation for the development of the electrochemical biosensor for the detection of miRNA-29a and the expected current signal in the absence and presence of target.

References

(1) Hernández-Rodríguez, J. F.; Rojas, D.; Escarpa, A. Electrochemical Sensing Directions for Next-Generation Healthcare: Trends, Challenges, and Frontiers. *Anal. Chem.* **2021**, *93* (1), 167–183. https://doi.org/10.1021/acs.analchem.0c04378.

(2) Miglione, A.; Spinelli, M.; Amoresano, A.; Cinti, S. Sustainable Copper Electrochemical Stripping onto a Paper-Based Substrate for Clinical Application. *ACS Meas. Au* **2022**. https://doi.org/10.1021/acsmeasuresciau.1c00059.

(3) Raucci, A.; Miglione, A.; Cimmino, W.; Cioffi, A.; Singh, S.; Spinelli, M.; Amoresano, A.; Musile, G.; Cinti, S. Technical Evaluation of a Paper-Based Electrochemical Strip to Measure Nitrite Ions in the Forensic Field. *ACS Meas. Sci. Au* **2023**. https://doi.org/10.1021/acsmeasuresciau.3c00050.

(4) Cheng, J.; Yang, G.; Guo, J.; Liu, S.; Guo, J. Integrated Electrochemical Lateral Flow Immunoassays (eLFIAs): Recent Advances. *Analyst* **2022**, *147* (4), 554–570. https://doi.org/10.1039/D1AN01478A.

(5) Blázquez-García, M.; Arévalo, B.; Serafín, V.; Benedé, S.; Mata, L.; Galán-Malo, P.; Segura-Gil, I.; Pérez, M. D.; Pingarrón, J. M.; Campuzano, S. Ultrasensitive Detection of Soy Traces by Immunosensing of Glycinin and β-Conglycinin at Disposable Electrochemical Platforms. *Talanta* **2022**, *241*, 123226. https://doi.org/10.1016/j.talanta.2022.123226.

(6) Kim, M.-S.; Ha, S.-E.; Wu, M.; Zogg, H.; Ronkon, C. F.; Lee, M.-Y.; Ro, S. Extracellular Matrix Biomarkers in Colorectal Cancer. *International Journal of Molecular Sciences* **2021**, *22* (17), 9185. https://doi.org/10.3390/ijms22179185.

(7) Miglione, A.; Raucci, A.; Amato, J.; Marzano, S.; Pagano, B.; Raia, T.; Lucarelli, M.; Fuso, A.; Cinti, S. Printed Electrochemical Strip for the Detection of miRNA-29a: A Possible Biomarker Related to Alzheimer's Disease. *Anal. Chem.* **2022**, *94* (45), 15558–15563. https://doi.org/10.1021/acs.analchem.2c03542.

(8) Cinti, S.; Moscone, D.; Arduini, F. Preparation of Paper-Based Devices for Reagentless Electrochemical (Bio)Sensor Strips. *Nature Protocols* **2019**, *14* (8), 2437–2451. https://doi.org/10.1038/s41596-019-0186-y.

(9) European Food Safety Authority. *EFSA Explains Risk Assessment: Nitrites and Nitrates Added to Food.*; Publications Office: LU, 2017.

(10) Anfossi, L.; Di Nardo, F.; Giovannoli, C.; Passini, C.; Baggiani, C. Increased Sensitivity of Lateral Flow Immunoassay for Ochratoxin A through Silver Enhancement. *Anal Bioanal Chem* **2013**, *405* (30), 9859–9867. https://doi.org/10.1007/s00216-013-7428-6.

(11) Parolo, C.; Sena-Torralba, A.; Bergua, J. F.; Calucho, E.; Fuentes-Chust, C.; Hu, L.; Rivas, L.; Álvarez-Diduk, R.; Nguyen, E. P.; Cinti, S.; Quesada-González, D.; Merkoçi, A. Tutorial: Design and Fabrication of Nanoparticle-Based Lateral-Flow Immunoassays. *Nat Protoc* **2020**, *15* (12), 3788–3816. https://doi.org/10.1038/s41596-020-0357-x.

(12) Di Nardo, F.; Chiarello, M.; Cavalera, S.; Baggiani, C.; Anfossi, L. Ten Years of Lateral Flow Immunoassay Technique Applications: Trends, Challenges and Future Perspectives. *Sensors* **2021**, *21* (15), 5185. https://doi.org/10.3390/s21155185.

(13) Cavalera, S.; Di Nardo, F.; Forte, L.; Marinoni, F.; Chiarello, M.; Baggiani, C.; Anfossi, L. Switching from Multiplex to Multimodal Colorimetric Lateral Flow Immunosensor. *Sensors* **2020**, *20* (22), 6609. https://doi.org/10.3390/s20226609.

(14) Baptista, P.; Pereira, E.; Eaton, P.; Doria, G.; Miranda, A.; Gomes, I.; Quaresma, P.; Franco, R. Gold Nanoparticles for the Development of Clinical Diagnosis Methods. *Anal Bioanal Chem* **2008**, *391* (3), 943–950. https://doi.org/10.1007/s00216-007-1768-z.

(15) Campuzano, S.; Pingarrón, J. M. Electrochemical Affinity Biosensors: Pervasive Devices with Exciting Alliances and Horizons Ahead. *ACS Sens.* **2023**, *8* (9), 3276–3293. https://doi.org/10.1021/acssensors.3c01172.

(16) Campuzano, S.; Pingarrón, J. M. Electrochemical Bioanalysis: All That Still Hides the Tip of the Iceberg. *Current Opinion in Electrochemistry* **2023**, *41*, 101359. https://doi.org/10.1016/j.coelec.2023.101359.

(17) Muñoz-San Martín, C.; Gamella, M.; Pedrero, M.; Montero-Calle, A.; Barderas, R.; Campuzano, S.; Pingarrón, J. M. Magnetic Beads-Based Electrochemical

Immunosensing of HIF-1α, a Biomarker of Tumoral Hypoxia. *Sensors and Actuators B: Chemical* **2020**, *307*, 127623. https://doi.org/10.1016/j.snb.2019.127623.

(18) Molinero-Fernández, Á.; Moreno-Guzmán, M.; López, M. Á.; Escarpa, A. Magnetic Bead-Based Electrochemical Immunoassays On-Drop and On-Chip for Procalcitonin Determination: Disposable Tools for Clinical Sepsis Diagnosis. *Biosensors* **2020**, *10* (6), 66. https://doi.org/10.3390/bios10060066.

(19) Cinti, S.; Cinotti, G.; Parolo, C.; Nguyen, E. P.; Caratelli, V.; Moscone, D.; Arduini, F.; Merkoci, A. Experimental Comparison in Sensing Breast Cancer Mutations by Signal ON and Signal OFF Paper-Based Electroanalytical Strips. *Anal. Chem.* **2020**, *92* (2), 1674–1679. https://doi.org/10.1021/acs.analchem.9b02560.

(20) Cinti, S.; Proietti, E.; Casotto, F.; Moscone, D.; Arduini, F. Paper-Based Strips for the Electrochemical Detection of Single and Double Stranded DNA. *Anal. Chem.* **2018**, *90* (22), 13680–13686. https://doi.org/10.1021/acs.analchem.8b04052.

(21) Singh, S.; Miglione, A.; Raucci, A.; Numan, A.; Cinti, S. Towards Sense and Sensitivity-Based Electrochemical Biosensors for Liquid Biopsy-Based Breast Cancer Detection. *TrAC Trends in Analytical Chemistry* **2023**, *163*, 117050. https://doi.org/10.1016/j.trac.2023.117050.

(22) Reddy, P. H.; Tonk, S.; Kumar, S.; Vijayan, M.; Kandimalla, R.; Kuruva, C. S.; Reddy, A. P. A Critical Evaluation of Neuroprotective and Neurodegenerative MicroRNAs in Alzheimer's Disease. *Biochemical and Biophysical Research Communications* **2017**, *483* (4), 1156–1165. https://doi.org/10.1016/j.bbrc.2016.08.067.

(23) *Loss of microRNA cluster miR-29a/b-1 in sporadic Alzheimer's disease correlates with increased BACE1/β-secretase expression*. PNAS. https://www.pnas.org/doi/abs/10.1073/pnas.0710263105 (accessed 2022-03-05).

CHAPTER 6. CONCLUSIONS AND FUTURE DIRECTIONS

The development of novel (bio)sensors and LC-HRMS approaches represents a significant advancement in the accurate and sustainable monitoring of emerging contaminants. These cutting-edge technologies offer several key benefits and present new opportunities for environmental and biological analysis. They enable the precise detection of a wide range of contaminants and toxins, including emerging and unknown compounds, at environmentally relevant concentrations. LC-HRMS approaches are investigating in order to allow targeted and non-target screening, enabling the characterization of a broader range of potentially toxic compounds, as emerging natural toxins. In this dissertation, several examples of LC-HRMS approaches are discussed and different classes of emerging natural toxins are studied. Among these, an untargeted approach is tested to analyze mucilage samples from the 2021 north-eastern Aegean Sea episode, and it allow to detect and confirm cyclic imines and in particular PnTX-G and Portimine A as main components of these samples. An untargeted LC-HRMS approach is also tested to identify microcystins in producing cyanobacterial cultures undergone to different chlorine-based treatments commonly used for water potabilization, suggesting that the choice of the oxidant to be used during raw water pre-treatment for potabilization purposes, as well as its dose and treatment time, should be taken into consideration. In this case the untargeted analysis allows the identification of a new cyanopeptoline-type peptide, structurally characterized through LC-HRMS^n experiments. In this study, the untargeted analysis has been implemented thanks to the use of the CyanoMetDB, an accessible database of cyanobacterial secondary metabolites, that can be uploaded on a specific software that allow a faster and easier suspect screening analysis of cyanometabolites. This workflow has been further explored during my permanence abroad, at Eawag

laboratories, where it is applied to monitor key metabolites from cyanobacterial blooms of *Planktothrix* sp. In the frame of monitoring palytoxin and its congeners, a novel Solid-Phase Toxin Adsorption (SPATT) method based on cross-linked cyclodextrins, is developed and currently in progress. From preliminary results, the resins are able to capture palytoxin and ovatoxins when used as powder in small scale experiments. Further experiments with SPATT units need to be evaluated to assess the usefulness of these kind of devices towards *Ostreopsis* proliferations in field.

Although these techniques have demonstrated high reliability, their use is strictly related to skilled personnel, equipped laboratory, sophisticated instruments and time-consuming procedures. Although validated laboratories are needed to confirm the presence/absence of a certain molecule, in situ measurements with portable analytical devices can be considered complementary: quick screening analysis can avoid loss of money and time in sending a suspected sample to laboratory.

Electrochemical sensors offer advantages such as low cost, portability, miniaturization, and high reliability, making them ideal for in-situ and continuous monitoring applications. Novel approaches in this field are deeply discussed in this dissertation; starting from the integration of a filter paper disk with a classic polyester system, we moved on a total paper-based platform; in these two studies, applied respectively towards nickel detection in cosmetics and paracetamol detection in wastewater, the advantages related to the use of paper are exploited: the integration with paper allow to store the reagents, collect real samples, and preconcentrate the analyte of interest. When the device is printed totally on paper, the entire platform become a self-contained platform, able to store all required reagents for the assay, process the sample by eliminating significant interferences, and display the results within minutes. Consequently, novel kinds

of sustainable substrates are investigated: porous PHBV-based bacterial polymers have been screen-printed with conductive inks to realize electrochemical strips able to detect organophosphate pesticides, highlighting the potentiality of these materials for future sustainable application in the electroanalytical field. Finally, the integration of our system directly on a glove able to detect organophosphate pesticides directly on fruit peels, is investigated. Organophosphate pesticide was detected down to a nanomolar range and due to the strength and flexibility obtained with this architecture, the system proved useful for in-situ monitoring. Considering the tight interconnection between emerging contaminants and human health, these novel approaches are successfully applied also in health monitoring field. In particular, biomimetic sensing platforms applied towards the detection of Alzheimer's disease related biomarkers applications in the miRNAs field, will be further investigated. While these technologies offer significant promise, they also face challenges that require ongoing research and development. Some of the key challenges include improving stability, reproducibility, and the ability to function accurately in complex sample matrices. Future advancements may involve the integration of advanced nanomaterials to enhance sensitivity and the development of self-contained sensing devices for miniaturization and integration of multiple components. During my PhD course, I had the opportunity in training these two different and complementary aspects of analytical chemistry applied to environment monitoring and health surveillance. The combination of I) easy-to-use and portable de-centralized approaches and II) validated and reference laboratory-bound methodologies, might represent a step forward beyond the current paradigm: each approach should be seen as an added point for the other one, with the common goal to preserve human health and ecosystems.

ACKNOWLEDGEMENTS

I am deeply grateful to my supervisors, Professors Stefano Cinti and Luciana Tartaglione, for giving me the opportunity to work in their laboratory; it was a truly important opportunity for my personal and professional growth. I would like to thank both of them for the scientific teachings, suggestions, help and support they gave me, introducing me to the world of research. I extend my appreciation to Professor Carmela dell'Aversano, Michela Varra and all the people who have been part of these years, I have tried to learn something from each of you!

I would like to thank Professor Elisabeth Janssen of the Eawag Institute (Swiss Federal Institute of Aquatic Science and Technology) and Professor Susana Campuzano Ruiz of the GEBE group (Electroanálisis y (bio)sensores electroquímicos, Universidad Complutense de Madrid), and all the people in their respective laboratories, for hosting me during my third year of my PhD and for their scientific commitment. I was welcomed by a great team and I felt at home from day one. These two experiences abroad had a great impact on my professional and personal growth.

Of course, I would like to thank all my friends and colleagues from N15/N16 Labs, Valentina, Fabio, Ada, Wanda, Sabrina, Giota, Sima and all the researchers and students I have had the pleasure to meet over the years, for all the happy and not so happy moments shared in this incredible journey, I will never forget you!

Special thanks to Elena, Alessio and Ernesto, you are, and I hope you will continue to be, the best place to find refuge. To Elle, you know everything.

Last but not least, I am infinitely grateful to my family, Rosa and Michele for their continued support, I hope to always make them proud of me.

I want to thank Sara, Carlotta and Carla for being there year after year.

And finally thanks to Andrea, always by my side.